frontiers | Research Topics

The 4th NACAN summit proceedings: Nutrition and food for a healthy life

Edited by
Ling Zhao, Zhiping Yu, Sheau Ching Chai, Fanbin Kong, Lei Hao and Zhi Chai

Published in
Frontiers in Nutrition

ISSN 1664-8714
ISBN 978-2-8325-2463-3
DOI 10.3389/978-2-8325-2463-3

About Frontiers

Frontiers is more than just an open access publisher of scholarly articles: it is a pioneering approach to the world of academia, radically improving the way scholarly research is managed. The grand vision of Frontiers is a world where all people have an equal opportunity to seek, share and generate knowledge. Frontiers provides immediate and permanent online open access to all its publications, but this alone is not enough to realize our grand goals.

Frontiers journal series

The Frontiers journal series is a multi-tier and interdisciplinary set of open-access, online journals, promising a paradigm shift from the current review, selection and dissemination processes in academic publishing. All Frontiers journals are driven by researchers for researchers; therefore, they constitute a service to the scholarly community. At the same time, the *Frontiers journal series* operates on a revolutionary invention, the tiered publishing system, initially addressing specific communities of scholars, and gradually climbing up to broader public understanding, thus serving the interests of the lay society, too.

Dedication to quality

Each Frontiers article is a landmark of the highest quality, thanks to genuinely collaborative interactions between authors and review editors, who include some of the world's best academicians. Research must be certified by peers before entering a stream of knowledge that may eventually reach the public - and shape society; therefore, Frontiers only applies the most rigorous and unbiased reviews. Frontiers revolutionizes research publishing by freely delivering the most outstanding research, evaluated with no bias from both the academic and social point of view. By applying the most advanced information technologies, Frontiers is catapulting scholarly publishing into a new generation.

What are Frontiers Research Topics?

Frontiers Research Topics are very popular trademarks of the *Frontiers journals series*: they are collections of at least ten articles, all centered on a particular subject. With their unique mix of varied contributions from Original Research to Review Articles, Frontiers Research Topics unify the most influential researchers, the latest key findings and historical advances in a hot research area.

Find out more on how to host your own Frontiers Research Topic or contribute to one as an author by contacting the Frontiers editorial office: frontiersin.org/about/contact

The 4th NACAN summit proceedings: Nutrition and food for a healthy life

Topic editors

Ling Zhao — The University of Tennessee, Knoxville, United States
Zhiping Yu — University of North Florida, United States
Sheau Ching Chai — University of Delaware, United States
Fanbin Kong — University of Georgia, United States
Lei Hao — Indiana University of Pennsylvania, United States
Zhi Chai — Icahn School of Medicine at Mount Sinai, United States

Citation

Zhao, L., Yu, Z., Chai, S. C., Kong, F., Hao, L., Chai, Z., eds. (2023). *The 4th NACAN summit proceedings: Nutrition and food for a healthy life*.
Lausanne: Frontiers Media SA. doi: 10.3389/978-2-8325-2463-3

Table of contents

frontiers | Frontiers in Nutrition

TYPE Editorial
PUBLISHED 04 May 2023
DOI 10.3389/fnut.2023.1200954

OPEN ACCESS

EDITED AND REVIEWED BY
Mauro Serafini,
University of Teramo, Italy

*CORRESPONDENCE
Ling Zhao
✉ ling.zhao@utk.edu

†These authors share first authorship

RECEIVED 05 April 2023
ACCEPTED 11 April 2023
PUBLISHED 04 May 2023

CITATION
Chai Z, Hao L, Chai SC, Chen G, Kong F, Wu C, Yu Z, Zhao L and Zhou J-R (2023) Editorial: The 4th NACAN summit proceedings: nutrition and food for a healthy life. *Front. Nutr.* 10:1200954. doi: 10.3389/fnut.2023.1200954

Editorial: The 4th NACAN summit proceedings: nutrition and food for a healthy life

Zhi Chai[1†], Lei Hao[2†], Sheau C. Chai[3], Guoxun Chen[4], Fanbin Kong[5], Chaodong Wu[6], Zhiping Yu[7], Ling Zhao[8*] and Jin-Rong Zhou[9]

[1]Department of Genetics and Genomic Sciences, Icahn School of Medicine at Mount Sinai, New York, NY, United States, [2]Department of Nursing and Allied Health Professions, Indiana University of Pennsylvania, Indiana, PA, United States, [3]Department of Behavioral Health and Nutrition, University of Delaware, Newark, DE, United States, [4]College of Biomedicine and Health, Huazhong Agricultural University, Wuhan, Hubei, China, [5]Department of Food Science and Technology, University of Georgia, Athens, GA, United States, [6]Department of Nutrition, Texas A&M University, College Station, TX, United States, [7]Department of Nutrition and Dietetics, University of North Florida, Jacksonville, FL, United States, [8]Department of Nutrition, The University of Tennessee, Knoxville, TN, United States, [9]Nutrition/Metabolism Laboratory, Department of Surgery, Beth Israel-Deaconess Medical Center, Harvard Medical School, Boston, MA, United States

KEYWORDS

diet, nutraceutical, metabolism, dietetics, disease, food, nutrition, health

Editorial on the Research Topic
The 4th NACAN summit proceedings: nutrition and food for a healthy life

Established in 2012, the North America Chinese Association for Nutrition (NACAN) celebrated its 10th anniversary in 2022 (https://www.nacan-us.org/). As a public, non-profit charitable organization under the US Internal Revenue Code Section 501(c)3 and a Commission on Dietetic Registration (CDR) accredited continuing professional education (CPE) provider to the US registered dietitians, NACAN continues to advance science and education among professionals with Chinese heritage in nutrition, health, and related fields of interest. NACAN aims to promote scientific exchange and networking, facilitate advanced education and training, support dissemination and application of nutrition knowledge, and advocate nutrition-related research and evidence-based practice to promote health and wellness.

Joined by their collaborators and co-sponsors, the Chinese American Food Society (CAFS), China Food Publishing Co (CFPC), Guangdong Nutrition Society (GNS), Hebei Nutrition Society (HNS), and College of Food Science and Engineering at Nanjing University of Finance & Economics (NUFE), NACAN hosted the 4th NACAN *Frontiers in Nutrition* Summit—The Joint Nutrition Scientific Symposia with meeting theme—"Nutrition for a healthy life: from the production of foods to healthy eating for everyone" in July of 2022. In collaboration with the journal *Frontiers in Nutrition*, NACAN launched a Research Topic to showcase the research contributed to the summit and beyond. This Research Topic collected research papers to address the following four themes:

- Emerging fields of research: New and innovative areas, especially revolutionary and/or multi-disciplinary approaches that address fundamental questions in nutrition, food, and health sciences.

- Scientific base of nutrition: Mechanistic studies that decipher the underlying links between nutrients, diet, and chronic diseases.
- Agriculture and food production: Functional foods, bioactive compounds, nutraceuticals, and novel food processing technologies that improve human health.
- Nutrition and public health: Clinical and population-based studies that examine the role of diet, food, and nutrition in health and disease.

Nutrition intervention is important for disease management. Li Z. et al. reviewed the potential mechanisms of diabetes mellitus combined with Alzheimer's disease and suggested nutrition therapy to reduce the risk of the comorbidity of those two diseases, which include the management of dietary intake, dietary patterns (e.g., ketogenic diet, Mediterranean diet), and nutrition supplements (e.g., probiotics, vitamins, minerals, omega-3 fatty acids).

Opportunities and challenges co-exist for nutritional intervention in childhood cancers. Wang K. et al. discussed the nutrition status among pediatric cancer patients. They reported nutrient dependencies on amino acids, glycolysis and oxidative phosphorylation, lipids, vitamins, and minerals. Several dietary modifications were reviewed, including calorie restriction, ketogenic diet, nutrient restriction, and nutrient supplementation.

Type 2 diabetes mellitus (T2DM) is the most common type of diabetes that has high comorbidity with obesity, renal impairments, and vitamin D (VD) deficiency. Multiple nutrients have been found to alleviate T2DM, shown in rodent models and in human subjects. Using Zucker diabetic fatty rats that were fed VD deficient diet, Wang D. et al. demonstrated $1,25(OH)_2D_3$ improved urinary Cu, Zn, Se, and Mo excretions, suggesting a protective effect against diabetic renal impairment. Using *in vitro* and *in vivo* models in another study, Wang Y. et al. reported that an olive-derived elenolic acid stimulated GLP-1 and PYY secretion, along with a series of ameliorations on the perturbated metabolic variables in obese diabetic mice. In a meta-analysis, Zhang, Ding et al. concluded that biotin (vitamin B7) supplementation may reduce fasting blood glucose, total cholesterol, and triglyceride levels.

Obesity is a major public health concern, which is closely related to chronic inflammation and brown adipose tissue dysfunction. Bae et al. examined the effects of naringenin, a citrus flavanone, on adipocyte browning, thermogenic activation and brown adipogenesis *in vitro*. The results suggest that naringenin may promote the development of functional brown adipose tissue, in part through PPARγ activation.

Cognition decline is associated with old age and chronic diseases, including neurodegenerative or neuropsychiatric disorders, diabetes and chronic kidney disease. Using an adenine-induced cognitive impairment mouse model, Abdolmaleky et al. demonstrated that mice treated with oligo-lactic acid (LAP) and fermented soy extract (IMB) had significantly improved cognitive performance. The neuroprotective effects of LAP and IMB are mediated by favorable alteration in the gut microbiome as well as through their anti-neuroinflammatory properties.

Inflammation contributes to the development of non-alcoholic fatty liver disease (NAFLD) and non-alcoholic steatohepatitis (NASH). While NAFLD is generally considered a benign condition, NASH can further progress to cirrhosis, liver failure, and liver cancer. Li H. et al. reviewed how hepatic and extra-hepatic signals activate the stimulator of interferon genes (STING) in macrophages, which triggers hepatic inflammation, a key factor driving the development of NAFLD/NASH. While more research is needed, current evidence suggests that STING plays a role in promoting liver inflammation and damage. Targeting the STING pathway may therefore represent a potential therapeutic approach for managing NAFLD/NASH in the future.

Vitamin A (VA) is vital for an individual's general health. Zhang, Tian et al. found that VA status regulates body weight, glucose, lipid levels, and hepatic gene expression in Zucker lean and Zucker fatty male rats. Furthermore, replenishing VA through the diet can restore the expression levels of hepatic genes for glucose and lipid metabolism in Zucker lean male rats.

Sphingomyelin and its metabolites have diverse biological functions. Yang and Chen explored their distribution, digestion, absorption, and metabolic pathways, and reviewed their nutritional functions in chronic metabolic diseases. While endogenous sphingomyelin production is linked to pathological changes, dietary supplementation has been shown to maintain lipid homeostasis. The paper also evaluated their possible implications in modern food preparations, skin improvement, delivery systems, and oil organogels.

In summary, the Joint Nutrition Scientific Symposia and all papers collected in the Research Topic offer insights into the development of research in nutrition and food for a healthy life.

Author contributions

All authors listed have made a substantial, direct, and intellectual contribution to the work and approved it for publication.

Conflict of interest

The authors declare that the research was conducted in the absence of any commercial or financial relationships that could be construed as a potential conflict of interest.

Publisher's note

frontiers | Frontiers in Nutrition

TYPE Original Research
PUBLISHED 06 October 2022
DOI 10.3389/fnut.2022.999323

OPEN ACCESS

EDITED BY
Lei Hao,
Indiana University of Pennsylvania, United States

REVIEWED BY
Martin Ronis,
Louisiana State University, United States
Min Chen,
Icahn School of Medicine at Mount Sinai, United States

*CORRESPONDENCE
Yan Zhang
Yank1223@sina.com

†These authors share first authorship

SPECIALTY SECTION
This article was submitted to Nutrition and Metabolism, a section of the journal Frontiers in Nutrition

RECEIVED 20 July 2022
ACCEPTED 16 September 2022
PUBLISHED 06 October 2022

CITATION
Zhang Y, Tian K and Chen G (2022) Replenishment of vitamin A for 7 days partially restored hepatic gene expressions altered by its deficiency in rats.
Front. Nutr. 9:999323.
doi: 10.3389/fnut.2022.999323

Replenishment of vitamin A for 7 days partially restored hepatic gene expressions altered by its deficiency in rats

Yan Zhang[1*†], Kui Tian[2†] and Guoxun Chen[3]

[1]Department of Gastroenterology, Affiliated Puren Hospital of Wuhan University of Science and Technology, Wuhan, Hubei, China, [2]Department of Radiology, Wuhan Pulmonary Hospital, Wuhan, Hubei, China, [3]Department of Nutrition, University of Tennessee at Knoxville, Knoxville, TN, United States

We investigated the effects of vitamin A (VA) status on metabolism of Zucker rats with different genders and genotypes, and of short-term refeeding of a VA sufficient (VAS) diet on VA deficient (VAD) animals. First, male and female Zucker lean (ZL) and fatty (ZF) rats at weaning were fed a VAD or VAS diet for 8 weeks. Second, male VAD ZL rats were fed a VAS diet for 3 (VAD-VAS3d) or 7 (VAD-VAS7d) days. The body weight (BW), blood parameters, and hepatic expressions of genes for metabolism were determined. VA deficiency reduced BW gain in ZL and ZF rats of either gender. VAD ZL rats had lower plasma glucose, insulin, and leptin levels than VAS ZL rats. VAD-VAS3d and VAD-VAS7d rats had higher plasma glucose, insulin, and leptin levels than that in the VAD rats. The hepatic mRNA levels of *Gck, Cyp26a1, Srebp-1c, Igf1, Rarb, Rxra, Rxrg, Pparg,* and *Ppard* were lowered by VA deficiency. Refeeding of the VAS diet for 3 days restored the *Gck* and *Cyp26a1* expressions, and for 7 days restored the *Gck, Cyp26a1, Igf1,* and *Rxrb* expressions significantly. The 7-day VA replenishment partially restored the hepatic gene expressions and metabolic changes in VAD ZL rats.

KEYWORDS

body weight, hepatic gene expression, plasma glucose, vitamin A deficient, vitamin A sufficient, Zucker rats

Introduction

Chronic metabolic diseases have become a concern of global health. For example, global diabetes prevalence in 2019 was about 463 million, which number is anticipated to be 700 million in 2045 (1). This also increases the financial burden globally as the total diabetic expenditure was estimated to be 760 billion dollars in 2019 worldwide (2). On the other hand, the world is also facing a challenge to feed the ever-increasing population on earth. The global food production has to rise 50% by the year 2030 to meet this demand, which may create two scenarios, malnutrition in certain areas and

overnutrition in others worldwide (3). Therefore, a clear understanding of nutrients' roles will benefit human health globally.

As an essential and lipophilic micronutrient, vitamin A (VA, retinol) plays crucial roles in the general health of an individual, such as vision, growth, and immune responses (4, 5). The active metabolite of retinol, retinoic acid (RA), exists in multiple isomeric forms, such as all-*trans* RA and 9-*cis* RA. Retinol is reversibly oxidized into retinal by (retinol) alcohol dehydrogenases and short-chain dehydrogenases/reductases. The conversion of retinal to RA is an irreversible process catalyzed by (retinal) aldehyde dehydrogenases. RA regulates gene expression through the activations of two families of nuclear receptors, retinoic acid receptors (RARα, β, and γ), and retinoid X receptors (RXRα, β, and γ). Additional transcription factors such as hepatocyte nuclear factor 4α, and chicken ovalbumin upstream transcription factor II may also mediate RA's effects on gene expressions (6, 7). RA is further catabolized into more polar metabolites for excretion by a RA-4-hydroxylase (gene *Cyp26a1*), a RA-responsive gene whose hepatic expression is induced after RA treatment (8). Recently, the effects of VA status on glucose and lipid metabolism have been recognized and appreciated (9, 10).

Metabolic abnormalities, such as obesity and diabetes, are often associated with profound changes in hepatic glucose and lipid metabolism (11, 12). In an attempt to find lipophilic molecules that influence insulin actions in hepatocytes, we found an activity that can modulate insulin-regulated expressions of the cytosolic form of phosphoenolpyruvate carboxyl kinase gene (*Pck1*) (13) and glucokinase gene (*Gck*) (14) in primary hepatocytes. The molecule responsible for this activity was identified as retinoids (14). RA also synergizes with insulin to induce the hepatic expression of sterol regulatory element-binding protein 1c gene (*Srebp-1c*), which is a master regulator of the expressions of genes responsible for the hepatic lipogenesis (15). The VA signaling regulates these genes' expression *via* retinoic acid responsive elements (RAREs) on their promoters (6, 16, 17). All these demonstrate the role of VA signaling in the regulation of the expression levels of genes for the hepatic glucose and lipid metabolism.

Vitamin A status regulates body weight (BW), glucose, and lipid levels in animals. VA deficiency reduced BW gain (18) and depleted hepatic glycogen (19) in rats. On the other hand, excessive dietary VA intake in the form of retinyl esters significantly induced the hepatic glycogen content (20). The Zucker Fatty (ZF) rats are an animal model which carries a spontaneous mutation in the leptin receptor gene, causing obesity and insulin resistance. Zucker Diabetic Fatty (ZDF) rats are a well characterized animal model of type 2 diabetes (T2D). ZDF rats were derived by selectively inbreeding of ZF rats, which led to a sub-strain that develops overt T2D at around 10 weeks of age. Studies have shown that when male Zucker lean (ZL) and ZF rats were fed a VA sufficient (VAS) or VA deficient (VAD) diet for 8 weeks, the VAD diet prevented obesity and hyperlipidemia in ZF rats (21–24). VA status regulates the respiratory exchange ratio in ZL rats (24). Recently, we have shown that reduction of dietary VA status prevents the obesity and T2D in ZDF rats (25). ZF and ZDF rats have leptin receptor mutations that lead to hyperphagia, overnutrition, and development of obesity and T2D (26, 27). We have shown that the expression of retinaldehyde dehydrogenase 1 (*Raldh1*) gene level was elevated in the liver and hepatocytes of ZF rats (28), which might have led to the excessive hepatic RA production and increase in lipogenesis. The *Raldh1* knockout mice are resistant to diet-induced obesity and insulin resistance (29). This was attributed to that the knockout mice have elevated retinaldehyde levels in adipose tissues, which probably suppressed adipogenesis (29). In humans with T2D, the plasma VA levels, and VA intake show some variations depending on population studied (30–33). Interestingly, RA treatment was shown to benefit blood glucose control in ZDF rats (34), and *ob/ob* mice (35). All these demonstrate that VA and its signaling play a role in the regulation of metabolism.

Given the important roles of VA in the regulation of metabolism, we hypothesize that the replenishment of VA in the diet will restore the expression levels of hepatic genes for glucose and lipid metabolism in the VAD animals. Here, ZL and ZF rats were fed a VAD diet for 8 weeks, and then ZL rats were refed a VAS diet for 3 or 7 days. We report that refeeding of a VAS diet for 3 or 7 days partially restored the hepatic expression levels of genes altered by VA deficiency in ZL rats.

Materials and methods

Reagents

The reagents for collecting plasma glucose were obtained from DiaSys Diagnostic Systems GmbH (Germany). The ELISA kits for insulin (#ml302840), leptin (#ml002969), and glucagon (#ml600102) were purchased from Shanghai Enzyme-linked Biotechnology Company (China). Reagents for cDNA synthesis, real-time PCR and other compounds were obtained from Shanghai Sangon Biotech Company (China).

Animals and diets

Male ZL (*fa*/+ or +/+) and ZF (*fa/fa*) rats were bred and maintained in the animal facility of the Taikang Medical Diagnosis Service (Hebei) Ltd. (Guan, Hebei, China). They were housed in colony cages in a temperature and humidity-controlled environment. The synthetic VAD and VAS diets were isocaloric and contained 4.05 kcal/g (1 cal = 4.184 J) diet, which had been used previously (23). The synthetic basal diet contained 18.3, 22.1, and 59.6% energy from protein,

fat (ether extract), and carbohydrate, respectively. Both diets had 10% (w/w) fat, in which the contents of total saturated, monounsaturated, and polyunsaturated fatty acids were 2.72, 3.31, and 3.42%, respectively. The VAS diet contained 22.1 IU VA/g diet, whereas the VAD diet contained 0 IU VA/g diet.

Two sets of experiments were conducted to evaluate the impacts of VA status on BW gain and metabolism in ZL and ZF rats. The first one was aimed to determine whether Zucker rats with different genotypes (+/+, +/*fa*, and *fa*/*fa*) and genders (male and female) respond differently to a VAD diet. Both male and female ZL (+/+ or *fa*/+) or ZF rats after weaning (3 weeks of age) were fed a VAD or a VAS diet for 8 weeks. Their BW and body length were measured weekly. The second experiment was aimed to determine whether refeeding of a VAS diet for 3 or 7 days will promote BW gain and restore the expression levels of hepatic genes involved in glucose and lipid metabolism. Here, ZL rats (+/+ and *fa*/+) after weaning were fed a VAD or VAS diet for 8 weeks. At the end of the 8-week feeding, the VAD rats were fed the VAS diet for 3 or 7 additional days. The 8-week protocol was sufficient to induce VA deficiency according to the original observation by McCollum and Davis (1913) (18) and our previous studies (21, 23). All animals were cared for in accordance with the Guide to the Care and Use of Experimental Animals (36). All procedures were approved by the Institutional Animal Care and Use Committee of Wuhan Puren Hospital (No.: 2020-10).

Genotyping

The genotypes of ZL (+/+ and *fa*/+) and ZF (*fa*/*fa*) rats were determined using a PCR based method as described in Durham et al. (37). In brief, a piece of ear tissue was obtained *via* punching, added to 75 μl of alkaline lysis buffer (25 mM NaOH/0.2 mM EDTA), and incubated at 95°C for 30 min to release genomic DNA. The lysate was mixed with 75 μl of 40 mM Tris–HCl buffer for neutralization and spun at 20,000 × *g* for 5 min to obtain supernatant, which was used as the template for PCR amplification. Each PCR reaction with a 25 μl volume contained 2.5 μl tissue lysate as the template, 2.5 μl 10 × PCR buffer, 2.5 μl 25 mM MgCl2, 1 μl 100 mM dNTP, 0.5 μl 5U/μl Taq DNA polymerase, 1 μl each of 10 μm forward (5′-CGTATGGAAGTCACAGA-3′) and reverse (5′GAATTCTCTAAATATTTCAGC-3′) primers, and 14 μl water. The reverse primer contains a single base substitution (C to G) at the 3′ end, which generates a *Pvu*II site in the wild type allele only. The PCR conditions were: 95°C for 5 min, and 40 cycles of 95°C for 30 s, 60°C for 30 s, and 72°C for 30 s. After that, 20 μl of the PCR product were digested in a 28 μl reaction containing 10 units of *Pvu*II at 37°C for 1 h, and subjected to gel electrophoresis in a 4% agarose gel with 10 mg/mL ethidium bromide and 0.5 × Tris-borate-EDTA buffer. The wildtype genotype (+/+), heterozygous (*fa*/+), and homozygous (*fa*/*fa*) genotypes showed the presence of one 80 bp band, 80 and 101 bp bands, and one 101 bp band, respectively.

Plasma and tissue sample collection and measurements

At the end of feeding, animals were fasted for 6 h after the diets were removed at around 7:00 AM, and euthanized under CO2 before tissue and plasma sample collections. Accumulated venous blood was collected into EDTA coated tubes and centrifugated at 2,000 ×*g* and 4°C for 20 min to obtain the plasma. The liver of both male and female rats, and two pads of epididymal white adipose tissue (WAT) of male rats was removed, weighted, and immediately frozen in liquid nitrogen. Tissue and plasma samples were stored at −80°C until be further processed. The plasma glucose level was determined using kits from DiaSys Diagnostic Systems GmbH (Germany) following the manufacture's manual. The plasma insulin, leptin and glucagon levels were measured using the ELISA kits according to the manufacture's manuals.

RNA extraction and real-time PCR

To extract total RNA, about 100 mg frozen rat liver sample was added to 1 ml of TRIzol reagent (#15596026, Thermo Fisher, Shanghai, China) according to the manufacture's protocol. Any contaminated DNA was removed using a DNA-free kit, and 2 μg of DNA-free RNA was used for the synthesis of cDNA. Each SYBR green based real-time PCR reaction in have a volume of 14 μl and contained cDNA reverse-transcribed from 14 ng of total RNA, 2.33 pmol forward and reverse primers, and 7 μl of 2 × SYBR Green PCR Master Mix (Applied Biosystems). The gene specific primers that will be provided upon request were used to amplify the corresponding cDNA, and some of them have been used previously (13, 14). PCR reactions in triplicates were carried out in 96-well plates using a 7300 Real-Time PCR system and were conducted as follow: 50°C for 2 min, 95°C for 10 min, followed by 40 cycles of 95°C for 15 s and 60°C for 1 min. The expression level of a particular gene was shown as -△ cycle threshold (CT) value by subtracting the CT value of 36B4 (an invariable control gene) from the CT value of the indicated gene.

Statistics analysis

SPSS 23.0 software was used for statistical analysis. Student's *t*-test with 95% confidence interval and one-way ANOVA with least significance difference *post-hoc* analysis tests were performed to compare two and more than two groups, respectively. If needed, natural log transformation

10.3389/fnut.2022.999323

was performed before analysis. Data were presented as means ± S.E.M. The *p*-value less than 0.05 was considered significantly different.

Results

Vitamin A deficiency reduced body weight gain and body fat in Zucker lean and Zucker fatty male rats

The effects of VA deficiency on ZL (+/+ or *fa*/+) or ZF (*fa*/*fa*) male rats were analyzed after they had been fed a VAD or a VAS diet for 8 weeks. As shown in **Table 1**, the initial BW of ZL male rats at weaning (3 weeks of age) fed a VAD diet was similar to that of the VAS group. At the end of the 8-week dietary treatment, VAD ZL male rats had significantly lower BW, body length, and BW gain than those of VAS rats ($P < 0.05$). In ZF male rats, the parameters of BW, length, and BW gain after 8 weeks followed the same trend as those in ZL rats ($P < 0.05$), demonstrating the reduced somatic growth when the rats were fed a VAD diet ($P < 0.05$). The liver weight, but not the liver/BW ratio, of the ZL male VAD rats was significantly lower than that of VAS rats. However, the liver/BW ratios in the ZF male rats were significantly different between VAD and VAS groups ($P < 0.05$). The WAT weight and the WAT/BW ratio of VAD male rats, regardless of lean or fatty, were all significantly lower than those of VAS rats ($P < 0.05$). All these data demonstrated that VA deficiency reduces the BW, liver weight and fat pad weight in male Zucker rats. There appears to be no difference between wild type (+/+) and heterozygous (+/*fa*) ZL male rats fed the VAD or VAS diet.

Vitamin A deficiency reduced body weight gain and body fat in Zucker lean and Zucker fatty female rats

To evaluate whether female Zucker rats respond to the change of VA status, ZL and ZF female rats were fed a VAD or VAS diet for 8 weeks. **Table 2** shows their BW, body length and liver weight, and liver/BW ratio of ZL (+/+ and *fa*/+) and ZF (*fa*/*fa*) female rats. Since female rats do not have epididymal fat, we did not have fat data. Different from that of the ZL male rats, values of body length of ZL female rats were similar between VAD and VAS groups. The difference in body length between VAD and VAS groups was only observed in ZF female rats ($P < 0.05$). The liver weight in VAD female rats, but not the liver/BW ratio, was still significantly lower than their corresponding VAS female rats in the same genotype. As in the ZL male rats, no difference was observed between wild type (+/+) and heterozygous (*fa*/+) ZL female rats fed the VAD or VAS diet.

TABLE 1 Body weight (BW), length, liver weight, white adipose tissue (WAT) weight, liver/BW ratio, WAT/BW ratio, and BW gain in male+/+, *fa*/+, and *fa*/*fa* Zucker rats fed a vitamin A deficient (VAD) or vitamin A sufficient (VAS) diet for 8 weeks.

Genotype	Diets (*n*)	Start BW (g)	End BW (g)	BW gain (g)	Length (cm)	Liver (g)	WAT (g)	Liver/BW	WAT/BW
+/+	VAD (7)	36.0 ± 4.2	170.8 ± 33.6a	134.8 ± 32.0a	34.9 ± 2.6	5.7 ± 0.7	0.70 ± 0.3a	0.034 ± 0.008a/b	0.004 ± 0.002a/b
	VAS (5)	32.9 ± 5.6	294.1 ± 29.5a′,*	261.3 ± 24.8a′,*	38.2 ± 1.4*	8.9 ± 0.9a′,*	3.10 ± 0.9a′,*	0.030 ± 0.003a′	0.010 ± 0.003a′,*
fa/+	VAD (8)	37.1 ± 4.7	166.1 ± 32.7a	129.0 ± 29.1a	34.9 ± 3.4	5.7 ± 0.6	0.59 ± 0.4 a	0.035 ± 0.006b	0.003 ± 0.002a
	VAS (8)	35.8 ± 5.6	254.5 ± 45.5a′*	218.7 ± 46.9a′,*	37.3 ± 2.2	8.7 ± 1.3a′,*	2.51 ± 0.8a′,*	0.035 ± 0.009b′	0.010 ± 0.002a′,*
fa/*fa*	VAD (7)	36.5 ± 2.3	244.9 ± 33.6b	208.5 ± 33.6 b	34.6 ± 1.59	6.6 ± 1.7	3.86 ± 3.8 b	0.027 ± 0.006a	0.014 ± 0.013b
	VAS (8)	37.2 ± 5.6	445.4 ± 38.6b′*	408.1 ± 38.3b′*	37.2 ± 5.6*	17.2 ± 1.8b′,*	15.1 ± 1.24b′,*	0.039 ± 0.003b′,*	0.034 ± 0.003b′,*

BW, body weight; cm, centimeters; g, grams; VAD, vitamin A deficient; VAS, vitamin A sufficient; WAT, epididymal white adipose tissue; *n*, animal number in the indicated group. *For comparing VAD with VAS in the same genotype using student's *t*-test; a < b, a′ < b′ for comparing the different genotypes within the same diet using one way ANOVA; All $P < 0.05$.

TABLE 2 Body weight (BW), body length, liver weight, liver/BW ratio, and BW gain in female +/+, *fa*/+, and *fa/fa* Zucker rats fed a vitamin A deficient (VAD) or vitamin A sufficient (VAS) diet for 8 weeks.

Genotype	Diets (*n*)	Start BW (g)	End BW (g)	BW gain (g)	Length (cm)	Liver (g)	Liver/BW
+/+	VAD (8)	33.0 ± 2.9	128.8 ± 21.3a	93.8 ± 20.7a	32.4 ± 3.1	4.7 ± 0.6	0.038 ± 0.008
	VAS (5)	34.3 ± 6.7	180.1 ± 18.3a′, *	145.8 ± 17.9a′, *	33.9 ± 1.5	6.1 ± 0.9a′, *	0.034 ± 0.003a′
fa/+	VAD (8)	33.7 ± 3.3	139.9 ± 26.8a	106.3 ± 25.8a	32.4 ± 2.3	4.8 ± 0.5	0.035 ± 0.006
	VAS (8)	35.4 ± 4.5	175.1 ± 19.0a′, *	139.7 ± 17.3a′, *	32.9 ± 3.2	6.9 ± 0.4a′, *	0.040 ± 0.005b′, *
fa/fa	VAD (8)	36 ± 2.8	238.3 ± 66.4b	202.3 ± 63.8b	31.3 ± 2.9	7.0 ± 0.8	0.031 ± 0.007
	VAS (7)	31.0 ± 3.4*	336.8 ± 60.8b′, *	305.8 ± 59.4b′, *	34.6 ± 2.0*	11.4 ± 1.5b′, *	0.034 ± 0.004a′

BW, body weight; cm, centimeters; g, grams; VAD, vitamin A deficient; VAS, vitamin A sufficient; *n*, animal number in the indicated group. *For comparing VAD with VAS in the same genotype using student's *t*-test; a < b, a′ < b′ for comparing the different genotypes within the same diet using one way ANOVA; All $P < 0.05$.

As for female rats fed the VAD or VAS diet, end BW and BW gain in ZL (+/+, *fa*/+) rats were obviously lower than that in ZF (*fa/fa*) rats, presenting similar trend as male ones ($P < 0.05$). The liver weight of ZF female rats fed the VAS diet was higher (11.4 g) than that of +/+ and *fa*/+ ZL rats (6.1 and 6.9 g, respectively). Interestingly, the live/BW ratio of heterozygous ZL (*fa*/+) female rats (0.040) was higher than that of ZF (*fa/fa*) female rats (0.034). All results indicate for the first time that ZL (+/+ and *fa*/+) and ZF female rats responded to the VAD diet largely like those male ones.

Refeeding of a vitamin A sufficient diet for 3 or 7 days increased body weight in Zucker lean male rats

As stated in our previous results, the responses to VAD or VAS are largely similar between male and female rats. Therefore, in order to determine the effects of refeeding of a VAS diet on the BW regain, ZL (+/+ and *fa*/+) male rats after weaning (3 weeks old) only were selected and then fed a VAS or a VAD diet for 8 weeks. After that, the VAD rats were refed the VAS diet for 3 or 7 days. As shown in Figure 1, ZL male rats fed a VAD diet grew at a similar rate as those fed a VAS diet did for the first 2 weeks. Starting from the week 3 (21 days), ZL male rats fed a VAD diet gained significantly less BW than those fed a VAS diet did ($P < 0.05$). After on the diets for 4 weeks (28 days), the BW values of rats in the VAD and VAD-VAS7d groups were lower than that of VAD-VAS3d and VAS groups (&). After on the diets for 5 weeks (35 days), the BW values of rats in the VAD and VAD-VAS7d groups were lower than that in the VAS group, and that in the VAD group were lower than that in the VAD-VAS3d group (#). After on the diets for 6 (42 days) to 8 weeks (56 days), the BW values of rats in the VAS group were higher than that in the VAD-VAS3d and VAD-VAS7d groups, and that in the VAD group were lower than that in VAD-VAS3d group (^). The BW values of ZL rats fed the VAD diet peaked at the sixth week, and started to drop after that. The BW of ZL rats fed the VAS diet continued to rise throughout the 8-week study period ($P < 0.05$). The BW of the ZL rats in the VAD-VAS-3d group were higher than that of VAD and VAD-VAS-7d group at week 4 ($P < 0.05$). When the VAS diet was refed to the VAD rats, the ZL rats in VAD-VAS3d and VAD-VAS7d groups started to gain significant amount of BW at 3 (59 days) and 7 (63 days) days comparing with that at the end of the 8-week (56 days) feeding of the VAD diet (**). These results demonstrate that restoration of VA in the diet promoted BW gain in ZL rats.

Refeeding of a vitamin A sufficient diet for 3 or 7 days increased plasma glucose, insulin, and leptin levels

Plasma glucose, insulin, leptin, and glucagon levels were measured in ZL rats fed a VAS or a VAD diet for 8 weeks, or those fed a VAD diet and followed by the VAS diet for 3 (VAD-VAS3d) or 7 (VAD-VAS7d). Table 3 shows that VAD ZL rats had

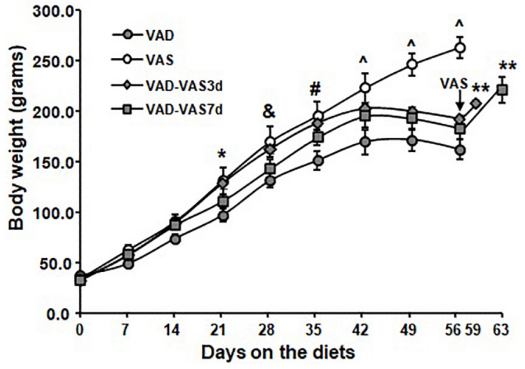

FIGURE 1
The body weight (BW) of Zucker lean (ZL) rats fed a vitamin A sufficient (VAS), a vitamin A deficient (VAD) diet for 8 weeks, or those fed a VAD diet for 8 weeks and followed by the VAS diet for 3 (VAD-VAS3d) or 7 (VAD-VAS7d). Mean ± SEM, *n* = 8 for each group; * For VAD < VAS, & for VAD/VAD-VAS7d < VAD-VAS3d/VAS; # for VAD and VAD-VAS7d < VAS and VAD < VAD-VAS3d, ^VAD < VAD-VAS3d < VAS and VAD-VAS7d < VAS using one way ANOVA; ** for comparing VAD-VAS3d or VAD-VAS7d at the indicated date with the BW of the group at 56 days (8 weeks).

10.3389/fnut.2022.999323

TABLE 3 Plasma glucose, insulin, leptin, and glucagon in Zucker lean (ZL) rats fed a vitamin A sufficient (VAS) or a vitamin A deficient (VAD) diet for 8 weeks, or those fed a VAD diet and followed by the VAS diet for 3 (VAD-VAS3d) or 7 (VAD-VAS7d).

Diets	Glucose (mg/dL)	Insulin (ng/mL)	Leptin (ng/mL)	Glucagon (pg/mL)
VAD	70.88 ± 9.06*	0.30 ± 0.08*	0.61 ± 0.23*	121.61 ± 77.09
VAS	100.25 ± 5.60	1.57 ± 0.75a	2.48 ± 2.47	171.08 ± 210.67
VAD + VAS 3 days	102.43 ± 9.38	0.68 ± 0.20	1.39 ± 0.94	67.47 ± 19.02
VAD + VAS 7 days	97.71 ± 8.28	0.66 ± 0.16	1.36 ± 0.57	65.43 ± 19.21

Plasma glucose, insulin, leptin, and glucagon were measured in ZL rats fed a VAS or a VAD diet for 8 weeks, or those fed a VAD diet and followed by the VAS diet for 3 (VAD-VAS3d) or 7 (VAD-VAS7d). Mean ± SEM, $n = 8$ for each group; *$P < 0.05$, as compared with VAS, VAD-VAS 3 days and VAD-VAS 7 days; a $P < 0.05$, for comparing with VAD-VAS 3 days, VAD-VAS 7 days.

lower plasma glucose, insulin, and leptin levels than the VAS ZL rats. The refeeding of the VAS diet for 3 or 7 days respectively increased the plasma levels of glucose, insulin, and leptin in ZL rats of the VAD-VAS3d and VAD-VAS7d groups significantly in comparison with that of the VAD group ($P < 0.05$). There was a trend of reduction of plasma glucagon levels in rats of the VAD-VAS3d and VAD-VAS7d groups in comparison with that of VAD and VAS groups, but did not reach statistical significance, probably due to large variations of the data. The increases in plasma insulin, leptin and glucose levels demonstrate that VA sufficiency promotes anabolism.

Refeeding of a vitamin A sufficient diet for 3 or 7 days partially recovered the hepatic expression levels of genes involved in vitamin A, glucose, and lipid metabolism

We next compared the hepatic mRNA levels of *Cyp26a1* (cytochrome P450 26a1 gene as an indicator of VA status), *Gck* (glucokinase gene in glycolysis), *Fas* (fatty acid synthase gene in the lipogenic pathway), *Me* (malic enzyme gene for the production of NADPH), *Acc1* (acetyl-CoA carboxylase gene in the lipogenic pathway), *Srebp-1c* (a key gene in lipogenesis), *G6pc* (Glucose-6-phosphatase catalytic subunit gene in the gluconeogenic pathway), *Pck1* (phosphoenolpyruvate carboxykinase gene in the gluconeogenic pathway), *Igfbp1* (Insulin-like growth factor-binding protein-1 gene for the binding of insulin-like growth factor 1), and *Igf1* Insulin-like growth factor 1 gene for the regulation of growth and metabolism) in ZL male rats of the VAD, VAS, VAD + VAS3d, and VAD + VAS7d groups. As shown in **Figure 2**, the hepatic expression level of *Cyp26a1* in ZL rats of the VAD group was significantly lower than that of VAS, VAD-VAS3d, and VAD-VAS7d, showing the improvement of VA status after refeeding of the VAS diet for 3 and 7 days in VAD-VAS3d and VAD-VAS7d groups. The expression level of *Gck* mRNA followed the same trend.

The hepatic expression level of *Fas* mRNA in the VAD-VAS7d, but not that in the VAS and VAD-VAS3d groups, was higher than that in the VAD group, suggesting the increase in the hepatic fatty acid synthesis after feeding the VAS diet for 7 days. Interestingly, the hepatic levels of *Me* mRNA in the VAS group was significantly higher than that VAD, VAD-VAS3d, and VAD-VAS7d groups, which are not different among them. The hepatic levels of *Acc1* and *Srebp-1c* mRNA in the VAS group were higher than that in the VAD group, which was not changed after refeeding of the VAS diet in the VAD-VAS3d and VAD-VAS-7d groups.

The expression levels of *G6pc* mRNA were not different among the four groups. The *Pck1* mRNA level in the VAD group was higher than that in the VAD-VAS3d group, but not different from that in the VAS and VAD-VAS7d groups. The *Igfbp1* mRNA level in the VAD group was significantly higher than that in the VAS, VAD-VAS3d, and VAD-VAS7d groups, showing the impacts of the VA status on metabolism. The *Igf1* mRNA levels in the VAD and VAD-VAS3d groups were lower than that in the VAS and VAD-VAS7d groups, showing that it took 7 days to restore the *Igf1* expression in the liver.

Refeeding of a vitamin A sufficient diet for 3 or 7 days partially recovered the hepatic expression levels of nuclear receptors responsible for vitamin A signaling

To determine whether the restoration of VA status affects the expression levels of nuclear receptors involved in mediating RA signaling and regulating glucose and fatty acid metabolism, we compared the hepatic mRNA levels of *Rara* (retinoic acid receptor alpha gene), *Rarb* (retinoic acid beta gene), *Rxra* (retinoid X receptor alpha gene), *Rxrb* (retinoid X receptor beta gene), *Rxrg* (retinoid X receptor gamma gene), *Ppargc1a* (peroxisome proliferator-activated receptor gamma coactivator 1 alpha gene), *Ppara* (peroxisome proliferator-activated receptor alpha gene), *Pparg* (peroxisome proliferator-activated receptor gamma gene), and *Ppard* (peroxisome proliferator-activated receptor delta gene), of the ZL rats in the four dietary groups. As shown in **Figure 3**, the hepatic levels of *Rara* mRNA in the VAD and VAS groups were not different, whereas that in the

10.3389/fnut.2022.999323

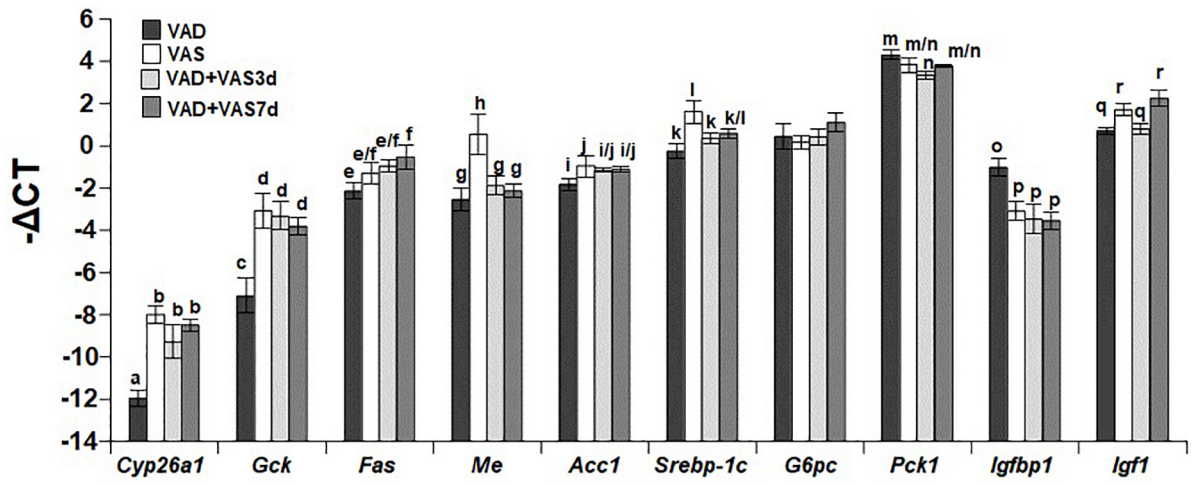

FIGURE 2
The hepatic mRNA levels of *Cyp26a1, Gck, Fas, Me, Acc1, Srebp-1c, G6pc, Pck1, Igfbp1,* and *Igf1* in Zucker lean (ZL) rats fed the vitamin A deficient (VAD) for 8 weeks, the vitamin A sufficient (VAS) diet for 8 weeks, or fed the VAD diet for 8 weeks followed by the VAS diet for 3 (VAD + VAS3d) or 7 (VAD + VAS 7d) days. Data are presented as mean ± SEM of minus delta Ct (cycle threshold); *n* = 7, 5, 5, and 5 for the VAD, VAS, VAD-VAS3d, and VAD-VAS7d, respectively; a < b for *Cyp26a1* (cytochrome P450 26a1), c < d for *Gck* (glucokinase), e < f for *Fas* (fatty acid synthase), g/h for *Me* (malic enzyme), i < j for *Acc1* (acetyl CoA carboxylase alpha), k < l for *Srebp-1c* (sterol regulatory element-binding protein 1c), m > n for *Pck1* (cytosolic form of phosphoenolpyruvate carboxykinase), o > p for *Igfbp1* (insulin like growth factor-binding protein 1), q < r for *Igf1* (insulin-like growth factor 1); all $P < 0.05$.

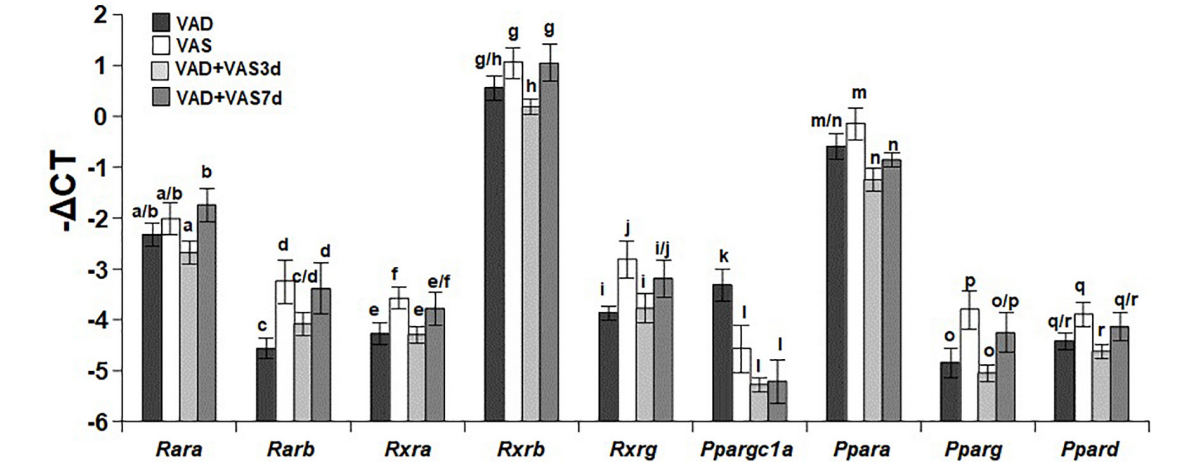

FIGURE 3
The hepatic mRNA levels of *Rara, Rarb, Rxra, Rxrb, Rxrg, Ppargc1a, Ppara, Pparg,* and *Ppard* in Zucker lean (ZL) rats fed a vitamin A deficient (VAD) or vitamin A sufficient (VAS) diet for 8 weeks or fed a VAD diet for 8 weeks and fed a VAS diet for 3 (VAD + VAS 3d) or 7 (VAD + VAS 7d) days. Data are presented as mean ± SEM of minus delta Ct (cycle threshold); *n* = 7, 5, 5, and 5 for the VAD, VAS, VAD-VAS3d, and VAD-VAS7d, respectively; a < b for *Rara* (retinoic acid receptor alpha), c < d for *Rarb* (Retinoic acid receptor beta), e < f for *Rxra* (rexinoid X receptor alpha), g > h for *Rxrb* (rexinoid X receptor beta), i < j for *Rxrg* (rexinoid X receptor gamma), k > l for *Ppargc1a* (peroxisome proliferative activated receptor gamma coactivator 1 alpha), m > n for *Ppara* (peroxisome proliferative activated receptor alpha), o < p for *Pparg* (peroxisome proliferative activated receptor gamma), q > r for *Ppard* (peroxisome proliferative activated receptor delta or beta).

VAD-VAS7d group was higher than that in the VAD-VAS3d group. The level of *Rarb* mRNA in the VAS group was higher than that in the VAD group, which was restored by the feeding of the VAS diet for 7, but not 3 days (c < d). The mRNA levels of *Rxra, Rxrg, Pparg* and *Ppard* in the VAS group were higher than that in the VAD and VAD-VAS3d groups, whereas that in the VAD-VAS7d group had a trend to return, but did not reach statistical significance. The mRNA levels of *Rxrb* in the VAS and VAD-VAS7d groups were higher than that in the VAD-VAS3d group. The mRNA level of *Ppargc1a* in the VAD group was higher than that in VAS, VAD-VAS3d, and VAD-VAS7d groups. The mRNA level of *Ppara* in the VAS

group was higher than that in the VAD-VAS3d and VAD-VAS7d groups.

Discussion

Here, we evaluated the effects of VA status on the BW gain in wild type (+/+), heterozygous (*fa*/+), and homozygous (*fa/fa*) Zucker rats of both genders, and the expression levels of hepatic genes in response to the refeeding of a VAS diet for 3 and 7 days in ZL male rats. We observed that VA deficiency leads to less BW gain in +/+, *fa*/+, and *fa/fa* rats of both genders. In addition, the refeeding of a VAS diet to VAD ZL male rats partially restored the expression levels of hepatic genes involved in metabolic controls.

We have shown previously that ZL and ZF male rats fed a VAD diet have lower BW than those fed a VAS diet for 8 weeks (21–24). This is the first time that the responses of female ZL (+/+ and *fa*/+) and ZF rats to a VAD diet were presented. Generally, the responses of female Zucker rats to the VAD diet like those of the male ones. The responses of BW and liver weight of +/+ and *fa*/+ female rats to VA deficiency do not differ from each other in either VAD or VAS condition, indicating the equivalence of the wild type and heterozygous ZL rats regarding the VA status.

Therefore, male ZL rats with both +/+ and *fa*/+ genotypes were used in the VAS refeeding experiment after they were weaned (3 weeks of age). Male ZL rats were fed the VAD diet for 8 weeks, and then those VAD rats were fed a VAS diet for 3 or 7 days. The refeeding of a VAS diet for 3 or 7 days is sufficient to increase the BW of those VAD rats significantly. What is noteworthy, we also noticed that ZL rats assigned to the VAD-VAS-3d had higher BW than the VAD and VAD-VAS-7d groups at certain time points, showing their slightly differential responses to the VAD diet during the course to develop VA deficiency. We attributed this difference to the variations of the original VA storage in ZL rats at weaning as they were derived from different breeding pairs, mothers with slightly different nutritional status and age. It is difficult to obtain animals with the same VA status at weaning, which is why we designed an 8-week protocol to ensure the animals in VAD groups to reach VA deficiency. Nevertheless, the BW gain of ZL rats in all three VAD groups stopped at round 6 weeks, demonstrating the success of VA deficiency. This served our original purpose to induce VA deficiency before the replenishment. The BW gain started to increase when the dietary VA became available, demonstrating clearly that VA plays an anabolic role in rats.

We have shown previously that the flux of dietary VA induces the expression of hepatic genes responsible for lipogenesis, such as *Gck* and *Srebp-1c* in the VAD ZL rats fed a VAS, but not a VAD diet (24). This occurs 6 h later after the intake of a VAS diet in the VAD ZL rats (24). Interestingly, in the current experimental setting, the expression levels of *Gck*, but not *Srebp-1c*, *Me* and *Acc1*, mRNA levels in the ZL VAD rats fed the VAS diet for 3 or 7 days were returned to that of the VAS rats. The *Fas* mRNA level in VAD-VAS7d, but not VAD-VAS3d, group is significantly higher than that in the VAD group. All these indicate that the presence of VA for 3 or 7 days in those VAD rats increase certain, but not all, mRNA levels of genes whose expression levels have been altered due to the VAD status.

Here, we demonstrate that the feeding of a VAS diet to the VAD rats restores their hepatic gene expression profile toward that of the VAS rats differentially. For certain genes such as *Cyp26a1, Gck, ppargc1a,* and *Igfbp1*, a 3-day refeeding of a VAS diet is sufficient, whereas for others such as *Rarb* and *Rxrb*, it took 7 days. As far as we know, this is the first time that the expression levels of genes involved in the hepatic glucose, and lipid metabolism are measured after VA returns to the body. Regarding the transcription factors and cofactors, the changes of *Ppargc1a* is similar to that of *Gck* and *Igfbp1*. On the other hand, the expression levels of *Rarb* and *Rxrb* in the VAD-VAS7d, but not VAD-VAS3d, group returned to level of the VAS group, which is similar to that of *Igf1*. It has been known that the binding of IGFBP-1 to IGF1 could reduce the IGF-1's action in metabolism during fasting (38). Our data show that the hepatic mRNA levels of *Igfbp-1* and *Igf1* are regulated differentially by the VA status. Actually, the hepatic *Igfbp-1* mRNA expression is regulated by insulin (39). The hepatic *Igfbp-1* mRNA is independent of circulating IGF-1 in humans. It is reasonable as there are other IGFBPs (40).

All these results show that the mRNA levels of those genes in the VAD rats return to the levels of VAS rats at different paces. For some of them, refeeding of a VAS diet for 3 days is sufficient. However, for others, the refeeding of a VAS for 7 days might not even enough. Whether this phenomenon is caused by the change of VA metabolism after the return of VA in the body or due to any permanent change of the gene expression due to VA deficiency remains to be answered. Future experiments with longer refeeding of a VAS diet are needed to answer this question.

We have also shown that VA status regulates the respiratory exchange ratio in ZL rats (24). It will be interesting to see how many days is sufficient for the VAD rats after refed a VAS diet to increase the anabolism as those VAS rats. Whether returning to a normal anabolism precedes the gene expression changes or after the recovery of the gene expression is an excellent future project.

Our current project has some limitations. First, we did not include groups with longer refeeding time of the VAS diet to show whether the expression levels of those genes changed by VA deficiency really can recover or not. This can be done in the future. Second, we only tested the refeeding in ZL rats, but not ZF rats. It will be interesting to see whether the reduced BW or the correction of obesity in VAD ZF rats is a transient phenomenon due to VA deficiency or a permanent change. Third, we only measured the hepatic gene expression due to limited resources. It will be interesting to see whether the gene

expression levels also change in other tissues such as fat. This can be done in the future as well.

Conclusion

In summary, both female and male ZL and ZF rats fed a VAD diet have lower BW gain, and liver mass than that fed a VAS diet, clearly demonstrating the role of VA in anabolism. Refeeding of a VAS diet in VAD ZL rats is sufficient to restore BW gain and partial expressions of genes affected by VA deficiency. These data demonstrated that the VAD rats are excellent molecular nutrition models to study the effects of VA on glucose and lipid metabolism after reintroducing VA in the animal body. They will certainly help our understanding of gene regulation *in vivo* and underlying mechanisms by which overnutrition leads to the development of metabolic diseases such as obesity and T2D.

Data availability statement

The original contributions presented in this study are included in the article/supplementary material, further inquiries can be directed to the corresponding author.

Ethics statement

This animal study was reviewed and approved by Institutional Animal Care and Use Committee of Wuhan Puren Hospital (No.: 2020-10).

Author contributions

YZ and KT contributed equally to this study as co-first authors. KT contributed to manuscript writing and data analyses. YZ and GC contributed to design the study and final revision of the manuscript. All authors have read and approved the submission.

Funding

The authors thank the Scientific Research Project of Wuhan Municipal Health Commission for research support to YZ (Number: WX19Y09).

Conflict of interest

The authors declare that the research was conducted in the absence of any commercial or financial relationships that could be construed as a potential conflict of interest.

Publisher's note

All claims expressed in this article are solely those of the authors and do not necessarily represent those of their affiliated organizations, or those of the publisher, the editors and the reviewers. Any product that may be evaluated in this article, or claim that may be made by its manufacturer, is not guaranteed or endorsed by the publisher.

References

1. Saeedi P, Petersohn I, Salpea P, Malanda B, Karuranga S, Unwin N, et al. Global and regional diabetes prevalence estimates for 2019 and projections for 2030 and 2045: Results from the International Diabetes Federation Diabetes Atlas, 9(th) edition. *Diabetes Res Clin Pract.* (2019) 157:107843. doi: 10.1016/j.diabres.2019.107843

2. Williams R, Karuranga S, Malanda B, Saeedi P, Basit A, Besançon S, et al. Global and regional estimates and projections of diabetes-related health expenditure: Results from the International Diabetes Federation Diabetes Atlas, 9th edition. *Diabetes Res Clin Pract.* (2020) 162:108072. doi: 10.1016/j.diabres.2020.108072

3. Pardue SL. Food, energy, and the environment. *Poult Sci.* (2010) 89:797–802. doi: 10.3382/ps.2009-00565

4. Ross AC. Retinoid production and catabolism: role of diet in regulating retinol esterification and retinoic acid oxidation. *J Nutr.* (2003) 133:291S–6S. doi: 10.1093/jn/133.1.291S

5. Blomhoff R, Blomhoff HK. Overview of retinoid metabolism and function. *J Neurobiol.* (2006) 66:606–30.

6. Li R, Zhang R, Li Y, Zhu B, Chen W, Zhang Y, et al. A RARE of hepatic *Gck* promoter interacts with RARa, HNF4a and COUP-TFII that affect retinoic acid- and insulin-induced *Gck* expression. *J Nutr Biochem.* (2014) 25:964–76. doi: 10.1016/j.jnutbio.2014.04.009

7. Zhang R, Wang Y, Li R, Chen G. Transcriptional factors mediating retinoic acid signals in the control of energy metabolism. *Int J Mol Sci.* (2015) 16:10210–44.

8. Wang Y, Zolfaghari R, Ross A. Cloning of rat cytochrome P450RAI (CYP26) cDNA and regulation of its gene expression by all-trans-retinoic acid in vivo. *Arch Biochem Biophys.* (2002) 401:235–43. doi: 10.1016/S0003-9861(02)00043-7

9. Blaner WS. Vitamin A signaling and homeostasis in obesity, diabetes, and metabolic disorders. *Pharmacol Ther.* (2019) 197:153–78. doi: 10.1016/j.pharmthera.2019.01.006

10. Chen W, Chen G. The roles of vitamin a in the regulation of carbohydrate, lipid, and protein metabolism. *J Clin Med.* (2014) 3:453–79.

11. McGarry JD. Banting lecture 2001: dysregulation of fatty acid metabolism in the etiology of type 2 diabetes. *Diabetes.* (2002) 51:7–18. doi: 10.2337/diabetes.51.1.7

12. Brown MS, Goldstein JL. Selective versus total insulin resistance: a pathogenic paradox. *Cell Metab.* (2008) 7:95–6. doi: 10.1016/j.cmet.2007.12.009

13. Chen G. Liver lipid molecules induce PEPCK-C gene transcription and attenuate insulin action. *Biochem Biophys Res Commun.* (2007) 361:805–10. doi: 10.1016/j.bbrc.2007.07.108

14. Chen G, Zhang Y, Lu D, Li N, Ross AC. Retinoids synergize with insulin to induce hepatic *Gck* expression. *Biochem J.* (2009) 419:645–53.

15. Li R, Chen W, Li Y, Zhang Y, Chen G. Retinoids synergized with insulin to induce *Srebp-1c* expression and activated its promoter via the two liver X receptor binding sites that mediate insulin action. *Biochem Biophys Res Commun.* (2011) 406:268–72. doi: 10.1016/j.bbrc.2011.02.031

16. Chen G, Liang G, Ou J, Goldstein JL, Brown MS. Central role for liver X receptor in insulin-mediated activation of *Srebp-1c* transcription and stimulation of fatty acid synthesis in liver. *Proc Natl Acad Sci USA*. (2004) 101:11245–50. doi: 10.1073/pnas.0404297101

17. Zhang Y, Li R, Chen W, Li Y, Chen G. Retinoids induced *Pck1* expression and attenuated insulin-mediated suppression of its expression via activation of retinoic acid receptor in primary rat hepatocytes. *Mol Cell Biochem.* (2011) 355:1–8. doi: 10.1007/s11010-011-0831-4

18. McCollum EV, Davis M. The necessity of certain lipins in the diet during growth. *J Biol Chem.* (1913) 15:167–75. doi: 10.1111/j.1753-4887.1973.tb07065.x

19. Wolf G, Lane MD, Johnson BC. Studies on the function of vitamin A in metabolism. *J Biol Chem.* (1957) 225:995–1008.

20. Singh M, Singh VN, Venkitasubramanian TA. Early effects of feeding excess vitamin A: Hepatic glycogen, blood lactic acid, plasma nefa and glucose tolerance in rats. *Life Sci.* (1968) 7:239–47. doi: 10.1016/0024-3205(68)90197-5

21. Chen W, Howell M, Li Y, Li R, Chen G. Vitamin A and feeding statuses modulate the insulin-regulated gene expression in Zucker lean and fatty primary rat hepatocytes. *PLoS One.* (2014) 9:e100868. doi: 10.1371/journal.pone.0100868

22. Li Y, Liu Y, Chen G. Vitamin A status affects the plasma parameters and regulation of hepatic genes in streptozotocin-induced diabetic rats. *Biochimie.* (2017) 137:1–11. doi: 10.1016/j.biochi.2017.02.012

23. Zhang Y, Li R, Li Y, Chen W, Zhao S, Chen G. Vitamin A status affects obesity development and hepatic expression of key genes for fuel metabolism in Zucker fatty rats. *Biochem Cell Biol.* (2012) 90:548–57. doi: 10.1139/o2012-012

24. Li Y, Li R, Chen W, Chen G. Vitamin A status and its metabolism contribute to the regulation of hepatic genes during the cycle of fasting and refeeding in rats. *J Nutr Biochem.* (2016) 30:33–43. doi: 10.1016/j.jnutbio.2015.11.012

25. Wang T, Tang X, Hu X, Wang J, Chen G. Reduction in the Dietary VA Status Prevents Type 2 Diabetes and Obesity in Zucker Diabetic Fatty Rats. *Biomolecules.* (2022) 12:528. doi: 10.3390/biom12040528

26. Zucker L, Zucker T. Fatty, a new mutation in the rat. *J Hered.* (1961) 52:275–8.

27. Iida M, Murakami T, Ishida K, Mizuno A, Kuwajima M, Shima K. Substitution at Codon 269 (Glutamine –> Proline) of the Leptin Receptor (OB-R) cDNA Is the Only Mutation Found in the Zucker Fatty (*fa/fa*) Rat. *Biochem Biophys Res Commun.* (1996) 224:597–604. doi: 10.1006/bbrc.1996.1070

28. Li Y, Zhang Y, Li R, Chen W, Howell M, Zhang R, et al. The Hepatic Raldh1 Expression Is elevated in Zucker Fatty Rats and Its Over-Expression Introduced the Retinal-Induced *Srebp-1c* Expression in INS-1 Cells. *PLoS One.* (2012) 7:e45210. doi: 10.1371/journal.pone.0045210

29. Ziouzenkova O, Orasanu G, Sharlach M, Akiyama TE, Berger JP, Viereck J, et al. Retinaldehyde represses adipogenesis and diet-induced obesity. *Nat Med.* (2007) 13:695–702.

30. Shah M, Vasandani C, Adams-Huet B, Garg A. Comparison of nutrient intakes in South Asians with type 2 diabetes mellitus and controls living in the United States. *Diabetes Res Clin Pract.* (2018) 138:47–56. doi: 10.1016/j.diabres.2018.01.016

31. Basualdo CG, Wein EE, Basu TK. Vitamin A (retinol) status of first nation adults with non-insulin-dependent diabetes mellitus. *J Am Coll Nutr.* (1997) 16:39–45. doi: 10.1080/07315724.1997.10718647

32. Olsen T, Blomhoff R. Retinol, retinoic acid, and retinol-binding protein 4 are differentially associated with cardiovascular disease, Type 2 diabetes, and obesity: an overview of human studies. *Adv Nutr (Bethesda, Md.).* (2020) 11:644–66. doi: 10.1093/advances/nmz131

33. Zhang Y, Wang T, Hu X, Chen G. Vitamin A and Diabetes. *J Med Food.* (2020) 24:11. doi: 10.1089/jmf.2020.0147

34. Nizamutdinova IT, Guleria RS, Singh AB, Kendall JA Jr., Baker KM, Pan J. Retinoic acid protects cardiomyocytes from high glucose-induced apoptosis through inhibition of NF-κB signaling pathway. *J Cell Physiol.* (2013) 228:380–92. doi: 10.1002/jcp.24142

35. Manolescu DC, Sima A, Bhat PV. All-trans retinoic acid lowers serum retinol-binding protein 4 concentrations and increases insulin sensitivity in diabetic mice. *J Nutr.* (2010) 140:311–6. doi: 10.3945/jn.109.115147

36. Council NR. *Guide for the Care and Use of Laboratory Animals*. Eighth ed. Washington, DC: The National Academies Press (2011). 246 p.

37. Durham HA, Truett GE. Development of insulin resistance and hyperphagia in Zucker fatty rats. *Am J Physiol Regul Integr Comp Physiol.* (2006) 290:R652–8. doi: 10.1152/ajpregu.00428.2004

38. Allard JB, Duan C. IGF-Binding Proteins: Why Do They Exist and Why Are There So Many? *Front Endocrinol (Lausanne).* (2018) 9:117. doi: 10.3389/fendo.2018.00117

39. Mounier C, Dumas V, Posner BI. Regulation of hepatic insulin-like growth factor-binding protein-1 gene expression by insulin: central role for mammalian target of rapamycin independent of forkhead box O proteins. *Endocrinology.* (2006) 147:2383–91. doi: 10.1210/en.2005-0902

40. Stanley TL, Fourman LT, Zheng I, McClure CM, Feldpausch MN, Torriani M, et al. Relationship of IGF-1 and IGF-Binding Proteins to Disease Severity and Glycemia in Nonalcoholic Fatty Liver Disease. *J Clin Endocrinol Metab.* (2021) 106:e520–33.

frontiers | Frontiers in Nutrition

TYPE Review
PUBLISHED 19 October 2022
DOI 10.3389/fnut.2022.1002574

OPEN ACCESS

EDITED BY
Fanbin Kong,
University of Georgia, United States

REVIEWED BY
Xuebing Xu,
Wilmar (Shanghai) Biotechnology Research & Development Center Co., Ltd., China
Qi Hu,
University of Florida, United States

*CORRESPONDENCE
Fang Yang
fangy521@hbtcm.edu.cn

SPECIALTY SECTION
This article was submitted to Nutrition and Metabolism, a section of the journal Frontiers in Nutrition

RECEIVED 25 July 2022
ACCEPTED 26 September 2022
PUBLISHED 19 October 2022

CITATION
Yang F and Chen G (2022) The nutritional functions of dietary sphingomyelin and its applications in food.
Front. Nutr. 9:1002574.
doi: 10.3389/fnut.2022.1002574

The nutritional functions of dietary sphingomyelin and its applications in food

Fang Yang[1]* and Guoxun Chen[2]

[1]School of Laboratory Medicine, Hubei University of Chinese Medicine, Wuhan, China, [2]Department of Nutrition, The University of Tennessee, Knoxville, TN, United States

Sphingolipids are common structural components of cell membranes and are crucial for cell functions in physiological and pathophysiological conditions. Sphingomyelin and its metabolites, such as sphingoid bases, ceramide, ceramide-1-phosphate, and sphingosine-1-phosphate, play signaling roles in the regulation of human health. The diverse structures of sphingolipids elicit various functions in cellular membranes and signal transduction, which may affect cell growth, differentiation, apoptosis, and maintain biological activities. As nutrients, dietary sphingomyelin and its metabolites have wide applications in the food and pharmaceutical industry. In this review, we summarized the distribution, classifications, structures, digestion, absorption and metabolic pathways of sphingolipids, and discussed the nutritional functioning of sphingomyelin in chronic metabolic diseases. The possible implications of dietary sphingomyelin in the modern food preparations including dairy products and infant formula, skin improvement, delivery system and oil organogels are also evaluated. The production of endogenous sphingomyelin is linked to pathological changes in obesity, diabetes, and atherosclerosis. However, dietary supplementations of sphingomyelin and its metabolites have been shown to maintain cholesterol homeostasis and lipid metabolism, and to prevent or treat these diseases. This seemly paradoxical phenomenon shows that dietary sphingomyelin and its metabolites are candidates for food additives and functional food development for the prevention and treatment of chronic metabolic diseases in humans.

KEYWORDS

sphingolipids, sphingomyelin, structure, metabolism, digestion, chronic metabolic diseases, applications

Introduction

Phospholipids act as the main component of biological membranes, emulsifier and surfactant. There are two types of phospholipids. The first one is glycerophospholipids with a glycerol backbone such as phosphatidylcholine, phosphatidylethanolamine, phosphatidylserine, phosphatidylglycerol, phosphatidylinositol, cardiolipin,

plasmalogen, phosphatidic acid and platelet activating factor (1). The other one is sphingolipids with sphingosine, the second largest group of membrane lipids. Sphingolipids such as ceramides, sphingomyelin, and glycosphingolipids have a polar head group and two non-polar tails (a long hydrocarbon fatty acyl group and a sphingoid base backbone) (2). Glycerophospholipids are important amphiphilic substances due to the presence of a hydrophilic head composed of substituent groups linked by phosphoric acid and a hydrophobic tail composed of fatty acyl groups. Currently, the LIPID MAPS database includes more than 4900 known sphingolipids, which are commonly found in all viruses, prokaryotes and eukaryotes (3). Sphingolipids are mainly found in membranes of cells, where the hydrophobic tail of phospholipids and other membrane lipids such as cholesterol are embedded. Both plasma and organelle membranes contain sphingomyelin, which distributes symmetrically throughout the membrane's bilayer. Contrarily, sphingolipids that are glycosylated (glycosphingolipids) are often arranged asymmetrically with their saccharide moieties facing the extracellular environment (4). Since the discovery in the 1880s (5), sphingolipids have been located on cell membranes, lipoproteins and other lipid-rich tissue structures, and are considered very important for maintaining membrane integrity, lipid raft formation, cell metabolism and signal transduction, cell growth, differentiation and apoptosis (6, 7). In foods, sphingolipids are present in dairy products, egg, meat product and soybeans, and some fruits and vegetables in small amounts (8).

The *de novo* synthesis of sphingolipids begins with the formation of ceramides, which is derived from serine and palmitate in a process that consists of condensation, reduction, acylation, and desaturation in the endoplasmic reticulum (ER). Then, ceramides are transported to the Golgi apparatus for the formations of sphingomyelin, ceramide-1-phosphate (C1P), inositol phosphorylceramides and glycosphingolipids (9–11). Sphingomyelin is one of the most important sphingolipids in animal tissues. Sphingomyelin from sources varies in sphingosine [long-chain bases (LCBs)] and fatty acyl groups (12). Sphingomyelin co-exists with phosphatidylcholine on the outer leaflet of the cell membrane. The dietary sphingomyelin is digested by intestinal alkaline SMase (Alk-SMase) and neutral ceramidase (N-CDase), and eventually hydrolyzed to ceramides, phosphorylcholine, sphingosine and fatty acids in the small intestine (3, 13). Unlike sphingomyelin and ceramides, sphingosine can be absorbed intact into intestinal mucosal cells and converted to sphingosine-1-phosphate (S1P), ceramides, sphingomyelin and glycosphingolipids, which are transported with chylomicrons into the lymph circulation and then the blood circulation, and newborn high-density lipoproteins (HDL) into the blood circulation (3, 13–15). The sphingomyelin metabolism and its plasma level are also affected by the types of fatty acids in the diet, vitamin B6, vitamin C, vitamin D, and vitamin K (16–23). The endogenous sphingomyelin is involved in adipose tissue function, obesity, diabetes and atherosclerosis related pathology (24–27), while exogenous dietary sphingomyelin may be beneficial for regulating cholesterol homeostasis and lipid metabolism, and for the prevention and treatment of chronic metabolic diseases (28–32). Due to the nutritional functions of dietary sphingomyelin and its metabolites, it has broad application prospects in food industry.

Classification and structures of sphingolipids

Classification of sphingolipids

When Johann Ludwig Wilhelm Thudichum isolated sphingolipids from the nerve tissues in 1880s, he named the molecule "sphingosine" after the Greek mythological creature sphinx, the beast of ancient Egyptian mythology that loved to present many enigmas to the inquirers (5). The LIPID MAPS Lipid Classification System classifies lipids into eight categories, fatty acyls, glycerolipids, glycerophospholipids, sphingolipids, sterol lipids, prenol lipids, saccharolipids, and polyketides. As shown in **Table 1**, sphingolipids have the most structural diversity and are subdivided into sphingoid bases, ceramides, phosphosphingolipids, phosphonosphingolipids, neutral glycosphingolipids, acidic glycosphingolipids, basic glycosphingolipids, amphoteric glycosphingolipids, arspidenosphingolipids and other sphingolipids (2). Sphingoid bases that include sphingosines, sphinganines, phytosphingosines, sphingoid base homologs and variants (C14, C16, and C17), sphingoid base S1P, lysosphingomyelins and lyso(glyco)sphingolipids, *N*-methylated sphingoid bases and sphingoid base analogs are the backbone of sphingolipids. A ceramide is generated when a fatty acyl group is linked to the sphingoid bases through an amide-linkage. There are ceramides, dihydroceramides, phytoceramides, acylceramides and its phosphate derivative C1P. Phosphosphingolipids such as sphingomyelins, ceramide phosphoethanolamines and ceramide phosphoinositols, are formed when the head group such as phosphocholine is linked to the ceramide via a phosphodiester linkage. In addition, simple and complex glycosphingolipids can be formed when mono or polysaccharides are attached to ceramide via glycosidic bonds such as in cerebrosides and gangliosides, respectively. Based on the polar parts, glycosphingolipids can be classified into three categories neutral, acidic, alkaline and amphoteric glycosphingolipids.

TABLE 1 Classification and representative structures for sphingolipids.

Common name	Systematic name	Formula	Structure
Sphingoid bases			
Sphingosine	Sphing-4-enine	$C_{18}H_{37}NO_2$	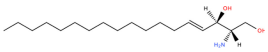
Sphinganine	Sphinganine	$C_{18}H_{39}NO_2$	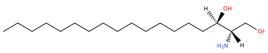
Phytosphingosines	4R-hydroxysphinganine	$C_{18}H_{39}NO_3$	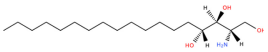
C16 Sphinganine	Hexadecasphinganine	$C_{16}H_{35}NO_2$	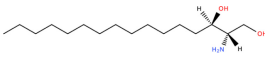
Sphingosine-1-phosphate	Sphing-4-enine-1-phosphate	$C_{18}H_{38}NO_5P$	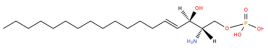
Sphingosine-1-phosphocholine	Sphing-4-enine-1-phosphocholine	$C_{23}H_{49}N_2O_5P$	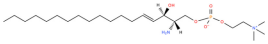
N,*N*-dimethylsphingosine	*N*,*N*-dimethylsphing-4-enine	$C_{20}H_{41}NO_2$	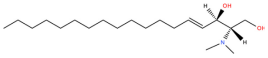
Ceramide			
Ceramide	*N*-acyl-sphing-4-enine	–	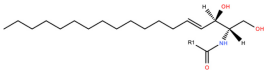
Dihydroceramide	*N*-acyl-sphinganine	–	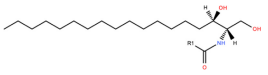
Cer(t18:0/16:0)	*N*-(hexadecanoyl)-4R-hydroxysphinganine	$C_{34}H_{69}NO_4$	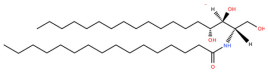
Omega-linoleoyloxy-Cer(d18:1/30:0)	*N*-(30-(9Z,12Z-octadecadienoyloxy)-triacontanoyl)-sphing-4-enine	$C_{66}H_{125}NO_5$	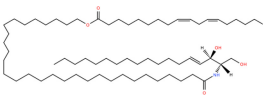
Ceramide-1-phosphate	*N*-(acyl)-sphing-4-enine-1-phosphate	–	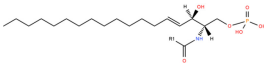
Phosphosphingolipids			
Sphingomyelin	*N*-acyl-sphing-4-enine-1-phosphocholine	–	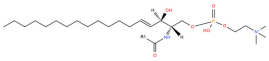
N-Acyl ceramide phosphoethanolamine	*N*-(acyl)-sphing-4-enine-1-phosphoethanolamine	–	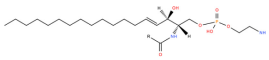
PI-Cer(d18:1/22:0)	*N*-(docosanoyl)-sphing-4-enine-1-phospho-(1′-myo-inositol)	$C_{46}H_{90}NO_{11}P$	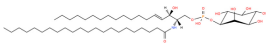
Phosphonosphingolipids			
Ceramide ciliatine	*N*-(acyl)-sphing-4-enine-1-(2-aminoethylphosphonate)	–	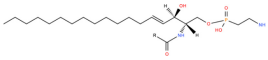
Neutral glycosphingolipids			
Glucosyl sphingosine	1-β-glucosyl-sphing-4-enine	$C_{24}H_{47}NO_7$	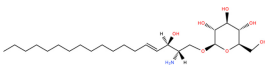
Gb3(d18:1/16:0)	Galα1-4Galβ1-4Glcβ-Cer(d18:1/16:0)	$C_{52}H_{97}NO_{18}$	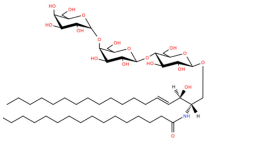
Asialo-GM2(d18:1/16:0)	GalNAcβ1-4Galβ1-4Glcβ-Cer(d18:1/16:0)	$C_{54}H_{100}N_2O_{18}$	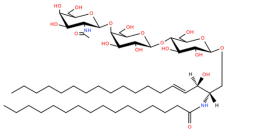

(Continued)

TABLE 1 (Continued)

Common name	Systematic name	Formula	Structure
Lc3Cer(d18:1/16:0)	GlcNAcβ1-3Galβ1-4Glcβ-Cer(d18:1/16:0)	$C_{54}H_{100}N_2O_{18}$	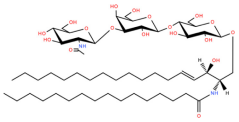
Acidic glycosphingolipids			
Gangliosides GM4(d18:1/16:0)	NeuAcα2-3Galβ-Cer(d18:1/16:0)	$C_{51}H_{94}N_2O_{16}$	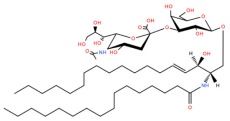
SulfoglycosphingolipidsGalbeta-Cer(d18:1/18:0)	*N*-octadecanoyl-1-β-(3′-sulfo)-glucosyl-sphing-4-enine	$C_{42}H_{81}NO_{11}S$	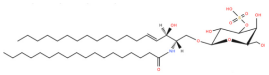
GlucuronosphingolipidsGlcAbeta-Cer(d18:1/18:0)	*N*-(octadecanoyl)-1-β-glucuronosyl-sphing-4-enine	$C_{42}H_{79}NO_9$	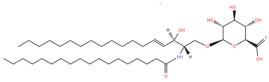
Basic glycosphingolipids			
Psychosine	1-β-galactosyl-sphing-4-enine	$C_{24}H_{47}NO_7$	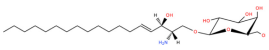
Amphoteric glycosphingolipids			
Psychosine sulfate	(2S,3R,4E)-2-amino-3-hydroxyoctadec-4-en-1-yl β-D-galactopyranoside 6-(hydrogen sulfate)	$C_{24}H_{47}NO_{10}S$	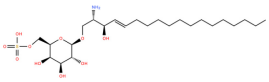

Structures of sphingolipids

Studies have identified more than 600 lipid species from 23 lipids classes and more than 2,300 novel features (33). The sphingoid base backbone is synthesized *de novo* from serine and a fatty acid. After a fatty acyl chain is added to the amine group of sphingoid bases, sphingosines, sphinganine and phytosphingosine are transformed to ceramide, dihydroceramide, and phytoceramide, respectively. The attachment of hydrophilic head groups to the OH-group of C-1 of the ceramide yields phosphosphingolipids, phosphonosphingolipids, glycosphingolipids, and other species, including protein adducts (34). Naturally derived sphingoid bases vary in alkyl chain length and branching, the level of saturation, the number of hydroxyl groups and other characteristics (35–37). The variations of sphingosine bases, fatty acyl and hydrophilic head groups together make them the most diverse and complex lipid class. As shown in **Table 1**, sphingosine has a double bond at the C-4 position, and sphinganine and phytosphingosine are fully saturated, while phytosphingosine has an extra hydroxyl group. The abbreviations "d" and "t" seen in the shorthand nomenclature in **Table 1** is to indicate the number of hydroxyl groups followed by the number of carbon atoms in the backbone and the number of double bonds in the fatty acyl group, while "d" is for the two (di-) hydroxyls group and "t" (tri-) for the additional hydroxyl group (38). So, sphingosine, sphinganine and phytosphingosine are designated as d18:1, d18:0, and t18:0, respectively. In addition, sphingoid base also includes the 1-phosphates, lysosphingolipids and *N*-methyl derivatives. The fatty acyl groups of ceramides are typically saturated or monounsaturated with various chain length from 14 to 36 carbons, while ceramides with C16, C18, and C24 are the most common ones in mammalian cells (2, 39, 40). When head groups (phosphate, phosphocholine or carbohydrate) are attached to ceramides at the C1-hydroxyl position, more complex sphingolipids such as C1P, phosphosphingolipids or glycosphingolipids are created (39). *N*-acylation of sphingosine creates dihydroceramides with C14 to C26 or in rare cases even up to C36 fatty acyl groups. The saturated or monounsaturated fatty acyl groups can be modified with an α and one additional hydroxylation. Sphingomyelin is composed of a sphingosine, a fatty acyl group and a phosphorylcholine head group (41). Its overall structure is roughly equivalent to replacing glycerol and a fatty acyl group in glycerophospholipid with sphingosine.

Glycosphingolipids can be divided into four sub-classes according to the types of carbohydrates and additional substituents, including neutral glycosphingolipids, acidic glycosphingolipids, basic glycosphingolipids and amphoteric glycosphingolipids (2). Neutral glycosphingolipids, also known as cerebrosides, contain one or more uncharged sugars, such as glucose (Glc), galactose (Gal) or N-acetylgalactosamine (GalNAc), *N*-acetylglucosamine (GlcNAc) and fucose. Acidic glycosphingolipids contain ionized groups adjoined

to neutral or charged carbohydrates such as sialic acid to form sulfoglycosphingolipids, glucuronosphingolipids and gangliosides. Gangliosides contain negatively charged sialic acids (N-acetylneuraminic acid or N-glycolylneuraminic acid), and are named and classified according to the number of sialic acid residues attached (M/D/T representing gangliosides containing 1, 2, or 3 sialic acids, respectively) and inner sugar moieties such as Glc, Gal or GalNAc connected to ceramides. For example, the subscripts 1, 2, 3, 4 of gangliosides usually can be expressed as: 1 is Gal-GalNAc-Gal-Glc-ceramide, 2 is GalNAc-Gal-Glc-ceramide, 3 is Gal-Glc-ceramide and 4 is Gal-ceramide (42). Basic glycosphingolipids refer only to psychosine or galactosylsphingosine that contains Gal residue, while psychosine sulfate belongs to amphoteric glycosphingolipids. Last, sphingolipids can be covalently attached to proteins to form adducts such as β-hydroxyceramides and inositol-phosphoceramides, which can be found on surface proteins of skin cells and membrane anchor proteins of fungi (43, 44). In cells, ceramides the building blocks of all sphingolipids, can be synthesized *de novo* from palmitoyl-CoA and serine or sphingosine and a fatty acyl CoA. Sphingomyelin contains phosphate, but not the glycerol backbone that glycerophospholipids have. When a glucosyl or a galactosyl group is attached to the C1 of ceramides, cerebrosides are formed. Galactocerebrosides are used to form sulfatides, whereas glucocerebrosides are used to synthesize gangliosides, globosides, and other related compounds (45).

Distribution of sphingolipids in foods

The contents of sphingolipids in foods vary from low in fruits and some vegetables to high in dairy products, egg and soybeans (8). **Table 2** summarizes the distribution and contents of sphingolipids in common foods. Since most sphingolipid research results have been focused on their structures, we could not collect contents of all sphingolipids in food. Based on the reported sphingolipid contents in nmol/g, the estimates in mg/100 g were converted using an average molecular weight for sphingosines of 299 g/mol, sphinganines of 301 g/mol, ceramides of 587 g/mol, sphingomyelin of 751 g/mol, and cerebroside of 779 g/mol. The first three sphingoid bases, sphingosines, sphinganine and phytosphingosine, are usually found in mammals, plants and fungi, and sphingosine (d18:1) is the most abundant of these three in mammalian cells (39, 46). In addition, substantial amounts of C20 and minor amounts of C12 to C22 as well as 1-deoxy and 1-deoxymethyl LCBs can also be found in animal products (47, 48). Phytosphingosines and their derivatives are usually found in plants to form plant sphingolipids, such as phytosphingosine (t18:0) and phytosphingosines 8-enine (t18:1) in potatoes and sweet potatoes, 9-Methyl-4, 8-sphingadienine (d19:2) and 2-Amino-4, 8, 10-octadecatriene-1, 3-diol (d18:3) in rice, mushroom and sea cucumber (49, 50). Many fungi also methylate the alkyl chain at C-9 to produce C19 bases, whereas *Saccharomyces cerevisiae* only produces sphingosine with predominant d18:0, t18:0, and some d20:0, t20:0 (51). Free sphingosine and LCBs are only present in cells at very low levels. Most of them can be phosphorylated to form S1P and other phosphorylated sphingosine bases.

Ceramides are widely distributed in mammals, especially in the skin (52). Sphingomyelins are high in animal-derived foods, such as aquatic products (2–10% of total phospholipids), meat products (5–10% of total phospholipids), eggs (approximately 1.5% of total phospholipids), and dairy products (approximately 25% of total phospholipids). Bioactive complex lipids are very abundant in milk and can be used as the main raw material for obtaining sphingomyelin and gangliosides (53). Insects mainly contain ceramide phosphate ethanolamine, and fungi have ceramide phosphate inositol and mannose-containing head group, and not found in most plants except legumes and nuts (2, 54). Soybeans are a good source of the plant-derived sphingolipids such as full-fat soy flakes (55). The types of fatty acids in sphingomyelins are different in foods. Taking eggs and milk for example, sphingomyelins derived from eggs have higher percentage of short-chain saturated fatty acids (SFAs) than that from milk (56). Although the content of glycosphingolipids in foods are lower than that of sphingomyelins, they are widely distributed in cereal, legumes and nuts, livestock and poultry meat, aquatic products, egg, milk and dairy products, vegetables, and fruits, as shown in **Table 2**. The sphingolipids in vegetables and fruits are relatively lower than other foods, mainly containing cerebrosides or glycosyl inositol phosphate ceramides (GIPCs) which can connect complex sugar chains (57, 58). Glucosylceramide-based sphingolipids, which have the basic structure of the tetrasaccharide ceramide series, are the main glycosphingolipids in plants, whereas some mannosylceramide series also exist (59). In invertebrates and vertebrates, different saccharides and their derivatives are added to the first sugar moiety of cerebroside, which is mainly glucose, to form hundreds of gangliosides with different head group structures. In addition, vertebrates also have a series of glycolipids containing galactose (60).

Metabolism of sphingolipids

Metabolic pathways of sphingolipids

In mammals, about 40 enzymes catalyze *de novo* synthesis, catabolism, recycling and interconversion of sphingolipids and

TABLE 2 Distribution and contents of sphingolipids in foods[a].

Content (mg/100 g) dietary sources	Sphingoid bases	Ceramide	Sphingomyelin	Cerebrosides	Gangliosides
Cereal					
Rice bran		5.6 (dw) (41)		11.5 (dw) (41)	
Rice (milled)				2.5 (ww) (205)	
Barley				14.4 (ww) (205)	
Corn				11.5 (ww) (205)	
Wheat flour				21.0 (ww) (205)	
Wheat flour				43.0 (dw) (8)	
Legumes and nuts					
Full-fat soy flakes	0.8 (dw) (55)	4.9–12.2 (dw) (206)	45.7 (dw) (55)	65.2–309.7 (dw) (206) 11.1–38.3 (dw) (207)	
Defatted soy flakes				19.2–23.9 (dw) (208)	
Almond			304.3 (dw) (209)	6.8 (dw) (210)	
Cashew nut			3.9 (dw) (209)	3.9 (dw) (210)	
Hazelnut			15.7 (dw) (209)	2.1 (dw) (210)	
Pine nut			376.9 (dw) (209)	4.2 (dw) (210)	
Peanut			5.9 (ww) (8)	3.9 (dw) (210)	
Pumpkin seed				3.1 (dw) (210)	
Walnut			612.9 (dw) (209)	2.5 (dw) (210)	
Pecans			373.5 (dw) (209)		
Pistachios			0.4 (dw) (209)		
Livestock and poultry meat					
Meat					0.35–1.1 (ww)
Pork			20.3 (ww) (52)		
Ham			17.8 (ww) (52)		
Beef			28.6–69.0 (ww) (41, 52)		
Fat cooked ground beef					1.7 (ww) (211)
Fat raw ground beef					1.6 (ww) (211)
Beef blade steak					1.0 (ww) (212)
Lamb			33.2 (ww) (52)		
Chicken			41.8 (ww) (52)		
Chicken thigh					1.4 (ww) (212)
Chicken breast					1.0 (ww) (212)
Turkey			35.0 (ww) (52)		
Aquatic products					
Plaice			9.6 (ww) (52)		
Herring			7.2 (ww) (52)		
Cod			6.5 (ww) (52)		
Turbot		2.9 (ww) (213)	6.4 (ww) (213)	0.3 (ww) (213)	0.9 (ww) (212)
Trout		2.5 (ww) (213)	4.2 (ww) (213)		
Mackerel		5.5 (ww) (213)	3.9 (ww) (213)		
Grass carp		11.5 (ww) (213)	1.7 (ww) (213)	0.3 (ww) (213)	
Shellfish			0.8 (ww) (214)		
Mussel		22.9 (ww) (214)		1.4 (ww) (214)	

(Continued)

TABLE 2 (Continued)

Content (mg/100 g) dietary sources	Sphingoid bases	Ceramide	Sphingomyelin	Cerebrosides	Gangliosides
Clam		19.3 (ww) (214)		7.4 (ww) (214)	
Scallop		16.7 (ww) (214)		6.8 (ww) (214)	
Oyster		12.1 (ww) (214)		2.2 (ww) (214)	
Island mackerel					6.6 (ww) (212)
King salmon					1.1 (ww) (212)
Snapper					0.8 (ww) (212)
Tuna					0.1 (ww) (211)
Microalgae			250–2760 (dw) (215)	2300 (dw) (215)	
Egg, milk, and dairy products					
Chicken egg yolk		4.4 (ww) (216)	190.0 (ww) (216)		1.7 (ww) (211)
Milk		0.1 (ww) (217)	23.4–47.3 (ww) (218)	13.6–175.2 (ww) (218)	0.05 (ww) (211)
Cheese	2.0 (ww) (55)		24.3–365.7 (ww) (218)	12.22–27.9 (ww) (218)	0.07 (ww) (211)
Butter			29.2–44.4 (ww) (218)	18.7–19.9 (ww) (218)	
Non-fat dry milk	43.8 (ww) (55)		15.2 (ww) (55)		
Yogurt	0.4 (ww) (55)		10.4 (ww) (55)		0.07 (ww) (211)
Vegetables					
Cauliflower			13.7 (ww) (8)		
Cucumber			2.0 (ww) (8)		
Lettuce			3.8 (ww) (8)		
Tomato			3.1 (ww) (8)		
Potato			5.2 (ww) (8)		
Sweet potato				50 (ww) (8)	
Spinach				5.0 (ww) (8)	
Soybeans				180 (ww) (8)	
Fruits					
Orange			1.8 (ww) (8)	4.9 (ww) (205)	
Banana			1.5 (ww) (8)	1.2 (ww) (205)	
Apple				7.1 (ww) (205)	
Grape				7.9 (ww) (205)	
Kiwifruit				6.2 (ww) (205)	
Lemon				4.9 (ww) (205)	
Pear				6.8 (ww) (205)	
Strawberry				3.4 (ww) (205)	

[a]dw means dry weight ratio, ww means wet weight ratio. Based on estimates of reported sphingolipid content (nmol/g), the conversion to mg/100 g was calculated using an average molecular weight for sphingosines of 299 g/mol, sphinganines of 301 g/mol, ceramide of 587 g/mol, sphingomyelin of 751 g/mol, and cerebroside of 779 g/mol.

products derived from them as summarized in Figure 1. The *de novo* synthesis of sphingolipids begins with the ceramide production. In general, 3-ketodihydrosphinganine is formed after the rate-limiting enzyme serine palmitoyltransferase (SPT) complex condenses palmitoyl-CoA and serine in a reaction that requires pyridoxal phosphate, NADPH, and Mn^{2+} (61, 62), and then reduced by 3-ketodihydrosphingosine reductase to generate sphinganine (47, 61). The mutations of the genes encoding SPTLC1 and SPTLC2, the key subunits of SPT, induce a permanent shift in the substrate specificity from L-serine to L-alanine and L-glycine, which results in the formations of atypical and neurotoxic metabolites, the 1-deoxy-sphingolipids and 1-deoxymethyl sphingoid bases, respectively, and their acylated ceramides (63). Besides, the recently discovered SPTLC3 prefers myristic acid to palmitic acid (64) and may use stearic acid as a fatty acid substrate (65). SPT can also

use alanine and glycine, as well as myristate and stearate, to produce a large amount of sphingosine bases. After that, the sphinganine is acylated by one of six ceramide synthases (CerS1-6) to form dihydroceramide (66), which is desaturated by dihydroceramide desaturase to generate ceramide (67). The other fatty acyl moiety in sphingolipids is long chain fatty acids (LCFAs) with 18–26 carbons, which are formed by a family of elongases extending myristic acid and palmitic acid in the ER (68). These variations in LCBs are combined with different acyl groups by the actions of CerS1-6, which makes ceramides a family of closely related but distinct molecules with different functions owing to variations in LCFA length and hydroxylation and desaturation of the LCB and LCFA components (69).

Ceramides are transported to the Golgi apparatus via vesicular and non-vesicular mechanisms (11). The latter mechanism *via* a ceramide transport protein (CERT) to assemble into sphingomyelin only exists in mammals (70), as shown in **Figure 1**. A variety of head groups are added to ceramide to form complex sphingolipids in the Golgi apparatus such as sphingomyelin, CIP, inositol phosphorylceramides and glycosphingolipids. The sphingomyelin synthase 1/2 (SMS1/2) enzymes located in the luminal side of the Golgi membrane transfer a phosphocholine headgroup from phosphatidylcholine to ceramide yielding diacylglycerol and sphingomyelin (71). According to Mitsutake and Igarashi, sphingomyelin synthase SMS2 on the plasma membrane dynamically regulates the activity of lipid microdomains and mice lacking SMS2 are resistant to the effects of a high-fat diet (HFD) on body weight, glucose intolerance, and fatty liver (72). Galactosylceramide (GalCer) and glucosylceramide (GlcCer) are synthesized by ceramide galactosyltransferase (CGT) and glucosylceramide synthase (GCS) transferring the monosaccharides from UDP-galactose and UDP-glucose to ceramide at the cytoplasmic side of the Golgi membrane, respectively (61, 73). The GlcCer is then translocated into the lumen of the Golgi *via* a membrane-bound transporter and further transformed to lactosylceramide (LacCer), which is synthesized by LacCer synthase transferring galactose from UDP-galactose to GlcCer (41, 74). The LacCer acts as a common backbone to produce more complex glycosphingolipids by various enzymes (41). Phosphatidylinositol-4-phosphate adaptor protein 2 (FAPP2) can transfer GlcCer among Golgi networks and couple it specifically to the synthesis of cerebrosides instead of anionic gangliosides (75). The sphingomyelin, cerebrosides and gangliosides are delivered to the plasma membrane *via* vesicular trafficking (76). Sphingomyelin and glycosphingolipids are delivered to the plasma membrane *via* vesicular transport, while C1P is transferred from the Golgi to other compartments such as the plasma membrane *via* non-vesicular translocation activity of C1P transfer protein (CPTP). On the cell membrane, sphingomyelin can be metabolized to ceramide on the outer leaflet of the membrane, where it is hydrolyzed to sphingosine by ceramidase, and metabolized to S1P by sphingosine kinase (SoK) (77).

Ceramides can be phosphorylated by ceramide kinase (CerK) to generate C1P, which can be dephosphorylated by a C1P phosphatase (78). Ceramides can also be acylated at the 1-OH position to form 1-O-acyl-ceramides (79). In addition, recent studies have shown that the ω-acylation of ceramides forms three-chained ceramides in the skin, thereby regulating epithelial permeability and skin barrier function (80). Ceramides can also be deacylated to generate sphingosine by ceramidase, and then phosphorylated by SoK to produce S1P in the lysosome and on plasma membrane (8). The S1P on the plasma membrane is flipped through the plasma membrane and transported to exocytoplasmic leaflets by the spinster homolog 2 (SPNS2), where it interacts with its receptors (81). The S1P lyase cleaves S1P (or dihydro S1P) into ethanolamine phosphate and fatty aldehydes, the latter are further metabolized and reduced to form acyl-CoA (76). All synthetic reactions to produce complex sphingolipids from ceramides are reversible. For instance, sphingomyelin, C1P and GlcCer are hydrolyzed by sphingomyelinase (SMase), C1P phosphatase and glucosylceramidase, respectively. This pathway may rapidly increase intracellular ceramide levels, while S1P catabolism is irreversible (82). S1P is catalyzed by S1P phosphatase (S1PP) and S1P lyase to dephosphorylate to sphingosine or irreversibly cleave to ethanolamine-1-phosphate and hexadecenal, respectively (83). The sphingolipids may be recirculated through endocytosis and transported from the endosome to the lysosome. In the lysosome, sphingomyelin, cerebrosides and gangliosides are metabolized to ceramides by hydrolases, and the ceramides are then degraded by acid ceramidase to generate sphingosine. Due to its positive charge, sphingosine is able to leave the lysosome and moves among the membranes such as ER membrane to be recycled (84). The sphingolipids have diverse biological activities in a receptor-dependent or -independent manner. Ceramide and sphingosines are mainly involved in cell apoptosis (85, 86), while S1P and C1P are related to cell survival (87), suggesting their antagonistic effects in some cases. Since ceramide and diacylglycerol may have opposite effects on cell proliferation and survival, SMS1/2 probably play an important role in regulating cellular fate. Therefore, the enzymes involved in these metabolic pathways maintain the homeostasis of bioactive sphingolipid metabolites.

Dietary factors affecting the metabolism of sphingolipids

Many prospective studies have shown that different dietary patterns affect *de novo* sphingolipids synthesis,

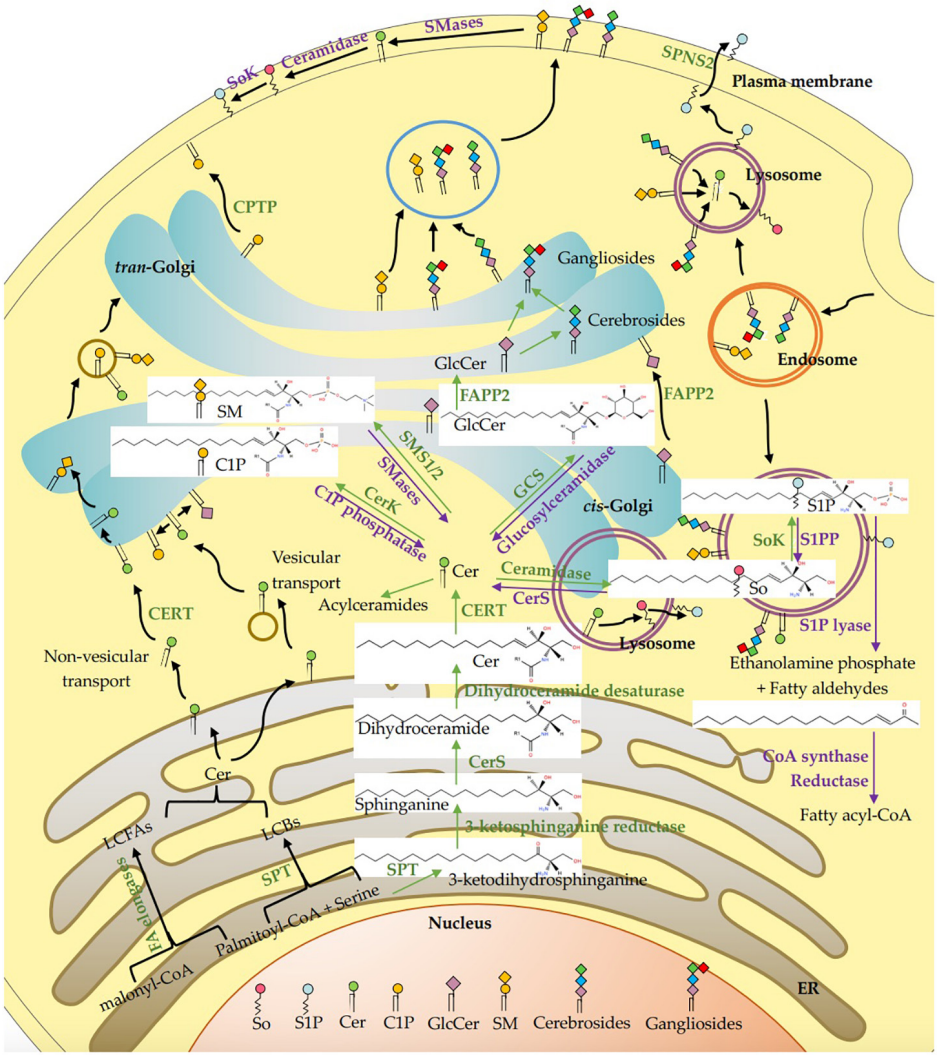

FIGURE 1

Intracellular metabolism and transport of sphingolipids in mammalian cells. The *de novo* synthesis of sphingolipids initiates with the synthesis of ceramide (Cer) through condensation by SPT complex utilizing palmitoyl-CoA and serine, which is followed by reduction, acylation, and desaturation on the cytosolic leaflet of the ER. Fatty acids with 12–16 carbons are extended by a family of elongase enzymes to form long-chain fatty acids (LCFAs, C18-C26) in the ER, which are used in the synthesis of Cer. Cers are transported to the Golgi apparatus through vesicular transport, and non-vesicular transport via the Cer transport protein (CERT). A variety of head groups are added to Cer to form complex sphingolipids in the Golgi apparatus such as sphingomyelin (SM), ceramide-1-phosphate (CIP), and glucosylceramide (GlcCer) by sphingomyelin synthase 1/2 (SMS1/2), ceramide kinase (CerK) and glucosylceramide synthase (GCS), respectively. The GlcCer is then translocated into the lumen of the Golgi apparatus via a membrane-bound transporter and further transformed into cerebrosides and gangliosides by different enzymes. C1P is transferred from the Golgi apparatus to plasma membrane via non-vesicular translocation of C1P transfer protein (CPTP). The SM, cerebrosides and gangliosides are delivered to the plasma membrane via vesicular trafficking, and then SM is metabolized to Cer, sphingosine (So) and sphingosine-1-phosphate (S1P). Cer is deacylated by ceramidase to generate So, and then phosphorylated by sphingosine kinase (SoK) to produce S1P in the lysosome and also in plasma membrane. The S1P lyase cleaves S1P into ethanolamine phosphate and fatty aldehydes, the latter are further metabolized and reduced to fatty acyl-CoA. All synthetic reactions to produce complex sphingolipids from Cer are reversible, such as SM, C1P, and GlcCer are hydrolyzed by sphingomyelinase (SMase), C1P phosphatase and glucosylceramidase, respectively. S1P is dephosphorylate by S1P phosphatase (S1PP) to get So, which is acylated by ceramide synthases (CerS) to form Cers. In the lysosome, SM, cerebrosides and gangliosides are metabolized by each hydrolase to produce Cer, and then degraded by acid ceramidase to generate sphingosine. In addition, Cers can also be acylated at the 1-OH position to form acylceramides. ER, Endoplasmic reticulum; SPT, serine palmitoyltransferase; CerS, ceramide synthase; CERT, ceramide transfer protein; Cer, ceramide; LCFAs, long chain fatty acids; LCBs, long chain bases; CerK, ceramide kinase; C1P, ceramide-1-phosphate; SMS1/2, sphingomyelin synthase; SMases, Sphingomyelinase; CerS, ceramide synthase; So, sphingosine; SoK, sphingosine kinase; S1P, sphingosine-1-phosphate; S1PP, sphingosine-1-phosphate phosphatase; GlcCer, glucosylceramide; GCS, glucosylceramide synthase; FAPP2, phosphatidylinositol-4-phosphate adaptor protein 2.

which in turn alters sphingolipid metabolism in human. The feeding of a HFD stimulates *de novo* synthesis of sphingolipids and alter sphingolipid metabolism in cells and tissues, which is associated systemic insulin resistance and imbalance of lipid accumulation, thereby exacerbating obesity-related diseases. HFD enhances *de novo* synthesis and turnover of sphingolipids through the salvage pathway, which promotes the synthesis and accumulation of ceramides, more specifically long chain ceramide species in skeletal muscle, plasma and liver tissues (88–90). Intake of SFAs enriched HFD can upregulate genes involved in ceramide synthesis (16), and promote releases of inflammatory cytokines such as tumor necrosis factor-α (TNF-α) and interleukin-1β (IL-1β) by inhibiting protein kinase B (Akt/PKB) (91). In addition, HFD can also increase the levels of sphingomyelin and S1P in the liver, skeletal muscle, adipose tissue, and cardiovascular tissue (89). Plant foods-based Mediterranean diet (92) has been negatively associated with the risks of cardiovascular diseases (CVDs) (93). This is associated with decrease in the plasma ceramide concentration. This may be attributed to the high ratio of monounsaturated fatty acids (MUFAs) to SFAs in the Mediterranean diet, which can inhibit the SFAs-induced accumulation of ceramides (17). In contrast, EPA (C20:5, n-3) and DHA (C22:6, n-3) decrease the expressions of genes involved in ceramide synthesis and ceramide content in the skeletal muscle and liver in rodents (88). Vitamins B6, C, D, and K have been shown to regulate sphingolipids metabolism (18–23). S1P lyase is a vitamin B6-dependent enzyme that can degrade S1P in the last step of sphingolipid metabolism. A genetic disease called SPL dysfunction syndrome (SPLIS) is caused by mutations in SGPL1, which encodes sphingosine phosphorylase (SPL). SPLIS patients exhibit lymphopenia, nephropathy, adrenal insufficiency, and/or neurological deficits. Vitamin B6 supplementation increases S1P abundance and activity levels, and decreases sphingolipids in the SPLIS patients (18). In addition, SPT responsible for 3-ketodihydrosphinganine synthesis is also a vitamin B6-dependent enzyme (19). One study has shown that the treatment with 1.2 mM calcium and 50 μg/mL vitamin C can significantly stimulate the content of ceramide in human keratinocytes (20). There may also be a relationship between the vitamin D intake and endogenous sphingolipids concentration in humans. Vitamin D supplementation can change levels of long-chain ceramides in the circulation and related sphingolipids metabolism, especially the increased levels of ceramide (C18) and dihydroceramide (C18) in subjects with type 2 diabetes (T2DM) (21). γ-tocotrienol, a form of vitamin E, can increase the levels of dihydroceramide and sphinganine but does not affect ceramide and sphingosine in cells (22). Vitamin K can regulate sphingolipids metabolism in the nervous system (23). However, more *in vivo* studies are needed to understand how vitamins regulate sphingolipid metabolism.

Absorption and utilization of dietary sphingomyelin

Pathways for the digestion and absorption of dietary sphingomyelin

The digestion and utilization of dietary sphingolipids starts in the jejunum section of the small intestine. The typical plasma membrane of mammalian cells contains about 20% cholesterol, 15–20% sphingomyelin, and 5% glycolipids of the total lipids, whereas the small intestinal brush border contains about 10% cholesterol, 5% sphingomyelin and over 30% glycolipids of the total lipids (7, 94). Bouhours and Guignard detected 750 nmol of sphingomyelin, 160 nmol of free ceramide, and 390 nmol of glucosylceramide from 1 mL of isolated rat intestinal epithelial cells (95). The levels of these sphingolipids change with the differentiation of rat epithelial cells and the development of the intestine (96, 97). Humans normally consume 2–8 g/day of phospholipids from the Western diet, accounting for 1–10% of total daily fat intake (98). Among them, sphingomyelin is about 0.3–0.4 g/day, which is mainly derived from fish, meat, milk and egg products. After digestion, about 3–6 g/day of phospholipids enter the blood through lipoproteins, of which sphingomyelin accounts for about 7%. In addition, sphingomyelin in human bile accounts for about 2% of total phospholipids, and about 0.1–0.2 g/day mainly palmitoyl and stearoyl species is delivered to the intestines (14).

Figure 2 shows the digestion and absorption of dietary sphingomyelin. After the dietary lipids are digested in gastrointestinal tract, triglyceride (TG) is hydrolyzed into free fatty acids, n-2 monoglycerides and a small amount of diacylglycerides by pancreatic lipase. Cholesterol esters are hydrolyzed by cholesterol esterase to form free cholesterol and fatty acids. Glycerophospholipids are cleaved by pancreatic phospholipase at n-1 or n-2 position to produce lysophospholipids and free fatty acids. Sphingomyelin is hydrolyzed to ceramide and phosphorylcholine by Alk-SMase in the intestinal mucosa under the optimal pH of 9.0 (99). Alk-SMase is produced by the liver and released into the jejunum vie bile, and is activated in the presence of bile salts and trypsin (3). Alk-SMase, with the hundred times of hydrolysis capacity higher than that of neutral SMase and acidic SMase, is strictly bile salt dependent and effectively stimulated by taurocholate and taurochenodeoxycholate (14, 100). Most sphingomyelin and its hydrolysate ceramides could not be absorbed intact and contribute to the chylomicron and plasma sphingomyelin pools (14). Ceramides are further hydrolyzed into sphingosine and fatty acids by intestinal N-CDase and bile salt-stimulated lipase (BSSL), while sphingosine could be absorbed into intestinal mucosal cells and rapidly metabolized in the enterocytes (13). BSSL from pancreatic

juice plays a key role in the digestion of TG and hydrolysis of the amide bond of ceramide between sphingosine and fatty acyl group. The activity of BSSL depends on bile salts with the optimal pH 8.5. It is worth noting that there is almost no ceramide formation in the proximal intestine where BSSL is most active (101, 102). All the digested products and bile acid (BA) can be assembled into micelles, which assist in crossing the unstirred water layer for entering the enterocytes.

When sphingosine is absorbed into the enterocytes, only a small amount of free sphingosine is incorporated into chylomicrons to be transported in the lymph and then, the blood. Most of the sphingosine receives a phosphate to generate S1P in the enterocytes, a process catalyzed by SoK. S1P is mainly degraded to ethanolamine phosphate and hexadecenal by S1P lyase, or to a less extend dephosphorylated to new sphingosine by S1PP and then to form ceramides and sphingomyelin. Fatty acids can be esterified into TG, and loaded with phospholipids and cholesterol esters onto chylomicrons, which enter the blood through lymphatic system (3, 14). Interestingly, the sphingosine first can be dephosphorylated by Sok to form S1P and secondly phosphorylated by S1PP to generate the new sphingosine, then acylated by CerS to form ceramide and more complex sphingolipids such as sphingomyelin and glycosphingolipids, which can be then incorporated into chylomicrons in the enterocytes for the release into the lymph. Dephosphorylation and then phosphorylation are prerequisites for the synthesis of sphingolipids by exogenous sphingosine in the enterocytes (13–15). In addition, dietary glycosphingolipids such as glucosylceramides, cerebrosides and gangliosides are degraded to produce ceramides by a series of enzymes such as glucosidase, galactosidase, glucosylceramidase, galactosylceramidase (3, 41). In the enterocytes, ceramides can also be synthesized from dietary palmitic acid and serine as shown in **Figure 1**.

Transport of sphingomyelin in plasma lipoproteins

Lipoproteins can be divided into chylomicrons, very low-density lipoproteins (VLDL), intermediate density lipoproteins (IDL), and low-density lipoproteins (LDL) and HDL according to their densities. HDL are further categorized into HDL_1, HDL_2, HDL_3 based on their densities. HDL_1 only appears after taking a high-cholesterol diet. Abnormal lipoprotein metabolism is associated with arteriosclerosis, diabetes, obesity and tumor occurrence (103). The concentrations of more than 200 sphingolipids in plasma lipoproteins vary. Sphingomyelin, LacCer, hexosylceramide, ceramides, S1P and dhS1P, C1P, sphingosine and dihydrosphingosine, are constituted 87.7, 5.8, 3.4, 2.8, 0.22, 0.15, and 0.005% of total sphingolipids in the human blood, respectively (104). Sphingolipids in lipoproteins can be secreted with apolipoprotein B (apoB) or apoA-I, and can be transferred from one lipoprotein to another. In addition, the complex sphingolipids in the lipoproteins can be modified from other existing sphingolipids, or decomposed into other sphingolipid components, such as ceramides, S1P, and Glc-ceramide (103). The human plasma contains 416 mg/ml sphingomyelin, which accounts for about 20% of total plasma phospholipids (104, 105) and 87.7% of total plasma sphingolipids (104, 105). The C_{16} and $C_{24:1}$-sphingomyelin are the major species in human plasma. Approximately 3.15, 32.85, 34.1, and 29.9% plasma sphingomyelin are present in VLDL, LDL, HDL_2, and HDL_3, respectively. The particle concentrations of these four lipoproteins in human plasma are 0.073, 1.514, 8.35, and 22.1 nmol/ml, and their molecular weights are 10.0×10^6, 2.0×10^6, 4.0×10^5, and 2.0×10^5, and percentages of protein composition are 10, 20, 40, and 55%, respectively (104). However, the amount of sphingomyelin has been significantly reduced in HDL and increased in LDL and VLDL in women with insulin-dependent diabetes (106). Approximately 75% of plasma sphingomyelin is present in LDL and VLDL, and about 25–37% is present in HDL, showing that the decrease of sphingomyelin, phosphatidylcholine and lysophosphatidylcholine may be potentially atherogenic. The reduction of phospholipid content in HDL may weaken its ability to promote the outflow of cholesterol from cells, and inhibit the transfer of cholesterol esters from HDL to larger lipoproteins containing apoB (106). Approximately 8.73, 39.94, 28.74, and 22.59% plasma ceramides are present in VLDL, LDL, HDL_2, and HDL_3, respectively. The prominent ceramide is C_{24}-ceramide in human plasma. About 1.33, 3.73, 16.3, and 78.64% plasma S1P are present in VLDL, LDL, HDL_2, and HDL_3, respectively. The ratios of sphingomyelin/ceramides in VLDL, LDL, HDL_2, and HDL_3 are 22.3:1, 50.9:1, 72.9:1, and 78.9:1,whereas the ratios of ceramides/S1P in those lipoproteins are 49.8:1, 80.7:1, 13.4:1, and 2.2:1, respectively (104). In addition, more than 50 species of complex glycosphingolipids account for about 9–10% of plasma sphingolipids, of which the most abundant ones are GlcCer and LacCer, accounting for about 8–14, 46–60, and 28–44% in VLDL, LDL, and HDL, respectively (103, 104).

Sphingomyelin formed in the enterocytes enters the body *via* chylomicrons as shown in **Figure 3**. The absorption of sphingosine leads to the formation of sphingomyelin and ceramides, which are incorporated into pre-chylomicron with TG, free cholesterol, cholesterol esters and other phospholipids under the action of microsomal triglyceride transfer protein (MTP) with apoB-48 in enterocytes. The pre-chylomicron then fuses with the lipid droplets to form chylomicron, which is secreted into the lymph circulation and then the blood circulation. TG in chylomicron is hydrolyzed into free fatty acids by lipoprotein lipase (LPL), which leads to the formation of chylomicron remnants in the circulation (14, 103, 107).

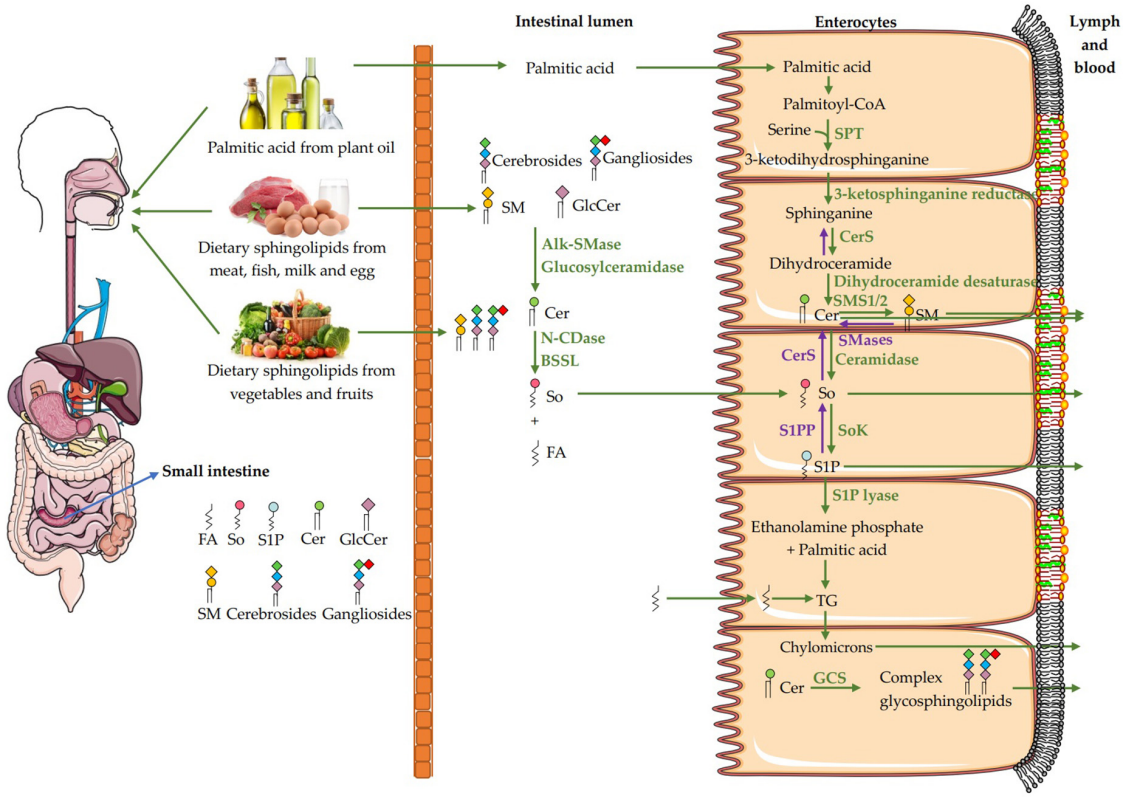

FIGURE 2
Pathways for the digestion and absorption of dietary sphingomyelin. The digestion of dietary sphingomyelin (SM) in the small intestinal lumen begins with the decomposition of SM to ceramide by Alk-SMase. Ceramide is further hydrolyzed into sphingosine (So) and fatty acids by N-CDase and BSSL, then the So is absorbed intact into the enterocytes. In the enterocytes, part of So comes from the *de novo* synthesis of palmitic acid and serine, and part of it comes from intestinal absorption. When the So is absorbed into the enterocytes, only a small amount of free So is transported with chylomicrons to the lymph and blood. Most of the So is catalyzed by sphingosine kinase (SoK) to generate sphingosine-1-phosphate (S1P), and then degraded to ethanolamine phosphate and hexadecenal by S1P lyase, or to a less extend dephosphorylated to new So by S1P phosphatase (S1PP) and then to form ceramides and sphingomyelin. Hexadecenal will be converted to palmitic acid and then esterified into triglycerides (TG), which can be incorporated into chylomicrons for transport. FA, fatty acid; So, sphingosine; S1P, sphingosine-1-phosphate; Cer, ceramide; GlcCer, glucosylceramide; SM, sphingomyelin; SMases, Sphingomyelinase; Alk-SMase, alkaline SMase; N-CDase, neutral ceramidase; BSSL, bile salt-stimulated lipase; SPT, serine palmitoyltransferase; CerS, ceramide synthase; SMS1/2, sphingomyelin synthase 1/2; CerS, ceramide synthase; SoK, sphingosine kinase; S1PP, sphingosine-1-phosphate phosphatase; TG, triglycerides; GCS, glucosylceramide synthase.

A part of sphingomyelin may also associate with apoA-I in the Golgi and be assembled into nascent HDL that is then secreted to the plasma and is responsible for reverse cholesterol transport to move cholesterol from extrahepatic tissues to the liver. New born HDL is mainly synthesized in the liver and can also be synthesized in the small intestine (14). The blood of healthy people mainly contains HDL_2 and HDL_3. ApoA-I interacts with the ATP binding cassette (ABC) transporters family and accepts sphingomyelin and glycosphingolipids to form pre-β HDL. Then lecithin–cholesterol acyltransferase (LCAT) converts free cholesterol to cholesterol esters in pre-β HDL, which move to the core of the newborn HDL and migrate with the lipoprotein particle in the blood to form mature HDL_2 and HDL_3 (103). *In vitro* experiments show that ABCA1, ABCA7, or ABCG1 expressed in HEK293 cells incubated with apoA-I efflux sphingomyelin (108–110). There are few studies on the transport of glycosphingolipids. Unlike sphingomyelin and ceramides, glycosphingolipids cannot be transported to apoB-containing lipoproteins by MTP. Instead, it may be assembled into HDL under the action of two possible transporters ABCA12 and ABCC1. Studies have shown that ABCC1 and ABCA12 are involved in the transport of glucosylceramide *in vivo*, but it is unclear whether its effluxes glucosylceramide to HDL or apoA1, or plays a role in plasma glycosphingolipid transport or metabolic disorders (103, 111, 112). Therefore, more *in vivo* evidence is needed to show that these transporters in basal levels play a role in sphingomyelin release, since their overexpression may limit the fluidity of membrane, which is conducive to outflow. As for ceramides, how they are involved in the assembly of HDL is still unknown.

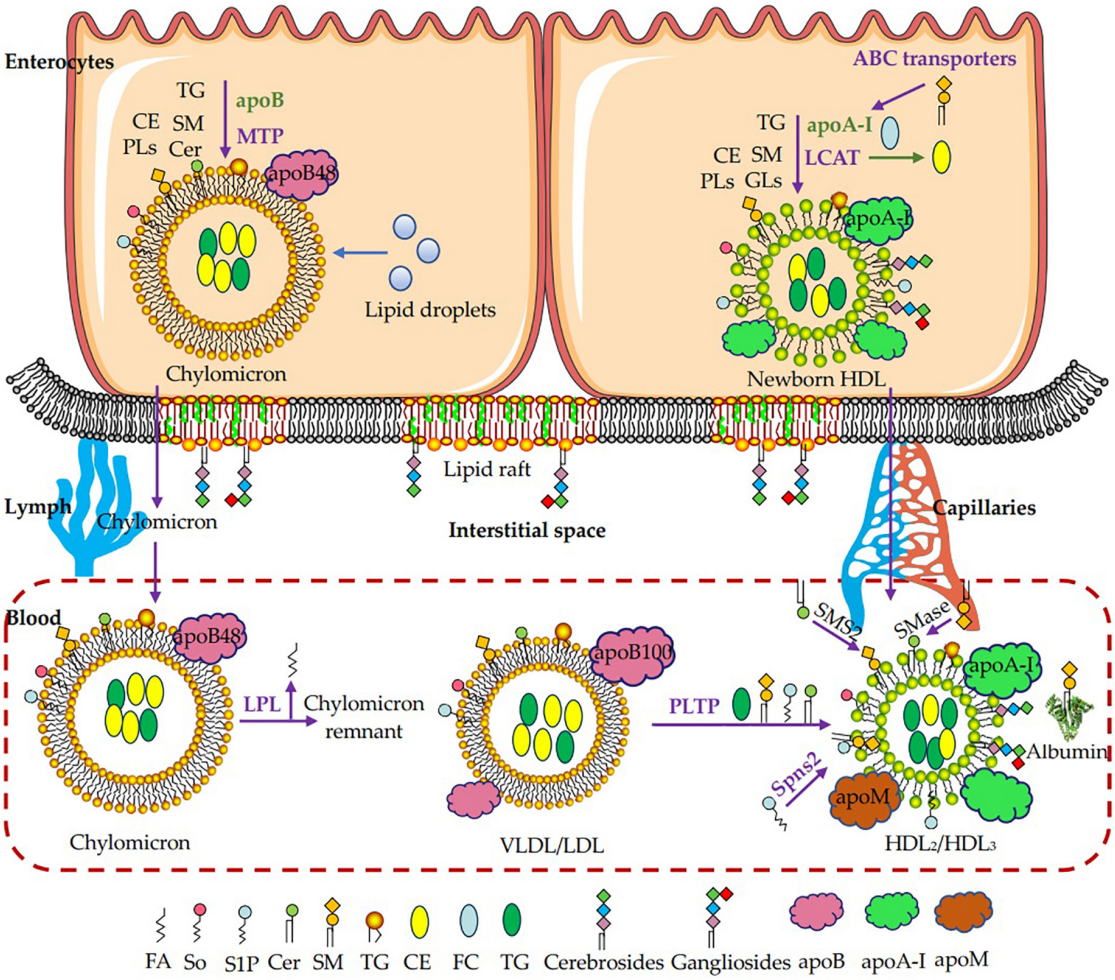

FIGURE 3
Transport of dietary sphingomyelin from enterocytes to plasma in lipoproteins. Most sphingomyelin (SM) and ceramide (Cer) can be reformed from sphingosine (So) in enterocytes, which will be transferred to the nucleation site with triglyceride (TG), free cholesterol (FC), cholesterol esters (CE) and other phospholipids (PLs) under the action of MTP and incorporated onto apolipoprotein B-48 (apoB-48) to form the original lipoprotein. The original lipoprotein then fuses with the lipid droplets to form chylomicron, which is secreted into the lymph and blood. TG in chylomicrons is hydrolyzed into free fatty acids by lipoprotein lipase (LPL), which leads to the formation of chylomicron residues in the circulation. Apolipoprotein A-I (apoA-I) interacts with the ATP binding cassette (ABC) transporters family and accepts SM and glycosphingolipids to form pre-β HDL. Then lecithin–cholesterol acyltransferase (LCAT) converts FC to CE in pre-β HDL, which moves to the core of the newborn HDL and is secreted into the blood to form mature HDL_2 and HDL_3. In the plasma membrane, synthesis of SM by SMS2 from Cer can contribute to SM in HDL, and degradation of SM by SMase may also increase Cer in HDL. S1P from the plasma membrane of peripheral tissues such as erythrocytes and platelets, is delivered to HDL with apolipoprotein M (apoM) and apoA-I *via* Spinster2 (Spns2). In addition, SM, Cer, S1P and TG are transferred from VLDL/LDL to HDL *via* phospholipid transfer protein (PLTP). FA, fatty acid; So, sphingosine; S1P, sphingosine-1-phosphate; Cer, ceramide; SM, sphingomyelin; PLs, phospholipids; CE, cholesterol esters; FC, free cholesterol; TG, triglyceride; apoB, apolipoprotein B; apoA-I, apolipoprotein A-I; apoM, apolipoprotein M; MTP, microsomal triglyceride transfer protein; LPL, lipoprotein lipase; GLs, glycosphingolipids; LCAT, lecithin–cholesterol acyltransferase; ABC transporters, ATP binding cassette transporters; SMases, Sphingomyelinase; SMS2, sphingomyelin synthase 2; PLTP, phospholipid transfer protein; Spns2, Spinster2.

Beside in the enterocytes, ABC transporters on the plasma membrane of macrophages, liver or other peripheral tissues can efflux sphingomyelin to HDL, apolipoprotein such as apoA-I, albumin or other receptors (103). Phospholipid transfer protein (PLTP) can maintain particle stability during the wide range of lipoprotein particle modifications in plasma. It can transfer sphingomyelin, ceramides, S1P and TG from VLDL/LDL to HDL (14). However, it is not clear whether PLTP can transfer GluCer, GalCer or other complex sphingolipids. On the plasma membrane, synthesis of sphingomyelin by SMS2 from ceramides can contribute to HDL sphingomyelin, degradation of sphingomyelin by SMase may also increase HDL ceramides (103). In addition, S1P from the plasma membrane of peripheral tissues such as erythrocytes and platelets, can be delivered to HDL with apoM and apoA-I *via* Spinster2 (Spns2) (103, 113). How other sphingolipids components

are incorporated into lipoprotein particles is unclear so far, and more research is needed to evaluate these and other possibilities.

Functions of dietary sphingomyelin in chronic metabolic diseases

Effects of dietary sphingomyelin on lipid profile

Metabolic syndrome (MetS) has become a global public health issue. It is the aggregate of pathological conditions in which proteins, fats, carbohydrates and other substances are metabolized abnormally, leading to central and abdominal obesity, insulin resistance, atherogenic dyslipidemia and systemic hypertension (114). Genetic defects of genes involved in metabolism may also lead to MetS. Additionally, dysfunctions of the liver or pancreas might result in MetS (115). Individual therapy of hypertriglyceridemia, hyperglycemia, and hypertension, as well as dietary restriction and frequent exercise, have been suggested as treatments for MetS. The dietary sphingomyelin and its metabolites may play an important role in regulating cholesterol homeostasis and lipid metabolism, and alleviating the symptoms of obesity, diabetes and atherosclerosis as shown in **Table 3**. Previous studies have shown that dietary sphingomyelin and its metabolites can significantly modify the plasma and hepatic cholesterol and TG metabolism in rats (116, 117) and inhibits the absorption of cholesterol both in Caco-2 cells and animal studies (118–120). Interestingly, sphingomyelin from milk is more effective in inhibiting cholesterol absorption than that from eggs, which may be attributed to the higher degree of saturation and longer chain length of fatty acyl group in milk sphingomyelin (56). Natural phospholipids, especially sphingomyelin, have high affinity for cholesterol to slow the rate of luminal hydrolysis, micellar solubilization, and transfer of micellar lipids to the enterocytes (121). We have found that the ability of egg sphingomyelin to inhibit cholesterol absorption, and simulate cholesterol transport at a higher rate than phosphatidylcholine in the Caco-2 monolayer. This is mediated by downregulation of the Niemann-Pick-Like Protein 1 (NPC1L1) mRNA, which is a key player in cholesterol absorption (122). A randomized crossover study shows for the first time that diets enriched with milk sphingomyelin, increased serum HDL cholesterol levels, but did not affect the serum TG, total cholesterol (TC), non-HDL cholesterol levels, also cholesterol absorption and cholesterol fractional synthesis rate in ten healthy adult males and females (123). The milk sphingomyelin also could regulate intestinal permeability and affect the intestinal tight junction protein expression through increasing the IL-8 secretion in Caco-2/TC7 cells, which may provide a clue to the protective role of obesity or leaky gut diseases (124). Sphingosine treatment significantly reduces cholesterol absorption in Caco-2 and HT-29-D4 cells (125). Due to the differences of sphingoid bases and fatty acid compositions, dietary sphingomyelin can improve lipids absorption and metabolism, probably *via* micellar solubilization, affinity to the hydrolases, or regulation of key proteins involved in cholesterol absorption.

Compared with other phospholipids, sphingomyelin has a larger interface area and stronger hydrogen bond formation capability, which is essential for the interactions between sphingomyelin and other lipids in the cell membrane (54). The important intermolecular hydrogen bond is formed by the 2-NH or choline nitrogen of sphingomyelin and the hydroxyl group of cholesterol. The phosphate oxygen and the 3-OH among sphingomyelin molecules may also form intermolecular hydrogen bonds and a network, thereby interfering with the release of cholesterol from these lipid complexes (126). Nilsson et al. (127) found that about 25% of dietary sphingomyelin can reach to the colon, in the form of 10% undegraded sphingomyelin, 30–90% ceramides and 3–6% free sphingosine. Dietary sphingomyelin in the colon may have the potential for reducing the development of aortic root plaque (128), affecting the gut microbiota such as *bifidobacterial* (129), neutralizing the intestinal inflammation caused by lipopolysaccharide (LPS) and improving in the intestinal barrier function attenuated by Western diet (130). Based on these, we hypothesize that dietary sphingomyelin inhibits the intestinal cholesterol absorption pathways, as shown in **Figure 4**. (i) Cell-independent effects. The strong hydrogen bonding or interaction between sphingomyelin and cholesterol causes the molecules in the micelles to pack more tightly, thereby slowing down the release of cholesterol in the micelles and inhibiting the absorption and transport of cholesterol in the enterocytes. Sphingomyelin may reduce the solubility of cholesterol in micelles, thereby reducing the thermodynamic movement of free cholesterol that is available to be absorbed by enterocytes. (ii) Cell-dependent effects. Sphingomyelin inhibits cholesterol absorption by reducing the expression of NPC1L1 in the enterocytes. *In vitro* studies have shown that LCBs such as sphingosine compete with palmitic acid for absorption through an acyl-CoA synthetase-dependent mechanism (54). Acyl-CoA synthetases convert intracellular long-chain fatty acids to their acyl-CoA, which promotes their retention in the cells, and in turn, facilitates their transport. (iii) Intestinal remodeling role. Sphingomyelin may improve the distribution and abundance of gut microbiota, prevent LPS from being transported to the mesenteric lymphatic circulation, or modulate its BA and short-chain fatty acid (SCFA) pathways to inhibit cholesterol absorption and transport.

TABLE 3 Effects of dietary sphingomyelin and its metabolites on human physiology and chronic metabolic diseases.

Metabolic disorders	SM and its' metabolites	Model	Treatment and duration	Results	References
Normal physiology	SLs from ox brain[a]	ExHC rats	0.5 and 2% (wt/wt) SLs for 2 weeks	[c]↓ Serum TG and liver CE levels; ↑ serum SM and liver PLs levels — Liver TG and serum CE levels	(116)
	SLs from bovine brain[b]	Donryu rats at 4 weeks old	1% (wt/wt) SLs during two generations	↓ Plasma TC levels; ↑ liver TG levels — Liver TC and plasma TG levels, tissue SLs and PLs levels	(117)
	Milk SM	SD rat	6.5–25 μmol/L ^{3}H-SM and ^{14}C-cholesterol for 4 h	↓ Cholesterol absorption	(118)
	Milk SM	Caco-2 cells C57L/J mice at 7 weeks old	2% (wt/wt) SM for 4 days	↓ Uptake and esterification of cholesterol in Caco-2 cells ↓ Cholesterol absorption in mice	(119)
	Egg yolk SM	SD rat at 8 weeks old	5 or 10 μmol/h SM and ^{14}C-cholesterol for 8 h	↓ Lymphatic absorption of cholesterol, α-tocopherol and fatty acid in a dose dependent manner	(120)
	Milk SM and egg yolk SM	SD rat at 8 weeks old	80 μmol/h SM and ^{14}C-cholesterol for 8 h	↓ Lymphatic absorption of cholesterol, fat, and other lipids Milk SM is more is more effective in inhibiting cholesterol absorption than egg SM	(121)
	Egg yolk SM	Caco-2 monolayer	0.6 mmol/L and ^{3}H-cholesterol for 2 h	↓ Cholesterol transport in a dose dependent manner alter the physicochemical properties of mixed micelles ↓ NPC1L1, Caveolin 1, SREBP-1/2 mRNA expression	(122)
	Milk SM	Ten healthy adult males and females (ages 18–45)	a randomized crossover study with 4-week washout period 1 g/day milk SM for 14 days	— Serum TG, TC, non-HDL cholesterol levels — Cholesterol absorption and cholesterol fractional synthesis rate — Intraluminal cholesterol solubilization ↑ HDL cholesterol levels	(123)
	So	Caco-2 and HT-29-D4 cells	0–50 μmol/L So and ^{3}H-cholesterol for 4 h	↓ Cholesterol uptake in a dose dependent manner ↓ NPC1L1 mRNA expression	(125)
Obesity	Chicken skin SM	Zucker rats fed with HFD at 6 weeks old	0.5 and 2% (wt/wt) SM for 45 days	↓ Hepatic lipid, plasma TC and insulin levels ↑ Adipor2, PPARR and Pdk4 mRNA and ↓Scd1 mRNA	(133)
	Egg yolk SM	C57BL/6 mice fed with HFD	0.3, 0.6, or 1.2% SM (wt/wt) with high-fat diet for 4 weeks	↓ Intestinal cholesterol absorption ↓ Total liver lipids (TC, TG) *via* the LXR-SREBP-1c pathway ↑ Fecal lipid and cholesterol output	(28)
	Milk SM Egg yolk SM	C57BL/6 mice fed with HFD at 8 weeks old	0.1% (wt/wt) milk or egg yolk SM for 10 weeks	↓ Body weight, serum TC, fasting glucose and liver TC, TG levels ↓ PPARγ-related mRNA expression (Scd1, Pparg2, Cd36, Fabp4, Ccl2) ↓ Epididymal adipose tissue inflammation and skeletal muscle lipid accumulation	(134)
	Milk SM Egg yolk SM	C57BL/6 mice fed with HFD at 8 weeks old	0.25% (wt/wt) milk or egg yolk SM for 4 weeks	↓ Body weight, serum TC, and liver TG *via* lipid absorption and metabolism regulation ↓ Serum LPS *via* bifidogenic effects and alterations in distal gut microbiota	(129)
	MPL with 25% SM	C57BL/6 mice fed with HFD at 8 weeks old	1.1 or 1.6% (wt/wt) MPL for 8 weeks	↓ Body weight gain – Plasma markers of inflammation 1.6% (wt/wt) MPL: ↓ hepatic gene expression of macrophage marker F4/80 and ↑ *Bifidobacterium animalis* in cecal microbiota 1.1% (wt/wt) MPL: ↓ *Lactobacillus reuteri* in cecal microbiota	(135)

(Continued)

TABLE 3 (Continued)

Metabolic disorders	SM and its' metabolites	Model	Treatment and duration	Results	References
	Milk SM and Cer	KK-A^y mice at 3 weeks old	1.7% (wt/wt) of LC-BS (0.13% SM; 0.18% Cer) or 0.5% (wt/wt) Cer-fraction (0.34% Cer) or 0.5% (wt/wt) SM-fraction (0.25% SM) for 4 weeks	LC-BS: ↓ plasma TC and LDL cholesterol and liver TG levels Cer-fraction: ↓ liver TC and TG levels ↓ Stearoyl-CoA desaturase-1 SM-fraction: –plasma and liver lipids	(136)
Diabetes	S1P	HIT-T 15 cells pancreatic islets from ICR mouse at 8 weeks old	10 μmol/L S1P	↑ Insulin secretion from isolated mouse islets ↓ Intracellular cyclic AMP levels in a dose dependent manner	(139)
	S1P	INS-1 cells pancreatic islets from SD rats	100–400 nmol/L S1P or dihydro-S1P for 4.5–5 h	↓ TUNEL analysis and caspase-3 activity ↑ PKC activity ↓ Cytochrome c release ↓ Nitric oxide synthase	(140)
	Milk SM	Obese/diabetic KK-A^y mice at 4 weeks old	1% (wt/wt) milk SM for 4 weeks	↓ Serum TC, non-HDL cholesterol, PLs and LDL-cholesterol levels; liver TG, TC, neutral and total lipids levels – Serum neutral lipids and cholesterol levels ↑ Fecal lipids (total lipids, TC, total bile acid and PLs) ↑ SREBP-2, HMG-CoA, and Cyp7a1 mRNA expression ↓ Scd1, Elovl2, Elovl5, Fads2 mRNA expression	(29)
	Sea cucumber Cer and GlcCer	SD rat fed with high-fructose-diet	0.16 g/kg Cer and 0.21 g/kg GlcCer of diet for 6 weeks	↓ Serum glucose levels and glycosylated hemoglobin ↓ Hypertension Cer ↑ glycogen levels, glycogen synthesis and insulin signal transduction in skeletal muscle GlcCer ↑ hepatic glycogen levels, glycogen synthesis and insulin signal transduction attenuated inflammation in adipose tissue	(141)
CVDs	Egg yolk SM	C57BL/6 mice fed with HFD at 4 weeks old	0.3, 0.6, or 1.2% (wt/wt) egg yolk SM for 4 weeks	↓ Serum TMAO level – Serum choline and betaine levels	(30)
		apoE$^{-/-}$ mice fed with HFD at 5 weeks old	1.2% (wt/wt) egg yolk SM for 16 weeks	↑ Body weight – Aortic lesions – Serum lipid levels (TC, TG, non-esterified fatty acid and SM)	
		apoE$^{-/-}$ mice at 5 weeks old	1.2% (wt/wt) egg yolk SM for 19 weeks	↓ Aortic lesion area in the aortic arch ↓ Lesion composition – Serum lipid, TMAO, choline and betaine levels	
	Egg yolk SM	apoE$^{-/-}$ mice fed with HFD at 6 weeks old	0.1% (wt/wt) egg yolk SM for 8 weeks	↓ Epididymal fat mass, alanine aminotransferase (ALT) activity ↓ Aortic root lipid accumulation ↑ Spleen weights – Serum TG, TC, HDL cholesterol, non-HDL cholesterol and non-esterified fatty acid levels	(128)
	Milk PLs	LDLr$^{-/-}$ mice fed with AMF-rich diet at 6 weeks old	0.2%, 0.4% (wt/wt) milk SM for 14 weeks	↓ Serum TG, TC, HDL cholesterol, non-HDL cholesterol and non-esterified fatty acid levels – Serum HDL-C, TG, liver enzymes, insulin, glucose, TNF-α, IL-1β, adiponectin, and resistin ↓ Inflammatory markers in the serum, liver, adipose and aorta ↓ Atherosclerosis development in both the thoracic aorta and the aortic root ↑ Relative abundance of Bacteroidetes, Actinobacteria, and Bifidobacterium, and ↓ Firmicutes in cecal feces	(31)

(Continued)

TABLE 3 (Continued)

Metabolic disorders	SM and its' metabolites	Model	Treatment and duration	Results	References
	Milk PLs	Fifty-eight overweight postmenopausal women (ages 56–62)	Multi-center double-blind randomized trial with 4–6 weeks washout period 0, 3, or 5 g of milk PLs for 4 weeks	↓ Blood lipids and associated cardiometabolic risk markers (TC/HDL cholesterol, apoB/apoA1) ↑ Fecal loss of coprostanol – Major bacterial populations and fecal short-chain fatty acids ↓ Cholesterol absorption but ↑ cholesterol-ileal efflux	(32)
	Milk PLs	Fifty-eight overweight postmenopausal women (ages 56–62)	Multi-center double-blind randomized trial with 4–6 weeks washout period 0, 3, or 5 g of milk PLs for 4 weeks	↓ Serum TC, LDL cholesterol and apoB levels ↓ Serum atherogenic C24:1 Cer, C16:1 SM, and C18:1 SM species ↓ Chylomicron content in total SM and C24:1 Cer, but ↑ total Cer in feces	(148)

[a]Sphingolipids contained 68.2% ceramide-monosaccharide, 27.8% sphingomyelin, 2.9% cholesterol. [b]Sphingolipids contained 64.8 % cerebroside and cerebroside sulfate, 29.0% sphingomyelin and 5.4% cholesterol and free fatty acids. [c]↓ refers the significantly decreasing index, ↑ refers the significantly increasing index, and – refers no significant changes. SM, sphingomyelin; SLs, sphingolipids; ExHC, exogenous hypercholesterolemic; TG, triglyceride; CE, cholesterol esters; TC, total cholesterol; SD rat, Sprague-Dawley rat; So, sphingosine; NPC1L1, Niemann-Pick-Like Protein 1; SREBP-1/2, sterol regulatory element-binding transcription factor 1/2; HFD, high-fat diet; Adipor2, adiponectin receptor 2; PPARγ, peroxisome proliferator activated receptor alpha; Pdk4, pyruvate dehydrogenase kinase 4; Scd1, stearoyl CoA desaturase; LPS, lipopolysaccharide; MPL, milk polar lipids; LC-BS, lipid-concentrated butter serum; S1P, sphingosine-1-phosphate; PLs, phospholipids; SREBP-2, sterol regulatory element-binding protein-2; HMG-CoA, 3-hydroxy-3-methylglutaryl coenzyme A reductase; Cyp7a1, cholesterol 7α-hydroxylase; Elovl2, elongases of very long chain fatty acids 2; Fads2, fatty acyl desaturase 2; Cer, ceramide; GlcCer, glucosylceramide; TMAO, trimethylamine *N*-oxide; ALT, alanine aminotransferase; LDLr, LDL receptor; AMF, anhydrous milk fat.

Effects of dietary sphingomyelin on obesity

Obesity, the excess accumulation of body fat, has become a major public health issue worldwide. Overweight and obesity rates were respectively 34.3 and 16.4% between 2015 and 2019 in adults based on Chinese criteria (131). The sphingomyelin and its metabolites play a role in lipogenesis (132). Endogenous sphingomyelin is involved in adipose tissue functions and obesity-related pathology (24, 25). Exogenous dietary sphingomyelin may be beneficial for obesity prevention and treatment (28, 129, 133, 134). The sphingomyelin purified from chicken skin could significantly decrease hepatic lipid, plasma non-HDL cholesterol and insulin levels *via* improvement of adiponectin signaling such as adiponectin receptor 2 (*Adipor2*), peroxisome proliferator activated receptor alpha (*Ppara*), pyruvate dehydrogenase kinase 4 (*Pdk4*), and stearoyl CoA desaturase (*Scd1*) in Zucker rats fed a HFD (133). Dietary supplementation of sphingomyelin from egg yolk lowered the hepatic lipid content in mice fed a HFD, and intestinal cholesterol absorption content *via* inactivation of the LXR-SREBP-1c pathway, and increased fecal lipid and cholesterol output (28). Furthermore, dietary sphingomyelin from milk and egg yolk attenuated the HFD-induced hepatic steatosis *via* regulating the lipid absorption and metabolism, and lowered blood LPS *via* bifidogenic effects and alterations in distal gut microbiota (129, 134). Milk polar lipids containing 25% sphingomyelin may also affect gut physiology and the abundance of metabolically relevant bacteria in mice fed a HFD such as *Bifidobacterium* spp., *Akkermansia muciniphila* and *Lactobacillus reuteri*, which are associated with the fecal excretion of lipids and bile salts (135). In addition, the milk lipid concentrated-butter serum (LC-BS) and its main lipid fractions including ceramides and sphingomyelin can decrease TG and cholesterol levels in the liver and plasma of obese KK-A^y mice (136). These results indicate that dietary supplementation of sphingomyelin and ceramides may prevent fatty liver and hypercholesterolemia, and attenuate obesity.

Effects of dietary sphingomyelin on diabetes

Insulin resistance in peripheral tissues is one characteristic for the occurrence and development of T2DM. Mitochondrial dysfunctions lead to the accumulation of lipid-derived metabolites such as ceramides, which may increase the risk of diabetes (137). Endogenous ceramides can cause T2DM and its chronic complications through a variety of ways. Therefore, either inhibition of ceramide *de novo* synthesis to enhance the mitochondrial functions in HFD-fed and *db/db* mice (26), or enhancement of the ceramide degradation to form S1P is a potential method to reduce ceramide level and attenuate lipotoxicity associated with it (138). For example, promoting ceramide degradation may reduce the synthesis of harmful lipids and promote synthesis of those beneficial ones such as S1P (138). The treatment

with exogenous S1P significantly increases non-glucose stimulated insulin secretion in isolated mouse islets and HIT-T 15 cells *via* the activation of phospholipase C-Ca^{2+} system (139). The extracellular S1P can also attenuate the cytokine-induced apoptosis in pancreatic β cell through acting on its receptors, suggesting that S1P in the blood has potential protective effects *in vivo* (140). Milk sphingomyelin supplementation significantly increased fecal lipids, but lowered serum non-HDL cholesterol, hepatic TC and neutral lipids *via* regulating the mRNA levels of related genes for lipid metabolism in obese KK-A_y mice (29). Recently, treatments with exogenous glucosylceramides and ceramides from sea cucumber improve glucose tolerance and alleviate insulin resistance in high-fructose-diet-fed SD rats *via* upregulating the IRS/PI3K/Akt signaling pathway (141).

Effects of dietary sphingomyelin on cardiovascular diseases

Atherosclerotic dyslipidemia, related to insulin resistance and visceral obesity, are important risk factors for CVDs (142). In the development of atherosclerosis, the endogenous sphingomyelin on the arterial wall can be degraded into ceramide by SMase, while the increase in ceramide content will promote the aggregation of lipoproteins (103). Studies have found that the content of ceramides in atherosclerotic LDL is 10–50 times of the normal level (143), and the endogenous sphingomyelin level in the plasma is correlated with atherosclerosis, which has been implicated as a risk factor for coronary artery disease (27). Therefore, the rate-limiting enzymes for the *de novo* synthesis of ceramides and sphingomyelin such as SPT andSMS1/2 may be targets for pharmacological intervention to prevent or treat atherosclerosis. The SMS2 and ApoE double knockout (KO) mice have lower sphingomyelin levels in lipoproteins, and contents of sphingomyelin, ceramides, free cholesterol, and cholesteryl ester contents in the brachiocephalic artery (144). Endogenous sphingomyelin synthesis promotes atherosclerosis. However, dietary sphingomyelin appears to prevent atherosclerosis by inhibiting cholesterol absorption (30, 118–120), modifying the plasma and hepatic cholesterol and TG metabolism (116, 117), and influencing lipoprotein formation and mucosal growth in the gut (14). Dietary sphingomyelin from egg yolk does not affect circulating sphingomyelin levels or increase atherosclerosis in apoE$^{-/-}$ mice fed a HFD, but it is anti-atherogenic in apoE$^{-/-}$ mice fed a normal chow diet, which may be related to sphingomyelin-mediated alterations in gut flora, a topic that needs further investigation (30). Dietary sphingomyelin from egg yolk reduced aortic neutral lipid accumulation in aortic root lipid accumulation of apoE$^{-/-}$ mice fed a HFD, without affecting serum or hepatic lipids, as well as hepatic gene expression. Furthermore, there was a modest modulation of gut microbiota in apoE$^{-/-}$ mice fed a HFD supplemented with sphingomyelin from egg yolk. It is worth noting that the mass ratio of sphingomyelin to cholesterol is 1:2 in the diet, which is similar to the ratio in egg yolk, indicating that egg yolk food matrix may have health benefits and/or counteract effects of dietary cholesterol (128).

Dietary sphingomyelin from milk also lowered atherogenic lipoprotein cholesterol, reduced inflammation and attenuated atherosclerosis development in LDLr$^{-/-}$ mice fed a diet supplemented with anhydrous milk fat (31). Milk fat globule membrane (MFGM) comprises a core of TG surrounded by a structural membrane composed of phospholipids, cholesterol, proteins, and glycoproteins (145, 146). While compared with other animal-derived phospholipids containing lower than 5% sphingomyelin or plant-derived phospholipids without sphingomyelin, MFGM extracts have received widespread attention as a potential nutrient, especially their natural phospholipid composition (98, 147). A multi-center double-blind crossover study containing 58 overweight postmenopausal women (ages 56–62) shows that diets enriched with milk phospholipids can improve the cardiometabolic health by decreasing levels of blood lipids associated cardiometabolic risks and cholesterol absorption involving in specific interactions in the small intestine, and increasing cholesterol-ileal efflux and fecal loss of coprostanol without affecting the major bacterial phyla of gut microbiota and fecal SCFAs (32). In addition, diets enriched with milk phospholipids decreased the levels of blood ceramide (C24:1) and sphingomyelin (C16:1, C18:1) species to improve atherosclerosis, and increased total ceramides in feces (148).

Application of dietary sphingomyelin in food

Dairy products and infant formula

Urbanization and the general lack of time have shortened the nursing period despite great attempts to support breastfeeding for newborns. Only 35% of infants between the ages of birth and 6 months are breastfed globally (149). Substantial research has been conducted to study the potential application of MFGM in dairy products and infant formula (150–153). A recent review critically analyzed preclinical and clinical research data involving MFGM and its bioactive components in connection to the formation of gut microbiota, infection resistance, cognitive development, and infant metabolism (151). MFGM is highly organized and made up of a variety of elements, including polar lipids (phospholipids and glycosphingolipids), apolar lipids (cholesterol and cerebrosides) and specialized proteins (mostly glycoproteins) (154). Among them, sphingomyelin accounts

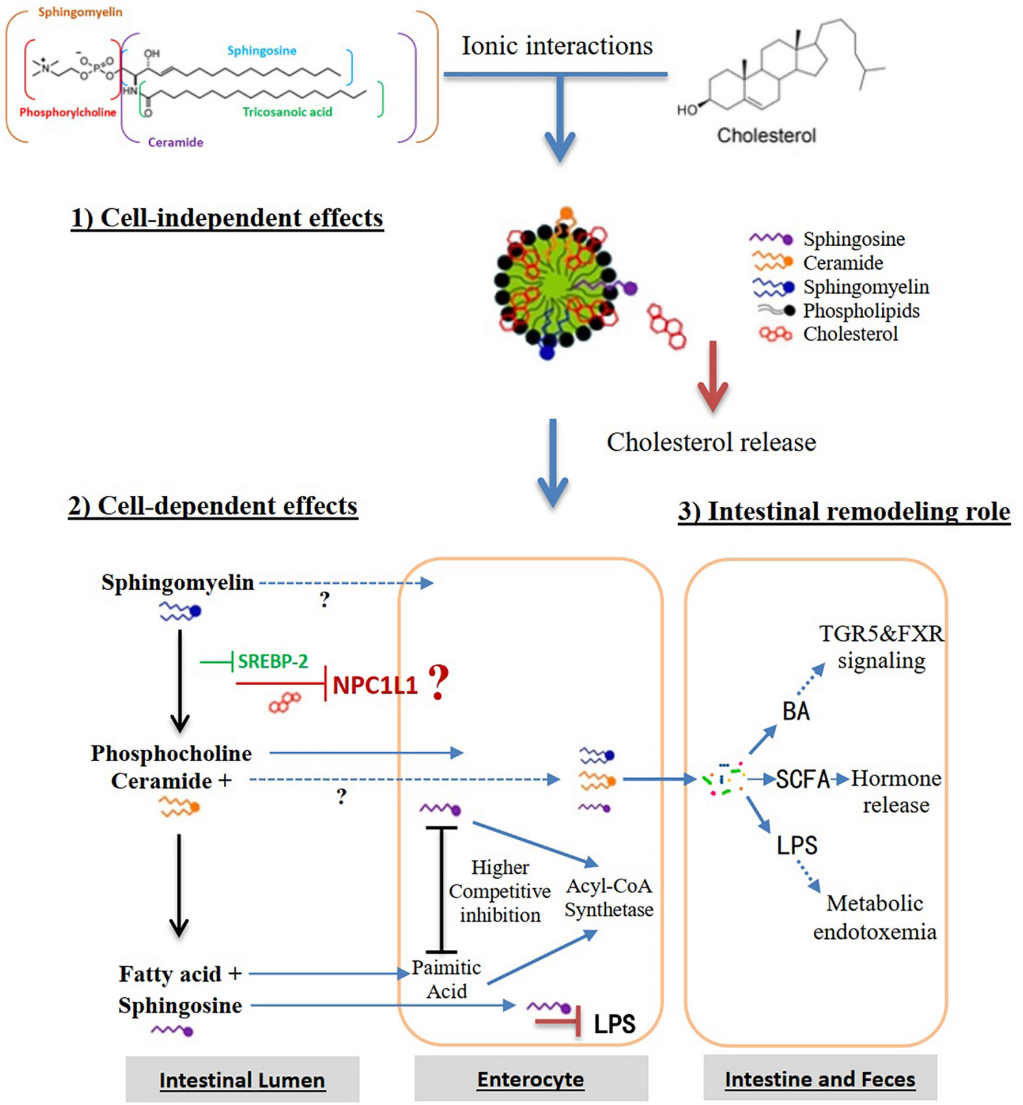

FIGURE 4
Hypothesis that dietary sphingomyelin inhibits the intestinal cholesterol absorption pathways. Alk-SMase, alkaline SMase; SREBP-2, sterol regulatory element-binding protein-2; NPC1L1, Niemann-Pick-Like Protein 1; N-CDase, neutral ceramidase; LPS, lipopolysaccharide; BA, bile acid; TGR5, Takeda G protein-coupled receptor 5; FXR, farnesoid X receptor; SCFA, short-chain fatty acids.

for over 25% of milk phospholipids (145, 146). Sphingomyelin is an essential component of the milk phospholipid fraction owing to its high concentration of the MFGM and positive impacts on human health, including brain development in babies and protection of neonates from bacterial infections (155). Interestingly, long-chain SFAs (C16:0, C22:0, C23:0, and C24:0) with high melting points make up around 97% of all MFGM sphingomyelins. Rarely, milk sphingomyelins include C23:0 fatty acids in amounts of 17% or higher (154). This distinguishing feature of milk sphingomyelins points to a distinct, most likely a biological, function much beyond its straightforward structural function in the MFGM. Albi et al. (152) hypothesized that the sphingomyelin in human breast milk is important for regulating gene expressions and forming myelin sheets to assist the neural development. Data of clinical and mechanistic preclinical studies indicate that full-fat dairy diets reduce cardiometabolic risk through boosting gut health, decreasing inflammation, and regulating dyslipidemia. These cardiometabolic advantages at the gut and systemic levels are attributed, at least in part, to milk polar lipids produced from the phospholipid- and sphingolipid-rich MFGM, which is more abundant in full-fat dairy milk (153). Deficiency of choline, a metabolite of sphingomyelin, may contribute to the decreased gain of lean body mass and pulmonary and neurocognitive development of premature newborns despite receiving enough macronutrients and gaining body

weight (156). At present, there are 3,939 patented inventions involving applications of sphingomyelin in infant formula milk worldwide.[1] As brain development occurs between 0 and 3 years of age, these findings suggest a novel intervention strategy to include sphingomyelin into newborn formulae to create products equivalent to breast feeding. Consequently, more patented inventions relate to infant formulae containing large lipid globules and/or those coated with sphingomyelin such as United States Patent No. 11389403 are developed to support infant growth trajectories or physical development during the first year of life more similar to those infants fed the breast milk (157). The synthetic composition described in United States Patent No. 11297872 includes sphingomyelin, choline, CIP, and other glycosphingolipids, as well as metabolic precursors and metabolites in formula milk. This composition may be used to support or optimize *de novo* myelination, as well as brain structure, brain connectivity, intellectual potential, cognitive potential, learning potential, and cognitive enjoyment in a formula fed subject (158). The creation of a lipid formulation that resembles the human milk fat composition would be a big step for the baby formula business and would allow to produce high-tech formulas for newborns.

Skin improvement

Any significant ultraviolet (UV) exposure sets off an inflammatory reaction in the epidermis, causing the skin to become dry and rough and compromising its barrier function (159). Photoaging, or prolonged exposure to UV radiation, affects both the dermal and epidermal layers of the skin, causing laxity, thickness, wrinkling, and changes in pigmentation (159, 160). Reactive oxygen species (ROS) are produced when skin is exposed to UV light. The oxidative damages due to the ROS production in keratinocytes and fibroblasts are reduced by protective and detoxifying non-enzymatic and enzymatic antioxidant molecules (161). Numerous dietary supplements have been shown to improve skin elasticity and health, including ascorbic acid, tocopherols, carotenoids, and polyphenols, which can be taken orally to prevent skin damages from UV radiation (159, 162, 163). The data of several animal research and clinical trials have shown the benefits of consumption of food-derived sphingomyelin and its' metabolites on skin health, which include those derived from plants, animals, and marine species (164–171). In comparison to control mice, the supplementation of sphingomyelin (146 mg/kg body weight/day) considerably reduced covalently bound ω-hydroxy ceramides and significantly attenuated an increase in transepidermal water loss (TEWL) (165). Dietary sphingomyelin seems to further improve skin condition even under normal circumstances. Using hairless mice, Haruta-Ono et al. found that dietary milk sphingomyelin markedly decreased TEWL and stratum corneum hydration on epidermal conditions in the sphingomyelin-fed animals (166–168). Dietary soy sauce Lees ceramide, which was more efficient than maize glucosylceramide, also dramatically improved epidermal barrier function and reduced TEWL in normal hairless mice (169). Evidence from clinical trials suggests that regular, long-term orally supplementation with sphingomyelin may improve skin health (170, 171). Oral sphingomyelin supplementation dramatically improved volunteers' perceptions of their skin's condition, including the moisture of their face skin and the appearance of wrinkles around their eyes, as well as the hydration of the skin at the heel and the flexibility of the skin under the eye (170). Sphingomyelin, glucosylceramide, and lactosylceramide were the key components of the milk sphingolipid-enriched fraction cream, which helped the skin's ability to retain water and maintain the barrier function (171). Experimental results suggest that the primary sphingoid bases in mammals, sphingosine and sphinganine from dietary sphingomyelin, may be partially reused in epidermal sphingolipids (168). Although the mechanism underlying skin condition enhancement is still not fully understood, previous studies have postulated some potential explanations. The fact that supplementary sphingomyelin reduced the covalently bound ω-hydroxy ceramides brought on by a single dose of UVB radiation is one reason for the mitigation of skin barrier deficiencies (165, 172). Dietary sphingolipids regulate the expressions of genes related to the development of the stratum corneum, which relates the production of the cornified envelope and tight junction proteins (173, 174). Another potential mechanism for the improvement of the skin barrier caused by dietary sphingomyelin is the reduction of the inflammatory response in the skin. According to Oba et al., in hairless mouse skin exposed to a single dose of UVB, the oral administration of milk sphingomyelin dramatically decreased the mRNA levels of genes linked to acute inflammation, such as thymic stromal lymphopoietin (TSLP), IL-1β, and IL-6 (165). The levels of thymus activation-regulated chemokine, and TSLP mRNA in hairless mice fed a magnesium-deficient diet were also markedly reduced by dietary milk sphingomyelin (172). Due to the functions of sphingomyelin and its metabolite ceramide to promote skin elasticity and health, there are more than 20,000 patents related to an effective ingredient of a skin beautifier and can be further blended with a food or feed to provide protection. Taking the United States Patent No. 20110065670 as an example, it relates to a meal or drink that improves the appearance of the skin as well as a skin beautifier that contains the useful element sphingomyelin and offers beauty benefits such skin moisturizing, skin beautification, wrinkle prevention, and skin roughness prevention (175).

1 https://www.freepatentsonline.com/

Delivery system

Vesicles, which include smaller vesicles, liposome, and exosomes with a diameter ranging from 30 to 100 nm, are biological entities encased by a membrane comprised of one or more lipid bilayers (176). Over the years, lipid vesicles have been regarded as effective medication delivery and carrier systems for bioactive compounds. Therefore, they are extensively employed in many different applications, including aesthetic, medicinal, therapeutic applications and growing food industry. Hydrophobic compounds can be solubilized inside of an aqueous vesicle since the vesicle is surrounded by a phospholipid bilayer (unilamellar vesicles or liposomes) or several concentric bilayers (multilamellar vesicles) (177). Lipid vesicles made of glycerophospholipids like soya lecithin or milk polar lipids, or model systems like dipalmitoyl-phosphatidylcholine, have been the primary focus of research for their potential use in the food industry (178, 179). Sphingomyelin molecules, the most abundant type of sphingolipid in biological membranes, perform structural functions and preferentially bind with cholesterol to create organized regions termed lipid rafts (126, 180). According to research by Morshed et al., lutein may be solubilized into the bilayers of egg-sphingomyelin vesicles, known as sphingosomes. This work opens up possibilities for the development of functional foods and drinks that are enriched with lutein and that have health benefits (177). The most thoroughly researched antimicrobial lipids are free fatty acids, monoglycerides, cholesteryl ester, sphingolipids, and others. Nano-sized lipid-based carriers may provide a tool of drug delivery for these antimicrobial agents, as they increase lipid solubility and dispersion in aqueous formulations. Additionally, nanocarriers may overcome drug resistance. Zhang et al. discussed several types of antimicrobial lipids in nanocarriers for the delivery of their activities. CAL02, a potential infection-controlling liposome composed of cholesterol and sphingomyelin, has been discussed as a novel anti-infection strategy, indicating that the antibacterial functions of antimicrobial lipids are worth to be investigated further (181). Sphingomyelin nanosystems are the promising form of carriers with potential for the combination of various types of medications (182–184). Bouzo et al. (182) encapsulated the anti-cancer drug etoposide in the sphingomyelin nanosystems, which mediated an antiproliferative response by interacting with colorectal cancer cells expressing the guanylyl cyclase receptor. Nagachinta et al. (183) designed sphingomyelin-based biocompatible nanosystems for intracellular delivery of microRNAs to colorectal cancer cells. Jatal et al. (184) revealed for the first time the possibility of combining sphingomyelin nanosystems with the 4N1Ks peptide for the development of novel senolytic cancer treatments. Therefore, sphingomyelin-based vesicles can be used to develop combination therapies. In addition, some inventions relate to the controlled delivery of different pharmaceutical agents (185–187). WIPO Patent No. WO/2001/041732 relates to compositions including sphingomyelins and methods for the intranasal delivery of active agents to the brain by means of neural pathways (188). WO/2022/047234 relates to devices and methods for the treatment of middle ear and/or inner ear disorders, and applicable to the treatment of other diseases in the human body. This kit includes sphingomyelins, stearyl, palmitoyl, tricosanyl sphingomyelins, ceramides, stearyl, palmitoyl ceramides, glycosphingolipids for delivering a drug formulation to treat diseases (189). The pharmaceutical agent protected by United States Patent No. 9186366 contains sphingomyelin and acts as a sialomucin secretion promoter, an antiallergic agent, an antioxidant, an infection defense agent, a hair growth agent, a therapeutic agent for demyelinating disease, an ant-pigmentation agent, an anti-inflammatory agent, or an agent that improves learning ability (190). As mentioned, sphingomyelin plays a role in cell structure, signaling, differentiation and functions. It is important to conduct more in *in vitro* and *in vivo* studies to assess the effectiveness of sphingomyelin vesicles in fortified foods.

Oil organogels

In food applications, the demand for plastic fats from plants and animals such as margarine and shortening is on the rise. However, the contents of SFAs and *trans* fatty acids (TFAs) are relatively high in the plastic fats, which has been linked to a number of negative health effects, including altered lipoprotein profiles and a higher risk of MetS and CVDs (191, 192). This has promoted the research of oil organogels instead of traditional plastic fats in the food industry. The organogelation of liquid vegetable oils has become a hot spot in the research of food-specific oils with the purpose of reducing the content of SFAs and TFAs and increasing the intake of MUFA and polyunsaturated fatty acids (PUFA) in our diets (193). Organogelation of liquid vegetable oil is to fix or confine the liquid vegetable oil in a thermally reversible network to obtain a three-dimensional supramolecular network and liquid oil co-exist structure system, so that it has specific structural and functional properties which is called oil organogels (194). Oil organogels are structural oils constructed by applying less than 5% oleogelators to liquid oil including vegetable waxes, fatty acids, hydroxylated fatty acids, fatty alcohols, fatty acid–fatty alcohol mixtures (stearic acid and stearyl alcohol), fatty esters, monoglycerides, diacylglycerides, phospholipids, ceramides, sorbitan monostearate, phytosterols, sterols (γ-oryzanol and β-sitosterol), tocopherol mixtures, polyphenols mixtures, lecithin–sorbitan tristearate mixtures (193–200). According to Rogers et al. (194), the architecture of mixed ceramide networks can be easily tailored to closely resemble colloidal fat crystal networks, such as translucent ceramide-canola oil gels with

2% synthetically pure ceramide, or opaque enzymatically hydrolyzed egg yolk sphingomyelin-canola oil gels with 7% crude extracts. Rogers et al. found that 2% *N*-acetyl-D-erythro-sphingosine (C2) and other short-chain ceramides were able to form edible oils like canola oil into self-assembling organogels without the addition of SFAs and TFAs. The viabilities of colon, prostate, ovarian, and leukemia cell lines were reduced by C2 ceramide, but not C18 ceramide (196). Due to the obvious side chain characteristics, the melting of the organogelator can be adjusted according to the application to obtain functional properties. Sphingomyelin-derived ceramides obtained from dairy products, eggs, and soybeans are mostly long-chain ceramides. The high melting temperature of ceramides might be beneficial since they provide thermal stability to systems such as chocolate. However, their application as food-grade oleogelators is limited due to their extremely crystalline fibril structures and high melting points. Guo et al. added phosphatidylcholine to the mixed gel system of ceramides, and optimized the gel performance by changing the molar ratio of the components and the gel formation temperature (197–199). Generally, the effect of multi-component systems of oleogelators is often better than that of a single-component, and the gel performance can be optimized by changing the ratios of the components. In addition, some inventions relate to oleogelators by adding sphingomyelin and its metabolites in foods, beverages, nutraceuticals, pharmaceuticals, pet foods, or animal feeds (201–203). Ceramides have limited applications in food-grade oleogelators due to their crystalline fibril structures and high melting points, but a variety of sphingomyelin and derivatives can be used for the food-grade oleogelators. Future study may be conducted on the functions of monomers and multi-component compounds in oil organogels.

Conclusion and perspectives

In this review, we summarized the content, structures, digestion, absorption, and metabolism of sphingolipids, and discussed the nutritional functioning of sphingomyelin in chronic metabolic diseases and the possible implications in food industry. Sphingolipids are a diverse category of chemically complicated molecules that are present in the brain, plasma, skin, and various foods including dairy, eggs, and soybeans. There is a need for a more comprehensive assessment of the varieties of sphingolipids in foods since certain diets may include adequate concentrations of atypical or typical sphingolipids that may have beneficial or detrimental impacts on human health. Many metabolites of sphingomyelin and derivatives are candidates for food-grade material, such as sphingoid bases, ceramides, C1P, whose structural formula are shown in **Table 1**. Sphingomyelin and ceramide are hardly absorbed in the small intestine. They can only be degraded into sphingosine to enter the circulation and be utilized by the body. Meanwhile, sphingoid bases, ceramides and sphingomyelin can also be interconverted, with ceramides being the central molecule. Ceramides can be desaturated to generate dihydroceramide, phosphorylated to form C1P and sphingomyelin, deacylated to generate sphingosine and then phosphorylated to produce S1P. Sphingomyelin is hydrolyzed by SMase to generate phosphorylcholine and ceramides, which in turn can be synthesized to C1P under the action of CerK. Phosphatidylcholine, sphingomyelin, and C1P are very similar in structure, with two long hydrophobic hydrocarbon chains and a polar head group. These characteristics of structure, absorption and metabolism can allow sphingomyelin and its metabolites to have wide applications in the food and pharmaceutical industry.

Clearly, dietary sphingomyelin benefits human health. Dietary sphingomyelin and its metabolites and derivatives have great potentials for clinical application in chronic diseases, cognitive development and intestinal health. **Table 3** summarizes the ways by which dietary sphingomyelin may be effective in chronic metabolic diseases, including inhibiting cholesterol absorption, modifying the plasma hepatic cholesterol and TG metabolism, influencing lipoprotein formation and mucosal growth in the gut, improving glucose tolerance and alleviating of insulin resistance, and modulating gut microbiota community. In addition, sphingolipids are prevalent in the brain, where they generate cell-type-specific profiles that vary throughout development, aging, and pathological brain changes. Bioactive metabolic intermediates of gangliosides and sphingomyelin, especially ceramides and S1P, have emerged as crucial players in the preservation of brain health (204). The related papers mentioned in this review provide important references for the design of dietary sphingomyelin in the future.

When compared to other nutrients, dietary sphingolipids have drawn less attention and remain to be fully understood. Since no indication of sphingomyelin deficiency has been observed, it is not considered an essential nutrient. Many hypotheses have been proposed to explain the functional mechanism of sphingomyelin and its metabolites. However, many questions how dietary sphingomyelin and its metabolites influence a variety of intricate cell functions still remain unanswered. Future investigations are needed to determine the fate of the exogenously added sphingomyelin, and differentiate the roles of sphingomyelin itself and its metabolites. Especially, endogenous sphingomyelin is involved in pathological changes in obesity, diabetes and atherosclerosis; however, exogenous dietary sphingomyelin and its metabolites have been shown to maintain cholesterol homeostasis and lipid metabolism, as well as the prevention or treatment of chronic metabolic diseases. This seemingly paradoxical phenomenon needs to be further verified by rigorous clinical trials and its mechanism should be explored in more depth. Understanding of the

underlying molecular mechanisms provide novel intervention strategies and target for the prevention and treatment of a variety of human illnesses. In general, the exciting but unexplained phenomenon shows that dietary sphingomyelin and its metabolites are candidates for food additives in food industry or natural medicines for metabolic related disease prevention.

Author contributions

FY searched the publications, summarized the data in tables, drew figures, discussed the literature, and wrote the review. GC modified the review. Both authors read and approved the final version of this review.

Funding

We gratefully acknowledge the financial support from the Scientific Research Project of Hubei Provincial Health Commission (WJ2021Q050) and the Scientific Research Project of Hubei Provincial Department of Education (Q20202009).

Conflict of interest

The authors declare that the research was conducted in the absence of any commercial or financial relationships that could be construed as a potential conflict of interest.

Publisher's note

All claims expressed in this article are solely those of the authors and do not necessarily represent those of their affiliated organizations, or those of the publisher, the editors and the reviewers. Any product that may be evaluated in this article, or claim that may be made by its manufacturer, is not guaranteed or endorsed by the publisher.

References

1. Lagace TA, Ridgway ND. The role of phospholipids in the biological activity and structure of the endoplasmic reticulum. *Biochim Biophys Acta.* (2013) 1833:2499–510. doi: 10.1016/j.bbamcr.2013.05.018

2. Fahy E, Subramaniam S, Brown HA, Glass CK, Merrill AH Jr, Murphy RC, et al. A comprehensive classification system for lipids. *J Lipid Res.* (2005) 46:839–61. doi: 10.1194/jlr.E400004-JLR200

3. Li W, Belwal T, Li L, Xu Y, Liu J, Zou L, et al. Sphingolipids in foodstuff: compositions, distribution, digestion, metabolism and health effects - A comprehensive review. *Food Res Int.* (2021) 147:110566. doi: 10.1016/j.foodres.2021.110566

4. Merrill AH. Chapter 13 - Sphingolipids. In: Vance DE, Vance JE editors. *Biochemistry of Lipids, Lipoproteins and Membranes.* San Diego, CA: Elsevier (2008). p. 363–97.

5. Nature Chemical Biology,. Unlocking the lipid labyrinth. *Nat Chem Biol.* (2010) 6:471. doi: 10.1038/nchembio.404

6. Duan R-D. Physiological functions and clinical implications of sphingolipids in the gut. *J Digest Dis.* (2011) 12:60–70. doi: 10.1111/j.1751-2980.2011.00481.x

7. Danielsen EM, Hansen GH. Lipid raft organization and function in brush borders of epithelial cells. *Mol Membr Biol.* (2006) 23:71–9. doi: 10.1080/09687860500445604

8. Vesper H, Schmelz EM, Nikolova-Karakashian MN, Dillehay DL, Lynch DV, Merrill AH Jr. Sphingolipids in food and the emerging importance of sphingolipids to nutrition. *J Nutr.* (1999) 129:1239–50. doi: 10.1093/jn/129.7.1239

9. Mandon EC, Ehses I, Rother J, van Echten G, Sandhoff K. Subcellular localization and membrane topology of serine palmitoyltransferase, 3-dehydrosphinganine reductase, and sphinganine N-acyltransferase in mouse liver. *J Biol Chem.* (1992) 267:11144–8.

10. Michel C, van Echten-Deckert G. Conversion of dihydroceramide to ceramide occurs at the cytosolic face of the endoplasmic reticulum. *FEBS Lett.* (1997) 416:153–5. doi: 10.1016/S0014-5793(97)01187-3

11. Kajiwara K, Ikeda A, Aguilera-Romero A, Castillon GA, Kagiwada S, Hanada K, et al. Osh proteins regulate COPII-mediated vesicular transport of ceramide from the endoplasmic reticulum in budding yeast. *J Cell Sci.* (2014) 127(Pt. 2):376–87. doi: 10.1242/jcs.132001

12. Barenholz Y, Gatt S. Chapter 4 Sphingomyelin: metabolism, chemical synthesis, chemical and physical properties. In: Hawthorne JN, Ansell GB editors. *New Comprehensive Biochemistry.* (Vol. 4), Amsterdam: Elsevier (1982). p. 129–77.

13. Ohlsson L, Hertervig E, Jönsson BA, Duan RD, Nyberg L, Svernlöv R, et al. Sphingolipids in human ileostomy content after meals containing milk sphingomyelin. *Am J Clin Nutr.* (2010) 91:672–8. doi: 10.3945/ajcn.2009.28311

14. Nilsson A, Duan RD. Absorption and lipoprotein transport of sphingomyelin. *J Lipid Res.* (2006) 47:154–71. doi: 10.1194/jlr.M500357-JLR200

15. Schmelz EM, Crall KJ, Larocque R, Dillehay DL, Merrill AH Jr. Uptake and metabolism of sphingolipids in isolated intestinal loops of mice. *J Nutr.* (1994) 124:702–12. doi: 10.1093/jn/124.5.702

16. Chocian G, Chabowski A, żendzian-Piotrowska M, Harasim E, Łukaszuk B, Górski J. High fat diet induces ceramide and sphingomyelin formation in rat's liver nuclei. *Mol Cell Biochem.* (2010) 340:125–31. doi: 10.1007/s11010-010-0409-6

17. Wang DD, Toledo E, Hruby A, Rosner BA, Willett WC, Sun Q, et al. Plasma ceramides, mediterranean diet, and incident cardiovascular disease in the PREDIMED trial (prevención con dieta mediterránea). *Circulation.* (2017) 135:2028–40. doi: 10.1161/circulationaha.116.024261

18. Zhao P, Liu ID, Hodgin JB, Benke PI, Selva J, Torta F, et al. Responsiveness of sphingosine phosphate lyase insufficiency syndrome to vitamin B6 cofactor supplementation. *J Inherit Metab Dis.* (2020) 43:1131–42. doi: 10.1002/jimd.12238

19. Beattie AE, Clarke DJ, Wadsworth JM, Lowther J, Sin HL, Campopiano DJ. Reconstitution of the pyridoxal 5′-phosphate (PLP) dependent enzyme serine palmitoyltransferase (SPT) with pyridoxal reveals a crucial role for the phosphate during catalysis. *Chem Commun.* (2013) 49:7058–60. doi: 10.1039/c3cc43001d

20. Kim KP, Shin KO, Park K, Yun HJ, Mann S, Lee YM, et al. Vitamin C stimulates epidermal ceramide production by regulating its metabolic enzymes. *Biomol Ther.* (2015) 23:525–30. doi: 10.4062/biomolther.2015.044

21. Koch A, Grammatikos G, Trautmann S, Schreiber Y, Thomas D, Bruns F, et al. Vitamin D supplementation enhances C18(dihydro)ceramide levels in type 2 diabetes patients. *Int J Mol Sci.* (2017) 18:1532. doi: 10.3390/ijms18071532

22. Jiang Q, Rao X, Kim CY, Freiser H, Zhang Q, Jiang Z, et al. Gamma-tocotrienol induces apoptosis and autophagy in prostate cancer cells by increasing

intracellular dihydrosphingosine and dihydroceramide. *Int J Cancer.* (2012) 130:685–93. doi: 10.1002/ijc.26054

23. Fischbeck A, Krüger M, Blaas N, Humpf H-U. Analysis of sphingomyelin in meat based on hydrophilic interaction liquid chromatography coupled to electrospray ionization-tandem mass spectrometry (HILIC-HPLC-ESI-MS/MS). *J Agric Food Chem.* (2009) 57:9469–74. doi: 10.1021/jf90 25376

24. Walls SM Jr., Attle SJ, Brulte GB, Walls ML, Finley KD, Chatfield DA, et al. Identification of sphingolipid metabolites that induce obesity *via* misregulation of appetite, caloric intake and fat storage in *Drosophila*. *PLoS Genet.* (2013) 9:e1003970. doi: 10.1371/journal.pgen.1003970

25. Le Barz M, Boulet MM, Calzada C, Cheillan D, Michalski M-C. Alterations of endogenous sphingolipid metabolism in cardiometabolic diseases: towards novel therapeutic approaches. *Biochimie.* (2020) 169:133–43. doi: 10.1016/j.biochi.2019. 10.003

26. Ussher JR, Koves TR, Cadete VJ, Zhang L, Jaswal JS, Swyrd SJ, et al. Inhibition of de novo ceramide synthesis reverses diet-induced insulin resistance and enhances whole-body oxygen consumption. *Diabetes.* (2010) 59:2453–64. doi: 10.2337/db09-1293

27. Jiang XC, Paultre F, Pearson TA, Reed RG, Francis CK, Lin M, et al. Plasma sphingomyelin level as a risk factor for coronary artery disease. *Arterioscler Thromb Vasc Biol.* (2000) 20:2614–8. doi: 10.1161/01.atv.20.12. 2614

28. Chung RW, Kamili A, Tandy S, Weir JM, Gaire R, Wong G, et al. Dietary sphingomyelin lowers hepatic lipid levels and inhibits intestinal cholesterol absorption in high-fat-fed mice. *PLoS One.* (2013) 8:e55949. doi: 10.1371/journal. pone.0055949

29. Yamauchi I, Uemura M, Hosokawa M, Iwashima-Suzuki A, Shiota M, Miyashita K. The dietary effect of milk sphingomyelin on the lipid metabolism of obese/diabetic KK-A(y) mice and wild-type C57BL/6J mice. *Food Funct.* (2016) 7:3854–67. doi: 10.1039/c6fo00274a

30. Chung RWS, Wang Z, Bursill CA, Wu BJ, Barter PJ, Rye KA. Effect of long-term dietary sphingomyelin supplementation on atherosclerosis in mice. *PLoS One.* (2017) 12:e0189523. doi: 10.1371/journal.pone.0189523

31. Millar CL, Jiang C, Norris GH, Garcia C, Seibel S, Anto L, et al. Cow's milk polar lipids reduce atherogenic lipoprotein cholesterol, modulate gut microbiota and attenuate atherosclerosis development in LDL-receptor knockout mice fed a Western-type diet. *J Nutr Biochem.* (2020) 79:108351. doi: 10.1016/j.jnutbio.2020. 108351

32. Vors C, Joumard-Cubizolles L, Lecomte M, Combe E, Ouchchane L, Drai J, et al. Milk polar lipids reduce lipid cardiovascular risk factors in overweight postmenopausal women: towards a gut sphingomyelin-cholesterol interplay. *Gut.* (2020) 69:487–501. doi: 10.1136/gutjnl-2018-318155

33. Yu D, Rupasinghe TWT, Boughton BA, Natera SHA, Hill CB, Tarazona P, et al. A high-resolution HPLC-QqTOF platform using parallel reaction monitoring for in-depth lipid discovery and rapid profiling. *Anal Chim Acta.* (2018) 1026:87–100. doi: 10.1016/j.aca.2018.03.062

34. Wang X, Wang Y, Xu J, Xue C. Sphingolipids in food and their critical roles in human health. *Crit Rev Food Sci Nutr.* (2021) 61:462–91. doi: 10.1080/10408398. 2020.1736510

35. Karlsson KA. On the chemistry and occurrence of sphingolipid long-chain bases. *Chem Phys Lipids.* (1970) 5:6–43. doi: 10.1016/0009-3084(70)90008-3

36. Karlsson KA. Sphingolipid long chain bases. *Lipids.* (1970) 5:878–91. doi: 10.1007/BF02531119

37. Stewart ME, Downing DT. Free sphingosines of human skin include 6-hydroxysphingosine and unusually long-chain dihydrosphingosines. *J Invest Dermatol.* (1995) 105:613–8. doi: 10.1111/1523-1747.ep12323736

38. Pruett ST, Bushnev A, Hagedorn K, Adiga M, Haynes CA, Sullards MC, et al. Biodiversity of sphingoid bases ("sphingosines") and related amino alcohols. *J Lipid Res.* (2008) 49:1621–39. doi: 10.1194/jlr.R800012-JLR200

39. Merrill AH Jr. Sphingolipid and glycosphingolipid metabolic pathways in the era of sphingolipidomics. *Chem Rev.* (2011) 111:6387–422. doi: 10.1021/ cr2002917

40. Maula T, Al Sazzad MA, Slotte JP. Influence of hydroxylation, chain length, and chain unsaturation on bilayer properties of ceramides. *Biophys J.* (2015) 109:1639–51. doi: 10.1016/j.bpj.2015.08.040

41. Norris GH, Blesso CN. Dietary and endogenous sphingolipid metabolism in chronic inflammation. *Nutrients.* (2017) 9:1180. doi: 10.3390/nu9111180

42. Cutillo G, Saariaho AH, Meri S. Physiology of gangliosides and the role of antiganglioside antibodies in human diseases. *Cell Mol Immunol.* (2020) 17:313–22. doi: 10.1038/s41423-020-0388-9

43. Simenel C, Coddeville B, Delepierre M, Latge JP, Fontaine T. Glycosylinositolphosphoceramides in *Aspergillus fumigatus*. *Glycobiology.* (2008) 18:84–96. doi: 10.1093/glycob/cwm122

44. Nemes Z, Marekov LN, Fesus L, Steinert PM. A novel function for transglutaminase 1: attachment of long-chain omega-hydroxyceramides to involucrin by ester bond formation. *Proc Natl Acad Sci U.S.A.* (1999) 96:8402–7. doi: 10.1073/pnas.96.15.8402

45. Engelking LR. Chapter 59 - Sphingolipids. Third ed. In: Engelking LR editor. *Textbook of Veterinary Physiological Chemistry*. Boston, MA: Academic Press (2015). p. 378–83. doi: 10.1016/j.jnutbio.2018.02.015

46. Kolter T. A view on sphingolipids and disease. *Chem Phys Lipids.* (2011) 164:590–606. doi: 10.1016/j.chemphyslip.2011.04.013

47. Han X, Jiang X. A review of lipidomic technologies applicable to sphingolipidomics and their relevant applications. *Eur J Lipid Sci Technol.* (2009) 111:39–52. doi: 10.1002/ejlt.200800117

48. Penno A, Reilly MM, Houlden H, Laurá M, Rentsch K, Niederkofler V, et al. Hereditary sensory neuropathy type 1 is caused by the accumulation of two neurotoxic sphingolipids. *J Biol Chem.* (2010) 285:11178–87. doi: 10.1074/jbc. M109.092973

49. Lynch DV, Dunn TM. An introduction to plant sphingolipids and a review of recent advances in understanding their metabolism and function. *New Phytol.* (2004) 161:677–702. doi: 10.1111/j.1469-8137.2004.00992.x

50. Sugawara T, Aida K, Duan J, Hirata T. Analysis of glucosylceramides from various sources by liquid chromatography-ion trap mass spectrometry. *J Oleo Sci.* (2010) 59:387–94. doi: 10.5650/jos.59.387

51. Ternes P, Sperling P, Albrecht S, Franke S, Cregg JM, Warnecke D, et al. Identification of fungal sphingolipid C9-methyltransferases by phylogenetic profiling. *J Biol Chem.* (2006) 281:5582–92. doi: 10.1074/jbc.M512864200

52. Hellgren LI. Occurrence of bioactive sphingolipids in meat and fish products. *Eur J Lipid Sci Technol.* (2001) 103:661–7. doi: 10.1002/1438-9312(200110)103: 103.0.CO;2-8

53. Hellgren LI, Nordby P. Chapter 17 - Bioactive lipids in dairy fat. In: Watson RR, Collier RJ, Preedy VR editors. *Dairy in Human Health and Disease Across the Lifespan*. Cambridge, MA: Academic Press (2017). p. 233–7.

54. Norris GH, Milard M, Michalski MC, Blesso CN. Protective properties of milk sphingomyelin against dysfunctional lipid metabolism, gut dysbiosis, and inflammation. *J Nutr Biochem.* (2019) 73:108224. doi: 10.1016/j.jnutbio.2019. 108224

55. Ahn EH, Schroeder JJ. Bioactive sphingolipids are constituents of soy and dairy products. *J Food Sci.* (2002) 67:522–4. doi: 10.1111/j.1365-2621.2002. tb10630.x

56. Blesso CN. Egg phospholipids and cardiovascular health. *Nutrients.* (2015) 7:2731–47. doi: 10.3390/nu7042731

57. Blaas N, Humpf H-U. Structural profiling and quantitation of glycosyl Inositol phosphoceramides in plants with fourier transform mass spectrometry. *J Agric Food Chem.* (2013) 61:4257–69. doi: 10.1021/jf4001499

58. Pata MO, Hannun YA, Ng CK. Plant sphingolipids: decoding the enigma of the Sphinx. *New Phytol.* (2010) 185:611–30. doi: 10.1111/j.1469-8137.2009.03123. x

59. Sperling P, Heinz E. Plant sphingolipids: structural diversity, biosynthesis, first genes and functions. *Biochim Biophys Acta.* (2003) 1632:1–15. doi: 10.1016/ s1388-1981(03)00033-7

60. Hannich JT, Umebayashi K, Riezman H. Distribution and functions of sterols and sphingolipids. *Cold Spring Harb Perspect Biol.* (2011) 3:a004762. doi: 10.1101/ cshperspect.a004762

61. Gault CR, Obeid LM, Hannun YA. An overview of sphingolipid metabolism: from synthesis to breakdown. *Adv Exp Med Biol.* (2010) 688:1–23. doi: 10.1007/ 978-1-4419-6741-1_1

62. Ha CE, Bhagavan NV. Chapter 16 - Lipids II: phospholipids, glycosphingolipids, and cholesterol. Third ed. In: Ha CE, Bhagavan NV editors. *Essentials of Medical Biochemistry*. San Diego, CA: Academic Press (2023). p. 355–83.

63. Bode H, Bourquin F, Suriyanarayanan S, Wei Y, Alecu I, Othman A, et al. HSAN1 mutations in serine palmitoyltransferase reveal a close structure-function-phenotype relationship. *Hum Mol Genet.* (2016) 25:853–65. doi: 10. 1093/hmg/ddv611

64. Hornemann T, Penno A, Rütti MF, Ernst D, Kivrak-Pfiffner F, Rohrer L, et al. The SPTLC3 subunit of serine palmitoyltransferase generates short chain sphingoid bases. *J Biol Chem.* (2009) 284:26322–30. doi: 10.1074/jbc.M109.023192

65. Harmon JM, Bacikova D, Gable K, Gupta SD, Han G, Sengupta N, et al. Topological and functional characterization of the ssSPTs, small activating

subunits of serine palmitoyltransferase. *J Biol Chem.* (2013) 288:10144–53. doi: 10.1074/jbc.M113.451526

66. Levy M, Futerman AH. Mammalian ceramide synthases. *IUBMB Life.* (2010) 62:347–56. doi: 10.1002/iub.319

67. Geeraert L, Mannaerts GP, van Veldhoven PP. Conversion of dihydroceramide into ceramide: involvement of a desaturase. *Biochem J.* (1997) 327 (Pt. 1):125–32. doi: 10.1042/bj3270125

68. Sassa T, Kihara A. Metabolism of very long-chain Fatty acids: genes and pathophysiology. *Biomol Ther.* (2014) 22:83–92. doi: 10.4062/biomolther.2014.017

69. Cingolani F, Futerman AH, Casas J. Ceramide synthases in biomedical research. *Chem Phys Lipids.* (2016) 197:25–32. doi: 10.1016/j.chemphyslip.2015.07.026

70. Hanada K, Kumagai K, Yasuda S, Miura Y, Kawano M, Fukasawa M, et al. Molecular machinery for non-vesicular trafficking of ceramide. *Nature.* (2003) 426:803–9. doi: 10.1038/nature02188

71. Tafesse FG, Ternes P, Holthuis JC. The multigenic sphingomyelin synthase family. *J Biol Chem.* (2006) 281:29421–5. doi: 10.1074/jbc.R600021200

72. Mitsutake S, Igarashi Y. Chapter Twelve - Sphingolipids in lipid microdomains and obesity. In: Litwack G editor. *Vitamins & Hormones.* (Vol. 91), Cambridge, MA: Academic Press (2013). p. 271–84.

73. Jeckel D, Karrenbauer A, Burger KN, van Meer G, Wieland F. Glucosylceramide is synthesized at the cytosolic surface of various Golgi subfractions. *J Cell Biol.* (1992) 117:259–67. doi: 10.1083/jcb.117.2.259

74. Chatterjee S, Castiglione E. UDPgalactose:glucosylceramide beta 1—-4-galactosyltransferase activity in human proximal tubular cells from normal and familial hypercholesterolemic homozygotes. *Biochim Biophys Acta.* (1987) 923:136–42. doi: 10.1016/0304-4165(87)90136-x

75. D'Angelo G, Polishchuk E, Di Tullio G, Santoro M, Di Campli A, Godi A, et al. Glycosphingolipid synthesis requires FAPP2 transfer of glucosylceramide. *Nature.* (2007) 449:62–7. doi: 10.1038/nature06097

76. Hannun YA, Obeid LM. Sphingolipids and their metabolism in physiology and disease. *Nat Rev Mol Cell Biol.* (2018) 19:175–91. doi: 10.1038/nrm.2017.107

77. Bartke N, Hannun YA. Bioactive sphingolipids: metabolism and function. *J Lipid Res.* (2009) 50(Suppl.):S91–6. doi: 10.1194/jlr.R800080-JLR200

78. Rovina P, Schanzer A, Graf C, Mechtcheriakova D, Jaritz M, Bornancin F. Subcellular localization of ceramide kinase and ceramide kinase-like protein requires interplay of their Pleckstrin Homology domain-containing N-terminal regions together with C-terminal domains. *Biochim Biophys Acta.* (2009) 1791:1023–30. doi: 10.1016/j.bbalip.2009.05.009

79. Ferreira NS, Engelsby H, Neess D, Kelly SL, Volpert G, Merrill AH, et al. Regulation of very-long acyl chain ceramide synthesis by acyl-CoA-binding protein. *J Biol Chem.* (2017) 292:7588–97. doi: 10.1074/jbc.M117.785345

80. Grond S, Eichmann TO, Dubrac S, Kolb D, Schmuth M, Fischer J, et al. PNPLA1 deficiency in mice and humans leads to a defect in the synthesis of Omega-O-Acylceramides. *J Invest Dermatol.* (2017) 137:394–402. doi: 10.1016/j.jid.2016.08.036

81. Nagahashi M, Takabe K, Terracina KP, Soma D, Hirose Y, Kobayashi T, et al. Sphingosine-1-phosphate transporters as targets for cancer therapy. *Biomed Res Int.* (2014) 2014:651727. doi: 10.1155/2014/651727

82. Kim YM, Park TS, Kim SG. The role of sphingolipids in drug metabolism and transport. *Expert Opin Drug Metab Toxicol.* (2013) 9:319–31. doi: 10.1517/17425255.2013.748749

83. Johnson KR, Johnson KY, Becker KP, Bielawski J, Mao C, Obeid LM. Role of human sphingosine-1-phosphate phosphatase 1 in the regulation of intra- and extracellular sphingosine-1-phosphate levels and cell viability. *J Biol Chem.* (2003) 278:34541–7. doi: 10.1074/jbc.M301741200

84. Riboni L, Bassi R, Caminiti A, Prinetti A, Viani P, Tettamanti G. Metabolic fate of exogenous sphingosine in neuroblastoma neuro2A cells. Dose-dependence and biological effects. *Ann N Y Acad Sci.* (1998) 845:46–56. doi: 10.1111/j.1749-6632.1998.tb09661.x

85. Hetz CA, Hunn M, Rojas P, Torres V, Leyton L, Quest AF. Caspase-dependent initiation of apoptosis and necrosis by the Fas receptor in lymphoid cells: onset of necrosis is associated with delayed ceramide increase. *J Cell Sci.* (2002) 115(Pt. 23):4671–83. doi: 10.1242/jcs.00153

86. Cuvillier O. Sphingosine in apoptosis signaling. *Biochim Biophys Acta.* (2002) 1585:153–62. doi: 10.1016/s1388-1981(02)00336-0

87. Cowart LA. Sphingolipids: players in the pathology of metabolic disease. *Trends Endocrinol Metab.* (2009) 20:34–42. doi: 10.1016/j.tem.2008.09.004

88. Blachnio-Zabielska AU, Chacinska M, Vendelbo MH, Zabielski P. The crucial role of C18-Cer in fat-induced skeletal muscle insulin resistance. *Cell Physiol Biochem.* (2016) 40:1207–20. doi: 10.1159/000453174

89. Choi S, Snider AJ. Sphingolipids in high fat diet and obesity-related diseases. *Mediators Inflamm.* (2015) 2015:520618. doi: 10.1155/2015/520618

90. Kahle M, Schäfer A, Seelig A, Schultheiß J, Wu M, Aichler M, et al. High fat diet-induced modifications in membrane lipid and mitochondrial-membrane protein signatures precede the development of hepatic insulin resistance in mice. *Mol Metab.* (2015) 4:39–50. doi: 10.1016/j.molmet.2014.11.004

91. Gomez-Muñoz A, Presa N, Gomez-Larrauri A, Rivera I-G, Trueba M, Ordoñez M. Control of inflammatory responses by ceramide, sphingosine 1-phosphate and ceramide 1-phosphate. *Prog Lipid Res.* (2016) 61:51–62. doi: 10.1016/j.plipres.2015.09.002

92. Trichopoulou A. Traditional Mediterranean diet and longevity in the elderly: a review. *Public Health Nutr.* (2004) 7:943–7. doi: 10.1079/PHN2004558

93. Estruch R, Ros E, Salas-Salvadó J, Covas MI, Corella D, Arós F, et al. Primary prevention of cardiovascular disease with a mediterranean diet supplemented with extra-virgin olive oil or nuts. *N Engl J Med.* (2018) 378:e34. doi: 10.1056/NEJMoa1800389

94. Jiang XC, Li Z. Sphingolipids and cholesterol. *Adv Exp Med Biol.* (2022) 1372:1–14. doi: 10.1007/978-981-19-0394-6_1

95. Bouhours JF, Guignard H. Free ceramide, sphingomyelin, and glucosylceramide of isolated rat intestinal cells. *J Lipid Res.* (1979) 20:879–907.

96. Breimer ME, Hansson GC, Karlsson KA, Leffler H. Studies on differentiating epithelial cells of rat small intestine. Alterations in the lipophilic part of glycosphingolipids during cell migration from crypt villus tip. *Biochim Biophys Acta.* (1982) 710:415–27. doi: 10.1016/0005-2760(82)90125-4

97. Bouhours JF, Bouhours D, Hansson GC. Developmental changes of glycosphingolipid composition of epithelia of rat digestive tract. *Adv Lipid Res.* (1993) 26:353–72.

98. Cohn JS, Kamili A, Wat E, Chung RW, Tandy S. Dietary phospholipids and intestinal cholesterol absorption. *Nutrients.* (2010) 2:116–27. doi: 10.3390/nu2020116

99. Norris GH, Blesso CN. Dietary sphingolipids: potential for management of dyslipidemia and nonalcoholic fatty liver disease. *Nutr Rev.* (2017) 75:274–85. doi: 10.1093/nutrit/nux004

100. Minamioka H, Imai H. Sphingoid long-chain base composition of glucosylceramides in *Fabaceae:* a phylogenetic interpretation of *Fabeae*. *J Plant Res.* (2009) 122:415. doi: 10.1007/s10265-009-0227-7

101. Nilsson Å, Duan RD, Ohlsson L. Digestion and absorption of milk phospholipids in newborns and adults. *Front Nutr.* (2021) 8:724006. doi: 10.3389/fnut.2021.724006

102. Nyberg L, Farooqi A, Bläckberg L, Duan RD, Nilsson A, Hernell O. Digestion of ceramide by human milk bile salt-stimulated lipase. *J Pediatr Gastroenterol Nutr.* (1998) 27:560–7. doi: 10.1097/00005176-199811000-00013

103. Iqbal J, Walsh MT, Hammad SM, Hussain MM. Sphingolipids and lipoproteins in health and metabolic disorders. *Trends Endocrinol Metab.* (2017) 28:506–18. doi: 10.1016/j.tem.2017.03.005

104. Hammad SM, Pierce JS, Soodavar F, Smith KJ, Al Gadban MM, Rembiesa B, et al. Blood sphingolipidomics in healthy humans: impact of sample collection methodology. *J Lipid Res.* (2010) 51:3074–87. doi: 10.1194/jlr.D008532

105. Dougherty RM, Galli C, Ferro-Luzzi A, Iacono JM. Lipid and phospholipid fatty acid composition of plasma, red blood cells, and platelets and how they are affected by dietary lipids: a study of normal subjects from Italy, Finland, and the USA. *Am J Clin Nutr.* (1987) 45:443–55. doi: 10.1093/ajcn/45.2.443

106. Bagdade JD, Subbaiah PV. Abnormal high-density lipoprotein composition in women with insulin-dependent diabetes. *J Lab Clin Med.* (1989) 113:235–40.

107. Illingworth DR. Lipoprotein metabolism. *Am J Kidney Dis.* (1993) 22:90–7. doi: 10.1016/s0272-6386(12)70173-7

108. Wang N, Lan D, Gerbod-Giannone M, Linsel-Nitschke P, Jehle AW, Chen W, et al. ATP-binding cassette transporter A7 (ABCA7) binds apolipoprotein A-I and mediates cellular phospholipid but not cholesterol efflux. *J Biol Chem.* (2003) 278:42906–12. doi: 10.1074/jbc.M307831200

109. Kobayashi A, Takanezawa Y, Hirata T, Shimizu Y, Misasa K, Kioka N, et al. Efflux of sphingomyelin, cholesterol, and phosphatidylcholine by ABCG1. *J Lipid Res.* (2006) 47:1791–802. doi: 10.1194/jlr.M500546-JLR200

110. Hotta N, Abe-Dohmae S, Taguchi R, Yokoyama S. Preferential incorporation of shorter and less unsaturated acyl phospholipids into high density lipoprotein-like particles in the ABCA1- and ABCA7-mediated biogenesis with apoA-I. *Chem Phys Lipids.* (2015) 187:1–9. doi: 10.1016/j.chemphyslip.2015.01.005

111. Raggers RJ, van Helvoort A, Evers R, van Meer G. The human multidrug resistance protein MRP1 translocates sphingolipid analogs across the plasma membrane. *J Cell Sci.* (1999) 112:415–22. doi: 10.1242/jcs.112.3.415

112. Ishibashi Y, Kohyama-Koganeya A, Hirabayashi Y. New insights on glucosylated lipids: metabolism and functions. *Biochim Biophys Acta.* (2013) 1831:1475–85. doi: 10.1016/j.bbalip.2013.06.001

113. Hammad SM. Blood sphingolipids in homeostasis and pathobiology. *Adv Exp Med Biol.* (2011) 721:57–66. doi: 10.1007/978-1-4614-0650-1_4

114. McCracken E, Monaghan M, Sreenivasan S. Pathophysiology of the metabolic syndrome. *Clin Dermatol.* (2018) 36:14–20. doi: 10.1016/j.clindermatol.2017.09.004

115. Zakir F, Mohapatra S, Farooq U, Mirza MA, Iqbal Z. Chapter 1 - Introduction to metabolic disorders. In: Dureja H, Murthy SN, Wich PR, Dua K editors. *Drug Delivery Systems for Metabolic Disorders*. Cambridge, MA: Academic Press (2022). p. 1–20.

116. Imaizumi K, Tominaga A, Sato M, Sugano M. Effects of dietary sphingolipids on levels of serum and liver lipids in rats. *Nutr Res.* (1992) 12:543–8. doi: 10.1016/S0271-5317(05)80024-7

117. Kobayashi T, Shimizugawa T, Osakabe T, Watanabe S, Okuyama H. A long-term feeding of sphingolipids affected the levels of plasma cholesterol and hepatic triacylglycerol but not tissue phospholipids and sphingolipids. *Nutr Res.* (1997) 17:111–4. doi: 10.1016/S0271-5317(96)00237-0

118. Nyberg L, Duan RD, Nilsson A. A mutual inhibitory effect on absorption of sphingomyelin and cholesterol. *J Nutr Biochem.* (2000) 11:244–9. doi: 10.1016/s0955-2863(00)00069-3

119. Eckhardt ER, Wang DQ, Donovan JM, Carey MC. Dietary sphingomyelin suppresses intestinal cholesterol absorption by decreasing thermodynamic activity of cholesterol monomers. *Gastroenterology.* (2002) 122:948–56. doi: 10.1053/gast.2002.32539

120. Noh SK, Koo SI. Egg sphingomyelin lowers the lymphatic absorption of cholesterol and alpha-tocopherol in rats. *J Nutr.* (2003) 133:3571–6. doi: 10.1093/jn/133.11.3571

121. Noh SK, Koo SI. Milk sphingomyelin is more effective than egg sphingomyelin in inhibiting intestinal absorption of cholesterol and fat in rats. *J Nutr.* (2004) 134:2611–6. doi: 10.1093/jn/134.10.2611

122. Yang F, Chen G, Ma M, Qiu N, Zhu L, Li J. Egg-yolk sphingomyelin and phosphatidylcholine attenuate cholesterol absorption in Caco-2 cells. *Lipids.* (2018) 53:217–33. doi: 10.1002/lipd.12018

123. Ramprasath VR, Jones PJ, Buckley DD, Woollett LA, Heubi JE. Effect of dietary sphingomyelin on absorption and fractional synthetic rate of cholesterol and serum lipid profile in humans. *Lipids Health Dis.* (2013) 12:125. doi: 10.1186/1476-511x-12-125

124. Milard M, Penhoat A, Durand A, Buisson C, Loizon E, Meugnier E, et al. Acute effects of milk polar lipids on intestinal tight junction expression: towards an impact of sphingomyelin through the regulation of IL-8 secretion? *J Nutr Biochem.* (2019) 65:128–38. doi: 10.1016/j.jnutbio.2018.12.007

125. Garmy N, Taïeb N, Yahi N, Fantini J. Interaction of cholesterol with sphingosine: physicochemical characterization and impact on intestinal absorption. *J Lipid Res.* (2005) 46:36–45. doi: 10.1194/jlr.M400199-JLR200

126. Slotte JP. The importance of hydrogen bonding in sphingomyelin's membrane interactions with co-lipids. *Biochim Biophys Acta.* (2016) 1858:304–10. doi: 10.1016/j.bbamem.2015.12.008

127. Nilsson A. Metabolism of sphingomyelin in the intestinal tract of the rat. *Biochim Biophys Acta.* (1968) 164:575–84. doi: 10.1016/0005-2760(68)90187-2

128. Millar CL, Norris GH, Vitols A, Garcia C, Seibel S, Anto L, et al. Dietary egg sphingomyelin prevents aortic root plaque accumulation in apolipoprotein-E knockout mice. *Nutrients.* (2019) 11:1124. doi: 10.3390/nu11051124

129. Norris GH, Jiang C, Ryan J, Porter CM, Blesso CN. Milk sphingomyelin improves lipid metabolism and alters gut microbiota in high fat diet-fed mice. *J Nutr Biochem.* (2016) 30:93–101. doi: 10.1016/j.jnutbio.2015.12.003

130. Norris GH, Porter CM, Jiang C, Blesso CN. Dietary milk sphingomyelin reduces systemic inflammation in diet-Induced obese mice and inhibits LPS activity in macrophages. *Beverages.* (2017) 3:37.

131. Pan XF, Wang L, Pan A. Epidemiology and determinants of obesity in China. *Lancet Diabetes Endocrinol.* (2021) 9:373–92. doi: 10.1016/s2213-8587(21)00045-0

132. Lambert JM, Anderson AK, Cowart LA. Sphingolipids in adipose tissue: what's tipping the scale? *Adv Biol Regul.* (2018) 70:19–30. doi: 10.1016/j.jbior.2018.10.002

133. Yunoki K, Renaguli M, Kinoshita M, Matsuyama H, Mawatari S, Fujino T, et al. Dietary sphingolipids ameliorate disorders of lipid metabolism in Zucker fatty rats. *J Agric Food Chem.* (2010) 58:7030–5. doi: 10.1021/jf100722f

134. Norris GH, Porter CM, Jiang C, Millar CL, Blesso CN. Dietary sphingomyelin attenuates hepatic steatosis and adipose tissue inflammation in high-fat-diet-induced obese mice. *J Nutr Biochem.* (2017) 40:36–43. doi: 10.1016/j.jnutbio.2016.09.017

135. Milard M, Laugerette F, Durand A, Buisson C, Meugnier E, Loizon E, et al. Milk polar lipids in a high-fat diet can prevent body weight gain: modulated abundance of gut bacteria in relation with fecal loss of specific fatty acids. *Mol Nutr Food Res.* (2019) 63:1801078. doi: 10.1002/mnfr.201801078

136. Watanabe S, Takahashi T, Tanaka L, Haruta Y, Shiota M, Hosokawa M, et al. The effect of milk polar lipids separated from butter serum on the lipid levels in the liver and the plasma of obese-model mouse (KK-Ay). *J Funct Foods.* (2011) 3:313–20. doi: 10.1016/j.jff.2011.06.002

137. Ross JS, Russo SB, Chavis GC, Cowart LA. Sphingolipid regulators of cellular dysfunction in Type 2 diabetes mellitus: a systems overview. *Clin Lipidol.* (2014) 9:553–69.

138. Bellini L, Campana M, Mahfouz R, Carlier A, Véret J, Magnan C, et al. Targeting sphingolipid metabolism in the treatment of obesity/type 2 diabetes. *Expert Opin Ther Targets.* (2015) 19:1037–50. doi: 10.1517/14728222.2015.1028359

139. Shimizu H, Okajima F, Kimura T, Ohtani K-I, Tsuchiya T, Takahashi H, et al. Sphingosine 1-phosphate stimulates insulin secretion in HIT-T 15 cells and mouse islets. *Endocrine J.* (2000) 47:261–9. doi: 10.1507/endocrj.47.261

140. Laychock SG, Sessanna SM, Lin MH, Mastrandrea LD. Sphingosine 1-phosphate affects cytokine-induced apoptosis in rat pancreatic islet beta-cells. *Endocrinology.* (2006) 147:4705–12. doi: 10.1210/en.2006-0456

141. Yang JY, Zhang TT, Dong Z, Shi HH, Xu J, Mao XZ, et al. Dietary supplementation with exogenous sea-cucumber-derived ceramides and glucosylceramides alleviates insulin resistance in high-fructose-diet-fed rats by upregulating the IRS/PI3K/Akt signaling pathway. *J Agric Food Chem.* (2021) 69:9178–87. doi: 10.1021/acs.jafc.0c06831

142. Huang PL. A comprehensive definition for metabolic syndrome. *Dis Model Mech.* (2009) 2:231–7. doi: 10.1242/dmm.001180

143. Ichi I, Nakahara K, Miyashita Y, Hidaka A, Kutsukake S, Inoue K, et al. Association of ceramides in human plasma with risk factors of atherosclerosis. *Lipids.* (2006) 41:859–63. doi: 10.1007/s11745-006-5041-6

144. Fan Y, Shi F, Liu J, Dong J, Bui HH, Peake DA, et al. Selective reduction in the sphingomyelin content of atherogenic lipoproteins inhibits their retention in murine aortas and the subsequent development of atherosclerosis. *Arterioscler Thromb Vasc Biol.* (2010) 30:2114–20. doi: 10.1161/atvbaha.110.213363

145. Bourlieu C, Michalski MC. Structure-function relationship of the milk fat globule. *Curr Opin Clin Nutr Metab Care.* (2015) 18:118–27. doi: 10.1097/mco.0000000000000138

146. Bourlieu C, Cheillan D, Blot M, Daira P, Trauchessec M, Ruet S, et al. Polar lipid composition of bioactive dairy co-products buttermilk and butterserum: emphasis on sphingolipid and ceramide isoforms. *Food Chem.* (2018) 240:67–74. doi: 10.1016/j.foodchem.2017.07.091

147. Jiménez-Flores R, Brisson G. The milk fat globule membrane as an ingredient: why, how, when? *Dairy Sci Technol.* (2008) 88:5–18. doi: 10.1051/dst:2007005

148. Le Barz M, Vors C, Combe E, Joumard-Cubizolles L, Lecomte M, Joffre F, et al. Milk polar lipids favorably alter circulating and intestinal ceramide and sphingomyelin species in postmenopausal women. *JCI Insight.* (2021) 6:e146161. doi: 10.1172/jci.insight.146161

149. Zhao J, Zhao Y, Du M, Binns CW, Lee AH. Maternal education and breastfeeding practices in China: a systematic review and meta-analysis. *Midwifery.* (2017) 50:62–71. doi: 10.1016/j.midw.2017.03.011

150. Silva RCD, Colleran HL, Ibrahim SA. Milk fat globule membrane in infant nutrition: a dairy industry perspective. *J Dairy Res.* (2021) 88:105–16. doi: 10.1017/s0022029921000224

151. Brink LR, Lönnerdal B. Milk fat globule membrane: the role of its various components in infant health and development. *J Nutr Biochem.* (2020) 85:108465. doi: 10.1016/j.jnutbio.2020.108465

152. Albi E, Arcuri C, Kobayashi T, Tomishige N, Cas MD, Paroni R, et al. Sphingomyelin in human breast milk might be essential for the hippocampus maturation. *Front Biosci.* (2022) 27:247. doi: 10.31083/j.fbl2708247

153. Bruno RS, Pokala A, Torres-Gonzalez M, Blesso CN. Cardiometabolic health benefits of dairy-milk polar lipids. *Nutr Rev.* (2021) 79(Suppl. 2):16–35. doi: 10.1093/nutrit/nuab085

154. Dewettinck K, Rombaut R, Thienpont N, Le TT, Messens K, Van Camp J. Nutritional and technological aspects of milk fat globule membrane material. *Int Dairy J.* (2008) 18:436–57. doi: 10.1016/j.idairyj.2007.10.014

155. Bourlieu C, Bouzerzour K, Ferret-Bernard S, Bourgot CL, Chever S, Ménard O, et al. Infant formula interface and fat source impact on neonatal digestion and gut microbiota. *Eur J Lipid Sci Technol.* (2015) 117:1500–12. doi: 10.1002/ejlt.201500025

156. Bernhard W, Poets CF, Franz AR. Choline and choline-related nutrients in regular and preterm infant growth. *Eur J Nutr.* (2019) 58:931–45. doi: 10.1007/s00394-018-1834-7

157. Van Der BEM. Abrahamse-berkeveld M, Acton, DS, Stefanie S. *Infant Formula with Special Lipid Architecture for Promoting Healthy Growth. United States Patent 11389403*. Washington, DC: U.S. Patent and Trademark Office (2022).

158. Schneider Nora HJ, Sean D, Tamas B, Jonathan O. *Nutritional Composition and Infant Formula for Promoting De Novo Myelination.* United States Patent 11297872. Washington, DC: U.S. Patent and Trademark Office (2022).

159. Morifuji M. The beneficial role of functional food components in mitigating ultraviolet-induced skin damage. *Exp Dermatol.* (2019) 28(Suppl. 1):28–31. doi: 10.1111/exd.13825

160. Imokawa G. Recent advances in characterizing biological mechanisms underlying UV-induced wrinkles: a pivotal role of fibrobrast-derived elastase. *Arch Dermatol Res.* (2008) 300(Suppl. 1):S7–20. doi: 10.1007/s00403-007-0798-x

161. Erden Inal M, Kahraman A, Köken T. Beneficial effects of quercetin on oxidative stress induced by ultraviolet A. *Clin Exp Dermatol.* (2001) 26:536–9. doi: 10.1046/j.1365-2230.2001.00884.x

162. Svobodová A, Psotová J, Walterová D. Natural phenolics in the prevention of UV-induced skin damage. A review. *Biomed Pap Med Fac Univ Palacky Olomouc Czech Repub.* (2003) 147:137–45.

163. Sugawara T. Sphingolipids as functional food components: benefits in skin improvement and disease prevention. *J Agric Food Chem.* (2022) 70:9597–609. doi: 10.1021/acs.jafc.2c01731

164. Tessema EN, Gebre-Mariam T, Neubert RHH, Wohlrab J. Potential applications of phyto-derived ceramides in improving epidermal barrier function. *Skin Pharmacol Physiol.* (2017) 30:115–38. doi: 10.1159/000464337

165. Oba C, Morifuji M, Ichikawa S, Ito K, Kawahata K, Yamaji T, et al. Dietary milk sphingomyelin prevents disruption of skin barrier function in hairless mice after UV-B irradiation. *PLoS One.* (2015) 10:e0136377. doi: 10.1371/journal.pone.0136377

166. Haruta-Ono Y, Ueno H, Ueda N, Kato K, Yoshioka T. Investigation into the dosage of dietary sphingomyelin concentrate in relation to the improvement of epidermal function in hairless mice. *Anim Sci J.* (2012) 83:178–83. doi: 10.1111/j.1740-0929.2011.00940.x

167. Haruta Y, Kato K, Yoshioka T. Dietary phospholipid concentrate from bovine milk improves epidermal function in hairless mice. *Biosci Biotechnol Biochem.* (2008) 72:2151–7. doi: 10.1271/bbb.80212

168. Haruta-Ono Y, Setoguchi S, Ueno HM, Higurashi S, Ueda N, Kato K, et al. Orally administered sphingomyelin in bovine milk is incorporated into skin sphingolipids and is involved in the water-holding capacity of hairless mice. *J Dermatol Sci.* (2012) 68:56–62. doi: 10.1016/j.jdermsci.2012.07.006

169. Ohta K, Hiraki S, Miyanabe M, Ueki T, Manabe Y, Sugawara T. Dietary ceramide prepared from soy sauce lees improves skin barrier function in hairless mice. *J Oleo Sci.* (2021) 70:1325–34. doi: 10.5650/jos.ess21128

170. Higurashi S, Haruta-Ono Y, Urazono H, Kobayashi T, Kadooka Y. Improvement of skin condition by oral supplementation with sphingomyelin-containing milk phospholipids in a double-blind, placebo-controlled, randomized trial. *J Dairy Sci.* (2015) 98:6706–12. doi: 10.3168/jds.2015-9529

171. Lee K, Kim S, Kim A, Suh HJ, Hong KB. Sphingolipid identification and skin barrier recovery capacity of a milk sphingolipid-enriched fraction (MSEF) from buttermilk powder. *Int J Cosmet Sci.* (2020) 42:270–6. doi: 10.1111/ics.12612

172. Morifuji M, Oba C, Ichikawa S, Ito K, Kawahata K, Asami Y, et al. A novel mechanism for improvement of dry skin by dietary milk phospholipids: effect on epidermal covalently bound ceramides and skin inflammation in hairless mice. *J Dermatol Sci.* (2015) 78:224–31. doi: 10.1016/j.jdermsci.2015.02.017

173. Ideta R, Sakuta T, Nakano Y, Uchiyama T. Orally administered glucosylceramide improves the skin barrier function by upregulating genes associated with the tight junction and cornified envelope formation. *Biosci Biotechnol Biochem.* (2011) 75:1516–23. doi: 10.1271/bbb.110215

174. Hasegawa T, Shimada H, Uchiyama T, Ueda O, Nakashima M, Matsuoka Y. Dietary glucosylceramide enhances cornified envelope formation *via* transglutaminase expression and involucrin production. *Lipids.* (2011) 46:529–35. doi: 10.1007/s11745-011-3546-0

175. Kato Ken UN, Susumu M, Toshimitsu Y. *Skin Beautifie.* United States Patent 20110065670. Washington, DC: U.S. Patent and Trademark Office (2011).

176. Morshed A, Karawdeniya BI, Bandara Y, Kim MJ, Dutta P. Mechanical characterization of vesicles and cells: a review. *Electrophoresis.* (2020) 41:449–70. doi: 10.1002/elps.201900362

177. Lopez C, Mériadec C, David-Briand E, Dupont A, Bizien T, Artzner F, et al. Loading of lutein in egg-sphingomyelin vesicles as lipid carriers: thermotropic phase behaviour, structure of sphingosome membranes and lutein crystals. *Food Res Int.* (2020) 138(Pt. A):109770. doi: 10.1016/j.foodres.2020.109770

178. Singh H. The milk fat globule membrane—A biophysical system for food applications. *Curr Opin Coll Interface Sci.* (2006) 11:154–63. doi: 10.1016/j.cocis.2005.11.002

179. Xia F, Hu D, Jin H, Zhao Y, Liang J. Preparation of lutein proliposomes by supercritical anti-solvent technique. *Food Hydrocoll.* (2012) 26:456–63. doi: 10.1016/j.foodhyd.2010.11.014

180. Lopez C, Madec M-N, Jimenez-Flores R. Lipid rafts in the bovine milk fat globule membrane revealed by the lateral segregation of phospholipids and heterogeneous distribution of glycoproteins. *Food Chem.* (2010) 120:22–33. doi: 10.1016/j.foodchem.2009.09.065

181. Zhang Q, Wu W, Zhang J, Xia X. Antimicrobial lipids in nano-carriers for antibacterial delivery. *J Drug Target.* (2020) 28:271–81. doi: 10.1080/1061186x.2019.1681434

182. Bouzo BL, Lores S, Jatal R, Alijas S, Alonso MJ, Conejos-Sánchez I, et al. Sphingomyelin nanosystems loaded with uroguanylin and etoposide for treating metastatic colorectal cancer. *Sci Rep.* (2021) 11:17213. doi: 10.1038/s41598-021-96578-z

183. Nagachinta S, Bouzo BL, Vazquez-Rios AJ, Lopez R, Fuente M. Sphingomyelin-based nanosystems (SNs) for the development of anticancer miRNA therapeutics. *Pharmaceutics.* (2020) 12:189. doi: 10.3390/pharmaceutics12020189

184. Jatal R, Mendes Saraiva S, Vázquez-Vázquez C, Lelievre E, Coqueret O, López-López R, et al. Sphingomyelin nanosystems decorated with TSP-1 derived peptide targeting senescent cells. *Int J Pharm.* (2022) 617:121618. doi: 10.1016/j.ijpharm.2022.121618

185. Fahmy Tarek MSE, Flavell Richard A, Jason P, Alyssa S. *Vehicles for Controlled Delivery of Different Pharmaceutical Agents.* WIPO Patent WO/2013/155487. Geneva: WIPO (2013).

186. Veldman Robert JVBWJ, Marcel V, Gerben K. *Pharmaceutical Formulations Employing Short-Chain Sphingolipids and Their Use.* United States Patent 7915227. Washington, DC: U.S. Patent and Trademark Office (2011).

187. Kulkarni VS. *Sphingolipid-Containing Cationic Liposomes for Topical Delivery of Bioactive Material.* WIPO Patent WO/2001/042424. Geneva: WIPO (2001).

188. Gore SL. *Compositions and Methods for Intranasal Delivery of Active Agents to the Brain.* WIPO Patent WO/2001/041732. Geneva: WIPO (2001).

189. Pavlichenko Ida AJ, Haritosh P, Michael A, Cathy Z. *Drug Combination Kits and Methods of Drug Delivery.* WIPO Patent WO/2022/047234. Geneva: WIPO (2022).

190. Kato Ken MS, Leo T, Hiroshi U, Noriko U, Yuko H, Toshimitsu Y. *Medicine, Food and Drink or Feed Containing Sphingomyelin.* United States Patent 9186366. Washington, DC: U.S. Patent and Trademark Office (2015).

191. Liu AG, Ford NA, Hu FB, Zelman KM, Mozaffarian D, Kris-Etherton PM. A healthy approach to dietary fats: understanding the science and taking action to reduce consumer confusion. *Nutr J.* (2017) 16:53. doi: 10.1186/s12937-017-0271-4

192. Zhu Y, Bo Y, Liu Y. Dietary total fat, fatty acids intake, and risk of cardiovascular disease: a dose-response meta-analysis of cohort studies. *Lipids Health Dis.* (2019) 18:91. doi: 10.1186/s12944-019-1035-2

193. Pehlivanoğlu H, Demirci M, Toker OS, Konar N, Karasu S, Sagdic O. Oleogels, a promising structured oil for decreasing saturated fatty acid concentrations: production and food-based applications. *Crit Rev Food Sci Nutr.* (2018) 58:1330–41. doi: 10.1080/10408398.2016.1256866

194. Rogers MA, Wright AJ, Marangoni AG. Oil organogels: the fat of the future? *Soft Matter.* (2009) 5:1594–6. doi: 10.1039/B822008P

195. Puscas A, Muresan V, Socaciu C, Muste S. Oleogels in food: a review ofcurrent and potential applications. *Foods.* (2020) 9:70. doi: 10.3390/foods9010070

196. Rogers MA, Spagnuolo PA, Wang TM, Angka L. A potential bioactive hard-stock fat replacer comprised of a molecular gel. *Food Sci Nutr.* (2017) 5:579–87. doi: 10.1002/fsn3.433

197. Guo S, Song M, He X, Yang F, Cao Y, Rogers M, et al. Water-induced self-assembly of mixed gelator system (ceramide and lecithin) for

edible oil structuring. *Food Funct.* (2019) 10:3923–33. doi: 10.1039/c9fo00473d

198. Guo S, Song M, Gao X, Dong L, Hou T, Lin X, et al. Assembly pattern of multicomponent supramolecular oleogel composed of ceramide and lecithin in sunflower oil: self-assembly or self-sorting? *Food Funct.* (2020) 11:7651–60. doi: 10.1039/d0fo00635a

199. Guo S, Lv M, Chen Y, Hou T, Zhang Y, Huang Z, et al. Engineering water-induced ceramide/lecithin oleogels: understanding the influence of water added upon pre- and post-nucleation. *Food Funct.* (2020) 11:2048–57. doi: 10.1039/c9fo02540e

200. Temkov M, Mure?an V. Tailoring the structure of lipids, oleogels and fat replacers by different approaches for solving the trans-fat issue-a review. *Foods.* (2021) 10:1376. doi: 10.3390/foods10061376

201. Savin Gabriela CV, Jin-mi J, Raffaele M, Martin L. *Oil Gel.* United States Patent 8796342. Washington, DC: U.S. Patent and Trademark Office (2014).

202. Thomas D. *Water-Based Emulsifier Wax Gels.* United States Patent 20040110851. Washington, DC: U.S. Patent and Trademark Office (2004).

203. Thomas D. *Emulgator-Wachs-Gele auf Wasserbasis.* German Patent DE10255554. München: The German Patent and Trade Mark Office (2004).

204. van Kruining D, Luo Q, van Echten-Deckert G, Mielke MM, Bowman A, Ellis S, et al. Sphingolipids as prognostic biomarkers of neurodegeneration, neuroinflammation, and psychiatric diseases and their emerging role in lipidomic investigation methods. *Adv Drug Deliv Rev.* (2020) 159:232–44. doi: 10.1016/j.addr.2020.04.009

205. Sugawara T, Miyazawa T. Separation and determination of glycolipids from edible plant sources by high-performance liquid chromatography and evaporative light-scattering detection. *Lipids.* (1999) 34:1231–7. doi: 10.1007/s11745-999-0476-3

206. Wang L, Wang T, Fehr WR. HPLC quantification of sphingolipids in soybeans with modified palmitate content. *J Agric Food Chem.* (2006) 54:7422–8. doi: 10.1021/jf061624c

207. Gutierrez E, Wang T, Fehr WR. Quantification of sphingolipids in soybeans. *J Am Oil Chem Soc.* (2004) 81:737–42. doi: 10.1007/s11746-004-0971-y

208. Gutierrez E, Wang T. Effect of processing on sphingolipid content in soybean products. *J Am Oil Chem Soc.* (2004) 81:971–7. doi: 10.1007/s11746-004-1009-1

209. Sullards MC, Merrill AH Jr. Analysis of sphingosine 1-phosphate, ceramides, and other bioactive sphingolipids by high-performance liquid chromatography-tandem mass spectrometry. *Sci STKE.* (2001) 2001:pl1. doi: 10.1126/stke.2001.67.pl1

210. Fang F, Ho C-T, Sang S, Rosen RT. Determination of sphingolipids in nuts and seeds by a single quadrupole liquid chromatography–mass spectrometry method. *J Food Lipids.* (2005) 12:327–43. doi: 10.1111/j.1745-4522.2005.00028.x

211. Pham PH, Duffy T-L, Dmytrash AL, Lien VW, Thomson AB, Clandinin MT. Estimate of dietary ganglioside intake in a group of healthy Edmontonians based on selected foods. *J Food Compos Anal.* (2011) 24:1032–7. doi: 10.1016/j.jfca.2011.01.011

212. Fong BY, Ma L, Khor GL, van der Does Y, Rowan A, McJarrow P, et al. Ganglioside composition in beef, chicken, pork, and fish determined using liquid chromatography–high-resolution mass spectrometry. *J Agric Food Chem.* (2016) 64:6295–305. doi: 10.1021/acs.jafc.6b02200

213. Wang X, Zhang H, Song Y, Cong P, Li Z, Xu J, et al. Comparative lipid profile analysis of four fish species by ultraperformance liquid chromatography coupled with quadrupole time-of-flight mass spectrometry. *J Agric Food Chem.* (2019) 67:9423–31. doi: 10.1021/acs.jafc.9b03303

214. Li H, Song Y, Zhang H, Wang X, Cong P, Xu J, et al. Comparative lipid profile of four edible shellfishes by UPLC-Triple TOF-MS/MS. *Food Chem.* (2020) 310:125947. doi: 10.1016/j.foodchem.2019.125947

215. Duan J, Sugawara T, Hirata T. Rapid quantitative analysis of sphingolipids in seafood using HPLC with evaporative light-scattering detection: its application in tissue distribution of sphingolipids in fish. *J Oleo Sci.* (2010) 59:509–13. doi: 10.5650/jos.59.509

216. Zhao Y-Y, Xiong Y, Curtis JM. Measurement of phospholipids by hydrophilic interaction liquid chromatography coupled to tandem mass spectrometry: the determination of choline containing compounds in foods. *J Chromatogr A.* (2011) 1218:5470–9. doi: 10.1016/j.chroma.2011.06.025

217. Liu Z, Li C, Pryce J, Rochfort S. Comprehensive characterization of bovine milk lipids: phospholipids, sphingolipids, glycolipids, and ceramides. *J Agric Food Chem.* (2020) 68:6726–38. doi: 10.1021/acs.jafc.0c01604

218. Rombaut R, Dewettinck K, Van Camp J. Phospho- and sphingolipid content of selected dairy products as determined by HPLC coupled to an evaporative light scattering detector (HPLC–ELSD). *J Food Compos Anal.* (2007) 20:308–12. doi: 10.1016/j.jfca.2006.01.010

frontiers | Frontiers in Nutrition

TYPE Systematic Review
PUBLISHED 31 October 2022
DOI 10.3389/fnut.2022.1046800

OPEN ACCESS

EDITED BY
Ling Zhao,
The University of Tennessee, Knoxville,
United States

REVIEWED BY
Zhaoyue Zhang,
The Rockefeller University,
United States
Guoxun Chen,
The University of Tennessee, Knoxville,
United States

*CORRESPONDENCE
Ling Wang
lingwang@must.edu.mo

SPECIALTY SECTION
This article was submitted to
Nutrition and Metabolism,
a section of the journal
Frontiers in Nutrition

RECEIVED 17 September 2022
ACCEPTED 17 October 2022
PUBLISHED 31 October 2022

CITATION
Zhang Y, Ding Y, Fan Y, Xu Y, Lu Y, Zhai L and Wang L (2022) Influence of biotin intervention on glycemic control and lipid profile in patients with type 2 diabetes mellitus: A systematic review and meta-analysis. *Front. Nutr.* 9:1046800. doi: 10.3389/fnut.2022.1046800

Influence of biotin intervention on glycemic control and lipid profile in patients with type 2 diabetes mellitus: A systematic review and meta-analysis

Yujia Zhang, Yiwang Ding, Yawen Fan, Yenan Xu, Yuting Lu, Lingzi Zhai and Ling Wang*

Faculty of Medicine, Macau University of Science and Technology, Macao, Macao SAR, China

Background: Biotin is a water-soluble vitamin acting as a covalently bound coenzyme in regulating energy production. Previous studies have reported that biotin supplementation may influence blood glucose and lipid level in patients with type 2 diabetes mellitus (T2DM).

Methods: We searched Pubmed, Embase, and Cochrane library databases up to 8th August 2022 for studies examining the effects of biotin supplementation in T2DM patients. Pooled effects were measured by weighted mean differences (WMDs) with 95% confidence intervals (CI) using random effects models. Inter-study heterogeneity was assessed and quantified.

Results: A total of five random controlled trials (RCT), involving 445 participants were included. It was suggested that biotin supplementation for 28 to 90 days significantly decreased the level of fasting blood glucose (FBG) (MD: −1.21 mmol/L, 95% CI: −2.73 to 0.31), total cholesterol (TC) (MD: −0.22 mmol/L, 95% CI: −0.25 to −0.19) and triglycerides (TG) (MD: −0.59 mmol/L, 95% CI: −1.21 to 0.03). No significant beneficial effects were observed on insulin (MD: 1.88 pmol/L 95% CI: −13.44 to 17.21). Evidence for the impact of biotin supplementation on the levels of glycated hemoglobin (HbA1c), low-density lipoprotein cholesterol (LDL-C), high-density lipoprotein cholesterol (HDL-C) and very low-density lipoprotein cholesterol (VLDL-C) was limited to draw conclusion.

Conclusions: Biotin supplementation may decrease FBG, TC and TG levels. However, its influence on insulin is not significant and further studies on the effects of biotin on HbA1c, LDL-C, HDL-C and VLDL-C are expected.

KEYWORDS

biotin, vitamin B, glycemic control, lipid profile, T2DM

Introduction

Diabetes mellitus is a global health problem with a prevalence of 11.3% and is projected to rise continuously (1). According to the World Health Organization, 422 million people worldwide are suffering from diabetes and 1.5 million deaths are directly attributed to diabetes every year. Type 2 diabetes mellitus (T2DM) is the most common type of diabetes and usually results in macro- and micro-vascular complications and comorbidities in the body, such as diabetic retinopathy (DR), diabetic foot, and diabetic kidney disease (DKD) (2). These chronic complications have caused severe adverse impact on the quality of life of human beings. Therefore, the prevention and management of T2DM is of vital importance to alleviate its disease burden.

Dietary vitamin supplementation is an easy and economic strategy for both pre-diabetic and diabetic patients to help control glucose and lipid metabolism. Vitamins are generally classified as fat-soluble and water-soluble. Various studies have systematically evaluated the effects of fat-soluble vitamins in lowering the risk of T2DM and improving glycemic indices, such as vitamin A (3), vitamin D (4–7), vitamin E (8) and vitamin K (9). Specifically, vitamin D supplementation has been proved to significantly ameliorate status of fasting blood glucose (FBG), homeostatic model assessment of insulin resistance (HOMA-IR), and glycated hemoglobin (HbA1c) (10). Similarly, the role of water-soluble vitamins is also important in maintaining energy metabolism. For example, vitamin B1 (thiamine) is a co-enzyme for several enzymes, including transketolase which is essential in the non-oxidative branch of the pentose phosphate pathway (PPP) (11). Many diabetic patients have been shown to have thiamine deficiency and lower blood thiamine pyrophosphate concentrations were associated with higher risk of DR (12). Moreover, vitamin B12 deficiency, usually caused by prolonged use of metformin, could result in severe oxidative stress and peripheral neuropathy (13, 14). As frequent urination and excessive thirst are two of the main symptoms of T2DM patients, it is unknown whether water soluble vitamins would be lost along with the extra urine discharge, thereby exacerbate the water-soluble vitamin deficiency in T2DM patients. Therefore, the study of individual water-soluble vitamin supplementation is necessary to determine their blood status and effects on T2DM patients.

Biotin, or vitamin B7, is a water-soluble vitamin that acts as a prosthetic group of carboxylases (15). It serves as the essential cofactor for the 6 biotin-dependent carboxylases: acetyl-CoA carboxylase (ACC), geranyl-CoA carboxylase (GCC), 3-methylcrotonyl-CoA carboxylase (MCC), pyruvate carboxylase (PC), propionyl-CoA carboxylase (PCC), and urea carboxylase (UC) (16). The first physiological function of biotin was found in 1968 and proved to increase hepatic glucokinase transcription (17). Subsequently, many *in vitro* studies reported that biotin could stimulate pancreatic islet glucokinase activity and expression (18), increase insulin secretion (19, 20), and induce insulin receptor synthesis (21). Meanwhile, various *in vivo* studies have also proven the efficiency of biotin in ameliorating diabetic status. Lazo et al. (22) investigated the effects of biotin in rodent pancreatic islets and confirmed that biotin supplementation could augment the proportion of beta cells and suppress mRNA expression of neural cell adhesion molecule. In animal studies, the results of glucose tolerance test (GTT) and insulin tolerance test (ITT) also supported the association between biotin treatment and improved tolerance condition (23, 24).

Current researches have demonstrated that biotin deficiency could impair energy production by decreasing glucose utilization and oxidative phosphorylation (25). Chuahan et al. (26) reported that biotin could regulate the glucokinase gene at the transcriptional stage in starved rats. In addition, insulin expression and secretion were found to be increased in response to biotin administration (18). On the other hand, excessive biotin intake may also ameliorate diabetic status. A study conducted in 43 Japanese T2DM patients demonstrated a decrease of approximately 45% of FBG concentration after one month of oral supplementation of 9 mg of biotin per day (15, 27). Similar effects were also observed in type 1 diabetic patients whose FBG levels decreased up to 50% after daily administration of 16 mg biotin for one week (28). High-dose biotin may compensate for subnormal insulin exposure by suppressing FOXO1 levels (29). Although the mechanism of hyperglycemia is different, biotin is effective in both type of diabetes mellitus (18, 30, 31). Moreover, many clinical trials have shown the hypoglycemic effect of biotin supplementation in overweight and obese individuals with T2DM (32, 33). A double-blind placebo-controlled trial including 348 participants reported a significant decrease in LDL-C, TC, HbA1c, and VLDL-C after 3 months intervention (34). However, another biotin intervention lasted for 4 weeks showed no significant change in plasma glucose, insulin, TG, TC or lactate concentration compared with placebos (35). The difference between these results may be caused by the small number of participants in one study and the specific conditions of the experiment such as the duration and dosage of the intervention.

Therefore, considering the lack of consensus, we performed a systematic review and meta-analysis for random controlled trials (RCTs) investigating the effects of biotin supplementation on glycemic control, including HbA1c, FBG, insulin, and lipid profile in T2DM patients. Prior to our research, no meta-analysis has been conducted in this regard.

Methods

This systematic review and meta-analysis was performed based on the Preferred Reporting Items for Systematic Reviews and Meta-Analysis reporting guidelines (36).

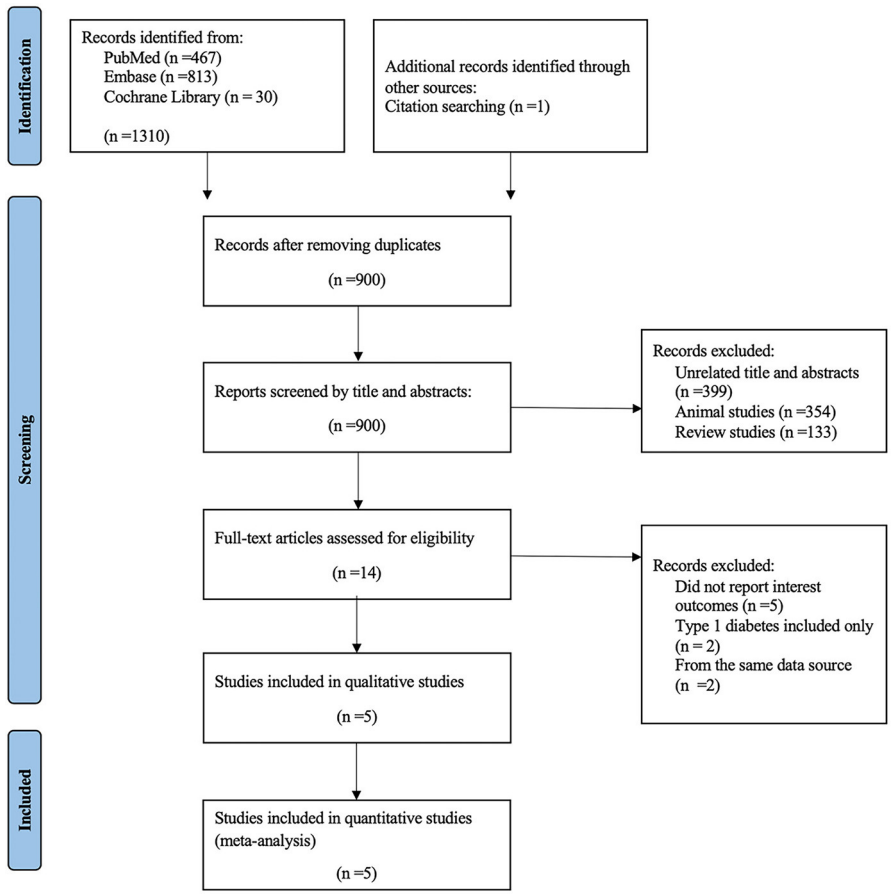

FIGURE 1
PRISMA flowchart of study selection.

Literature search strategy

We searched the Pubmed, Embase, and Cochrane library electronic databases to identify RCTs that reported the effects of biotin on glycemic control in patients with type 2 diabetes, through 8th August 2022. The following medical subject headings (MeSH) terms and non-MeSH search terms were included: ((“Biotin” OR “Vitamin B7” OR Water-Soluble Vitamins) AND (“Type 2 diabetes” OR T2DM OR diabetes mellitus OR non-insulin dependent diabetes) AND [Intervention OR randomized OR trial OR “controlled trials” OR “clinical trials” OR “cross-over” OR parallel)]. The detailed search strategy is listed in the Supplemental materials. Articles satisfying the intervention, ending point, and study design criteria were pulled. We also manually reviewed the reference lists of the included studies to avoid missing related researches.

Study selection

Two authors (ZY and FY) independently screened the titles and abstracts of every paper retrieved by the literature search to identify potentially eligible studies. We excluded studies that are letters, comments, conference papers, meta-analysis, reviews, RCTs with duplicate data or studies with insufficient data. RCTs that reported at least one of the following outcomes were included: 1) HbA1c, 2) FBG level, 3) insulin level, 4) TC level, 5) TG level, 6) HDL-C level, 7) LDL-C level, 8) VLDL-C level, 9) TG/HDL-C ratio. Any discrepancies regarding on the selection process were resolved by a third author (DY).

Data extraction

Data extraction was conducted by two authors independently (ZY and DY). The following data were extracted from each study: first author, publication year, location of the study, study design and duration, age, gender, sample size, type of intervention, the doses of biotin supplementation, BMI, main glycemic control (mean and SD) for both control and supplementation groups at baseline and end of the studies. Outcomes that were measured in different units were unified by mathematical conversion.

10.3389/fnut.2022.1046800

TABLE 1 Baseline characteristic of the included studies.

Authors	Year	Country	Design	Duration	Male (%)	Age (years)		BMI (kg/m^2)		Intervention		Sample size		Reference
						EG	PG	EG	PG	EG	PG	EG	PG	
Cristina et al.	2006	Mexico	Parallel	28 days	38.9%	48.6± 3.5	49.0±3.7	29.7±1.5	29.7±1.4	15mg/d	Placebo	10	8	(32)
Cesar et al.	2007	United States	Parallel	90 days	59.7%	57.6±10.1	59.6±8.3	30.5±3.3	30.4±3.1	2mg/d biotin plus 0.6mg/d chromium	Placebo	226	122	(34)
Gregory et al.	2006	United States	Parallel	28 days	52.8%	53±9	48±9	30±4	30±4	2mg/d biotin plus 0.6mg/d chromium	Placebo	20	16	(39)
Armida	2004	Mexico	Parallel	28 days	48.7%	50.4±7.7		28.6±4.9		1.5mg/d	Placebo	10	5	(35)
Masaru	1993	Japan	Parallel	30 days	-	46±10		-		9mg/d	Placebo	18	10	(27)

EG, experiment group, PG, placebo group.

Quality assessment

Cochrane criteria was applied to assess the risk of bias and quality of the included studies (37). The assessment criteria include random sequence generation, allocation concealment, blinding of participants, blinding of outcome, incomplete outcome data, selective report and other bias. Each study was classified as low, high or unclear risk of bias regarding on each segment.

Statistical analysis

All statistical analysis was performed using Review Manger V5.4 (Copenhagen: The Nordic Cochrane Center, Cochrane). To estimate the effect size of biotin on glycemic control, random-effects model was used to evaluate the WMD, SD and corresponding 95% confidence intervals (CI). Statistical heterogeneity was assessed in the meta-analysis using the I^2 and χ^2 statistics, and heterogeneity was considered substantial if I^2 >50% and P-value of < 0.10 in the χ^2 test (38). A sensitivity analysis was performed by removing each study one by one, to explore the contribution of each study to the overall mean difference. Subgroup analysis was performed according to the dosage of intervention (< or ≥ 9 mg/d). Trials not applicable for meta-analysis were reported in a narrative form.

Results

Search results

A total of 1,310 articles were identified through database searching and citation searching, with 900 remained after removing duplicates. Among the remaining articles, 886 records were excluded due to the following reasons: unrelated title and abstracts, animal studies and review studies. After a full-text assessment for eligibility, five trials were included in the qualitative and quantitative analysis (Figure 1).

Characteristics of the studies

The baseline characteristic of the included studies is demonstrated in Table 1. The five trials were conducted in three different countries including two in the United States, two in Mexico and one in Japan from 1993 to 2007. All of the trials were placebo controlled parallel RCTs and the intervention period varied from 4 weeks to 3 months, while 284 patients were in the experiment group and 161 were in the placebo group. One trial (27) did not report the gender of participants, while the male and female participants

distribution was even in two trials (35, 39). But the other two trials (32, 34) showed male predominance and female predominance, respectively. Baseline mean age and BMI varied from 46 to 59 years and 28.6 to 30.5 kg/m^2, respectively. The dosage of biotin intervention ranged from 1.5 mg/d to 15 mg/d.

Quality assessment

The results of the quality assessment for the included studies are presented in Figure 2. Three trials had a rigorous experimental design and were considered to be at low risk. Two trials (27, 39) were considered to be at a moderate risk due to either unclear or lack of reporting on various potential biases.

The heterogeneity among studies for FBG ($I^2 = 0\%$, $P = 0.33$), insulin ($I^2 = 48\%$, $P = 0.12$), TC ($I^2 = 33\%$, $P = 0.21$), TG ($I^2 = 0\%$, $P = 0.38$), HDL-C ($I^2 = 0\%$, $P = 1.00$), LDL-C ($I^2 = 0\%$, $P = 0.93$) and TG/HDL ratio ($I^2 = 0\%$, $P = 0.33$) was not detected. Heterogeneity measured for VLDL-C ($I^2 = 88\%$, $P = 0.004$) was significant, which might be caused by using random effects model.

Effects of biotin on FBG levels

All of the five included studies examined the effect of biotin supplementation on FBG levels. Overall, biotin supplementation significantly reduced FBG levels (MD: −1.21 mmol/L, 95% CI: −2.73 to 0.31, $P = 0.33$, $I^2 = 0\%$). Regarding on subgroup analysis, two trials with supplementation of biotin dosage ≥ 9 mg/d significantly decreased FBG levels (MD: −3.02 mmol/L, 95% CI: −8.15 to 2.46). Three trials with supplementation dosage of < 9 mg/d biotin demonstrated no significant difference compared with placebos (MD: −0.10 mmol/L, 95% CI: −2.38 to 2.18) (Figure 3). In addition, although two trials used the combination of biotin and chromium, subgroup analysis showed no significant difference in the effects of supplementation between the groups with or without chromium (34, 39) (Supplementary Figure S2).

Effects of biotin on insulin levels

Four studies (32, 34, 35, 39) investigated the effects of biotin supplementation on insulin levels. Overall, no significant difference was observed in this meta-analysis (MD: 1.88 pmol/L, 95% CI: −13.44 to 17.21) (Figure 4). Regarding on subgroup analysis, one trial involved 18 participants, ten of which took biotin at the dosage of ≥ 9 mg/d and the other eight took the placebo, both groups showed a significant decrease in insulin levels, while the decrease was more remarkable in biotin group (MD: −16.6 pmol/L, 95% CI: −41.65 to 8.45). However, three

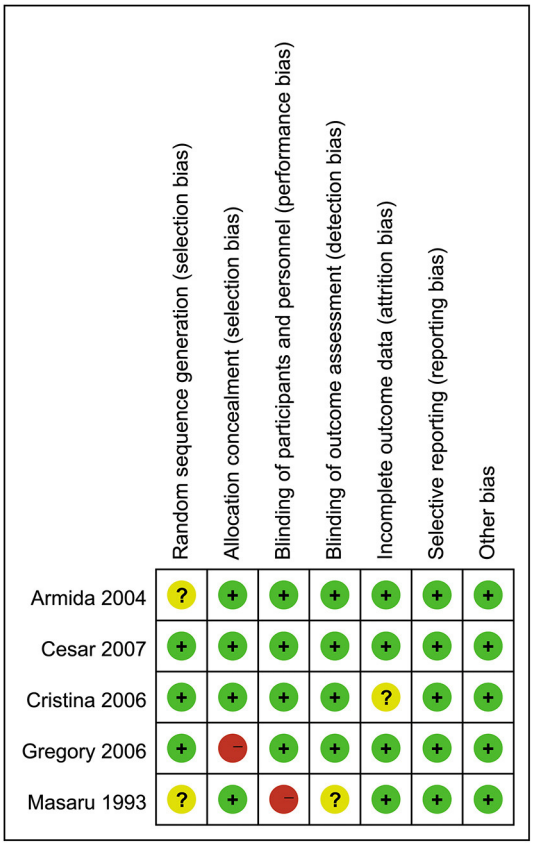

FIGURE 2
Quality assessment for the included studies.

trials with supplementation dosage < 9mg/d biotin presented a contrary trend where insulin levels were raised after intervention (MD: 6.79 pmol/L, 95% CI: −9.20 to 22.78). Besides, the combination of biotin and chromium supplementation did not show any significant difference with the subgroup of individual biotin supplementation (34, 39) (Supplementary Figure S3).

Effects of biotin on HbA1c levels

Only one trial (34) reported the effects of biotin supplementation on HbA1c levels in T2DM patients. Although it's not enough for a meta-analysis, according to the original article, the experiment group involving 226 patients showed a significant reduction in HbA1c levels compared with the placebo group (MD: −0.18%, 95% CI: −0.39 to 0.03).

Effects of biotin on TC and TG levels

Four studies (32, 34, 35, 39) investigated the effects of biotin supplementation on TC levels (Figure 5A) and three studies

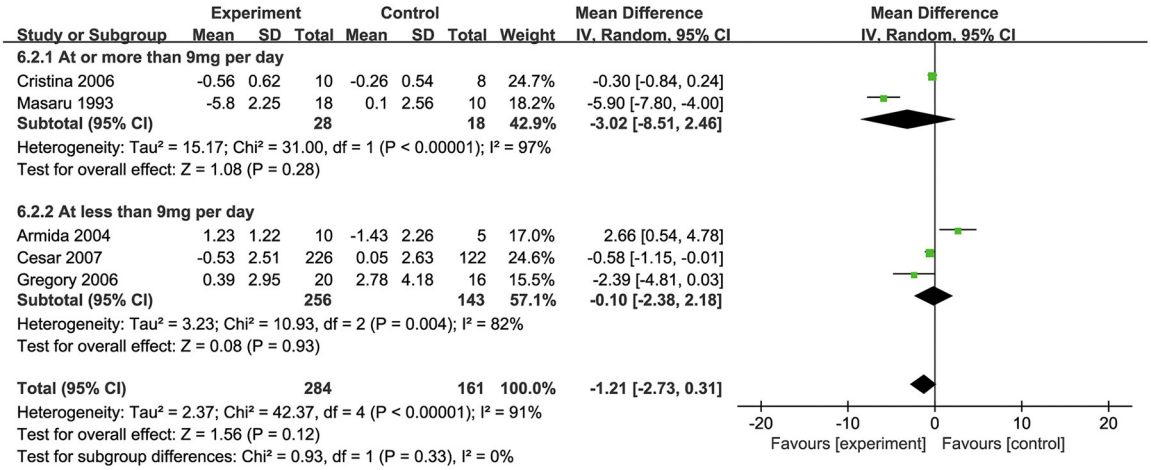

FIGURE 3
Effects of biotin supplementation on FBG levels < or ≥ 9 mg/d.

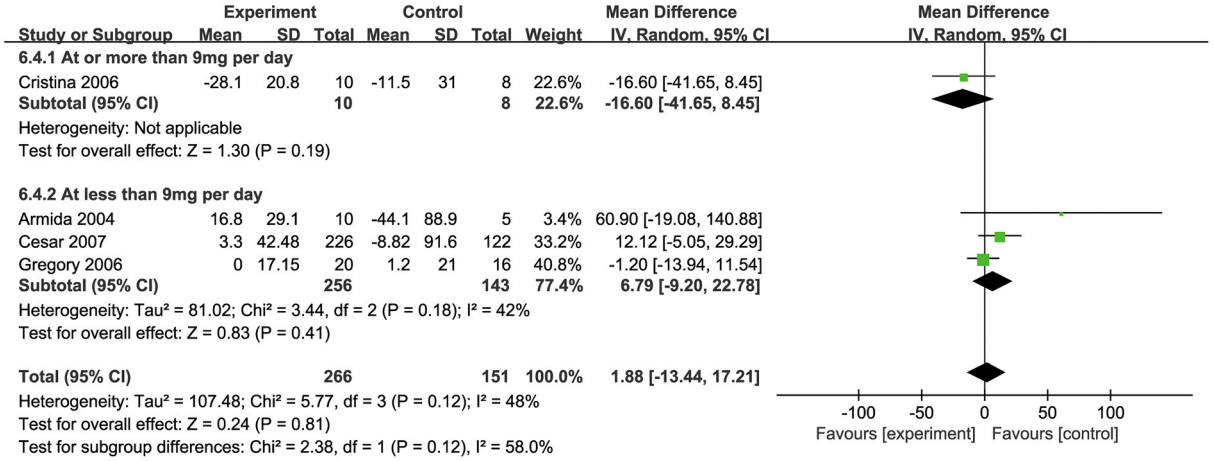

FIGURE 4
Effects of biotin supplementation on insulin levels < or ≥ 9 mg/d.

(34, 35, 39) reported TG levels (Figure 5B). Overall, biotin supplementation significantly reduced TC (MD: −0.22 mmol/L, 95% CI: −0.25 to 0.19) and TG levels (MD: −0.59 mmol/L, 95% CI: −1.21 to 0.03). Meta-regression analysis did not demonstrate any significant linear relationship between dosage of biotin supplementation and changes in TC (Coefficient = −0.03) (Supplementary Figure S1).

Effects of biotin on HDL-C, LDL-C, VLDL-C, and TG/HDL-C levels

Two studies (34, 39) pooled for this meta-analysis revealed no significant effect of biotin supplementation on HDL-C levels (MD: 0.00 mmol/L, 95% CI: −0.04 to 0.04) (Figure 6A). But the supplementation mildly reduced LDL-C levels (MD: −0.03 mmol/L, 95% CI: −0.19 to 0.14) and a significant decrease was found regarding TG/HDL-C ratio (MD: −0.77, 95% CI: −1.46 to −0.08) (Figures 6B,D).

Two studies (32, 34) investigated the effects of biotin supplementation on VLDL-C levels. However, no significant difference was observed in this meta-analysis (MD: −0.02 mmol/L, 95% CI: −0.19 to 0.14) (Figure 6C).

Sensitivity analysis

A sensitivity analysis was also performed to test the influence of every individual trial on the overall effect size. Each trial was removed from the sensitivity analysis orderly. After removing

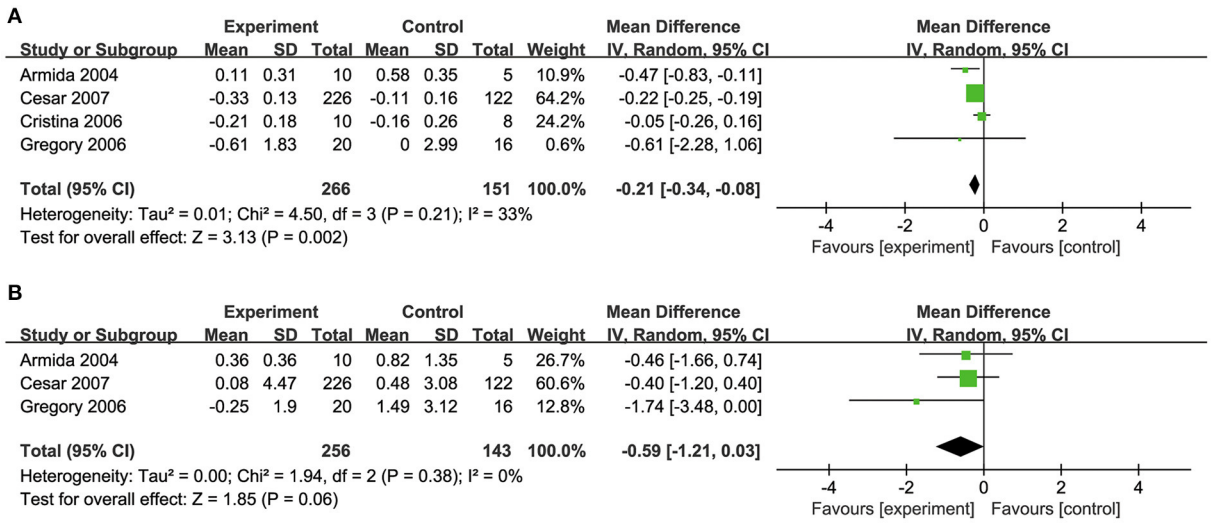

FIGURE 5
(A) Effects of biotin supplementation on TC levels. **(B)** Effects of biotin supplementation on TG.

the trails conducted by George et al. (39) or Cristina et al. (32), sensitivity analysis showed that the effects of biotin supplementation on serum insulin levels presented a significant increase [(MD: 5.61 pmol/L, 95% Cl: −23.19. to 34.41) (MD: 6.79 pmol/L, 95% Cl: −9.20 to 22.78)] (Figure 7).

Discussion

In this meta-analysis, we evaluated the effects of biotin supplementation on glycemic control in T2DM patients. The results indicate that biotin supplementation significantly improved lipid profile by decreasing TC, TG and TG/HDL-C ratio, but no linear association was observed for these changes and biotin dosage. The influence of biotin on LDL-C, HDL-C and VLDL-C was mild to none. Supplementation with or without chromium did not cause a difference on the influence of TC and TG changes. Regarding on FBG levels, T2DM patients receiving biotin supplementation at the dosage of $\geq$ 9 mg/d showed a significant decrease, but the reduction was not significant on those receiving $<$ 9 mg/d according to the subgroup analysis. Moreover, results for the effect on insulin levels were inconsistent between subgroups divided by dosage of the supplement. Evidence for HbA1c was not enough because only one trial reported this parameter. Therefore, considering the small number of included studies, no conclusion can be made on the effects of biotin supplementation on insulin, HbA1c, LDL-C, HDL-C and TG/HDL-C ratio so far.

The effects of biotin on glycemic outcomes are mainly caused by two pathways. First, biotin can increase the activity and expression of glucokinase expressed in hepatocyte and pancreatic β cell (40). Glucokinase phosphorylates glucose to glucose 6-phosphate inside the hepatocyte, ensuring an adequate flow of glucose enters the cell to be metabolized (41). Glucokinase activity is essential for glucose-induced insulin secretion, post-prandial hepatic glucose uptake, and suppression of hepatic glucose output and gluconeogenesis by elevated plasma glucose (33). Diabetic patients often have subnormal hepatic glucokinase activities, which affects the rate at which glucose is converted into glucose-6-phosphate in the liver, thus hindering the breakdown of glucose and hepatic glycogen. Biotin can stimulate glucokinase to accelerate the conversion of glucose into pyruvate, thereby reducing FBG levels (41, 42). Meanwhile, after the increase of glucokinase, the carbon from glucose are provided for *de novo* lipogenesis (43). Glucokinase mRNA expression has been proven to be associated with markers of *de novo* lipogenesis and liver triglyceride content in humans (44). The overexpression of glucokinase can promote pathways that convert glucose to fatty acids, which suggests that increased glucokinase activity may leads to reduced blood glucose and induces hypertriglyceridemia and hepatic steatosis (45, 46). Secondly, biotin acts as a key coenzyme for PC in gluconeogenesis. In biotin-deficient patients, biotin administration can increase PCC activity and maintain blood glucose stability (47). Biotin can also repress both the gluconeogenic genes and their transcription factors, such as phosphoenolpyruvate carboxykinase (PCK1), glucose-6-phosphatase (G6PC), forkhead box protein O1 (FoxO1) and hepatocyte nuclear factor 4α (HNF4α) through a pathway independent of insulin-signaling (48). The role of biotin in glucokinase and PC together make up for the efficacy of its potential clinical value.

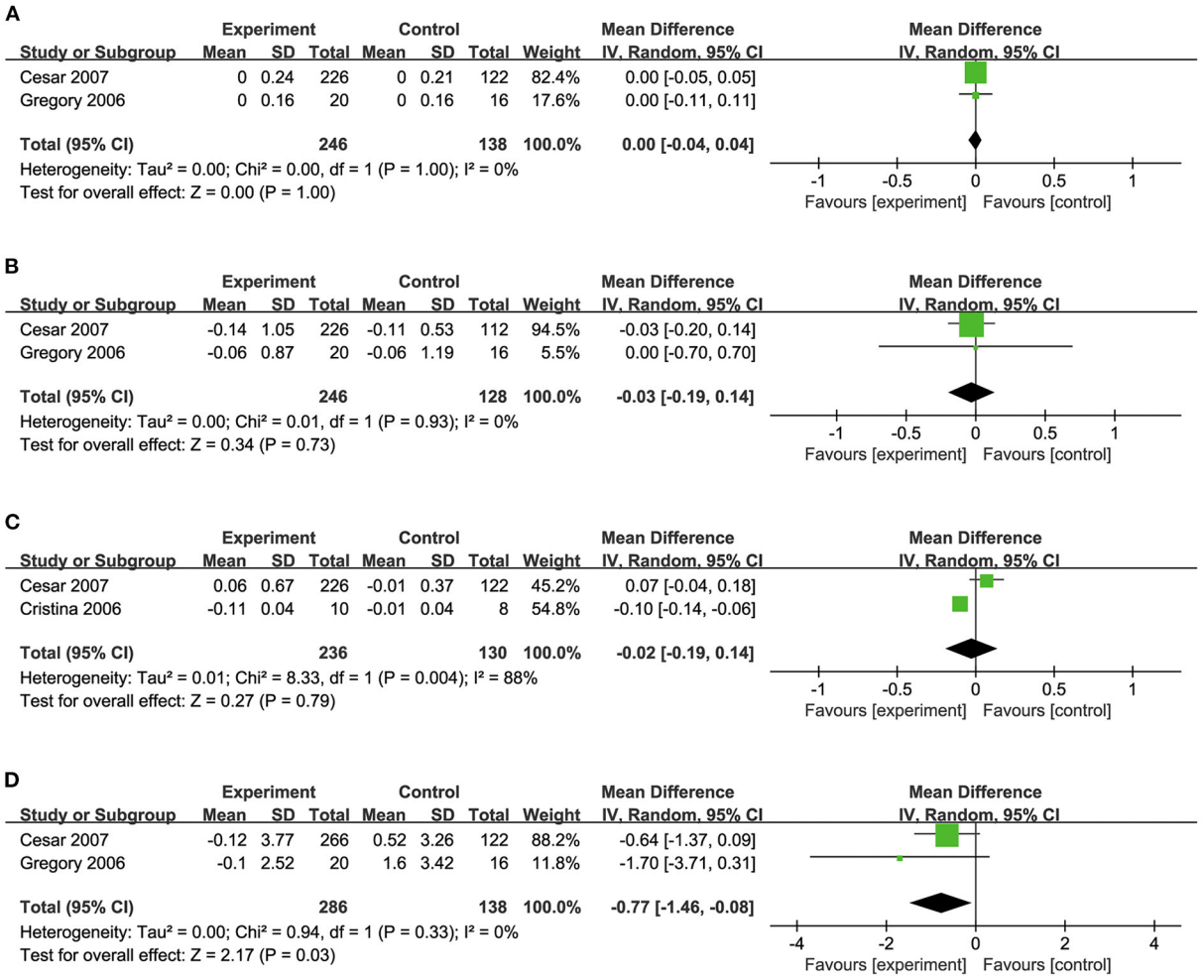

FIGURE 6
(A) Effects of biotin supplementation on HDL-C. **(B)** Effects of biotin supplementation on LDL-C. **(C)** Effects of biotin supplementation on VLDL-C. **(D)** Effects of biotin supplementation on TGHDL-C ratio.

Regarding on lipid profile, biotin can regulate lipid metabolism by reducing the expression of adipogenesis genes in liver and adipose tissues. As the coenzyme of ACC1 and ACC2, biotin helps to catalyze the reaction of acetyl CoA to malonyl CoA in the synthesis of long-chain fatty acids, which is related to the synthesis of acetylcholine and cholesterol (49). Biotin supplementation can reduce lipogenesis by increasing cGMP content and activating AMP-activated protein kinase (AMPK) (50), thereby inactivating ACC1. It is also able to increase fatty acid oxidation by decreasing ACC2 activity (32). In patients with atherosclerosis and hyperlipidemia, decreased blood cholesterol concentration was found after biotin supplementation, especially those with exacerbated hyperlipidemia (51). The triglyceride-lowering effect of biotin was also reported in patients with T2DM (32). Meanwhile, another study suggested that biotin could also potentiate the suppression of appetite by upregulating ACC2 gene expression in the hypothalamus, which lead to the suppression of food intake and contribute to the prevention of diabetes (49).

Although non-human experiments have provided strong evidence for the possible effects of biotin in the prevention and treatment of diabetes, there is a huge blank regarding data from clinical trials or RCTs. The latest article included in this meta-analysis was conducted fifteen years ago. Similarly, RCTs for thiamine supplementation in T2DM subjects also dated back to nearly ten years ago (52). The notion of using vitamin a preventive or therapeutic agent for T2DM is not new, but many have focused on fat-soluble vitamins (4, 8, 9, 53). The effects of water-soluble vitamins, especially individual vitamins in the vitamin B family, have far less been emphasized on. Only a few studies have suggested the effects of vitamins

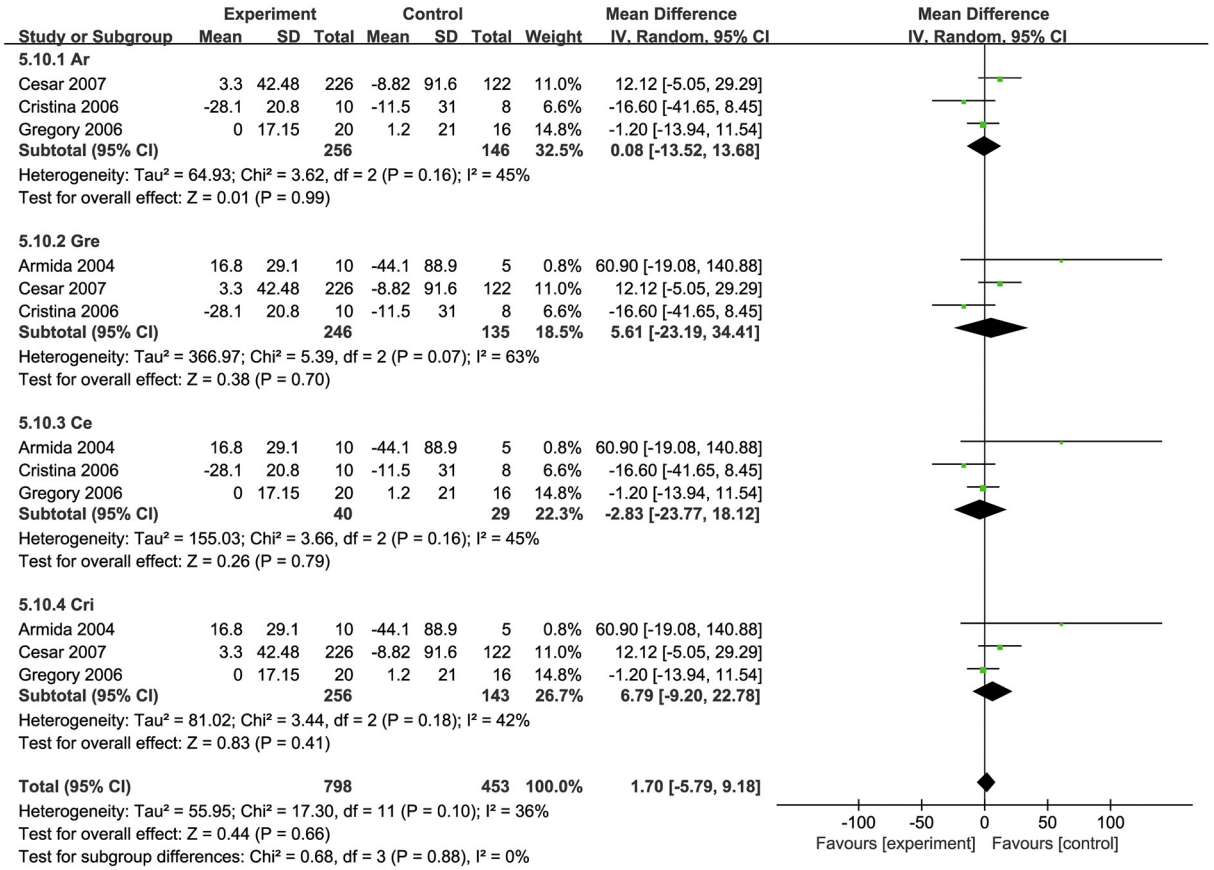

FIGURE 7
Sensitivity analysis for the effects of biotin supplementation on insulin levels.

C and individual vitamins within the vitamin B family in blood lipids and blood glucose levels. Results from a meta-analysis of 15 studies indicated that vitamin C supplementation significantly decreased TG and TC, but failed to improve LDL-C and HDL-C in T2DM patients (54). Another meta-analysis including six RCTs showed no significant beneficial effects of thiamine supplementation were observed on glycemic control (55).

Potential differences among included trials may be caused by the duration of diabetes, underlying health condition, dietary interference, and individual genetic and microbiota responses to biotin (56). More importantly, water-soluble vitamins could be largely expelled from the body due to T2DM patients' poor absorption ability and frequent urination. Thiamine deficiency (57), Vitamin B12 deficiency (58), niacin deficiency (59), biotin deficiency (27) and other vitamin B deficiency were widely reported in patients with T2DM. Whether and how much of the water-soluble vitamin supplementation would be lost in urine and how that influenced the ultimate effects needs further clarification. The baseline biotin level of the participants was not reported, the supplementation methods were not specified, and the dosage of biotin supplementation used in some studies was low and could easily be influenced by normal diet. All of these factors may be related to the lack of significant difference in insulin levels. Therefore, besides high quality RCTs on the effect of individual vitamin supplement, cross-sectional studies on the blood and urine vitamin levels of T2DM patients are all expected.

Limitations of this study include the quantity of included RCTs, as few trials have been conducted in this area. Besides, none of the RCTs in this meta-analysis had a treatment or follow-up period longer than three months, which could weaken the observations of long-term effect. Moreover, the dietary intake of biotin was not considered in all of the studies. Although the intervention effect did not meet the requirements for clinical significance due to the small sample sizes, we believe that our study provides important information to the current knowledge of the impact of biotin on glycemic control and lipid profile of T2DM patients.

Conclusions

In conclusion, our systematic review and meta-analysis suggests that biotin supplementation may decrease TC and TG levels while limited evidence suggested that its influence on insulin, LDL-C, HDL-C, VLDL-C is not significant. T2DM patients receiving higher dose of biotin demonstrated a decrease in FBG levels. Biotin supplementation could be economical and potentially beneficial to T2DM patients. However, more robust-designed and updated studies with long-term follow-up and large sample sizes are expected to further evaluate the veracity of biotin supplement in T2DM patients.

Data availability statement

The original contributions presented in the study are included in the article/Supplementary material, further inquiries can be directed to the corresponding author.

Author contributions

YZ designed the protocol, collected, analyzed the data, and wrote the manuscript. YD collected, analyzed the data, and wrote the manuscript. YF collected the data and wrote the manuscript. YX collected and analyzed the data. YL and LZ collected the data and edited the manuscript. LW conceived the idea and edited the manuscript. All authors contributed to the article and approved the submitted version.

Funding

This research was supported by the Faculty Research Grants of Macau University of Science and Technology (No. FRG-21-036-FMD).

Conflict of interest

The authors declare that the research was conducted in the absence of any commercial or financial relationships that could be construed as a potential conflict of interest.

Publisher's note

All claims expressed in this article are solely those of the authors and do not necessarily represent those of their affiliated organizations, or those of the publisher, the editors and the reviewers. Any product that may be evaluated in this article, or claim that may be made by its manufacturer, is not guaranteed or endorsed by the publisher.

Supplementary material

The Supplementary Material for this article can be found online at: https://www.frontiersin.org/articles/10.3389/fnut.2022.1046800/full#supplementary-material

References

1. Arokiasamy P, Salvi S, Selvamani Y. Global burden of diabetes mellitus: prevalence, pattern, and trends. *Handbook Global Health.* (2021) 21:495–538. doi: 10.1007/978-3-030-45009-0_28

2. Cole JB, Florez JC. Genetics of diabetes mellitus and diabetes complications. *Nat Rev Nephrol.* (2020) 16:377–90. doi: 10.1038/s41581-020-0278-5

3. Xiong K, Wang J, Ma A. Adjunctive vitamin a and d for the glycaemic control in patients with concurrent type 2 diabetes and tuberculosis: a randomised controlled trial. *Br J Nutr.* (2022) 127:556–62. doi: 10.1017/S0007114521001185

4. Zhang Y, Tan H, Tang J, Li J, Chong W, Hai Y, et al. Effects of vitamin D supplementation on prevention of type 2 diabetes in patients with prediabetes: a systematic review and meta-analysis. *Diabetes Care.* (2020) 43:1650–8. doi: 10.2337/dc19-1708

5. Yu Y, Tian L, Xiao Y, Huang G, Zhang M. Effect of Vitamin D Supplementation on some inflammatory biomarkers in type 2 diabetes mellitus subjects: a systematic review and meta-analysis of randomized controlled trials. *Ann Nutr Metab.* (2018) 73:62–73. doi: 10.1159/000490358

6. Wang S, Cai B, Han X, Gao Y, Zhang X, Wang R, et al. Vitamin d supplementation for nonalcoholic fatty liver disease in type 2 diabetes mellitus: A protocol for a systematic review and meta-analysis. *Medicine (Baltimore).* (2020) 99:e20148. doi: 10.1097/MD.0000000000020148

7. Barbarawi M, Zayed Y, Barbarawi O, Bala A, Alabdouh A, Gakhal I, et al. Effect of Vitamin D Supplementation on the Incidence of Diabetes Mellitus. *J Clin Endocrinol Metab.* (2020) 105:dgaa335. doi: 10.1210/clinem/dgaa335

8. Xu R, Zhang S, Tao A, Chen G, Zhang M. Influence of Vitamin E Supplementation on glycaemic control: a meta-analysis of randomised controlled trials. *PLoS ONE.* (2014) 9:e95008. doi: 10.1371/journal.pone.0095008

9. Shahdadian F, Mohammadi H, Rouhani MH. Effect of vitamin K supplementation on glycemic control: a systematic review and meta-analysis of clinical trials. *Horm Metab Res.* (2018) 50:227–35. doi: 10.1055/s-0044-100616

10. Sahebi R, Rezayi M, Emadzadeh M, Salehi M, Tayefi M, Parizadeh SM, et al. The effects of vitamin D supplementation on indices of glycemic control in iranian diabetics: a systematic review and meta-analysis complement. *Ther Clin Pract.* (2019) 34:294–304. doi: 10.1016/j.ctcp.2018.12.009

11. Alexander-Kaufman K, Harper C. Transketolase: observations in alcohol-related brain damage research. *Int J Biochem Cell Biol.* (2009) 41:717–20. doi: 10.1016/j.biocel.2008.04.005

12. Cinici E, Dilekmen N, Senol O, Arpali E, Cinici O, Tanas S. Blood thiamine pyrophosphate concentration and its correlation with the stage of diabetic retinopathy. *Int Ophthalmol.* (2020) 40:3279–84. doi: 10.1007/s10792-020-01513-2

13. Valdés-Ramos R, Guadarrama-López AL, Martínez-Carrillo BE, Benítez-Arciniega AD. Vitamins and type 2 diabetes mellitus. *Endocr Metab Immune Disord Drug Targets.* (2015) 15:54–63. doi: 10.2174/1871530315666150416130242

14. Khalaf KM, Khudhair MS, Ashor AW. Vitamin B12 status and peripheral neuropathy in patients with type 2 diabetes mellitus. *J Pak Med Assoc.* (2019) 69(Suppl. 3):S40–4.

15. Fernandez-Mejia C. Pharmacological effects of biotin. *J Nutr Biochem.* (2005) 16:424–7. doi: 10.1016/j.jnutbio.2005.03.018

16. Tong L. Structure and function of biotin-dependent carboxylases. *Cell Mol Life Sci.* (2013) 70:863–91. doi: 10.1007/s00018-012-1096-0

17. Dakshinamurti K, Cheah-Tan C. Biotin-mediated synthesis of hepatic glucokinase in the rat. *Arch Biochem Biophys.* (1968) 127:17–21. doi: 10.1016/0003-9861(68)90195-1

18. Romero-Navarro G, Cabrera-Valladares G, German MS, Matschinsky FM, Velazquez A, Wang J, et al. Biotin regulation of pancreatic glucokinase and insulin in primary cultured rat islets and in biotin-deficient rats. *Endocrinology.* (1999) 140:4595–600. doi: 10.1210/endo.140.10.7084

19. Sone H, Ito M, Shimizu M, Sasaki Y, Komai M, Furukawa Y. Characteristics of the biotin enhancement of glucose-induced insulin release in pancreatic islets of the rat. *Biosci Biotechnol Biochem.* (2000) 64:550–4. doi: 10.1271/bbb.64.550

20. Sone H, Ito M, Sugiyama K, Ohneda M, Maebashi M, Furukawa Y. Biotin enhances glucose-stimulated insulin secretion in the isolated perfused pancreas of the rat. *J Nutr Biochemistry.* (1999) 10:237–43. doi: 10.1016/S0955-2863(99)00003-0

21. De la Vega LA, Stockert RJ. Regulation of the insulin and asialoglycoprotein receptors via cgmp-dependent protein kinase. *Am J Physiol-Cell Physiol.* (2000) 279:C2037–42. doi: 10.1152/ajpcell.2000.279.6.C2037

22. Lazo de la Vega-Monroy ML, Larrieta E, German MS, Baez-Saldana A, Fernandez-Mejia C. Effects of biotin supplementation in the diet on insulin secretion, islet gene expression, glucose homeostasis and beta-cell proportion. *J Nutr Biochem.* (2013) 24:169–77. doi: 10.1016/j.jnutbio.2012.03.020

23. Larrieta E, Vega-Monroy ML, Vital P, Aguilera A, German MS, Hafidi ME, et al. Effects of biotin deficiency on pancreatic islet morphology, insulin sensitivity and glucose homeostasis. *J Nutr Biochem.* (2012) 23:392–9. doi: 10.1016/j.jnutbio.2011.01.003

24. Reddi A, DeAngelis B, Frank O, Lasker N, Baker H. Biotin supplementation improves glucose and insulin tolerances in genetically diabetic Kk mice. *Life Sci.* (1988) 42:1323–30. doi: 10.1016/0024-3205(88)90226-3

25. Dakshinamurti K, Modi VV, Mistry SP. Some aspects of carbohydrates metabolism in biotin-deficient rats. In: *Proceedings of the Society for Experimental Biology and Medicine.* New York, NY: Society for Experimental Biology and Medicine (1968) 127:396–400. doi: 10.3181/00379727-127-32699

26. Chauhan J, Dakshinamurti K. Transcriptional regulation of the glucokinase gene by biotin in starved rats. *J Biol Chem.* (1991) 266:10035–8. doi: 10.1016/S0021-9258(18)99181-7

27. Maebashi M, Makino Y, Furukawa Y, Ohinata K, Kimura S, Sato T. Therapeutic evaluation of the effect of biotin on hyperglycemia in patients with non-insulin dependent diabetes mellitus. *J Clin Biochem Nutr.* (1993) 14:211–8. doi: 10.3164/jcbn.14.211

28. Coggeshall JC, Heggers JP, Robson Mc, Baker H. Biotin status and plasma glucose in diabeticsa. *Annal New York Academy Sci.* (1985) 447:389–92. doi: 10.1111/j.1749-6632.1985.tb18454.x

29. McCarty MF. In type 1 diabetics, high-dose biotin may compensate for low hepatic insulin exposure, promoting a more normal expression of glycolytic and gluconeogenic enyzymes and thereby aiding glycemic control. *Med Hypotheses.* (2016) 95:45–8. doi: 10.1016/j.mehy.2016.08.002

30. Hemmati M, Babaei H, Abdolsalehei M. Survey of the effect of biotin on glycemic control and plasma lipid concentrations in type 1 diabetic patients in Kermanshah in Iran (2008-2009). *Oman Med J.* (2013) 28:195–8. doi: 10.5001/omj.2013.53

31. Ferre T, Pujol A, Riu E, Bosch F, Valera A. Correction of diabetic alterations by glucokinase. *Proc Natl Acad Sci U S A.* (1996) 93:7225–30. doi: 10.1073/pnas.93.14.7225

32. Revilla-Monsalve C, Zendejas-Ruiz I, Islas-Andrade S, Báez-Saldaña A, Palomino-Garibay MA, Hernández-Quiróz PM, et al. Biotin supplementation reduces plasma triacylglycerol and vldl In type 2 diabetic patients and in nondiabetic subjects with hypertriglyceridemia. *Biomed Pharmacother.* (2006) 60:182–5. doi: 10.1016/j.biopha.2006.03.005

33. Albarracin CA, Fuqua BC, Evans JL, Goldfine ID. Chromium picolinate and biotin combination improves glucose metabolism in treated, uncontrolled overweight to obese patients with type 2 diabetes. *Diabetes Metab Res Rev.* (2008) 24:41–51. doi: 10.1002/dmrr.755

34. Albarracin C, Fuqua B, Geohas J, Juturu V, Finch MR, Komorowski JR. Combination of chromium and biotin improves coronary risk factors in hypercholesterolemic type 2 diabetes mellitus: a placebo-controlled, double-blind randomized clinical trial. *J CardioMetab Syndrome.* (2007) 2:91–7. doi: 10.1111/j.1559-4564.2007.06366.x

35. Báez-Saldana A, Zendejas-Ruiz I, Revilla-Monsalve C, Islas-Andrade S, Cárdenas A, Rojas-Ochoa A, et al. Effects of biotin on pyruvate carboxylase, acetyl-coa carboxylase, propionyl-coa carboxylase, and markers for glucose and lipid homeostasis in type 2 diabetic patients and nondiabetic subjects. *Am J Clin Nutr.* (2004) 79:238–43. doi: 10.1093/ajcn/79.2.238

36. Moher D, Liberati A, Tetzlaff J, Altman DG. Group* P. Preferred reporting items for systematic reviews and meta-analyses: the Prisma Statement. *Annal Int Med.* (2009) 151:264–9. doi: 10.7326/0003-4819-151-4-200908180-00135

37. Higgins JP, Altman DG, Gøtzsche PC, Jüni P, Moher D, Oxman AD, et al. The cochrane collaboration's tool for assessing risk of bias in randomised trials. *BMJ.* (2011) 343:d5928. doi: 10.1136/bmj.d5928

38. Higgins JP, Thompson SG, Deeks JJ, Altman DG. Measuring inconsistency in meta-analyses. *BMJ.* (2003) 327:557–60. doi: 10.1136/bmj.327.7414.557

39. Singer GM, Geohas J. The effect of chromium picolinate and biotin supplementation on glycemic control in poorly controlled patients with type 2 diabetes mellitus: a placebo-controlled, double-blinded, randomized trial. *Diabetes Technol Ther.* (2006) 8:636–43. doi: 10.1089/dia.2006.8.636

40. McCarty MF. High-dose biotin, an inducer of glucokinase expression, may synergize with chromium picolinate to enable a definitive nutritional therapy for type Ii diabetes. *Med Hypotheses.* (1999) 52:401–6. doi: 10.1054/mehy.1997.0682

41. Adeva-Andany María M, Pérez-Felpete N, Fernández-Fernández C, Donapetry-García C, Pazos-García C. Liver glucose metabolism in humans. *Biosci Rep.* (2016) 36:160385. doi: 10.1042/BSR20160385

42. Matschinsky FM, Wilson DF. The central role of glucokinase in glucose homeostasis: a perspective 50 years after demonstrating the presence of the enzyme in islets of langerhans. *Front Physiol.* (2019) 10:148. doi: 10.3389/fphys.2019.00148

43. Dentin R, Girard J, Postic C. Carbohydrate responsive element binding protein (Chrebp) and sterol regulatory element binding protein-1c (Srebp-1c): two key regulators of glucose metabolism and lipid synthesis in liver. *Biochimie.* (2005) 87:81–6. doi: 10.1016/j.biochi.2004.11.008

44. Peter A, Stefan N, Cegan A, Walenta M, Wagner S, Königsrainer A, et al. Hepatic glucokinase expression is associated with lipogenesis and fatty liver in humans. *J Clin Endocrinol Metab.* (2011) 96:E1126–E30. doi: 10.1210/jc.2010-2017

45. Morral N, Edenberg HJ, Witting SR, Altomonte J, Chu T, Brown M. Effects of glucose metabolism on the regulation of genes of fatty acid synthesis and triglyceride secretion in the liver. *J Lipid Res.* (2007) 48:1499–510. doi: 10.1194/jlr.M700090-JLR200

46. Niswender KD, Shiota M, Postic C, Cherrington AD, Magnuson MA. Effects of increased glucokinase gene copy number on glucose homeostasis and hepatic glucose metabolism. *J Biol Chem.* (1997) 272:22570–5. doi: 10.1074/jbc.272.36.22570

47. Wolf B, Rosenberg LE. Stimulation of propionyl coa and beta-methylcrotonyl coa carboxylase activities in human leukocytes and cultured fibroblasts by biotin. *Pediatr Res.* (1979) 13:1275–9. doi: 10.1203/00006450-197911000-00014

48. Matschinsky FM. Glucokinase, glucose homeostasis, and diabetes mellitus. *Curr Diab Rep.* (2005) 5:171–6. doi: 10.1007/s11892-005-0005-4

49. Sone H, Kamiyama S, Higuchi M, Fujino K, Kubo S, Miyazawa M, et al. Biotin augments acetyl coa carboxylase 2 gene expression in the hypothalamus, leading to the suppression of food intake in mice. *Biochem Biophys Res Commun.* (2016) 476:134–9. doi: 10.1016/j.bbrc.2016.04.152

50. Aguilera-Méndez A, Fernández-Mejía C. The hypotriglyceridemic effect of biotin supplementation involves increased levels of cgmp and ampk activation. *BioFactors.* (2012) 38:387–94. doi: 10.1002/biof.1034

51. Marshall M, Kliman P, Washington V, Mackin J, Weinland B. Effects of Biotin on lipids and other constituents of plasma of healthy men and women. *Artery.* (1980) 7:330–51.

52. Alaei Shahmiri F, Soares MJ, Zhao Y, Sherriff J. High-dose thiamine supplementation improves glucose tolerance in hyperglycemic individuals: a randomized, double-blind cross-over trial. *Eur J Nutr.* (2013) 52:1821–4. doi: 10.1007/s00394-013-0534-6

53. Iqbal S, Naseem I. Role of vitamin a in type 2 diabetes mellitus biology: effects of intervention therapy in a deficient state. *Nutrition.* (2015) 31:901–7. doi: 10.1016/j.nut.2014.12.014

54. Namkhah Z, Ashtary-Larky D, Naeini F, Clark CCT, Asbaghi O. Does vitamin C supplementation exert profitable effects on serum lipid profile in patients with type 2 diabetes? a systematic review and dose-response meta-analysis. *Pharmacol Res.* (2021) 169:105665. doi: 10.1016/j.phrs.2021.105665

55. Muley A, Fernandez R, Green H, Muley P. Effect of thiamine supplementation on glycaemic outcomes in adults with type 2 diabetes: a systematic review and meta-analysis. *BMJ Open.* (2022) 12:e059834. doi: 10.1136/bmjopen-2021-059834

56. Voland L, Le Roy T, Debédat J, Clément K. gut microbiota and vitamin status in persons with obesity: a key interplay. *Obesity Rev.* (2022) 23:e13377. doi: 10.1111/obr.13377

57. Page GL, Laight D, Cummings MH. Thiamine deficiency in diabetes mellitus and the impact of thiamine replacement on glucose metabolism and vascular disease. *Int J Clin Pract.* (2011) 65:684–90. doi: 10.1111/j.1742-1241.2011.02680.x

58. Aroda VR, Edelstein SL, Goldberg RB, Knowler WC, Marcovina SM, Orchard TJ, et al. Long-term metformin use and vitamin B12 deficiency in the diabetes prevention program outcomes study. *J Clin Endocrinol Metab.* (2016) 101:1754–61. doi: 10.1210/jc.2015-3754

59. Zillikens MC, van Meurs JB, Sijbrands EJ, Rivadeneira F, Dehghan A, van Leeuwen JP, et al. Sirt1 genetic variation and mortality in type 2 diabetes: interaction with smoking and dietary niacin. *Free Radic Biol Med.* (2009) 46:836–41. doi: 10.1016/j.freeradbiomed.2008.12.02

frontiers | Frontiers in Nutrition

TYPE Original Research
PUBLISHED 01 November 2022
DOI 10.3389/fnut.2022.1051452

OPEN ACCESS

EDITED BY
Ling Zhao,
The University of Tennessee, Knoxville, United States

REVIEWED BY
Zhaoyue Zhang,
The Rockefeller University, United States
Hiroshi Hara,
Fuji Women's University, Japan

*CORRESPONDENCE
Dongmin Liu
doliu@vt.edu
Bin Xu
bxu@nccu.edu

†PRESENT ADDRESS
Yao Wang,
Diabetes Center,
School of Medicine, UCSF,
San Francisco, CA, United States

SPECIALTY SECTION
This article was submitted to Nutrition and Metabolism, a section of the journal Frontiers in Nutrition

RECEIVED 22 September 2022
ACCEPTED 11 October 2022
PUBLISHED 01 November 2022

CITATION
Wang Y, Wu Y, Wang A, Wang A, Alkhalidy H, Helm R, Zhang S, Ma H, Zhang Y, Gilbert E, Xu B and Liu D (2022) An olive-derived elenolic acid stimulates hormone release from L-cells and exerts potent beneficial metabolic effects in obese diabetic mice.
Front. Nutr. 9:1051452.
doi: 10.3389/fnut.2022.1051452

An olive-derived elenolic acid stimulates hormone release from L-cells and exerts potent beneficial metabolic effects in obese diabetic mice

Yao Wang[1†], Yajun Wu[1], Aiping Wang[2], Aihua Wang[3], Hana Alkhalidy[4], Richard Helm[3], Shijun Zhang[5], Hongguang Ma[5], Yan Zhang[5], Elizabeth Gilbert[6], Bin Xu[7*] and Dongmin Liu[1,8*]

[1]Department of Human Nutrition, Foods, and Exercise, College of Agricultural and Life Sciences, Virginia Tech, Blacksburg, VA, United States, [2]College of Life Sciences, Zhengzhou University, Zhengzhou, Henan, China, [3]Department of Biochemistry, College of Agriculture and Life Sciences, Virginia Tech, Blacksburg, VA, United States, [4]Department of Nutrition and Food Technology, Jordan University of Science and Technology, Irbid, Jordan, [5]Department of Medicinal Chemistry, School of Pharmacy, Virginia Commonwealth University, Richmond, VA, United States, [6]School of Animal Sciences, College of Agricultural and Life Sciences, Virginia Tech, Blacksburg, VA, United States, [7]Department of Pharmaceutical Sciences, Biomanufacturing Research Institute and Technology Enterprise, North Carolina Central University, Durham, NC, United States, [8]Virginia Tech Drug Discovery Center, Virginia Tech, Blacksburg, VA, United States

Insulin resistance and progressive decline in functional β-cell mass are two key factors for developing type 2 diabetes (T2D), which is largely driven by overweight and obesity, a significant obstacle for effective metabolic control in many patients with T2D. Thus, agents that simultaneously ameliorate obesity and act on multiple pathophysiological components could be more effective for treating T2D. Here, we report that elenolic acid (EA), a phytochemical, is such a dual-action agent. we show that EA dose-dependently stimulates GLP-1 secretion in mouse clonal L-cells and isolated mouse ileum crypts. In addition, EA induces L-cells to secrete peptide YY (PYY). EA induces a rapid increase in intracellular $[Ca^{2+}]_i$ and the production of inositol trisphosphate in L-cells, indicating that EA activates phospholipase C (PLC)-mediated signaling. Consistently, inhibition of (PLC) or $G\alpha_q$ ablates EA-stimulated increase of $[Ca^{2+}]_i$ and GLP-1 secretion. *In vivo*, a single dose of EA acutely stimulates GLP-1 and PYY secretion in mice, accompanied with an improved glucose tolerance and insulin levels. Oral administration of EA at a dose of 50 mg/kg/day for 2 weeks normalized the fasting blood glucose and restored glucose tolerance in high-fat diet-induced obese (DIO) mice to levels that were comparable to chow-fed mice. In addition, EA suppresses

appetite, reduces food intake, promotes weight loss, and reverses perturbated metabolic variables in obese mice. These results suggest that EA could be a dual-action agent as an alternative or adjuvant treatment for both T2D and obesity.

KEYWORDS

elenolic acid, glucagon-like peptide-1, peptide YY, obesity, type 2 diabetes, mice

Introduction

Type 2 diabetes (T2D) is a result of chronic insulin resistance and loss of β-cell function and mass (1–3). In both experimental animals and people, obesity is a leading pathogenic factor for developing insulin resistance and T2D, which is regarded as a significant obstacle for effective metabolic control in many patients with T2D. Constant insulin resistance will progress to T2D when β-cells become unable to secrete adequate amounts of insulin to compensate for decreased insulin sensitivity, which is largely due to loss of functional β-cell mass (1–3). Metformin has been widely used for the treatment of T2D. While it is effective in ameliorating hyperglycemia primarily by reducing hepatic glucose production and enhancing insulin sensitivity, it is unable to promote desired weight loss and stop the progressive decline in β-cell function and mass (4, 5).

It is well-established that the incretin hormone glucagon-like peptide-1 (GLP-1), which is primarily secreted from intestinal L-cells, plays a critical role in maintaining glycemic homeostasis *via* potentiating glucose-stimulated insulin secretion (GSIS) and promoting β-cell proliferation and survival (6–8). Recently, GLP-1-based drugs, including GLP-1 analogues and dipeptidyl peptidase-IV (DPP-IV) inhibitors that inhibit breakdown of GLP-1, have been developed for treating T2D (9–11), but patients given GLP-1-based drugs suffer from side effects such as nausea and vomiting (12). In addition, the weight loss efficacy of these monotherapies is often limited (13). Compared with GLP-1, peptide YY (PYY) secreted from L-cells may play a more important role in regulating satiety and food intake in both humans and rodents (14, 15). Recent studies further showed that GLP-1 and PYY synergistically inhibit appetite in mice (16) and humans (17, 18). Therefore, agents that are capable of targeting both GLP-1 and PYY secretion could be a safe and effective strategy in the prevention and treatment of T2D by promoting obesity and insulin resistance control and simultaneously improving functional β -cell mass.

A recent study showed that consumption of extra virgin olive oil (EVO) provided better glycemic control as compared with pure olive oil (POO) in human subjects (19). EVO has a nearly identical fatty acid composition but considerably higher amount of phytochemicals than POO (20), suggesting that the beneficial effect of EVO may be at least partially attributed to one or more of its phytochemical components. Interestingly, EVO intake resulted in higher serum GLP-1 and insulin levels but lower postprandial glycemia relative to POO in patients with morbid obesity (19). However, the specific compound(s) that are responsible for the observed metabolic beneficial actions of EVO are unclear. Oleuropein and its derivatives such as hydroxytyrosol and elenolic acid (EA) are major phytochemicals in olives (21). EA is present in mature olives and EVO, and is derived from decomposition of oleuropein during fruit maturation (22). Oleuropein and its aglycone oleacein have moderate glucose-lowering effects and ameliorate high-fat-diet (HFD)-induced metabolic alterations in rodent models, but it has not been investigated either *in vitro* or *in vivo* whether EA exerts beneficial actions related to healthy or disease states such as diabetes. In this study, we generated EA by hydrolyzing oleuropein and investigated the effects of EA on GLP-1 and PYY secretion in L-cells and further explored the underlying mechanism of EA's action. In addition, we explored the anti-diabetic effects of EA in diet-induced obese (DIO), glucose intolerant mice.

Materials and methods

Chemicals and reagents

Oleuropein (purity ≥ 80%, HPLC) for EA synthesis was from Shaanxi Huike Botanical Development Co. (Xi'an, China); metformin was from Cayman Chemicals (Ann Arbor, MI, USA); U73122 was from Tocris Bioscience (Pittsburgh, PA); YM 254,890 was from Focus Biomolecules (Plymouth Meeting, PA, USA); DMEM media, fetal bovine serum (FBS), and other cell culture supplements were from Hyclone (GE Healthcare Bio-Sciences, Pittsburgh, PA, USA); fluro-4AM was from ThermoFisher Scientific (Waltham, MA); antibodies for western blotting were from Santa Cruz Biotechnology (Dallas, TX, USA); assay kits for measuring active GLP-1 [GLP-1 (7–36) amide and GLP-1 (7–37)], triglyceride, human PYY as well as dipeptidyl peptidase IV (DPP4) inhibitor assay kit were from Cayman Chemical (Ann Arbor, MI); oleacein, hydroxytyrosol, oleocanthal, tyrosol, and oleuropein (≥ 95% pure) for GLP-1 secretion assays, RPMI1640 medium, and all other chemicals

were purchased from Millipore Sigma (Burlington, MA, USA); IP_3 ELISA kit was from Amsbio (Cambridge, MA, USA); mouse insulin and leptin ELISA kits and mouse total GLP-1 ELISA kits were from Crystal Chem (Elk Grove Village, IL); glucose meter and strips were from AgaMatrix (Salem, NH); and free fatty acid (FFA) assay kits were from BioAssay Systems (Hayward, CA, USA).

Generation of elenolic acid

Oleuropein was dissolved in tetrahydrofuran (THF), followed by the addition of 1 N aqueous H_2SO_4 and stirring for 48 h at room temperature. After removing THF under vacuum, the solution was neutralized to pH 7.5 with 1 N NaOH solution. The solution was washed with ethyl acetate (EtOAc) three times. The neutral solution was acidified with 1 N HCl and extracted with EtOAc. The organic layer was collected and dried with anhydrous sodium sulfate overnight. After evaporating the solvent, the residue was purified by flash chromatographic procedures, using dichloromethane-methanol (contain 1% acetic acid) as mobile phase to obtain EA. The final product identity and purity was confirmed by liquid chromatography-mass spectrometry (LC-MS) (SHIMADZU Scientific Instruments, Inc., Columbia, MD, USA), ^{1}H-NMR, and ^{13}C-NMR analyses.

Glucagon-like peptide-1 secretion measurement

GLUTag L-cells (provided by Dr. Daniel J. Drucker, Lunenfeld Tanenbaum Research Institute, Toronto, ON, Canada) were cultured as previous described (23). For GLP-1 secretion assays, cells were incubated with Krebs-Ringer Modified (KRB) buffer containing 0.2% bovine serum albumin (BSA) for 30 min and then treated with EA (0.1, 1, or 10 μM), 10 μM oleacein, hydroxytyrosol, oleocanthal, tyrosol, oleuropein, or 1 μM forskolin and 1 μM 3-isobutyl-1-methylxanthine (IBMX) for 1 h. For some experiments, cells were pretreated with various inhibitors for 30 min prior to the addition of 10 μM EA for 1 h. Supernatants were collected for measuring GLP-1 [7–36 (NH2) and GLP-1 (7–37)] concentrations using an assay kit, which was then normalized to the protein content in the same sample. The ileum crypts were isolated from mice as previously described (24, 25). The crypts were maintained for 48 h, and then treated with EA or forskolin (10 μM) plus IBMX for 1 h to measure GLP-1 secretion.

Peptide YY secretion assay

NCI-H716 cells (ATCC, CCL-251) were maintained in RPMI1640 medium supplemented with 10% fetal bovine serum (FBS), 2 mM L-Glutamine, and 1% penicillin streptomycin in a humidified incubator at 37°C and 5% CO_2. For PYY secretion, 2×10^5 NCI-H716 cells were seeded into a 12-well plate that was precoated with Matrigel. Before the treatment, cells were incubated with KRB buffer containing 0.2% BSA for 30 min and then treated with EA or 2 mM butyrate for 1 h. Supernatants were collected for measuring PYY (in the form of 3–36) concentration using an assay kit, which was then normalized to the protein content in the same sample.

Intracellular calcium measurement

To identify whether EA induces intracellular calcium influx, GLUTag cells were loaded with 2 μM Fluo-4AM in Ca^{2+}-free KRB and incubated at 37°C for 1 h. The cells were then washed and resuspended in Ca^{2+}-free KRB buffer at 2×10^6 cell/ml and transferred to opaque 96-well microplates. Basal fluorescence signals of Fluro-4AM-loaded cells were measured at 495 nm excitation and 518 nm emission using a spectrofluorophotometer (FLUOstar OPATIMA, Cary, NC, USA). After 10 sec, EA or inhibitor was injected into culture plates, and fluorescence was continuously recorded for 240 s.

Inositol trisphosphate assay

GLUTag cells (10^5 cells/well) were treated with vehicle or 10 μM EA for 30 sec, followed by addition of 10% perchloric acid to terminate the reaction. IP_3 concentrations in the cell lysates were measured using an ELISA kit.

Trypsin protection assay

To investigate whether EA binds with Gα subunits, the isolation of plasma membranes and subsequent trypsin protection assays were performed as described (26) with modifications. The inactive Gα can be readily cleaved by trypsin, whereas the active Gα due to the agonist-stimulated binding of GTP protects it from trypsinolysis (26). In brief, GLUTag cells were lysed in 10 mM Tris–HCl (pH 7.4) buffer containing 5 mM EDTA, 10 μg/ml benzamidine, 10 μg/ml soybean trypsin inhibitor (type II-S), and 5 μg/ml leupeptin, and plasma membranes were isolated. Cell membranes (30 μg) were then incubated in 25 mM HEPES (pH 7.5) buffer containing 1 mM EDTA, 20 mM β-mercaptoethanol, 25 mM $MgCl_2$, 100 mM NaCl, 10 μM GDP, and 50 μM GTPγS in the presence or absence of EA or vehicle at 37°C for 15 min. Afterward, the cell membranes were digested with 100 μg/ml of N-tosyl-L-phenylamine chloromethyl ketone (TPCK)-trypsin (1:25 ratio of trypsin to total protein) at room temperature for 15 min, and the reaction was terminated by the addition of gel loading

buffer and heating at 95°C. The samples were then analyzed by immunoblotting with antibodies against $G\alpha_s$, $G\alpha_i$, or $G\alpha_q$.

Animals

Male C57/BL6J mice (male, 8 weeks old) were purchased from the Jackson Laboratory (Bar Harbor, ME, USA). All mice were kept under constant temperature (23°C) and Light cycle (12 h Light/12 h dark) with *ad libitum* access to water and either a standard chow diet (SD, 11% kcal from fat) or high-fat-diet (HFD, 58% kcal from fat) (Research Diets, Inc., New Brunswick, NJ, USA). All protocols for the following animal experiments were approved by the Institutional Animal Care and Use Committee at Virginia Tech.

Acute effects of elenolic acid on glucagon-like peptide-1 and peptide YY secretion and glucose intolerance in mice

Next, we used DIO mice to assess whether acute administration of EA improves glucose tolerance, thereby exerting potential anti-diabetic potential consistent with its stimulatory action in GLP-1 and PYY secretion. In that regard, C57B6 mice (male, 8 weeks old) were fed a control, standard chow diet (SD; Research Diets, NJ, containing 11, 73, and 16% kcal from fat, carbohydrate and protein, respectively) or a HFD (containing 58% kcal from fat) for 12 weeks (wks) to induce obesity, insulin resistance, and glucose intolerance (27). To perform intraperitoneal glucose tolerance test (IPGTT), mice (n = 8/group) were fasted for 14 h followed by measuring basal blood glucose levels using samples drawn from tail vein. Mice were then given 50 mg/kg EA or same amount of vehicle *via* oral gavage. EA was dissolved in 0.1 M $NaHCO_3$ and then suspended in 2% methylcellulose before administration. At 30 min after EA administration, blood samples were drawn for glucose measurements, and then an IPGTT (1.5 g glucose/kg) was performed. The area under the curve (AUC) from these tests was calculated as previously described (28). For assessing the effects of EA on GLP-1 and PYY levels, obese mice were fasted for 6 h and blood samples from tail vein were collected into pre-chilled tubes containing 50 μM diprotin A and 5 mM EDTA for baseline analyses. Mice were then administered 50 mg/kg EA or vehicle (n = 8/group) and blood was drawn at 15 min post-injection for measuring total GLP-1 (tGLP-1, C) and PYY (D) levels using ELISA kits. To examine the effect of EA on glucose stimulated insulin secretion (GSIS), mice were fasted for 6 h and then administered 1.5 g/kg glucose *via* IP injection. Tail vein blood samples were obtained before and 30 min after glucose administration, and plasma insulin levels were measured with an ELISA kit.

Metabolic effects of elenolic acid on obese mice

C57BL6 mice (8 weeks old, male) were fed either a SD or a HFD (n = 8 mice/group) for 10 weeks to induce obesity. Obese mice were divided into two groups with similar body weight (BW) and blood glucose and then given either EA (50 mg/kg once daily) or vehicle *via* oral gavage for 2 weeks. Age-matched mice fed a SD were used as healthy controls and were administered the vehicle orally for 2 weeks. Body weight, non-fasting blood glucose (NFBG), and fasting blood glucose (FBG) were recorded weekly. For measuring food intake, pre-weighed food pellets were provided and replaced twice a week, and cumulative food intake was calculated. IPGTT was performed at the end of this experiment. Body composition of mice was evaluated by NMR Analyzer for small animals (Bruker, Billerica, MA, USA) at the beginning and end of the study. Following these procedures, mice were fasted overnight, euthanized, an blood was collected immediately *via* cardiopuncture. Plasma insulin, leptin, FFA and triglycerides were measured using assay kits.

Statistical analysis

Data were analyzed by unpaired student's t-test or one-way ANOVA using SigmaPlot software. Significant differences between multiple groups were subjected to Tukey's test. A $p < 0.05$ was considered statistically significant. Values are presented as mean ± standard error (SE) or SE of mean (SEM), where appropriate.

Results

Synthesis and validation of elenolic acid

Elenolic acid (EA) was synthesized by hydrolysis of oleuropein followed by multiple steps of extraction and purification procedures. The purity of generated EA was > 95% as determined by LC-MS analysis, which showed that the predominant EA peak has a retention time of 5.50 min $[M-H]^-$ of 241.07 (**Supplementary Figure 1A**). The isolated EA is an aldehyde form as confirmed with high-resolution mass spectrometry fragmentation (**Supplementary Figure 1B**), and its chemical structure and calculated mass are shown in the inset. The aldehyde form of EA was further determined by ^{13}C and ^{1}H nuclear magnetic resonance (NMR) spectroscopy (**Supplementary Figures 1C,D**). The chemical shift of aldehyde EA is 13C (> 200 ppm) and 1H (9.7 ppm) from ^{13}C-NMR to ^{1}H-NMR analysis, respectively.

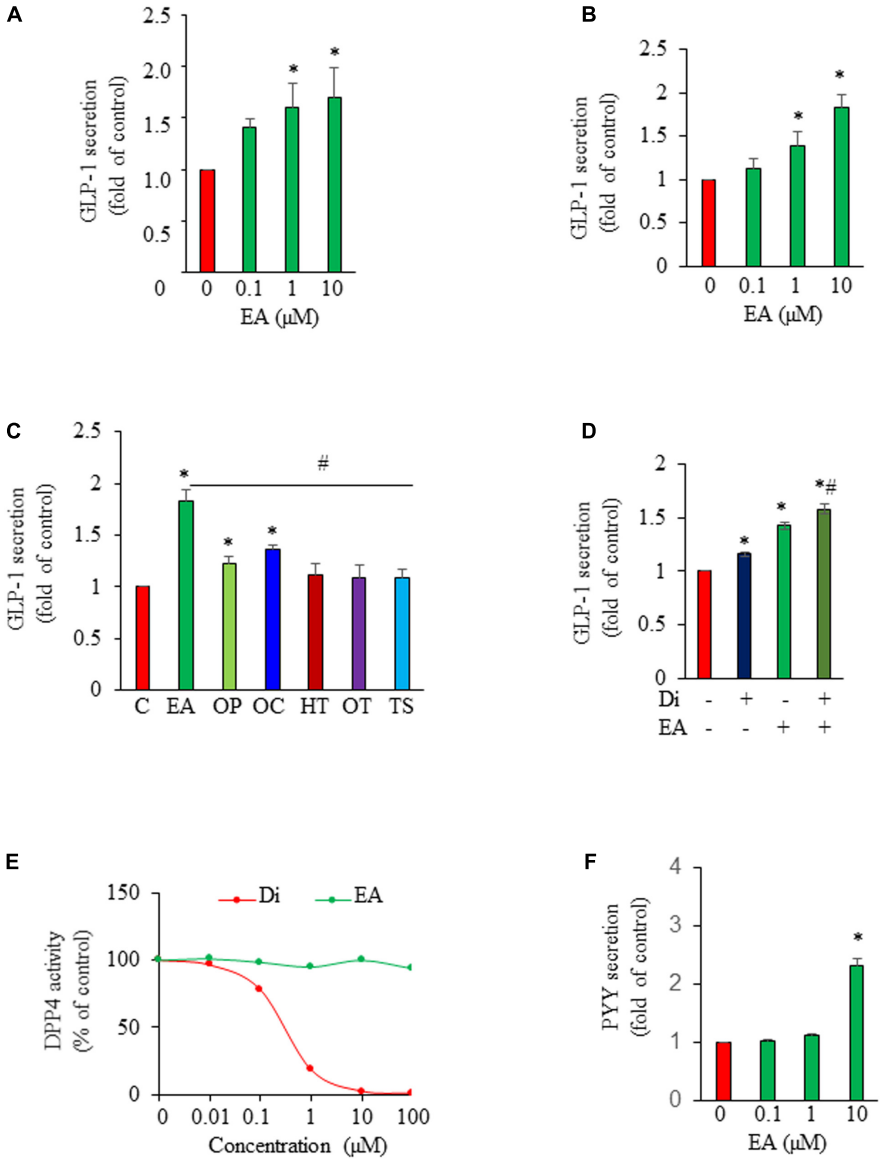

FIGURE 1
Elenolic acid (EA) induces both glucagon-like peptide-1 (GLP-1) and peptide YY (PYY) secretion from L-cells. GLUTag L-cells **(A)** or mouse ileum crypts **(B)** were incubated with various concentrations of EA or vehicle for 1 h. GLP-1 secreted into medium was measured by ELISA, and the GLP-1 secretion was normalized to protein content of each treatment and converted to the percentage of the control. **(C)** GLP-1 secretion from cells treated with 10 μM EA, oleuropein (OP), oleacein (OC), hydroxytyrosol (HT), oleocanthal (OT), or tyrosol (TS) for 1 h. **(D)** GLUTag cells were pre-incubated with or without DPP4 inhibitor vildagliptin (Di; 50 μM) for 30 min and then treated with vehicle or 10 μM EA for another 1 h. Supernatants were collected for GLP-1 secretion measurement. **(E)** The DPP4 activity in the presence of EA or DI was analyzed using a fluorescence reader at an excitation wavelength of 360 and emission wavelength of 465. **(F)** NCI-H716 L-cells were incubated with EA or vehicle for 1 h. PYY released into supernatants were measured using an assay kit. Data are mean ± SEM (n = 3–4). *$p < 0.05$ vs. control; #$p < 0.05$ vs. EA.

Elenolic acid is an intestinal L-cell functional agonist with anti-diabetic potential

We show that EA is an incretin secretagogue, with 1–10 μM concentration inducing significant GLP-1 release from GLUTag L-cells after 1 h of exposure (Figure 1A). Similarly, EA treatment significantly increased GLP-1 secretion from isolated mouse ileum crypts (Figure 1B), suggesting that the EA effect on L-cells is physiologically relevant. Next, we compared the effect of EA on GLP-1 secretion with that of other secoiridoids, including oleuropein (OP), oleacein (OC), hydroxytyrosol (HT), as well as oleocanthal (OT) and tyrosol (TS). We found that EA is much more potent in stimulating GLP-1 secretion than OP and OC,

whereas OT, HT, and TS are inactive (Figure 1C), indicating that EA is unique in inducing GLP-1 secretion. To determine whether EA induces GLP-1 secretion through inhibition of DPP-IV, we pre-incubated the cells with 50 μM vildagliptin, a DPP-IV inhibitor. As shown in Figure 1D, vildagliptin alone increased GLP-1 level by 16% ($p < 0.05$), which was only about 30% of that achieved by exposure to EA. In the presence of vildagliptin, EA-stimulated GLP-1 release was further increased, which should be due to the inhibitory effect of vildagliptin on GLP-1 degradation. We further confirmed that vildagliptin was very potent in inhibiting DPP-IV with doses > 10 μM completely ablating its enzymatic activity while EA at the same doses was inactive (Figure 1E). These results demonstrate that EA action on GLP-1 secretion from L-cells is mediated *via* a DPP-IV-independent mechanism. Last, to examine whether EA also directly induces PYY secretion from L-cells, we cultured NCI-H716 cells in the presence or absence of EA. Consistent with its effect *in vivo*, EA stimulated PYY secretion from L-cells, with 10 μM increasing PYY secretion by over 100% (Figure 1F).

Elenolic acid stimulates glucagon-like peptide-1 secretion through a $G\alpha_q$-PLC-IP_3-Ca^{2+}-dependent mechanism

To explore the signaling mechanism that mediated EA-stimulated GLP-1 secretion, we first examined whether EA increases intracellular $[Ca^{2+}]_i$, which is critical for triggering GLP-1 secretion (29). We found that L-cells exposed to EA displayed a rapid increase in intracellular $[Ca^{2+}]_I$ (Figure 2A). We then examined the effect of EA on the activity of phospholipase C (PLC), which hydrolyzes phosphatidylinositol 4,5-bisphosphate (PIP_2) to the Ca^{2+}-mobilizing second messenger inositol triphosphate (IP_3), thereby elevating cytosolic $[Ca^{2+}]$ (30). The result showed that EA treatment elicited a rapid IP_3 production in L-cells, indicating that EA stimulated PLC activity (Figure 2B). Further, incubation of L-cells with U73122, a specific antagonist of PLC, completely ablated EA-elicited intracellular $[Ca^{2+}]_i$ increase (Figure 2C) and GLP-1 secretion (Figure 2D), suggesting that EA induced-GLP-1 secretion was mediated *via* the PLC-dependent pathway. Next, we determined whether EA induces GLP-1 secretion *via* $G\alpha_q$, as the secretion of GLP-1 could be regulated *via* G-protein-coupled receptors, which signal primarily through $G\alpha_q$, leading to activation of PLC/Ca^{2+} signaling (31–35). We found that blockage of $G\alpha_q$ with the $G\alpha_q$ specific inhibitor, YM 254890, diminished EA-induced GLP-1 secretion (Figure 2E). We further examined whether EA activates $G\alpha_q$ by performing a trypsin sensitivity assay (26), Cell membranes incubated with EA exhibited a clear and strong $G\alpha_q$ band, which was completely absent in vehicle-treated plasma membranes (Figure 2F). Collectively, these results provide evidence that EA-stimulated hormone secretion from L-cells is mediated by activating $G\alpha_q$/PLC/Ca^{2+} signaling.

Acute administration of elenolic acid improved glycemic control and increased blood glucagon-like peptide-1, peptide YY, and insulin levels

We next assessed the acute effect of EA on glucose excursion in HFD-induced obese, glucose intolerant mice. The results from IPGTT showed that administration of EA significantly reduced blood glucose levels at 15, 30, and 60 min post-injection of glucose as compared with the control mice (Figures 3A,B), which is consistent with the established role of GLP-1 in glucose homeostasis. Next, we determined the effect of oral administration of EA on GLP-1, PYY, and insulin secretion in obese mice under glucose challenge. Acute administration of EA increased blood GLP-1 (Figure 3C) and PYY (Figure 3D) levels by about 50% ($p < 0.05$), demonstrating that EA-evoked GLP-1 and PYY (3–36) secretion from L-cells *ex vitro* is recapitulated *in vivo*. Acute administration of EA also increased plasma insulin levels in obese mice under glucose challenge (Figure 3E), suggesting that it promoted glucose-stimulated insulin secretion (GSIS), which is consistent with such a role of GLP-1 in pancreatic beta-cells. Importantly, EA did not alter blood glucose levels in SD-fed lean mice (Figure 3F), indicating that it has no hypoglycemic effect in metabolically healthy mice.

Elenolic acid reverses hyperglycemia in diet-induced obese mice

We then conducted an animal study to evaluate whether EA has potential as a therapeutic for the treatment of obesity and T2D. In that regard, C57B6 mice were fed a SD or a HFD for 10 wks to induce obesity, insulin resistance, and glucose intolerance (27), followed by oral administration of EA (50 mg/kg) once per day for 2 weeks. Remarkably, treatment with EA completely reversed hyperglycemia (Figures 4A,B). Consistently, EA also fully corrected glucose intolerance (Figures 4C,D) in obese mice.

Elenolic acid promotes body weight loss and reverses obesity-associated perturbation of metabolic variables in diet-induced obese mice

Oral administration of EA promoted weight loss in DIO mice during 2 wks of treatment, which reduced BW from

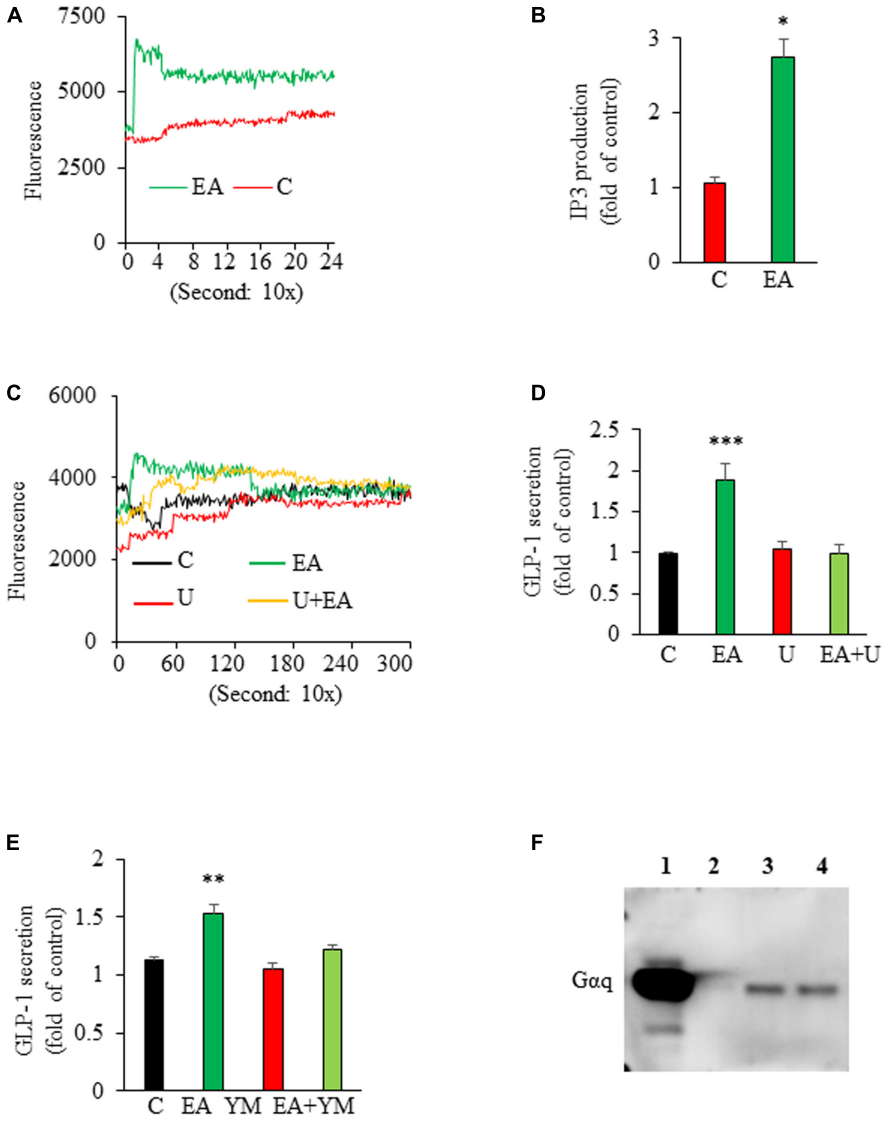

FIGURE 2
Elenolic acid (EA)-induced glucagon-like peptide-1 (GLP-1) secretion is mediated *via* a Gαq-PLC-IP3-Ca^{2+}-dependent mechanism. **(A)** GLUTag L-cells were pretreated with Fluo-4AM and treated with vehicle or 10 μM EA. The $[Ca^{2+}]_i$ response was measured using a fluorescence plate reader. A representative graph from 4 experiments is shown. **(B)** L-cells were treated with 10 μM EA or vehicle for 20 s. The intracellular IP_3 contents were measured using an ELISA kit. **(C)** GLUTag cells were labeled with Fluo-4 AM in the presence or absence of 10 μM U73122 (U) for 30 min, followed by an injection of 10 μM EA or vehicle. The $[Ca^{2+}]_i$ response was measured as stated above. **(D)** GLUTag cells were pretreated with 10 μM U73122 (U) for 30 min, followed by addition of 10 μM EA or vehicle for another 1 h. Supernatants were collected for GLP-1 measurement. **(E)** L-cells were preincubated with 10 μM $G\alpha_q$ inhibitor, YM 254,890 (YM) for 30 min followed by incubation with 10 μM EA or vehicle for 1 h. Supernatants were collected for measuring GLP-1 secretion. **(F)** Cell membranes isolated from L-cells were treated with vehicle or EA for 15 min. Western blotting was performed with $G\alpha_q$ antibody. L, ladder; Lane 1: assay control (without trypsin); Lane 2: vehicle; Lane 3: 1 μM EA; Lane 4: 10 μM EA. Data are means ± SEM; n = 5–6. $^*P < 0.05$; $^{**}P < 0.01$; $^{***}P < 0.001$ vs. control.

37.3 ± 1.4 g to 35.4 ± 1.42 g, corresponding to a decrease of 5.0 ± 1.4% ($P < 0.05$), whereas the BW of vehicle-treated DIO mice increased by 6.4% over their initial BW, 37.3 ± 1.4 (Figure 5A). In addition, EA reduced food intake, with cumulative food intake at the end of 2 weeks reduced to 28.0 ± 1.5 g/mouse in EA-treated mice from 35.6 ± 1.1 g/mouse in control group, corresponding to a 21.4% reduction (Figure 5B). The result of body composition analysis showed that EA treatment significantly reduced fat percentage, whereas the lean mass was increased by 8% relative to vehicle-treated mice (Figure 5C), suggesting that EA is likely a non-toxic, novel anti-obesity agent. As expected, blood leptin and insulin levels in obese mice were greater than in SD mice ($p < 0.01$), demonstrating that obese mice developed insulin resistant (36). Strikingly, treatment with EA for only 2 weeks reduced the obesity-elevated leptin and insulin levels by 69.3%

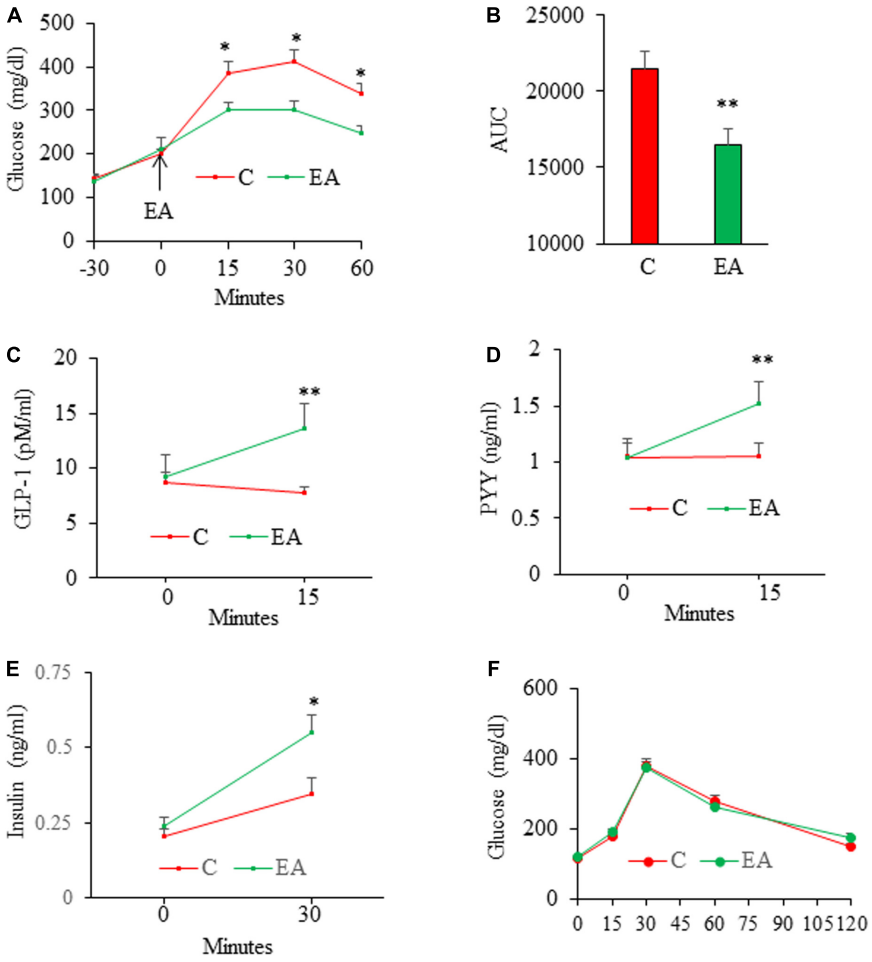

FIGURE 3
Acute effects of elenolic acid (EA) on glucose tolerance, glucagon-like peptide-1 (GLP-1), peptide YY (PYY), and insulin secretion in mice. C57BL6 male mice (8 weeks old) on high-fat-diet (HFD) for 12 weeks were fasted for 14 h and then were given EA (50 mg/kg, oral gavage) or vehicle, followed by performing intraperitoneal glucose (1.5 g/kg) tolerance test (IGTT) **(A)**, and the area under the curve (AUC) from GTT was calculated **(B)**. For assessing the effects of EA on GLP-1 and PYY levels, obese mice were fasted for 6 h and blood was drawn for baseline analyses. Mice were then given EA (50 mg/kg) or vehicle. Blood total GLP-1 [tGLP-1, **(C)**] and PYY **(D)** levels were measured at 15 min after gavage. **(E)** Plasma insulin levels in 6-h fasted mice before (0) and 30 min following sequential administration of EA (50 mg/kg, gavage) and by glucose (1.5 g/kg, ip. Injection). The results of IPGTT from lean **(F)** mice following administration of EA (50 mg/kg) *via* gavage. Data are mean ± SE. $^{*}p < 0.05$, $^{**}p < 0.01$ (n = 4–8 mice/group).

(Figure 5D) and 58.5% (Figure 5E), respectively, in obese mice, which is likely due to improved obesity and insulin resistance consistent with previous findings in this mouse model (37, 38). EA almost completely reversed the elevated plasma triglyceride concentrations in obese mice to those in SD mice (Figure 5F; $P < 0.05$). Similarly, plasma FFA concentrations in EA-treated mice were lower relative to control obese mice (Figure 5G; $P < 0.05$).

Discussion

While many naturally occurring compounds have been explored for their potential anti-obesity and anti-diabetic properties, the ones with both strong hypoglycemic and anti-obesity activities are rarely discovered. In the present study, we found for the first time that an olive-derived small molecule EA exerts potent glucose-lowering activity while also suppressing food intake and BW gain in DIO mice. On a cellular level, EA directly stimulates intestinal L-cells to release GLP-1 and PYY. Therefore, EA could be a potent dual-action, anti-diabetic and anti-obesity compound.

Secretion of GLP-1 and PYY from L-cells in the intestine is increased in response to ingested macronutrients, primarily fatty acids (31, 32, 39), although glucose (40, 41), some amino acids, and dietary fibers (42) may also induce hormone release. In addition, a variety of neurotransmitters and neuropeptides released by the enteric nervous system and enteroendocrine

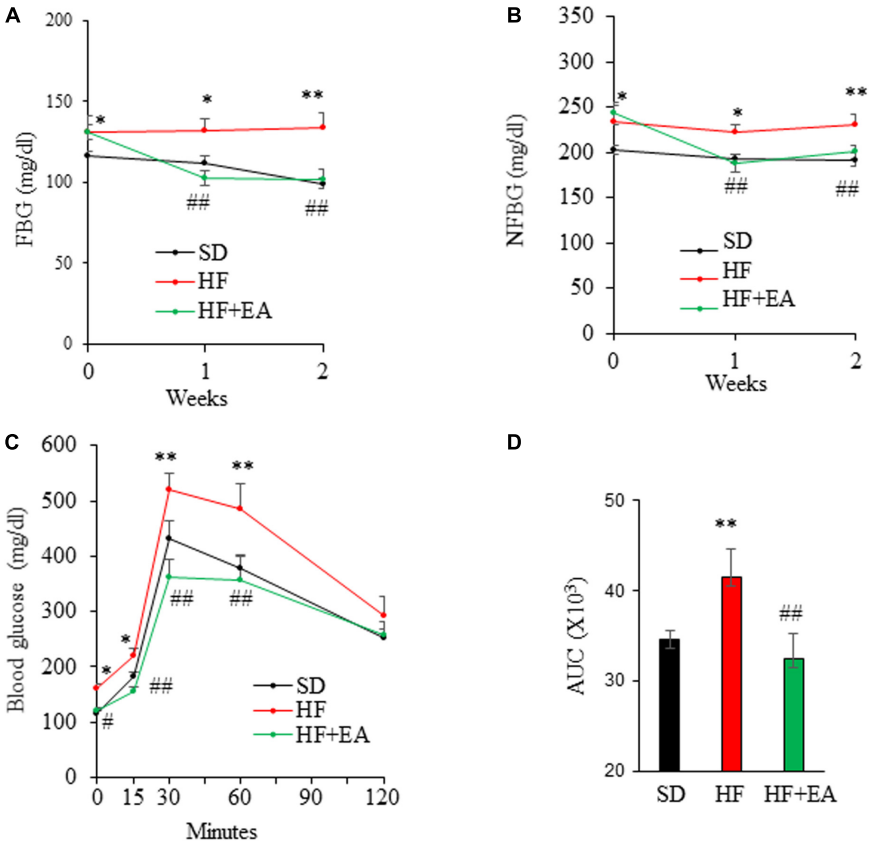

FIGURE 4
Elenolic acid (EA) is a potent anti-diabetic agent in high-fat diet (HF)-induced obese mice. C57BL6 mice (8 weeks old, male) were fed either a SD or a HF for 10 weeks, followed by treatment with EA (50 mg/kg/d) or vehicle *via* oral gavage for 2 weeks. Fasting blood glucose (FBG) **(A)** and non-fasting blood glucose (NFBG) **(B)** were measured once per week. Blood glucose levels during IPGTT (1.5 g glucose/kg) **(C)** and the area under the curve (AUC) was calculated **(D)**. Data are Mean ± SE (n = 8). $^{*}p < 0.05$, and $^{**}p < 0.01$ vs. SD-fed mice; $^{\#}p < 0.05$; and $^{\#\#}p < 0.01$ vs. high-fat-diet (HF) alone-fed mice.

cell types, such as acetylcholine (43) and gastrin-releasing peptide (44), have been implicated in the regulation of GLP-1 secretion. However, no therapeutic strategy based on these stimuli has been successfully developed for treating T2D. While GLP-1-based drugs are effective for treating T2D, there are safe concerns that these drugs may induce gastrointestinal adverse events (45) and acute gallbladder disease (46). In addition, GLP-1 analogs are not potent in BW control and do not mimic endogenous GLP-1 secretory pattern in response to a meal intake (47). In the present study, we sought to identify agents to induce both endogenous GLP-1 and PYY secretion, thereby providing a safe and alternative strategy for obesity and T2D management. We provide strong evidence from studies of cells, intestinal tissues, and mice that EA is a novel GLP-1 and PYY secretagogue. We then found that acute administration of EA greatly improved glucose disposal in response to glucose challenge. Interestingly, acute administration of EA had no effect on glucose excursion of lean mice during glucose tolerance test, which is in line with some previous findings (48, 49) but not others (50, 51) from examining GLP-1 analogs. The lean mice used in the present study are young adult that are metabolically healthy with presumably stronger counterregulatory response to hyperglycemia as compared with obese mice. It is possible that EA-induced GLP-1 secretion and subsequent increase in circulating insulin didn't reached levels high enough to significantly reduces blood glucose in lean mice under glucose loading. Indeed, it was found that at least 10 pM/L of GLP-1 analogs in the blood is required for achieving significant glucose lowering effect in lean mice (52). Nevertheless, using DIO mouse models, we show that EA treatment for 2 weeks already nearly reversed metabolic abnormalities caused by long-term feeding with HFD in obese mice consistent with expected metabolic effects of GLP-1 and PYY, thus providing evidence that this agent may have substantial therapeutic potential for T2D. However, it should be noted that this is only a short-term treatment (due to limited quantity of EA generated in our lab at that time) using a DIO mice that are insulin resistant and glucose intolerant, but are not overt diabetic. Therefore, the persistence and efficacy of EA in in treating obesity and diabetes

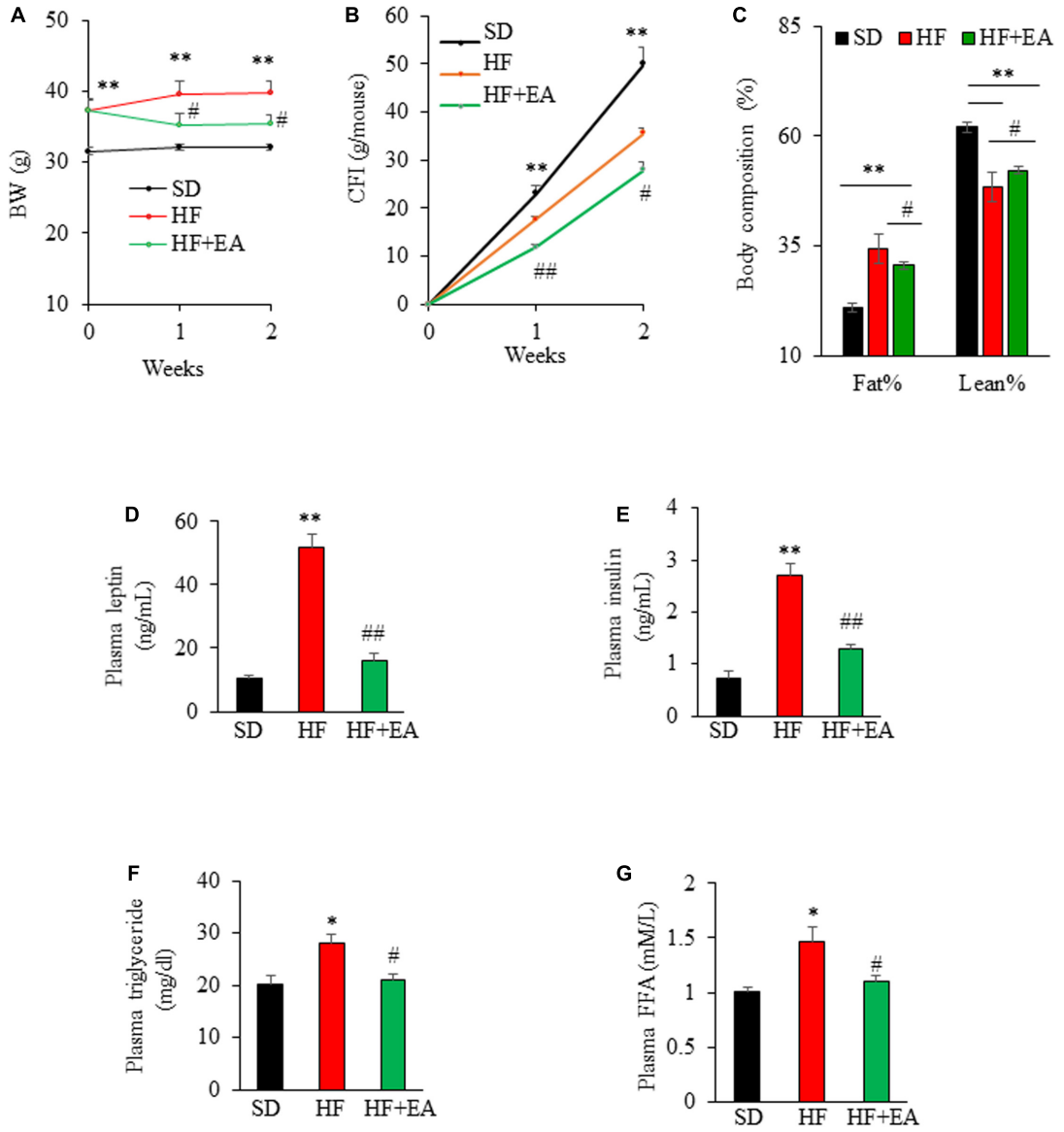

FIGURE 5
Elenolic acid (EA) promotes weight loss and reverses obesity-associated biochemical alterations. Weekly body weight **(A)** and cumulative food intake **(B)** of obese mice on the vehicle or EA treatment for 2 weeks as described in **Figure 5**. Body composition was measured at the end of the experiment **(C)**. Effects of EA treatment for 2 weeks on fasting plasma leptin **(D)**, insulin **(E)**, triglyceride **(F)**, and free fatty acid [**(G)**, FFA] levels in obese mice as measured using ELISA kits. Data are Mean ± SE (n = 8). *p < 0.05, and **P < 0.01 vs. SD-fed mice; #P < 0.05; and ##p < 0.01 vs. high-fat-diet (HF) alone-fed mice.

need to be confirmed through a long-term study using overt obese diabetic rodent models.

The EA dose (50 mg/kg/day *via* gavage) used in this study is likely pharmacological, as it may be impossible to get this amount of EA by dietary intake of olive products, given that the content of EA in mature olives is 7–12 mg/g dry weight, and 5–22 mg/kg in extra olive oil (53, 54). We chose this dose of EA, which is equivalent to dietary intake of about 243 mg/day for a 60 kg human as calculated according to an allometric scaling method for converting doses between species (55), because it is within the dosage range of previously tested various bioactive compounds in mouse studies as well as in clinical trials. However, the optimal dose and its safety profile are still unknown, which can be identified by determining the dose-effect relationship in combination with evaluating its pharmacokinetics.

One of the most interesting observations from this study is that EA elicited robust reductions in food intake. While several naturally occurring compounds have been reported to change food palatability due to their bitter taste (56), which

may modulate the reward system in the brain, thereby affecting food intake (57), we believe that EA suppression of food intake should not be secondary to the induction of taste aversion, given that EA was administered *via* oral gavage, resulting in the direct passage of EA to the stomach without inducing taste in the mouth. Rather, EA regulation of food intake is at least partially executed through stimulated release of the metabolic hormones from the gut. Food intake is controlled primarily by a variety of orexigenic and anorexigenic signals that are integrated in the hypothalamus. It was recently found that the GLP-1 receptor is expressed in several brain regions such as the paraventricular nucleus (PVN) and the arcuate nucleus (ARC) of the hypothalamus, and that GLP-1 targets control circuits in these regions to induce satiety and reduce food intake (58). PYY is an anorectic hormone that regulates gut mobility and directly suppresses appetite in the brain *via* an Y2 receptor-mediated pathway (16). It was found that mice deficient in PYY are hyperphagic and obese while PYY replacement restored their lean phenotype (15). In addition, PYY may also promote β-cell function and survival (59), thereby contributing to maintaining glucose homeostasis. In addition to stimulating GLP-1 secretion *in vitro* and *in vivo*, we found that EA also greatly increased circulating PYY in mice and directly stimulated PYY release from cultured L-cells, which should be a major contributing factor for the hypophagic and anti-obesity effects of EA treatment. Previous studies show that GLP-1 and PYY synergistically inhibit appetite in mice (16) and humans (17, 18), suggesting that simultaneous activation of these gut hormones might work additively to provide better metabolic outcomes than those achieved by GLP-1 or its receptor agonist alone. Thus, it is intriguing to test in the future whether EA could be potentially a more effective anti-diabetic and anti-obesity agent than some of the currently prescribed monotherapeutic drugs such as DPP4 inhibitors, metformin, and GLP-1 analogs. In addition, as several other intestinal hormones secreted in response to meal ingestion, such as glucose-dependent insulinotropic polypeptide (60) and cholecystokinin (61), also play a role in promoting satiety, studies of transgenic mouse models combined with analyses of hypothalamic pathway controlling food intake are needed to determine whether EA regulation of food intake and body weight is exclusively mediated *via* GLP-1 and PYY-mediated mechanisms.

In the present study, we performed a series of experiments *in vitro* with the results indicating that EA activation of GLP-1 secretion is mediated *via* the PLC/IP_3/Ca^{2+} signaling pathway, and that $G\alpha_q$ activation in cell membranes is upstream of the PLC signaling and GLP-1 secretion elicited by EA. Cell membrane-associated G-proteins are typically activated by GPCRs. Previous studies demonstrated that the secretion of GLP-1 is largely regulated *via* GPCRs (62), which signal primarily through $G\alpha_q$, leading to activation of PLC/Ca^{2+} signaling. Therefore, it is tempting to speculate that EA-triggered signaling in L-cells may be transmitted *via* a $G\alpha_q$-coupled receptor. In that regard, it is possible that EA binds to the short chain fatty acid (SCFA) receptors, which are coupled to $G\alpha_q$ to mediate SCFA-induced GLP-1 secretion from L-cells (32, 63). It was suggested that the binding of SCFAs to their receptors depends on the carboxylic acid group (64), and EA is also a carboxylic acid. In this study, we did not explore the mechanism by which EA stimulates PYY secretion. It was shown that activation $G\alpha_q$/PLC/Ca^{2+} signaling in L-cells elicited both GLP-1 and PYY secretion (63), suggesting that EA stimulation of PYY secretion could also be mediated by this signaling pathway. However, our data show that EA at 1 μM stimulated GLP-1 secretion, whereas it was inactive at this dose in inducing PYY secretion. It is presently unclear whether this discrepancy is due to different L-cell lines used for GLP-1 (GLUTag mouse L-cells) and PYY (human NCI-H716 L-cells) secretion assays or different mechanisms involved, which remain to be determined.

In conclusion, we found for the first time that EA is a novel agent with potent anti-diabetic and anti-obesity effects in mouse models of obesity and T2D, which were associated with increased secretion of GLP-1 and PYY. These metabolically important hormones may act additively, resulting in more effective metabolic control. Mechanistically, EA directly induces incretin hormone secretion from intestinal L-cells *via* a $G\alpha_q$/PLC-mediated mechanism (**Supplementary Figure 2**). Further studies are still needed to uncover the exact mechanism by which EA regulates food intake, which may play a significant role in its blood glucose lowering and anti-obesity effects. The outcomes from this research could lay the foundation for developing approaches using this small molecule for safe and effective treatment of both obesity and T2D.

Data availability statement

The original contributions presented in the study are included in the article/**Supplementary material**, further inquiries can be directed to the corresponding authors.

Ethics statement

The animal study was reviewed and approved by Institutional Animal Care and use Committee at Virginia Tech.

Author contributions

DL and YW designed the experiments. APW, BX, RH, SZ, HM, YZ, and EG provided essential research tools. YJW, YW, AHW, and HA performed the experiments. YW and DL analyzed the data and wrote the manuscript. All authors have approved the final manuscript.

Funding

This work was partially supported by a grant from Diabetes Research Action and Education Foundation (USA), a grant from Virginia Tech Discovery Center, and a Virginia Tech Pratt Fellowship Award. The publication charge was partially supported by Open Access Subvention Fund from Virginia Tech Library.

Conflict of interest

The authors declare that the research was conducted in the absence of any commercial or financial relationships that could be construed as a potential conflict of interest.

Publisher's note

All claims expressed in this article are solely those of the authors and do not necessarily represent those of their affiliated organizations, or those of the publisher, the editors and the reviewers. Any product that may be evaluated in this article, or claim that may be made by its manufacturer, is not guaranteed or endorsed by the publisher.

Supplementary material

The Supplementary Material for this article can be found online at: https://www.frontiersin.org/articles/10.3389/fnut.2022.1051452/full#supplementary-material

References

1. Stoffers DA. The development of beta-cell mass: recent progress and potential role of GLP-1. *Horm Metab Res.* (2004) 36:811–21. doi: 10.1055/s-2004-826168

2. Cozar-Castellano I, Fiaschi-Taesch N, Bigatel TA, Takane KK, Garcia-Ocana A, Vasavada R, et al. Molecular control of cell cycle progression in the pancreatic beta-cell. *Endocr Rev.* (2006) 27:356–70. doi: 10.1210/er.2006-0004

3. Butler AE, Janson J, Bonner-Weir S, Ritzel R, Rizza RA, Butler PC. Beta-cell deficit and increased beta-cell apoptosis in humans with type 2 diabetes. *Diabetes.* (2003) 52:102–10. doi: 10.2337/diabetes.52.1.102

4. Turner RC, Cull CA, Frighi V, Holman RR. Glycemic control with diet, sulfonylurea, metformin, or insulin in patients with type 2 diabetes mellitus: progressive requirement for multiple therapies (UKPDS 49). UK prospective diabetes study (UKPDS) group. *JAMA.* (1999) 281:2005–12. doi: 10.1001/jama.281.21.2005

5. Tajima K, Shirakawa J, Okuyama T, Kyohara M, Yamazaki S, Togashi Y, et al. Effects of metformin on compensatory pancreatic beta-cell hyperplasia in mice fed a high-fat diet. *Am J Physiol Endocrinol Metab.* (2017) 313:E367–80. doi: 10.1152/ajpendo.00447.2016

6. Thorens B. Expression cloning of the pancreatic beta cell receptor for the gluco-incretin hormone glucagon-like peptide 1. *Proc Natl Acad Sci U.S.A.* (1992) 89:8641–5. doi: 10.1073/pnas.89.18.8641

7. Schmidt W, Siegel E, Creutzfeldt W. Glucagon-like peptide-1 but not glucagon-like peptide-2 stimulates insulin release from isolated rat pancreatic islets. *Diabetologia.* (1985) 28:704–7. doi: 10.1007/BF00291980

8. Liu Z, Habener JF. Glucagon-like peptide-1 activation of TCF7L2-dependent Wnt signaling enhances pancreatic beta cell proliferation. *J Biol Chem.* (2008) 283:8723–35. doi: 10.1074/jbc.M706105200

9. Nauck M, Kleine N, Ørskov C, Holst JJ, Willms B, Creutzfeldt W. Normalization of fasting hyperglycaemia by exogenous glucagon-like peptide 1 (7-36 amide) in type 2 (non-insulin-dependent) diabetic patients. *Diabetologia.* (1993) 36:741–4. doi: 10.1007/BF00401145

10. Nauck MA, Heimesaat M, Orskov C, Holst JJ, Ebert R, Creutzfeldt W. Preserved incretin activity of glucagon-like peptide 1 [7-36 amide] but not of synthetic human gastric inhibitory polypeptide in patients with type-2 diabetes mellitus. *J Clin Investig.* (1993) 91:301. doi: 10.1172/JCI116186

11. Nauck MA, Heimesaat MM, Behle K, Holst JJ, Nauck MS, Ritzel R, et al. Effects of glucagon-like peptide 1 on counterregulatory hormone responses, cognitive functions, and insulin secretion during hyperinsulinemic, stepped hypoglycemic clamp experiments in healthy volunteers. *J Clin Endocr Metab.* (2002) 87:1239–46. doi: 10.1210/jcem.87.3.8355

12. Neumiller JJ. Incretin-based therapies. *Med Clin North Am.* (2015) 99:107–29. doi: 10.1016/j.mcna.2014.08.013

13. Spreckley E, Murphy KG. The L-cell in nutritional sensing and the regulation of appetite. *Front Nutr.* (2015) 2:23. doi: 10.3389/fnut.2015.00023

14. Perry B, Wang Y. Appetite regulation and weight control: the role of gut hormones. *Nutr Diabetes.* (2012) 2:e26. doi: 10.1038/nutd.2011.21

15. Batterham RL, Heffron H, Kapoor S, Chivers JE, Chandarana K, Herzog H, et al. Critical role for peptide YY in protein-mediated satiation and body-weight regulation. *Cell Metab.* (2006) 4:223–33. doi: 10.1016/j.cmet.2006.08.001

16. Talsania T, Anini Y, Siu S, Drucker DJ, Brubaker PL. Peripheral exendin-4 and peptide YY(3-36) synergistically reduce food intake through different mechanisms in mice. *Endocrinology.* (2005) 146:3748–56. doi: 10.1210/en.2005-0473

17. Steinert RE, Poller B, Castelli MC, Drewe J, Beglinger C. Oral administration of glucagon-like peptide 1 or peptide YY 3-36 affects food intake in healthy male subjects. *Am J Clin Nutr.* (2010) 92:810–7. doi: 10.3945/ajcn.2010.29663

18. Schmidt JB, Gregersen NT, Pedersen SD, Arentoft JL, Ritz C, Schwartz TW, et al. Effects of PYY3-36 and GLP-1 on energy intake, energy expenditure, and appetite in overweight men. *Am J Physiol Endocrinol Metab.* (2014) 306:E1248–56. doi: 10.1152/ajpendo.00569.2013

19. Garcia-Serrano S, Ho-Plagaro A, Santiago-Fernandez C, Rodriguez-Diaz C, Martin-Reyes F, Valdes S, et al. An isolated dose of extra-virgin olive oil produces a better postprandial gut hormone response, lipidic, and anti-inflammatory profile that sunflower oil: effect of morbid obesity. *Mol Nutr Food Res.* (2021) 65:e2100071. doi: 10.1002/mnfr.202100071

20. Bogani P, Galli C, Villa M, Visioli F. Postprandial anti-inflammatory and antioxidant effects of extra virgin olive oil. *Atherosclerosis.* (2007) 190:181–6. doi: 10.1016/j.atherosclerosis.2006.01.011

21. Charoenprasert S, Mitchell A. Factors influencing phenolic compounds in table olives (*Olea europaea*). *J Agric Food Chem.* (2012) 60:7081–95. doi: 10.1021/jf3017699

22. Yuan JJ, Wang CZ, Ye JZ, Tao R, Zhang YS. Enzymatic hydrolysis of oleuropein from *Olea europea* (olive) leaf extract and antioxidant activities. *Molecules.* (2015) 20:2903–21. doi: 10.3390/molecules20022903

23. Reimann F, Gribble FM. Glucose-sensing in glucagon-like peptide-1-secreting cells. *Diabetes.* (2002) 51:2757–63. doi: 10.2337/diabetes.51.9.2757

24. Psichas, A, Tolhurst G, Brighton CA, Gribble FM, Reimann F. Mixed primary cultures of murine small intestine intended for the study of gut hormone secretion and live cell imaging of enteroendocrine cells. *J Vis Exp.* (2017) 20:55687. doi: 10.3791/55687

25. Wang Y, Wang A, Alkhalidy H, Luo J, Moomaw E, Neilson AP, et al. Flavone hispidulin stimulates glucagon-like peptide-1 secretion and ameliorates hyperglycemia in streptozotocin-induced diabetic mice. *Mol Nutr Food Res.* (2020) 64:1900978. doi: 10.1002/mnfr.201900978

26. Liu F, Usui I, Evans LG, Austin DA, Mellon PL, Olefsky JM, et al. Involvement of both Gq/11 and Gs proteins in gonadotropin-releasing hormone receptor-mediated signaling in LβT2 cells. *J Biol Chem.* (2002) 277:32099–108. doi: 10.1074/jbc.M203639200

27. Wang C-Y, Liao JK. A mouse model of diet-induced obesity and insulin resistance. *Methods Mol Biol.* (2012) 821:421–33. doi: 10.1007/978-1-61779-430-8_27

28. Luo J, Wang A, Zhen W, Wang Y, Si H, Jia Z, et al. Phytonutrient genistein is a survival factor for pancreatic beta-cells via GPR30-mediated mechanism. *J Nutr Biochem.* (2018) 58:59–70. doi: 10.1016/j.jnutbio.2018.04.018

29. Reimann F, Ward PS, Gribble FM. Signaling mechanisms underlying the release of glucagon-like peptide 1. *Diabetes.* (2006) 55(Suppl. 2):S78–85. doi: 10.2337/db06-S010

30. Jang H-J, Kokrashvili Z, Theodorakis MJ, Carlson OD, Kim B-J, Zhou J, et al. Gut-expressed gustducin and taste receptors regulate secretion of glucagon-like peptide-1. *Proc Natl Acad Sci U.S.A.* (2007) 104:15069–74. doi: 10.1073/pnas.0706890104

31. Hirasawa A, Tsumaya K, Awaji T, Katsuma S, Adachi T, Yamada M, et al. Free fatty acids regulate gut incretin glucagon-like peptide-1 secretion through GPR120. *Nat Med.* (2005) 11:90–4. doi: 10.1038/nm1168

32. Tolhurst G, Heffron H, Lam YS, Parker HE, Habib AM, Diakogiannaki E, et al. Short-chain fatty acids stimulate glucagon-like peptide-1 secretion via the G-protein–coupled receptor FFAR2. *Diabetes.* (2012) 61:364–71. doi: 10.2337/db11-1019

33. Edfalk S, Steneberg P, Edlund H. Gpr40 is expressed in enteroendocrine cells and mediates free fatty acid stimulation of incretin secretion. *Diabetes.* (2008) 57:2280–7. doi: 10.2337/db08-0307

34. Christensen LW, Kuhre RE, Janus C, Svendsen B, Holst JJ. Vascular, but not luminal, activation of FFAR1 (GPR40) stimulates GLP-1 secretion from isolated perfused rat small intestine. *Physiol Rep.* (2015) 3:e12551. doi: 10.14814/phy2.12551

35. Hauge M, Vestmar MA, Husted AS, Ekberg JP, Wright MJ, Di Salvo J, et al. GPR40 (FFAR1)–combined Gs and Gq signaling in vitro is associated with robust incretin secretagogue action ex vivo and in vivo. *Mol Metab.* (2015) 4:3–14. doi: 10.1016/j.molmet.2014.10.002

36. Lackey DE, Lazaro RG, Li P, Johnson A, Hernandez-Carretero A, Weber N, et al. The role of dietary fat in obesity-induced insulin resistance. *Am J Physiol Endocrinol Metab.* (2016) 311:E989–97. doi: 10.1152/ajpendo.00323.2016

37. Cakir I, Lining Pan P, Hadley CK, El-Gamal A, Fadel A, Elsayegh D, et al. Sulforaphane reduces obesity by reversing leptin resistance. *Elife.* (2022) 11:e67368. doi: 10.7554/eLife.67368

38. Lu HF, Lai YH, Huang HC, Lee IJ, Lin LC, Liu HK, et al. Ginseng-plus-Bai-Hu-Tang ameliorates diet-induced obesity, hepatic steatosis, and insulin resistance in mice. *J Ginseng Res.* (2020) 44:238–46. doi: 10.1016/j.jgr.2018.10.005

39. Lauffer LM, Iakoubov R, Brubaker PL. GPR119 is essential for oleoylethanolamide-induced glucagon-like peptide-1 secretion from the intestinal enteroendocrine L-cell. *Diabetes.* (2009) 58:1058–66. doi: 10.2337/db08-1237

40. Kuhre RE, Frost CR, Svendsen B, Holst JJ. Molecular mechanisms of glucose-stimulated GLP-1 secretion from perfused rat small intestine. *Diabetes.* (2015) 64:370–82. doi: 10.2337/db14-0807

41. Gribble FM, Williams L, Simpson AK, Reimann F. A novel glucose-sensing mechanism contributing to glucagon-like peptide-1 secretion from the GLUTag cell line. *Diabetes.* (2003) 52:1147–54. doi: 10.2337/diabetes.52.5.1147

42. Diakogiannaki E, Gribble FM, Reimann F. Nutrient detection by incretin hormone secreting cells. *Physiol Behav.* (2012) 106:387–93. doi: 10.1016/j.physbeh.2011.12.001

43. Anini Y, Hansotia T, Brubaker PL. Muscarinic receptors control postprandial release of glucagon-like peptide-1: in vivo and in vitro studies in rats. *Endocrinology.* (2002) 143:2420–6. doi: 10.1210/endo.143.6.8840

44. Mulherin AJ, Oh AH, Kim H, Grieco A, Lauffer LM, Brubaker PL. Mechanisms underlying metformin-induced secretion of glucagon-like peptide-1 from the intestinal L cell. *Endocrinology.* (2011) 152:4610–9. doi: 10.1210/en.2011-1485

45. Horowitz M, Aroda VR, Han J, Hardy E, Rayner CK. Upper and/or lower gastrointestinal adverse events with glucagon-like peptide-1 receptor agonists: I ncidence and consequences. *Diabetes Obes Metab.* (2017) 19:672–81. doi: 10.1111/dom.12872

46. Woronow D, Chamberlain C, Niak A, Avigan M, Houstoun M, Kortepeter C. Acute cholecystitis associated with the use of glucagon-like peptide-1 receptor agonists reported to the US food and drug administration. *JAMA Intern Med.* (2022) 182:1104–6. doi: 10.1001/jamainternmed.2022.3810

47. Petersen N, Reimann F, van Es JH, van den Berg BM, Kroone C, Pais R, et al. Targeting development of incretin-producing cells increases insulin secretion. *J Clin Invest.* (2015) 125:379–85. doi: 10.1172/JCI75838

48. Ellenbroek JH, Tons HA, Westerouen van Meeteren MJ, de Graaf N, Hanegraaf MA, Rabelink TJ, et al. Glucagon-like peptide-1 receptor agonist treatment reduces beta cell mass in normoglycaemic mice. *Diabetologia.* (2013) 56:1980–6. doi: 10.1007/s00125-013-2957-2

49. Hao T, Zhang H, Li S, Tian H. Glucagon-like peptide 1 receptor agonist ameliorates the insulin resistance function of islet beta cells via the activation of PDX-1/JAK signaling transduction in C57/BL6 mice with high-fat diet-induced diabetes. *Int J Mol Med.* (2017) 39:1029–36. doi: 10.3892/ijmm.2017.2910

50. Henderson SJ, Konkar A, Hornigold DC, Trevaskis JL, Jackson R, Fritsch Fredin M, et al. Robust anti-obesity and metabolic effects of a dual GLP-1/glucagon receptor peptide agonist in rodents and non-human primates. *Diabetes Obes Metab.* (2016) 18:1176–90. doi: 10.1111/dom.12735

51. Elvert R, Herling AW, Bossart M, Weiss T, Zhang B, Wenski P, et al. Running on mixed fuel-dual agonistic approach of GLP-1 and GCG receptors leads to beneficial impact on body weight and blood glucose control: a comparative study between mice and non-human primates. *Diabetes Obes Metab.* (2018) 20:1836–51. doi: 10.1111/dom.13212

52. Briere DA, Bueno AB, Gunn EJ, Michael MD, Sloop KW. Mechanisms to elevate endogenous GLP-1 beyond injectable GLP-1 analogs and metabolic surgery. *Diabetes.* (2018) 67:309–20. doi: 10.2337/db17-0607

53. Bruno L, Picardi E, Pacenza M, Chiappetta A, Muto A, Gagliardi O, et al. Changes in gene expression and metabolic profile of drupes of *Olea europaea* L. cv Carolea in relation to maturation stage and cultivation area. *BMC Plant Biol.* (2019) 19:428. doi: 10.1186/s12870-019-1969-6

54. Faci M, Douzane M, Hedjal M, Daas MS, Fougere L, Lesellier E. Changes in secoiridoids content and chemical characteristics of cultivated and wild Algerian olive oil, in term of fruit maturation. *PLoS One.* (2021) 16:e0260182. doi: 10.1371/journal.pone.0260182

55. Nair AB, Jacob S. A simple practice guide for dose conversion between animals and human. *J Basic Clin Pharm.* (2016) 7:27–31. doi: 10.4103/0976-0105.177703

56. Drewnowski A, Gomez-Carneros C. Bitter taste, phytonutrients, and the consumer: a review. *Am J Clin Nutr.* (2000) 72:1424–35. doi: 10.1093/ajcn/72.6.1424

57. Erlanson-Albertsson C. How palatable food disrupts appetite regulation. *Basic Clin Pharmacol Toxicol.* (2005) 97:61–73. doi: 10.1111/j.1742-7843.2005.pto_179.x

58. Secher A, Jelsing J, Baquero AF, Hecksher-Sorensen J, Cowley MA, Dalboge LS, et al. The arcuate nucleus mediates GLP-1 receptor agonist liraglutide-dependent weight loss. *J Clin Invest.* (2014) 124:4473–88. doi: 10.1172/JCI75276

59. Sam AH, Gunner DJ, King A, Persaud SJ, Brooks L, Hostomska K, et al. Selective ablation of peptide YY cells in adult mice reveals their role in beta cell survival. *Gastroenterology.* (2012) 143:459–68. doi: 10.1053/j.gastro.2012.04.047

60. Zhang Q, Delessa CT, Augustin R, Bakhti M, Collden G, Drucker DJ, et al. The glucose-dependent insulinotropic polypeptide (GIP) regulates body weight and food intake via CNS-GIPR signaling. *Cell Metab.* (2021) 33:833–44.e5. doi: 10.1016/j.cmet.2021.01.015

61. Clerc P, Coll Constans MG, Lulka H, Broussaud S, Guigne C, Leung-Theung-Long S, et al. Involvement of cholecystokinin 2 receptor in food intake regulation: hyperphagia and increased fat deposition in cholecystokinin 2 receptor-deficient mice. *Endocrinology.* (2007) 148:1039–49. doi: 10.1210/en.2006-1064

62. Lee JH, Wen X, Cho H, Koo SH. CREB/CRTC2 controls GLP-1-dependent regulation of glucose homeostasis. *FASEB J.* (2018) 32:1566–78. doi: 10.1096/fj.201700845R

63. Psichas A, Sleeth M, Murphy K, Brooks L, Bewick G, Hanyaloglu A, et al. The short chain fatty acid propionate stimulates GLP-1 and PYY secretion via free fatty acid receptor 2 in rodents. *Int J Obes.* (2015) 39:424. doi: 10.1038/ijo.2014.153

64. Bindels LB, Dewulf EM, Delzenne NM. GPR43/FFA2: physiopathological relevance and therapeutic prospects. *Trends Pharmacol Sci.* (2013) 34:226–32. doi: 10.1016/j.tips.2013.02.002

frontiers | Frontiers in Nutrition

TYPE Original Research
PUBLISHED 10 November 2022
DOI 10.3389/fnut.2022.1036655

OPEN ACCESS

EDITED BY
Bo Wang,
China Agricultural University, China

REVIEWED BY
Yao Wang,
University of California, San Francisco, United States
Yan Cao,
Women's Hospital of Nanjing Medical University, China

*CORRESPONDENCE
Ling Zhao
lzhao7@utk.edu

†PRESENT ADDRESSES
Jiyoung Bae,
Department of Nutritional Sciences, Oklahoma State University, Stillwater, OK, United States
Yang Yang,
John Hopkins All Children's Hospital, St. Petersburg, FL, United States
Jamie Flaherty,
Children's Hospital Colorado, Aurora, CO, United States
Haley Overby,
Division of Cardiovascular Medicine, Vanderbilt University Medical Center, Nashville, TN, United States
Kelsey Hildreth,
NHC HealthCare, Oak Ridge, TN, United States

‡These authors have contributed equally to this work

SPECIALTY SECTION
This article was submitted to Nutrition and Metabolism, a section of the journal Frontiers in Nutrition

RECEIVED 04 September 2022
ACCEPTED 19 October 2022
PUBLISHED 10 November 2022

CITATION
Bae J, Yang Y, Xu X, Flaherty J, Overby H, Hildreth K, Chen J, Wang S and Zhao L (2022) Naringenin, a citrus flavanone, enhances browning and brown adipogenesis: Role of peroxisome proliferator-activated receptor gamma.
Front. Nutr. 9:1036655.
doi: 10.3389/fnut.2022.1036655

Naringenin, a citrus flavanone, enhances browning and brown adipogenesis: Role of peroxisome proliferator-activated receptor gamma

Jiyoung Bae[1†‡], Yang Yang[1†‡], Xinyun Xu[1], Jamie Flaherty[1†], Haley Overby[1†], Kelsey Hildreth[1†], Jiangang Chen[2], Shu Wang[3] and Ling Zhao[1*]

[1]Department of Nutrition, The University of Tennessee, Knoxville, Knoxville, TN, United States, [2]Department of Public Health, The University of Tennessee, Knoxville, Knoxville, TN, United States, [3]College of Health Solutions, Arizona State University, Phoenix, AZ, United States

Identifying functional brown adipose tissue (BAT) has provided new hope for obesity treatment and prevention. Functional BAT includes classical BAT and brown-like adipose tissue converted from white adipose tissue. By promoting thermogenesis (i.e., heat production) *via* uncoupling protein 1 (UCP1), functional BAT can increase energy expenditure and aid obesity treatment and prevention. Naringenin (NAR) is a flavanone primarily found in citrus fruits. NAR has been reported to decrease body weight, increase energy expenditure in treated mice, and promote browning in human adipocytes. Here, we examined the effects of NAR on 3T3-L1 adipocytes' browning and β-adrenergic agonist isoproterenol (ISO)-stimulated thermogenic activation and classical murine brown adipogenesis. In addition, we demonstrated the signaling pathways and involvement of peroxisome proliferator-activated receptor gamma (PPARγ) in the process. We found that NAR did not increase *Ucp1* mRNA expression at the basal (i.e., non-ISO stimulated) condition. Instead, it enhanced *Ucp1* and *Pgc-1α* up-regulation and thermogenesis under ISO-stimulated conditions in 3T3-L1 adipocytes. NAR promoted protein kinase A (PKA) activation and phosphorylation of p38 MAPK downstream of ISO stimulation and activated PPARγ. Pharmacological inhibition of either PKA or p38 and PPARγ knockdown attenuated *Ucp1* up-regulation by NAR. Moreover, NAR promoted brown adipogenesis by increasing lipid accumulation, brown marker expression, and thermogenesis in murine brown adipocytes, which was also attenuated by PPARγ knockdown. Together, our

results suggest that NAR may promote the development of functional BAT in part through PPARγ activation. NAR's role in combating human obesity warrants further investigation.

KEYWORDS

naringenin, browning, brown adipogenesis, PPARγ, citrus flavanone

Introduction

Obesity has become a pandemic across the globe over the past decades. In addition to well-recognized higher risks of developing many chronic diseases, such as diabetes, cardiovascular diseases, and some types of cancer (1), obesity is also associated with increased severity and mortality of coronavirus disease (COVID-19), an ongoing pandemic infectious disease caused by SARS-CoV-2 virus (2, 3).

White adipose tissue (WAT) and brown adipose tissue (BAT) contribute to energy homeostasis. BAT is responsible for non-shivering thermogenesis *via* uncoupling protein 1 (UCP1), leading to energy expenditure. In addition, animal and *in vitro* studies have demonstrated inducible brown-like adipocytes, also known as beige adipocytes, in WAT. These brown-like adipocytes can be generated by β-adrenergic stimulation from cold exposure or synthetic β-adrenergic receptor (β-AR) agonists (4–6). Activation of peroxisome proliferator-activated receptor gamma (PPARγ) by its agonists, such as rosiglitazone (ROSI), also promotes browning and enhances thermogenic activation induced by β-adrenergic stimulation (7–10). It is well recognized that functional BAT, including classical brown and brown-like adipose tissue, exists in humans (11–14). Their mass or activities negatively correlate with body mass index, total, or visceral fat mass (15), blood glucose, and HbA1c levels (16). Moreover, cold exposure or daily intake of capsinoids increases BAT activation and energy expenditure and decreases body fat mass in human subjects (17). Therefore, strategies that promote functional BAT are promising for combating human obesity.

Naringenin (4′,5,7-trihydroxyflavanone, NAR), a flavanone commonly found in citrus fruits, has been reported with many beneficial health effects, including anti-inflammatory, anti-oxidative, and anti-carcinogenic effects (18–22). In addition, NAR was reported to activate PPARγ and other nuclear receptors (23). PPARγ activation by its agonist enhances both browning and brown adipogenesis (24, 25). Therefore, it is conceivable that NAR may induce browning and brown adipogenesis to confer anti-obesity benefits. Indeed, NAR decreased body weight with increases in energy expenditures in both chow-fed lean and high-fat diet-fed obese Ldlr-/-mice (26, 27) and reversed the attenuation of *Ucp1* mRNA expression in the BAT by a high-fat diet in rats (28). Consistently, NAR induced thermogenic *UCP1*, *PGC1α*, and *PGC1β* expression in human white adipocytes (29). However, the direct effects of NAR on thermogenic activation by a β-adrenergic agonist in brown-like adipocytes and classical brown adipogenesis remain unknown, and the underlying molecular mechanisms are not completely understood.

In this report, we examined the effects of NAR on browning and thermogenic activation by isoproterenol, a β-adrenergic receptor agonist, in 3T3-L1 white adipocytes and classical brown adipogenesis in murine brown pre-adipocytes. We further explored the molecular pathways by which NAR promotes thermogenic activation and the role of PPARγ in the process.

Materials and methods

Reagents

Naringenin, ROSI, insulin, 3-isobutyl-L-methylxanthine, dexamethasone, and isoproterenol (ISO) were from MilliporeSigma (St. Louis, MO, USA). Calf serum (CS) was purchased from Hyclone (Logan, UT, USA), and fetal bovine serum (FBS) was purchased from Bio-techne (Minneapolis, MN, USA). The pharmacological inhibitors for p38 (SB203580) and PKA (H-89) were from Tocris Bioscience (Ellisville, MI, USA). Anti-phospho-p38 (Thr180/Tyr182) (Catalog# 9211, RRID:AB_331641), anti-p38 (Catalog# 9212, RRID:AB_330713), and anti-ERK1/2 (Catalog# 4695, RRID:AB_390779) antibodies and horseradish peroxidase-conjugated goat anti-rabbit were from Cell Signaling Technology (Danvers, MA, USA). Anti-UCP1 (Catalog# U6382, RRID:AB_261838) was purchased from Sigma Aldrich (St. Louis, MO, USA); Anti-PGC1α antibody (Catalog# AB3242, RRID:AB_2268462) was purchased from Millipore (Temecula, CA, USA). Other reagents, if not specified, were purchased from MilliporeSigma.

Naringenin was dissolved in dimethyl sulfoxide (DMSO) to make 50 mM stock, followed by dilution in DMSO to make 0, 5, 10, and 20 mM stocks for treatment. The final DMSO concentration in the cell culture medium was 0.1% (v/v).

Cell culture and treatment

Murine 3T3-L1 cells were grown in DMEM containing 10% calf serum at 37°C humidified incubator with 5% CO_2. The cells were differentiated as described (30). Briefly, at the confluence (day 0), the cells were induced to differentiate in DMEM containing 10% FBS, 0.5 mM/L 3-isobutyl-1-methylxanthine, 1 μM/L dexamethasone, and 10 μg/mL insulin for 3 days, followed by DMEM containing 10% FBS and 10 μg/mL of insulin for 2 days. The cells were then kept in DMEM containing 10% FBS until day 7, when the cells were fully differentiated.

To study NAR's effects, 3T3-L1 cells were differentiated in the presence or absence of various doses of NAR from day 0. Fresh NAR was replaced at each change of the media. ROSI (1 μM) served as a positive control. On day 7, the cells were treated with isoproterenol (ISO, 1 μM) or the vehicle control (H_2O) for 6 h for mRNA analysis or 24 h for protein analysis. In a separate experiment, the cells were pre-treated with the pharmacological inhibitor of PKA (H-89), p38 (SB203580), or the vehicle control (DMSO) for 1 h before ISO treatment, as indicated in the figure legends.

Murine primary stromal cells were isolated from the white fat pads (both the subcutaneous and epididymal fat) of C57BL/6 J male mice (12 weeks old) and differentiated as described with modification (31). The animal study has been approved by the University of Tennessee Knoxville Institutional Animal Care and Use Committee under animal protocol 2,320. After reaching confluence (day 0), the primary stromal cells were differentiated in DMEM containing 10% FBS, 1 μM/L dexamethasone, 0.5 mM/L 3-isobutyl-1-methylxanthine and 10 μg/mL insulin for 7 days, followed by DMEM containing 10% FBS for another 7 days. NAR (10 μM) or the vehicle control (DMSO) was added to the media from day 0. The treatments were replaced at each change of media.

Murine brown pre-adipocyte cell line was a gift from Dr. Klein (32). Murine brown pre-adipocytes were grown in DMEM containing 20% FBS until they reached confluence (day 0). The cells were differentiated in DMEM containing 20% FBS, 1 nM T3, and 20 nM insulin (differentiation media) for 6 days, with media change every 2 days. To study NAR's effects, NAR (10 μM), the vehicle control (DMSO), or ROSI (1 μM, a positive control) were added to the media from day 0. The treatments were replaced at each change of media.

Peroxisome proliferator-activated receptor gamma knockdown (PPARγ-KD)

3T3-L1 with PPARγ-KD or a scrambled non-targeting control have been described elsewhere (33). Murine brown pre-adipocytes with PPARγ-KD or a scrambled non-targeting control were generated by lentiviral shRNA infection. Briefly, murine brown pre-adipocytes were plated at ∼50% confluence in a 6-well plate overnight. The cells were then infected with MISSION lentiviral shRNA transduction-ready particles against mouse *Pparg* or a scrambled non-targeting control according to the manufacturer's instructions (MilliporeSigma). Stably infected cells were selected by puromycin for 2 weeks.

Protein kinase A activity

On day 7, 3T3-L1 adipocytes treated with NAR (10 μM), the vehicle control, or ROSI (1 μM) were serum starved with 0.25% FBS containing DMEM for 1 h. Then the cells were treated with ISO (1 μM) or the vehicle control (H_2O) for an additional 6 h. Protein kinase A (PKA) activities were measured from total cell lysates using the DetectX PKA activity kit (Arbor Assays, Ann Arbor, MI, USA) according to the manufacturer's instructions.

Western blot analysis

Total cell lysates were prepared with lysis buffer (Cell Signaling, Danvers, MA, USA). Protein concentrations were measured by a BCA assay kit (Thermo Fisher Scientific, Waltham, MA, USA). Total cell lysates were subjected to 10% SDS-PAGE and transferred overnight to polyvinylidene difluoride membranes (Bio-Rad, Hercules, CA, USA). The membranes were blocked in 137 mM NaCl, 20 mM Tris·HCl, and 0.1% Tween 20 (pH 7.4) solution with 5% non-fat milk, followed by immunoblotting with primary antibodies at 4°C overnight and secondary antibody conjugated with horseradish peroxidase for 1 h. ERK1/2 served as the loading control for **Figures 1**, **6**, **7**, as previously reported (32–34). The signals were produced by incubating the membranes with ECL Western blot detection reagents (GE Healthcare, Piscataway, NJ, USA) and captured by X-ray films or ChemiDoc Imaging Systems (Bio-Rad, Hercules, CA, USA). The membranes were stripped in the stripping buffer (100 mM 2-mercaptoethanol, 62.5 mM Tris-HCl, and 2% SDS) for 10 min at 50°C and re-probed with different antibodies.

Total RNA isolation and semi-quantitative reverse-transcription PCR analysis

Total RNA was isolated with TRI reagent (Molecular Research Center, Cincinnati, OH, USA) according to the manufacturer's instructions. Total RNA abundance was measured by a NanoDrop ND-1,000 spectrophotometer (NanoDrop Technologies, Wilmington, DE, USA). Reverse transcription was performed using a High Capacity cDNA Reverse Transcription kit (Thermo Scientific, Waltham, MA, USA) according to the manufacturer's instructions. Analysis of mRNA expression of the target genes and the housekeeping gene *36b4* [encodes acidic ribosomal phosphoprotein P0 (RPLP0)]

were carried out using Absolute Blue QPCR SYBR Green ROX mix (Thermo Fisher Scientific, Waltham, MA, USA). PCR reactions were carried out in 96-well plates in an ABI 7300HT instrument. The conditions were set at 50°C 2 min and 95°C 15 min, followed by 40 cycles of 95°C 15 s/60°C 1 min. Relative gene expression was calculated using the $2^{-\Delta\Delta Ct}$ method (35), which normalizes against *36b4*. The primer sequences were reported in our previous study (25).

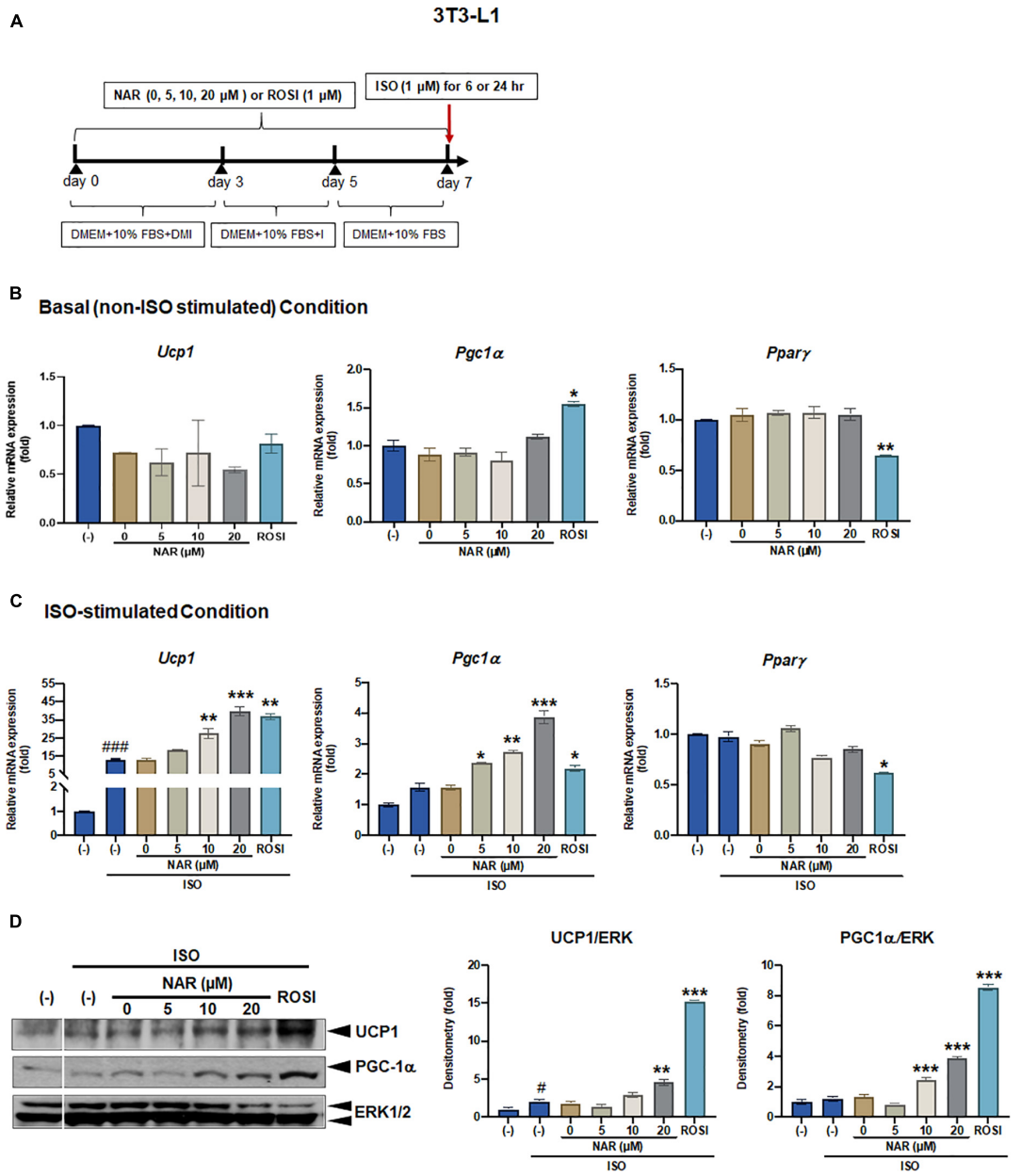

FIGURE 1
Naringenin dose-dependently enhances UCP-1 expression in isoproterenol (ISO)-stimulated 3T3-L1 adipocytes. 3T3-L1 cells were differentiated in the presence or absence of NAR (5, 10, 20 μM) for 7 days. ROSI (1 μM) was included as a positive control. On day 7, the cells were stimulated with isoproterenol (ISO, 1 μM) or the vehicle control (H_2O) for 6 h for mRNA analysis or 24 h for protein analysis. **(A)** A diagram of the cell treatment and timeline. As described in the Materials and Methods, DMEM + 10% FBS + DMI refer to DMEM containing 10% FBS, 0.5 mM/L 3-isobutyl-1-methylxanthine, 1 μM/L dexamethasone, and 10 μg/mL insulin. DEME + 10% FBS + I refer to DMEM containing 10% FBS and 10 μg/mL insulin. DMEM + 10% FBS refer to DMEM containing 10% FBS. **(B,C)** Relative mRNA levels of *Ucp1, Pgc1α*, and *Pparγ* at the basal **(B)** and ISO-stimulated conditions **(C)**. mRNA expression is presented relatively to the loading control *36b4*. **(D)** Protein expression of UCP1, PGC1α, and the loading control ERK1/2. Bar graphs show the densitometry of each protein to the loading control ERK1/2. Data = Mean ± SEM (n = 3). *, **, ***$p < 0.05$, $p < 0.01$, and $p < 0.001$ compared to the 0 μM NAR (i.e., DMSO) samples, respectively **(B–D)**. #, ###$p < 0.05$, $p < 0.001$ compared to the non-ISO stimulated (–) samples, respectively **(C,D)**.

Reporter gene assays

3T3-L1 cells were seeded at 2.5 × 10 (4) per well in 24-well plates overnight. The following day, the cells were transiently transfected with either PPRE X3-TK-Luc, a PPAR response element driven luciferase reporter, a gift from Dr. Bruce Spiegelman (Addgene plasmid # 1015[1]; RRID:Addgene_1015) (36) or murine PPARγ *trans*-activation reporters that include murine PPARγ ligand binding domain (LBD) linked to the Gal4 DNA binding domain (DBD) (mPPARγ-Gal4) and a reporter with an upstream activating sequence linked to luciferase, 4xUAS-TK-Luc (TK: thymidine kinase) (37) and β-galactosidase (β-gal) plasmid with Fugene HD transfection reagent (Promega, Madison, WI, USA). The cells were then treated with NAR, DMSO, or ROSI for 18 h. Luciferase and β-gal activities were measured from the cell lysates with GloMax Multi Detection System (Promega, Madison, WI, USA). Relative luciferase activities were presented by normalizing the luciferase activities with β-gal activities.

1 http://n2t.net/addgene:1015

Cellular bioenergetics measurements

3T3-L1 cells were differentiated in the presence or absence of NAR (10 μM) or ROSI (1 μM) for 6 days before they were seeded at 20,000 cells per well into XFe24 assay plates in DMEM containing 10% FBS overnight. Murine brown pre-adipocytes

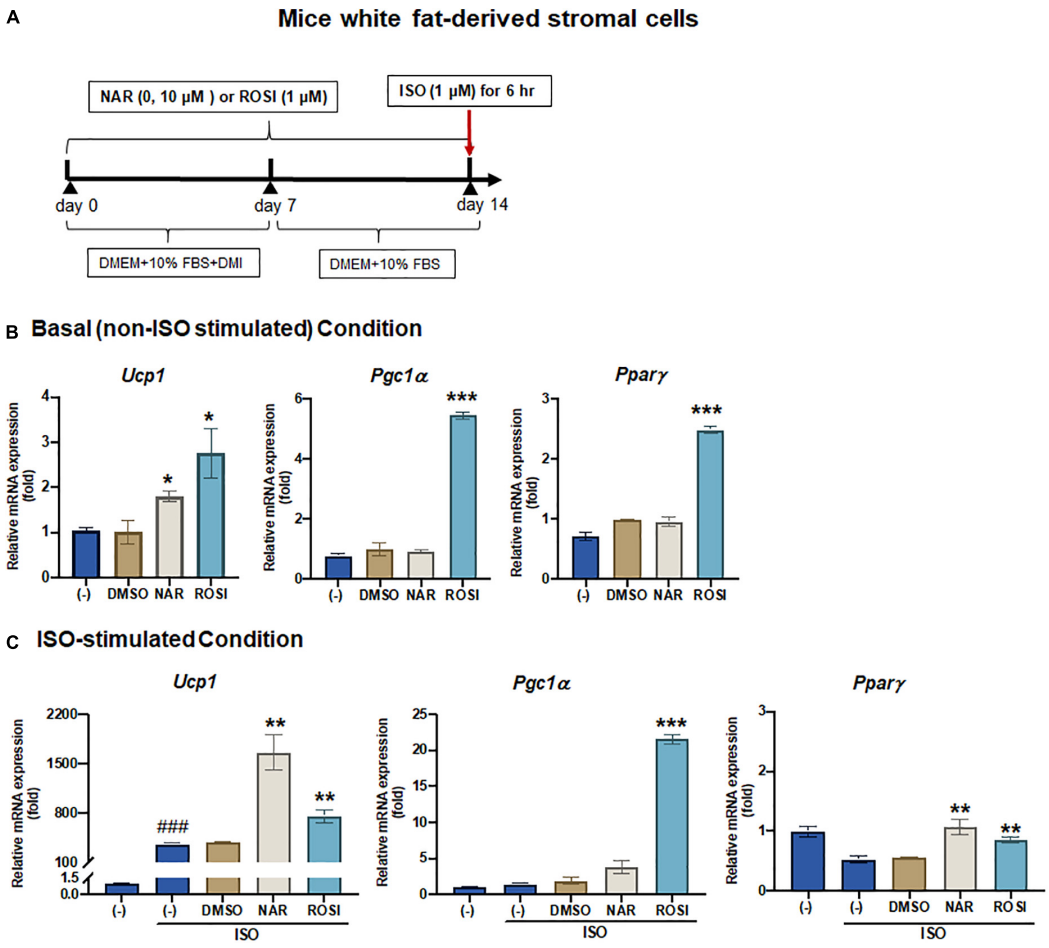

FIGURE 2
Naringenin enhances basal and isoproterenol (ISO)-stimulated up-regulation of *Ucp1* mRNA expression in primary white adipocytes differentiated from mice white fat-derived stromal cells. Mice white fat-derived primary stromal cells were induced to differentiate in the presence or absence of NAR (10 μM) or ROSI (1 μM) for 14 days. On day 14, the cells were stimulated with ISO (1 μM) or the vehicle control for 6 h for mRNA analysis. **(A)** A diagram of the cell treatment and timeline. As described in the Materials and Methods, DMEM + 10% FBS + DMI refer to DMEM containing 10% FBS, 0.5 mM/L 3-isobutyl-1-methylxanthine, 1 μM/L dexamethasone, and 10 μg/mL insulin. DMEM + 10% FBS refer to DMEM containing 10% FBS. **(B,C)** Relative mRNA levels of *Ucp1*, *Pgc1α*, and *Pparγ* at the basal **(B)** and ISO-stimulated conditions **(C)**. mRNA expression is presented relatively to the loading control *36b4*. Data = Mean ± SEM (n = 3). *, **, ***$p < 0.05$, $p < 0.01$, and $p < 0.001$ compared to the DMSO samples, respectively **(B,C)**. ###$p < 0.001$ compared to the non-ISO stimulated (−) samples **(C)**.

were differentiated in the presence or absence of NAR (10 μM) or ROSI (1 μM) for 4 days before they were seeded at 20,000 cells per well into XFe24 assay plates in the differentiation media overnight.

To start cellular bioenergetics measurements, cells were washed three times with XF assay buffer (DMEM without $NaHCO_3$, 10 mM glucose, 2 mM pyruvate, and 2 mM GlutaMAX, and 2% bovine serum albumin, pH 7.4). The cells were then equilibrated at 37°C in a non-CO_2 incubator for 1 h in the XF assay buffer. Oxygen consumption rates (OCR) were measured in an XFe24 Extracellular Flux Analyzer (Agilent, Santa Clara, CA, USA). To carry out mitochondria stress tests, ISO (10 μM, only for 3T3-L1 adipocytes), oligomycin (1 μM), carbonyl cyanide-ptrifluoromethoxyphenylhydrazone (FCCP; 6.5 μM), rotenone/antimycin A (1 μM each) were injected in sequential order, and three readings were taken after each injection. OCR readings were recorded by XFe24 software. OCR linked to proton leak and ATP production, coupling efficiency, and maximal respiration were calculated according to the manufacturer's instructions.

Oil red O staining

Lipid accumulation in the differentiated brown adipocytes was assessed by oil red O (ORO) staining and ORO absorbance, as described (25).

Statistical analysis

All data are shown as mean ± SE. Triplicates were performed in each experiment. Statistical analysis was conducted using Prism 9.3.0 (GraphPad Software, San Diego, CA, USA). One-way ANOVA with repeated measures followed by multiple comparisons test (Student-Newman-Keuls

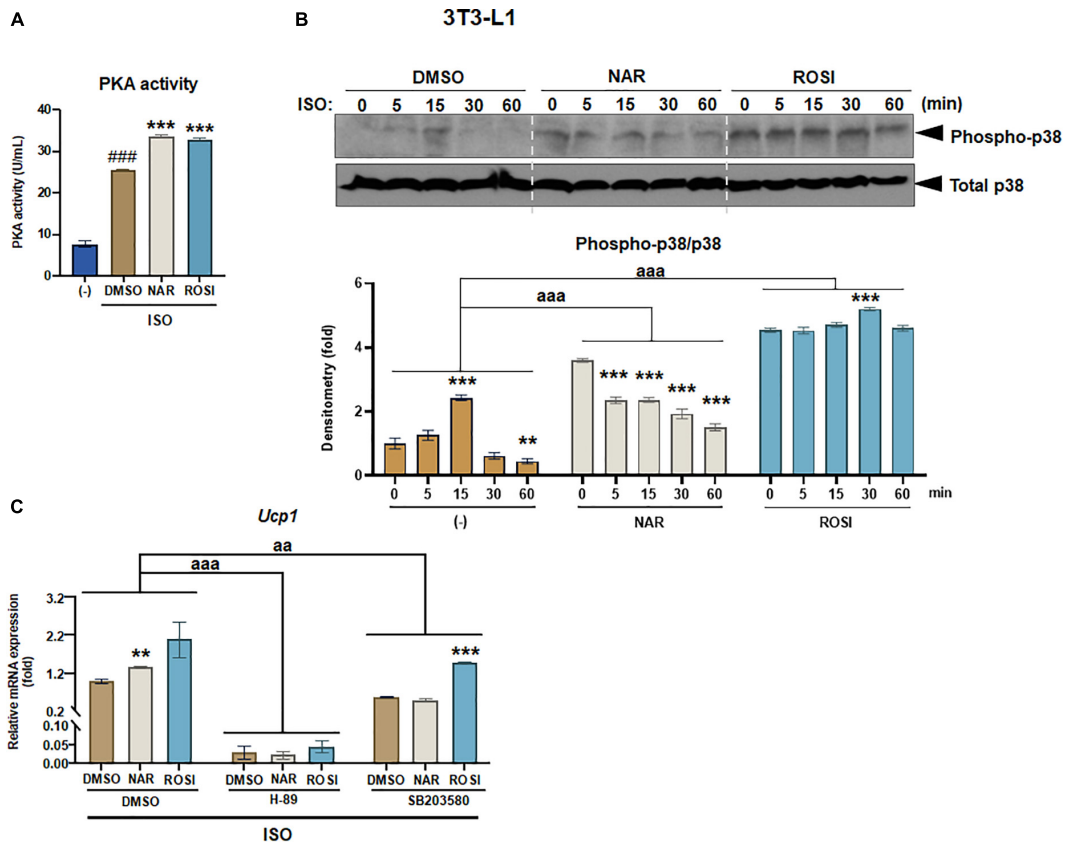

FIGURE 3
Naringenin enhances protein kinase A (PKA) activation and phosphorylation of p38 MAPK required for *Ucp1* up-regulation in isoproterenol (ISO)-stimulated 3T3-L1 adipocytes. 3T3-L1 cells were differentiated in the presence or absence of NAR (10 μM) or ROSI (1 μM) for 7 days. On day 7, the cells were stimulated with ISO (1 μM) or the vehicle control for 6 h for PKA activity analysis (A) or 1 h for analysis of phosphorylation of p38 (B). In a separate experiment, the cells were pretreated with the pharmacological inhibitors of PKA (H-89) and p38 (SB203580) or the vehicle control (DMSO) for 1 h before ISO stimulation for 6 h for mRNA expression analysis (C). **(A)** PKA activity. **(B)** p38 phosphorylation analysis. **(C)** Effects of PKA and p38 inhibitors on ISO-stimulated *Ucp1* up-regulation by NAR. *Ucp1* mRNA expression is presented relatively to the loading control *36b4*. Data = Mean ± SEM (n = 3). ###$p < 0.001$ compared to the non-ISO stimulated (–) samples **(A)**. *, **, ***$p < 0.05$, $p < 0.01$, and $p < 0.001$ compared to the ISO-stimulated time 0 **(B)** or DMSO samples **(C)** within each group, respectively. aa and aaa, $p < 0.01$ and $p < 0.001$ compared to the DMSO group, respectively, by two-way ANOVA **(B,C)**.

method) was used to detect significant differences in group mean between the treatment groups or between time points. Two-way ANOVA was used to detect differences between treatment groups. Student's *t*-tests were used as needed. The level of significance was set at $p < 0.05$.

Results

Naringenin dose-dependently enhances uncoupling protein 1 expression in isoproterenol-stimulated white adipocytes

To examine the effects of NAR on browning, 3T3-L1 cells were differentiated in the presence of increasing concentrations of NAR (5, 10, 20 μM) or its vehicle control DMSO. ROSI served as a positive control (Figure 1A). At basal (i.e., non-stimulated) condition (Figure 1B), ROSI induced mRNA expression of established brown specific markers *Ucp1*, *Pgc1α*, and suppressed *Pparγ* mRNA expression, as reported (9). In contrast, NAR did not change the mRNA expression of *Ucp1*, *Pgc1α*, and *Pparγ* when used up to 20 μM at the basal condition (Figure 1B). When stimulated with ISO, NAR dose-dependently enhanced ISO-induced *Ucp1* mRNA expression (Figure 1C). Similar effects were seen in *Pgc1α*, but not *Pparγ* (Figure 1C). ROSI also significantly enhanced ISO-induced *Ucp1* and *Pgc1α* up-regulation but suppressed *Pparγ* mRNA expression (Figure 1C). Consistently, NAR dose-dependently increased UCP1 and PGC1α protein expression in ISO-stimulated 3T3-L1 adipocytes (Figure 1D and Supplementary Figure 1A).

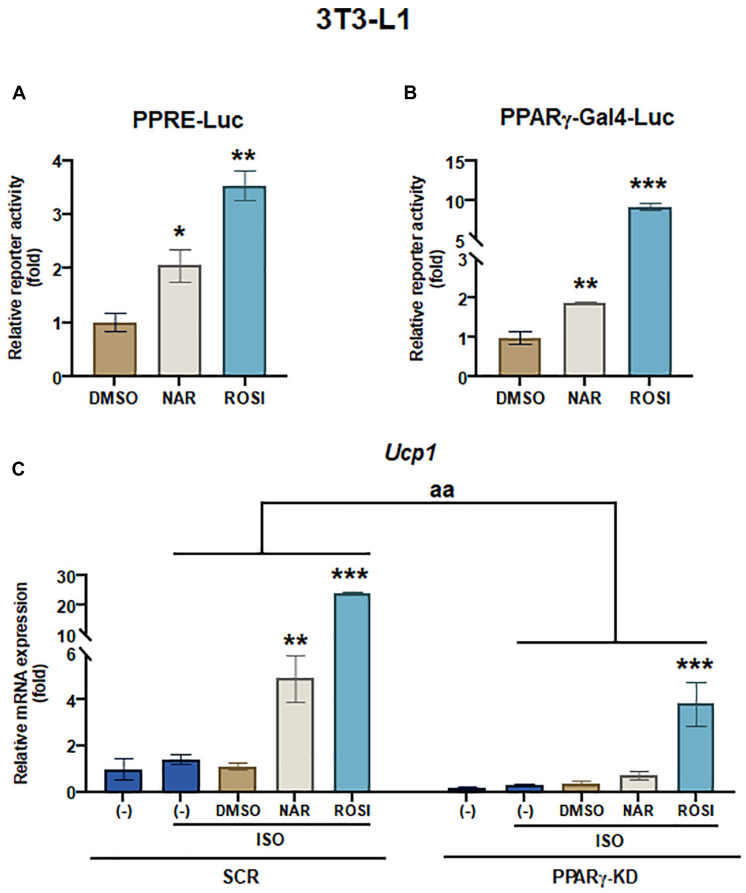

FIGURE 4
Naringenin activates PPRE and peroxisome proliferator-activated receptor gamma (PPARγ) reporters, and peroxisome proliferator-activated receptor gamma (PPARγ) knockdown attenuates the up-regulation of *Ucp1* mRNA expression by naringenin in isoproterenol (ISO)-stimulated 3T3-L1 adipocytes. **(A,B)** Effects of NAR on PPAR activation. 3T3-L1 cells were transiently transfected with PPRE-Luc **(A)** or murine PPARγ *trans*-activation reporter and the β-gal control plasmid **(B)** as described. Then the cells were treated with NAR, ROSI, or DMSO for 18 h, and the reporter activities were measured. Relative luciferase activities were calculated and presented as a fold with the DMSO sample set as 1. **(C)** Effects of PPARγ knockdown on ISO-stimulated *Ucp1* up-regulation by NAR. 3T3-L1 cells with PPARγ knockdown (PPARγ-KD) and a scrambled non-targeting control (SCR) were differentiated in the presence or absence of NAR (10 μM) or ROSI (1 μM) for 7 days. On day 7, the cells were stimulated with ISO (1 μM) for 6 h for mRNA analysis. *Ucp1* mRNA expression is presented relatively to the loading control *36b4*. Data = Mean ± SEM ($n = 3$). *, **, ***$p < 0.05$, $p < 0.01$, and $p < 0.001$ compared to the DMSO samples **(A,B)** or ISO-stimulated DMSO samples **(C)**, respectively. aa, $p < 0.01$ compared to the SCR control group by two-way ANOVA **(C)**.

Since it has been reported that the physiologically achievable serum level of NAR in human subjects is ~8 μM (38), we, therefore, focused our studies on NAR at 10 μM. We further examined the effects of NAR on murine primary stromal cells derived from white fat pads from C57BL/6 J mice. Primary stromal cells derived from the mice white fat pads were differentiated in the presence or absence of NAR (10 μM) or ROSI for 14 days (**Figure 2A**). NAR significantly increased *Ucp1* mRNA expression at the basal condition (**Figure 2B**) and enhanced ISO-stimulated up-regulation of *Ucp1* and *Pparγ* mRNA in these primary adipocytes (**Figure 2C**).

Naringenin enhances protein kinase A activation and phosphorylation of p38 MAPK in isoproterenol-stimulated 3T3-L1 adipocytes

β-adrenergic activation induced by cold exposure increases cAMP levels, leading to activation of PKA and downstream p38 MAPK phosphorylation and, consequently, UCP1 protein expression in brown adipocytes (39). To understand the molecular mechanisms by which NAR increases ISO-stimulated UCP1 expression in 3T3-L1 adipocytes, we explored the effects

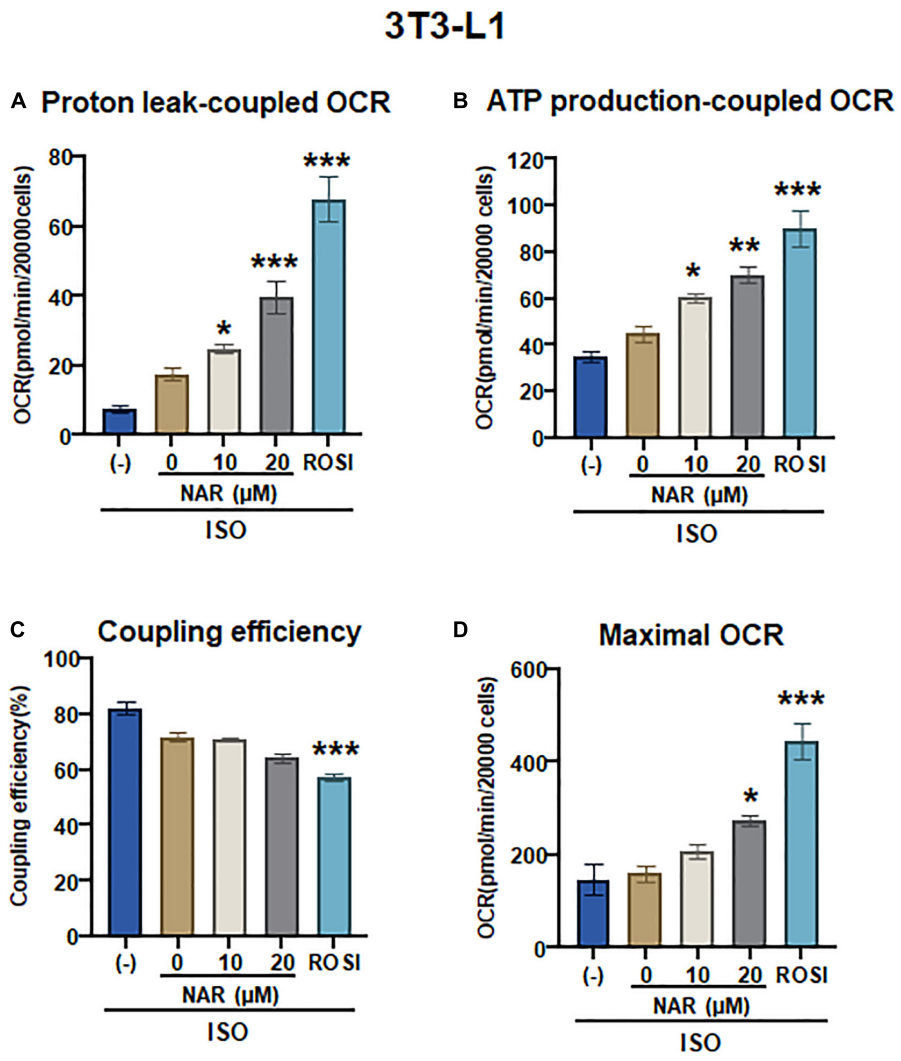

FIGURE 5
Naringenin enhances mitochondrial respiration and uncoupling in isoproterenol (ISO)-stimulated 3T3-L1 adipocytes. **(A–D)** 3T3-L1 cells were differentiated in the presence or absence of NAR (10 and 20 μM) or ROSI (1 μM) for 6 days. Then the cells were reseeded at 20,000 per well into an XFe24 assay plate. After 24 h, the cells were subjected to real-time OCR measurements using an XFe24 Extracellular Flux Analyzer. ISO was injected after three basal OCRs were taken, followed by oligomycin, FCCP, and rotenone/antimycin A injections as described. OCR linked to proton leak **(A)** and ATP production **(B)**, coupling efficiency **(C)**, and maximal respiration **(D)** were calculated and presented. Data = Mean ± SEM (n = 3–7). *, **, ***$p < 0.05$, $p < 0.01$, and $p < 0.001$ compared to the 0 μM NAR sample, respectively.

of NAR on PKA activation and p38 phosphorylation in ISO-stimulated 3T3-L1 adipocytes (Figure 3). ISO stimulation led to ∼3-fold increase of PKA activities, compared with the non-stimulated controls (Figure 3A). Both NAR and ROSI significantly enhanced PKA activation induced by ISO (Figure 3A).

We further examined p38 phosphorylation downstream of PKA activation in ISO-stimulated 3T3-L1 adipocytes (Figures 3B,C). As shown, ISO induced a peak of p38 phosphorylation at 15 min upon the stimulation in the control (DMSO treated) cells (Figure 3B). In contrast, p38 phosphorylation was significantly higher at time 0 but gradually decreased upon the stimulation in the NAR treated cells. ROSI induced the highest p38 phosphorylation at time 0 and a small peak at 30 min upon the stimulation in 3T3-L1 adipocytes (Figure 3B).

To examine whether PKA/p38 pathways underlie ISO-stimulated *Ucp1* up-regulation by NAR, we employed PKA and p38 pharmacological inhibitors. The PKA inhibitor H-89 blocked *Ucp1* mRNA expression at the basal condition and the up-regulation induced by NAR and ROSI (Figure 3C). The p38 inhibitor SB203580 also significantly attenuated the basal as well as NAR- and ROSI-induced, *Ucp1* mRNA expression, although to a less extent compared to H-89 (Figure 3C).

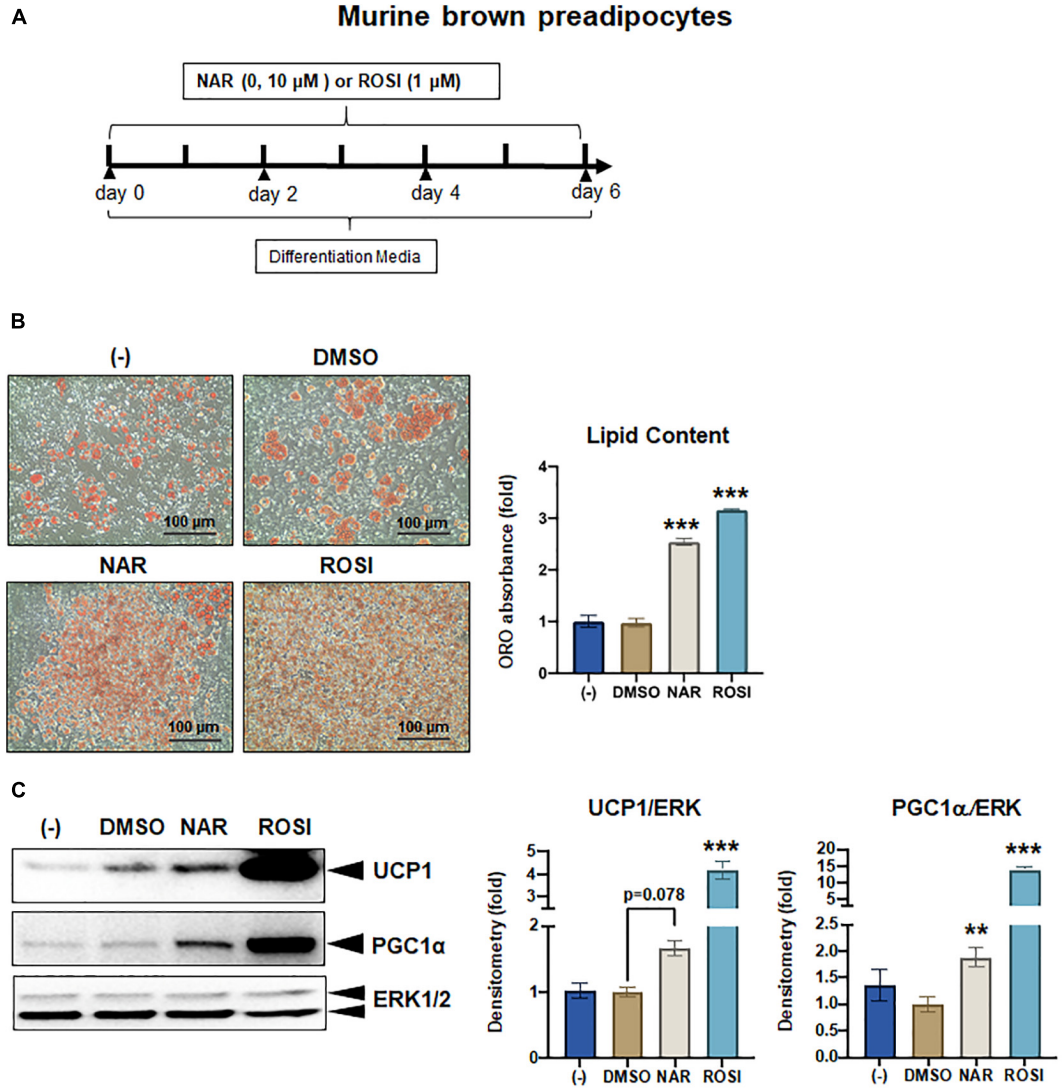

FIGURE 6
Naringenin promotes brown adipogenesis and thermogenic protein expression in murine brown adipocytes. Murine brown pre-adipocytes were differentiated in the presence or absence of NAR (10 μM) or ROSI (1 μM) for 6 days. **(A)** A diagram of the cell treatment and timeline. **(B)** Oil red O (ORO)-stained cell morphology and ORO absorbance. Scale bar = 100 μm. **(C)** Protein expression of thermogenic genes UCP1, PGC1α, and the loading control ERK1/2. Bar graphs show the densitometry of each protein normalized to the loading control ERK1/2. Data = Mean ± SEM (n = 3). *, **, ***$p < 0.05$, $p < 0.01$, and $p < 0.001$ compared to the DMSO samples, respectively.

Naringenin enhances *Ucp1* mRNA expression in isoproterenol-stimulated 3T3-L1 adipocytes through peroxisome proliferator-activated receptor gamma activation

It has been reported that as one of the downstream targets of the PKA/p38 pathway, PPARγ interacts with PGC1α and activates the PPRE site in the *Ucp1* promotor, leading to *Ucp1* transcription (39, 40). To understand whether NAR's effects were specifically mediated through PPARγ in 3T3-L1 pre-adipocytes, we first performed reporter gene assays. At 10 μM, NAR activated PPRE-Luc reporter by ∼2-fold, whereas ROSI activated the reporter by ∼3.5-fold compared to the controls (**Figure 4A**). Moreover, NAR at the same concentration *trans*-activated PPARγ *via* its ligand binding domain in 3T3-L1 cells (**Figure 4B**), consistent with the previous report (23). Furthermore, using 3T3-L1 with PPARγ knockdown (PPARγ-KD) and the scrambled non-targeting control (SCR) we have generated (25), we found that ISO-induced *Ucp1* mRNA expression was significantly enhanced by NAR or ROSI in the SCR cells but was significantly attenuated in PPARγ-KD cells (**Figure 4C**).

Naringenin enhances isoproterenol-stimulated mitochondrial respiration and uncoupling in 3T3-L1 adipocytes

To determine whether UCP1 up-regulation by NAR upon ISO stimulation leads to increases in mitochondrial respiration

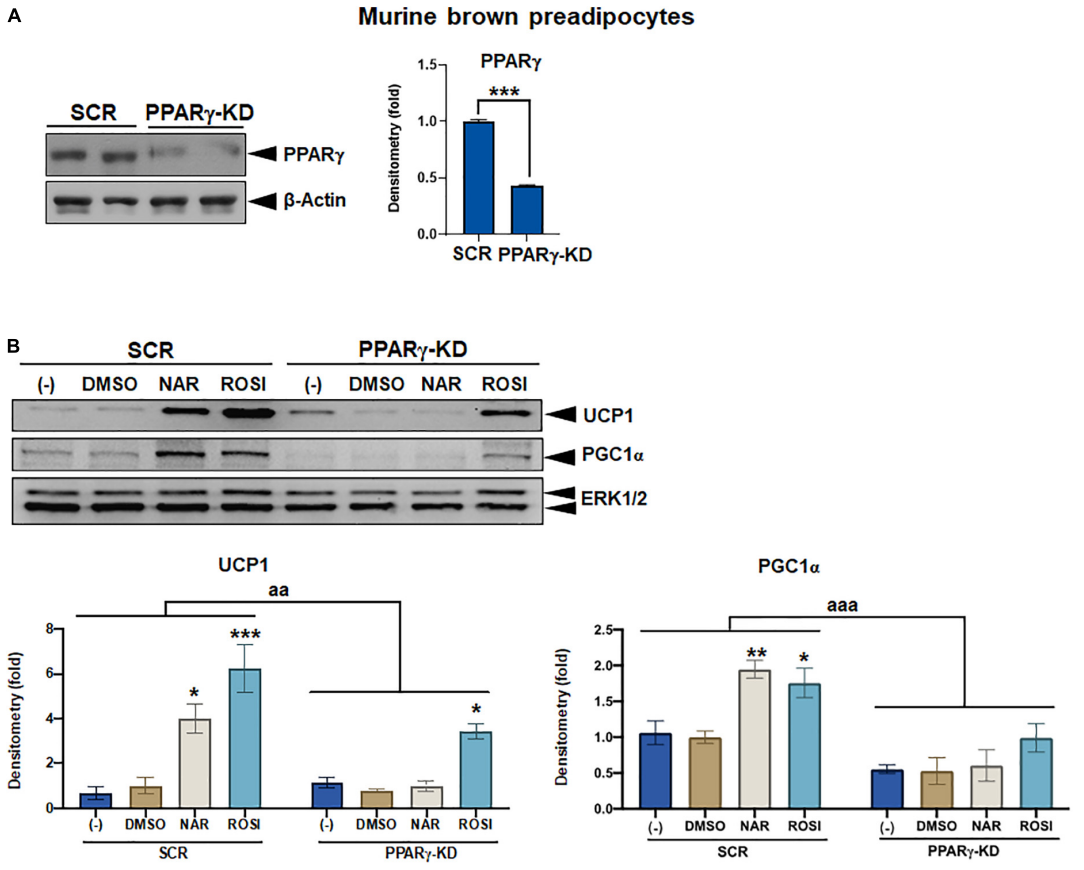

FIGURE 7
Attenuation of thermogenic protein expression by peroxisome proliferator-activated receptor gamma (PPARγ) knockdown in naringenin-treated murine brown adipocytes. **(A)** Knockdown efficiency in murine brown pre-adipocytes with PPARγ knockdown (PPARγ-KD) compared to the cells with a scrambled non-targeting control (SCR). Two individual clones were analyzed. Average knockdown efficiency is shown. **(B)** PPARγ-KD and SCR cells were differentiated in the presence or absence of NAR (10 μM) or ROSI (1 μM) for 6 days. Protein expression of thermogenic markers UCP1, PGC1α, and the loading control ERK1/2 are shown. Bar graphs show the densitometry of each protein normalized to the loading control ERK1/2. Data = Mean ± SEM (n = 3). *, **, ***$p < 0.05$, $p < 0.01$, and $p < 0.001$ compared to the SCR clones **(A)** or the DMSO samples within SCR or PPARγ-KD group **(B)**, respectively. aa and aaa, $p < 0.01$ and $p < 0.001$ compared to the SCR group, respectively, by two-way ANOVA **(B)**.

and uncoupling, we measured oxygen consumption rates (OCR) in mitochondrial stress tests in 3T3-L1 adipocytes that were differentiated in the presence of NAR, the vehicle control, or ROSI using an XFe24 Extracellular Flux Analyzer (**Figure 5** and **Supplementary Figure 1B**). We found that NAR dose-dependently enhanced OCR linked to proton leak (i.e., uncoupling) (**Figure 5A**) and ATP production (**Figure 5B**) and increased maximal OCR (**Figure 5D**) while had no significant effects on coupling efficiency (**Figure 5C**) in ISO-stimulated 3T3-L1 adipocytes. Note that significant increases in OCR linked to proton leak and ATP production by NAR were detected starting at 10 μM.

Naringenin promotes brown adipogenesis and thermogenic protein expression in murine brown adipocytes through peroxisome proliferator-activated receptor gamma

As a part of functional brown adipose tissue, classical brown adipocytes are responsible for non-shivering thermogenesis in response to cold, leading to energy expenditure. However, despite the effects on browning, the effects of NAR on brown adipogenesis have not been reported. Here, we examined the effects of NAR on brown adipogenesis in a murine brown pre-adipocyte cell line. Murine brown pre-adipocytes were differentiated in the presence or absence of NAR or ROSI (**Figure 6A**). NAR at 10 μM significantly enhanced brown adipogenesis as indicated by the oil red O-stained cell morphology (**Figure 6B** left) and lipid accumulation (**Figure 6B** right) and increased protein expression of brown markers UCP1 and PGC1α (**Figure 6C**) and other general differentiation markers PPARγ, fatty acid binding protein 4 (FABP4), and perilipin (PLIN) (**Supplementary Figure 2A**). We further assessed the role of PPARγ in the process using the brown pre-adipocytes with stable knockdown of PPARγ (PPARγ-KD) and a scrambled non-targeting control (SCR). PPARγ-KD reduced endogenous PPARγ protein expression by ∼60% (**Figure 7A**). While NAR at 10 μM significantly increased UCP1 and PGC1α protein expression in the SCR cells, it did not cause significant changes in the PPARγ-KD cells (**Figure 7B**). ROSI's effects were also significantly attenuated in PPARγ-KD cells as expected (**Figure 7B**).

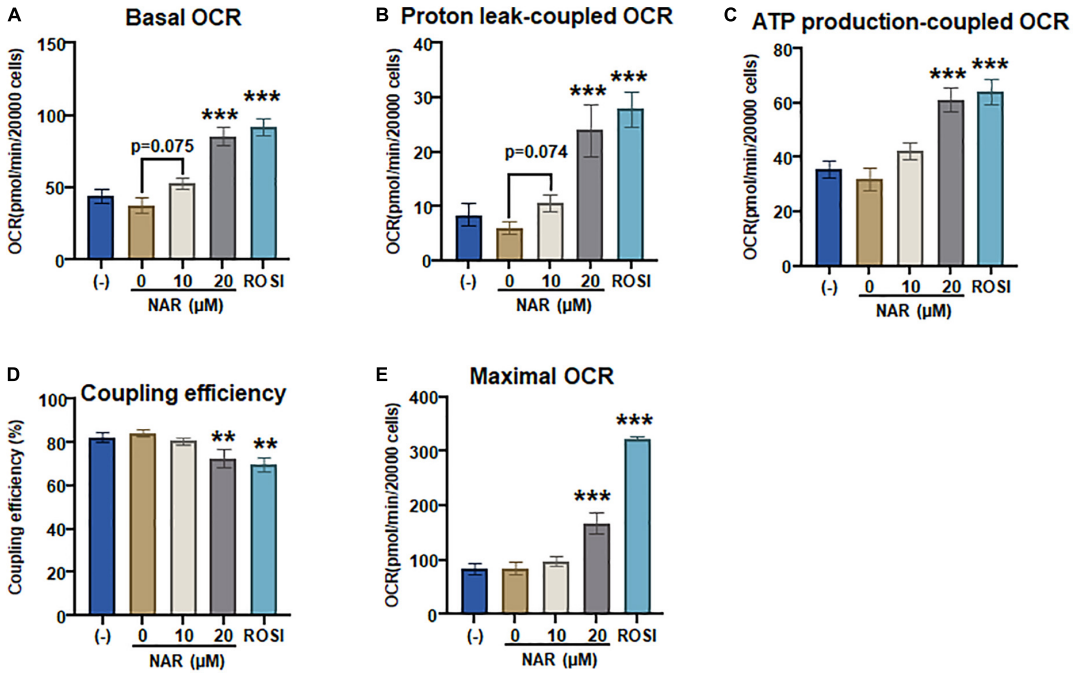

FIGURE 8
Naringenin enhances mitochondrial respiration and uncoupling in murine brown adipocytes. **(A–E)** Murine brown pre-adipocytes were differentiated in the presence or absence of NAR (10 and 20 μM) or ROSI (1 μM) for 4 days. Then cells were reseeded at 20,000 cells per well into an XFe24 assay plate. After 24 h, the cells were then subjected to real-time measurements of OCR coupled with a mitochondrial stress test using an XFe24 Extracellular Flux Analyzer as described. Basal OCRs **(A)**, OCR linked to proton leak **(B)** and ATP production **(C)**, coupling efficiency **(D)**, and maximal respiration **(E)** were calculated and presented. Data = Mean ± SEM (n = 3–7). *, **, ***$p < 0.05$, $p < 0.01$, and $p < 0.001$ compared to the 0 μM NAR samples, respectively.

Naringenin enhances mitochondrial respiration and uncoupling in murine brown adipocytes

To confirm that NAR also enhances mitochondrial respiration and thermogenesis in parallel with its effects on lipid accumulation and brown marker protein expression, we measured OCR coupled with mitochondrial stress tests in the murine brown adipocytes that were differentiated in the presence or absence of NAR or ROSI using the XFe24 Extracellular Flux Analyzer (**Figure 8**). We found that there were dose-dependent increases in the basal OCR (**Figure 8A** and **Supplementary Figure 2B**), OCR linked to proton leak (i.e., uncoupling) (**Figure 8B**) and ATP production (**Figure 8C**) and maximal OCR (**Figure 8E**) and a decrease in the coupling efficiency (**Figure 8D**) in brown adipocytes treated by NAR. However, significant changes in those measures were found by NAR at 20 μM only. As expected, ROSI significantly increased similar changes in those measures but to a greater extent compared to NAR at 20 μM (**Figure 8**).

Discussion

Functional brown adipose tissue has become a novel target for obesity treatment and prevention. We report that NAR enhances ISO-stimulated UCP1 expression, mitochondrial respiration, and uncoupling in 3T3-L1 adipocytes. NAR enhances ISO-stimulated PKA activation and phosphorylation of p38, accompanied by PPARγ activation. Moreover, NAR enhances murine brown adipogenesis and increases brown adipocytes' mitochondrial respiration and uncoupling. We further demonstrate that PPARγ is required for enhanced *Ucp1* expression in 3T3-L1 adipocytes and brown adipocytes by NAR.

3T3-L1 cells, a commonly used white fat cell model, have been used to identify and characterize strategies to induce

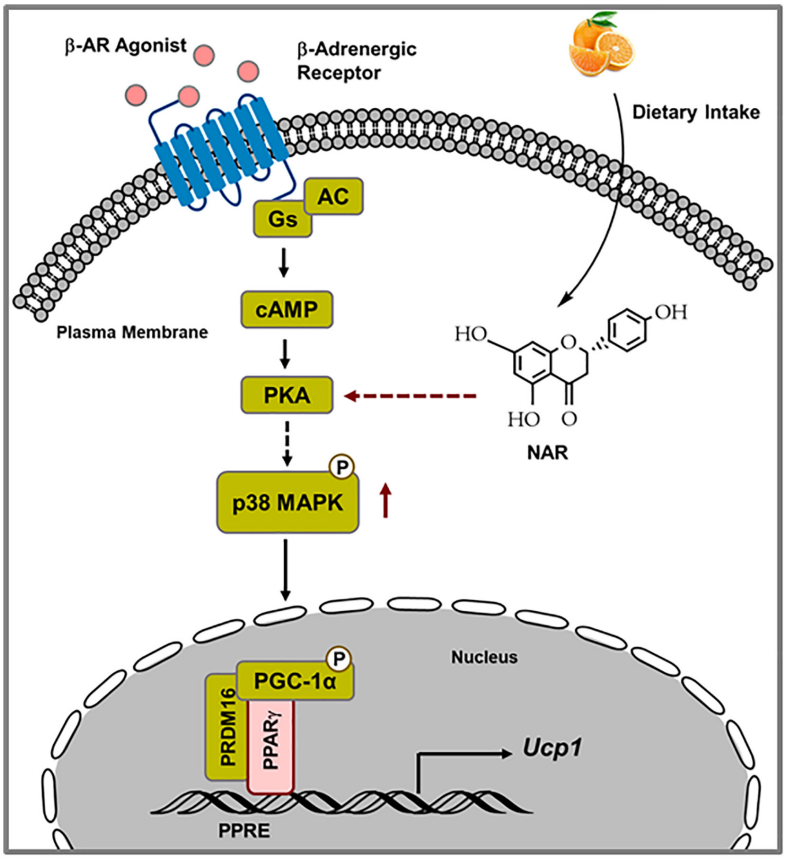

FIGURE 9
Schematic diagram illustrating the proposed mechanisms by which naringenin enhances isoproterenol (ISO)-stimulated UCP1 expression in 3T3-L1 adipocytes. Upon ISO binding to the β-adrenergic receptor (AR), cAMP is produced through Gs-coupled adenylyl cyclase (AC), leading to PKA activation. Through yet unknown steps, PKA activation results in p38 phosphorylation and subsequent phosphorylation and activation of downstream targets, such as PGC1α. Activated PGC1α co-activates PPARγ on the PPRE site in the promoter of the *Ucp1* gene, leading to enhanced *Ucp1* transcription. NAR enhances ISO-stimulated PKA activation and p38 phosphorylation and further activates PPARγ, leading to increased *Ucp1* up-regulation upon ISO stimulation in 3T3-L1 adipocytes.

browning (41–47). To our knowledge, this is the first report that NAR, a dietary bioactive compound, enhances ISO-stimulated thermogenic activation (*Ucp1* expression and mitochondrial uncoupling) in 3T3-L1 adipocytes at 10 μM, a level that is achievable through dietary consumption in human subjects (38).

The hallmark of brown-like adipocytes is inducible UCP1 expression and thermogenesis upon β adrenergic stimulation, such as cold exposure. As a β adrenergic receptor agonist, ISO has been used to induce thermogenic activation in brown (32, 48) and brown-like adipocytes (33, 41, 44, 48). It was reported that ISO induced increases in *Ucp1* mRNA expression in 3T3-L1 adipocytes (41). Therefore, our findings are consistent with the report and further highlight the browning capacity of NAR as a dietary factor in enhancing ISO-stimulated *Ucp1* expression in 3T3-L1 adipocytes. Moreover, we report that NAR at 10 μM, a reported dietary achievable dose in human subjects (29, 38), enhances *Ucp1* mRNA expression at both basal (non-ISO stimulated) and ISO-stimulated conditions in the primary white adipocytes differentiated from stromal cells isolated from mice white fat pads. These findings are consistent with the reported increase of UCP1 expression by NAR at the same dose in human white adipocytes under non-ISO-stimulated conditions (29). The effects of NAR on ISO-stimulated UCP1 up-regulation in human white adipocytes were not reported in that study and, therefore, warrant further investigation.

The findings that NAR does not induce *Ucp1* mRNA expression at the basal conditions but enhances *Ucp1* expression and mitochondrial uncoupling in response to ISO in 3T3-L1 adipocytes prompted us to investigate the mechanisms by which NAR enhances ISO-stimulated *Ucp1* up-regulation in these adipocytes. Upon adrenergic stimulation by cold or other β-AR agonists, cyclic AMP (cAMP) is produced through activated Gs protein coupled-adenylyl cyclase (AC) associated with β-AR, leading to PKA activation and subsequent p38 phosphorylation and activation (49, 50). Activated p38 further phosphorylates and activates target proteins, such as PGC1α [a coactivator of PPARγ on the PPAR response elements (PPRE) site], leading to up-regulation of *Ucp1* transcription (39, 40; **Figure 9**). We report, for the first time, that NAR at a dietary achievable dose enhances ISO-stimulated PKA activation in 3T3-L1 adipocytes. Moreover, NAR-treated 3T3-L1 adipocytes have a higher basal p38 phosphorylation before ISO stimulation. NAR enhances PPARγ transactivation in 3T3-L1 cells. Furthermore, we demonstrate that NAR's effects on ISO-stimulated *Ucp1* up-regulation are attenuated by the inhibition of PKA and p38 and by PPARγ knockdown. Our results suggest that NAR may act through PKA/p38/PPARγ pathway to enhance ISO-stimulated *Ucp1* up-regulation in 3T3-L1 adipocytes (**Figure 9**).

As a well-known browning agent, ROSI is shown to enhance PKA activation and basal p38 phosphorylation, leading to up-regulation of ISO-stimulated *Ucp1* transcription, mitochondrial respiration, and uncoupling in 3T3-L1 adipocytes in our studies, consistent with a previous report that demonstrated enhanced cAMP levels and ISO-stimulated oxygen consumption in ROSI-treated white adipocytes (10). Our results shed new light on the mechanisms by which ROSI promotes the browning of white adipocytes.

For the first time, we also report that, similar to ROSI, NAR enhances brown adipogenesis with increased brown marker gene expression and mitochondrial respiration and uncoupling. We further demonstrate that PPARγ is required for the increased UCP1 expression by NAR in the brown adipocytes with PPARγ knockdown. Together, our results suggest that NAR promotes the development of functional brown adipocytes *in vitro* through PPARγ activation. Our results may help explain the increased energy expenditure found in NAR-treated mice (26, 27). However, whether there were significant increases in functional BAT mass or activities in those treated mice is unclear in those studies. Future studies on how NAR supplementation increases energy expenditure *in vivo* are warranted.

In conclusion, our results demonstrate that NAR at a dietary achievable dose enhances ISO-stimulated UCP1 up-regulation and mitochondrial respiration and uncoupling in 3T3-L1 adipocytes, possibly through enhancement of PKA/p38/PPARγ pathways downstream of ISO. Moreover, NAR also enhances cellular brown adipogenesis through PPARγ activation. Combined with other published reports, our results suggest that NAR may be beneficial in promoting the development of functional BAT. Further studies of NAR in promoting thermogenesis and energy expenditure to combat human obesity through enhancing functional BAT are warranted.

Data availability statement

The original contributions presented in the study are included in the article/**Supplementary material**, further inquiries can be directed to the corresponding author.

Ethics statement

The animal study was reviewed and approved by University of Tennessee Knoxville IACUC animal protocol 2320.

Author contributions

JB and YY performed the experiments, data analysis, and wrote the manuscript. XX, JF, HO, KH, and JC performed the experiments and data analysis. SW contributed to the study

designs and provided funding support. LZ wrote the manuscript and provided funding support. All authors have read and approved the manuscript.

Funding

This study was supported by NIH 1R15AT008733 and 1R15AT010395 to SW and 1R15DK114790-01A1 and 1R15DK132728-01 to LZ. Partial funding for open access to this research was provided by the University of Tennessee's Open Publishing Support Fund.

Acknowledgments

Some of the results were presented as part of the work in the dissertation and thesis by JB and JF (as Jamie Ann Kearns), respectively, and deposited in Tennessee Research and Creative Exchange (TRACE) database.

Conflict of interest

The authors declare that the research was conducted in the absence of any commercial or financial relationships that could be construed as a potential conflict of interest.

Publisher's note

Supplementary material

The Supplementary Material for this article can be found online at: https://www.frontiersin.org/articles/10.3389/fnut.2022.1036655/full#supplementary-material

SUPPLEMENTARY FIGURE 1
The effects of Naringenin on UCP1 and PGC1α protein expression and mitochondrial respiration under ISO-stimulated conditions in 3T3-L1 adipocytes. 3T3-L1 cells were differentiated in the presence or absence of NAR (5, 10, 20 μM) for 7 days. ROSI (1 μM) was included as a positive control. **(A)** The cells were stimulated with isoproterenol (ISO, 10 μM) or the vehicle control (H_2O) for 24 h. Protein samples were prepared, and UCP1, PGC1α, and ERK1/2 protein expression are shown. **(B)** The cells were reseeded at 20,000 per well into an XFe24 assay plate. After 24 h, the cells were subjected to real-time OCR measurements using an XFe24 Extracellular Flux Analyzer as described in **Figure 5**. OCR readings over time are shown.

SUPPLEMENTARY FIGURE 2
Naringenin increases protein expression of general differentiation markers and mitochondrial respiration in murine brown adipocytes. Murine brown pre-adipocytes were differentiated in the presence or absence of NAR (10 μM) or ROSI (1 μM). **(A)** After 6 days, protein expression of PPARγ, FABP4, perilipin (PLIN), and the loading control ERK1/2 are shown (left panel). Bar graphs show the densitometry of each gene normalized to the loading control ERK1/2 (right panels). Data = Mean ± SEM (n = 3). *, **, ***$p < 0.05$, $p < 0.01$, and $p < 0.001$ compared to the DMSO samples, respectively. **(B)** The cells were reseeded at 20,000 cells per well on day 4 into an XFe24 assay plate. After 24 h, the cells were then subjected to OCR measurements using an XFe24 Extracellular Flux Analyzer as described in **Figure 8**. OCR readings over time are shown.

References

1. CDC. Adult obesity causes & consequences. *Retriev Dec.* (2021) 1:2021.

2. Atkins D. Unraveling the connection between obesity and outcomes in COVID-19. *Obesity.* (2021) 29:786–7.

3. Foulkes AS, Selvaggi C, Shinnick D, Lumish H, Kim E, Cao T, et al. Understanding the link between obesity and severe COVID-19 outcomes: causal mediation by systemic inflammatory response. *J Clin Endocrinol Metab.* (2021) 107:e698–707.

4. Cousin B, Cinti S, Morroni M, Raimbault S, Ricquier D, Penicaud L, et al. Occurrence of brown adipocytes in rat white adipose tissue: molecular and morphological characterization. *J Cell Sci.* (1992) 103:931–42. doi: 10.1242/jcs.103.4.931

5. Guerra C, Koza RA, Yamashita H, Walsh K, Kozak LP. Emergence of brown adipocytes in white fat in mice is under genetic control. Effects on body weight and adiposity. *J Clin Invest.* (1998) 102:412–20.

6. Himms-Hagen J, Melnyk A, Zingaretti MC, Ceresi E, Barbatelli G, Cinti S. Multilocular fat cells in WAT of CL-316243-treated rats derive directly from white adipocytes. *Am J Physiol Cell Physiol.* (2000) 279:C670–81. doi: 10.1152/ajpcell.2000.279.3.C670

7. Fukui Y, Masui S, Osada S, Umesono K, Motojima K. A new thiazolidinedione, NC-2100, which is a weak PPAR-gamma activator, exhibits potent antidiabetic effects and induces uncoupling protein 1 in white adipose tissue of KKAy obese mice. *Diabetes.* (2000) 49:759–67. doi: 10.2337/diabetes.49.5.759

8. Sell H, Berger JP, Samson P, Castriota G, Lalonde J, Deshaies Y, et al. Peroxisome proliferator-activated receptor gamma agonism increases the capacity for sympathetically mediated thermogenesis in lean and ob/ob mice. *Endocrinology.* (2004) 145:3925–34. doi: 10.1210/en.2004-0321

9. Petrovic N, Walden TB I, Shabalina G, Timmons JA, Cannon B, Nedergaard J. Chronic peroxisome proliferator-activated receptor gamma (PPARgamma) activation of epididymally derived white adipocyte cultures reveals a population of thermogenically competent, UCP1-containing adipocytes molecularly distinct from classic brown adipocytes. *J Biol Chem.* (2010) 285:7153–64.

10. Merlin J, Sato M, Nowell C, Pakzad M, Fahey R, Gao J, et al. The PPARgamma agonist rosiglitazone promotes the induction of brite adipocytes, increasing beta-adrenoceptor-mediated mitochondrial function and glucose uptake. *Cell Signal.* (2018) 42:54–66. doi: 10.1016/j.cellsig.2017.09.023

11. Cypess AM, Lehman S, Williams G, Tal I, Rodman D, Goldfine AB, et al. Identification and importance of brown adipose tissue in adult humans. *N Engl J Med.* (2009) 360:1509–17.

12. Virtanen KA, Lidell ME, Orava J, Heglind M, Westergren R, Niemi T, et al. Functional brown adipose tissue in healthy adults. *N Engl J Med.* (2009) 360:1518–25.

13. Wu J, Bostrom P, Sparks LM, Ye L, Choi JH, Giang AH, et al. Beige adipocytes are a distinct type of thermogenic fat cell in mouse and human. *Cell.* (2012) 150:366–76.

14. Jespersen NZ, Larsen TJ, Peijs L, Daugaard S, Homoe P, Loft A, et al. A classical brown adipose tissue mRNA signature partly overlaps with brite in the supraclavicular region of adult humans. *Cell Metab.* (2013) 17:798–805. doi: 10.1016/j.cmet.2013.04.011

15. Saito M, Okamatsu-Ogura Y, Matsushita M, Watanabe K, Yoneshiro T, Nio-Kobayashi J, et al. High incidence of metabolically active brown adipose tissue in healthy adult humans: effects of cold exposure and adiposity. *Diabetes.* (2009) 58:1526–31. doi: 10.2337/db09-0530

16. Matsushita M, Yoneshiro T, Aita S, Kameya T, Sugie H, Saito M. Impact of brown adipose tissue on body fatness and glucose metabolism in healthy humans. *Int J Obes.* (2014) 38:812–7. doi: 10.1038/ijo.2013.206

17. Yoneshiro T, Aita S, Matsushita M, Kayahara T, Kameya T, Kawai Y, et al. Recruited brown adipose tissue as an anti-obesity agent in humans. *J Clin Invest.* (2013) 123:3404–8.

18. Coelho RA, Hermsdorff HM, Bressan J. Anti-inflammatory properties of orange juice: possible favorable molecular and metabolic effects. *Plant Foods Hum Nutr.* (2013) 68:1–10. doi: 10.1007/s11130-013-0343-3

19. Alam MA, Subhan N, Rahman MM, Uddin SJ, Reza HM, Sarker SD. Effect of citrus flavonoids, naringin and naringenin, on metabolic syndrome and their mechanisms of action. *Adv Nutr.* (2014) 5:404–17.

20. Mir IA, Tiku AB. Chemopreventive and therapeutic potential of naringenin, a flavanone present in citrus fruits. *Nutr Cancer.* (2015) 67:27–42.

21. Sharma M, Akhtar N, Sambhav K, Shete G, Bansal AK, Sharma SS. Emerging potential of citrus flavanones as an antioxidant in diabetes and its complications. *Curr Top Med Chem.* (2015) 15:187–95. doi: 10.2174/1568026615666141209163013

22. Yang Y, Trevethan M, Wang S, Zhao L. Beneficial effects of citrus flavanones naringin and naringenin and their food sources on lipid metabolism: an update on bioavailability, pharmacokinetics, and mechanisms. *J Nutr Biochem.* (2022) 104:108967. doi: 10.1016/j.jnutbio.2022.108967

23. Goldwasser J, Cohen PY, Yang E, Balaguer P, Yarmush ML, Nahmias Y. Transcriptional regulation of human and rat hepatic lipid metabolism by the grapefruit flavonoid naringenin: role of PPARalpha, PPARgamma and LXRalpha. *PLoS One.* (2010) 5:e12399. doi: 10.1371/journal.pone.0012399

24. Petrovic N I, Shabalina G, Timmons JA, Cannon B, Nedergaard J. Thermogenically competent nonadrenergic recruitment in brown preadipocytes by a PPARgamma agonist. *Am J Physiol Endocrinol Metab.* (2008) 295:E287–96. doi: 10.1152/ajpendo.00035.2008

25. Overby H, Yang Y, Xu X, Graham K, Hildreth K, Choi S, et al. Soluble epoxide hydrolase inhibition by t-TUCB promotes brown adipogenesis and reduces serum triglycerides in diet-induced obesity. *Int J Mol Sci.* (2020) 21:19. doi: 10.3390/ijms21197039

26. Mulvihill EE, Allister EM, Sutherland BG, Telford DE, Sawyez CG, Edwards JY, et al. Naringenin prevents dyslipidemia, apolipoprotein B overproduction, and hyperinsulinemia in LDL receptor-null mice with diet-induced insulin resistance. *Diabetes.* (2009) 58:2198–210. doi: 10.2337/db09-0634

27. Burke AC, Telford DE, Edwards JY, Sutherland BG, Sawyez CG, Huff MW. Naringenin supplementation to a chow diet enhances energy expenditure and fatty acid oxidation, and reduces adiposity in lean, pair-fed Ldlr(-/-) mice. *Mol Nutr Food Res.* (2019) 63:e1800833. doi: 10.1002/mnfr.201800833

28. Mehanna ET, El-Sayed NM, Ibrahim AK, Ahmed SA, Abo-Elmatty DM. Isolated compounds from *Cuscuta pedicellata* ameliorate oxidative stress and upregulate expression of some energy regulatory genes in high fat diet induced obesity in rats. *Biomed Pharmacother.* (2018) 108:1253–8. doi: 10.1016/j.biopha.2018.09.126

29. Rebello CJ, Greenway FL, Lau FH, Lin Y, Stephens JM, Johnson WD, et al. Naringenin promotes thermogenic gene expression in human white adipose tissue. *Obesity.* (2019) 27:103–11. doi: 10.1002/oby.22352

30. Zhao L, Hu P, Zhou Y, Purohit J, Hwang D. NOD1 activation induces proinflammatory gene expression and insulin resistance in 3T3-L1 adipocytes. *Am J Physiol Endocrinol Metab.* (2011) 301:E587–98.

31. Hausman DB, Park HJ, Hausman GJ. Adipose tissue protocol: chapter 15 isolation and culture of preadipocytes from rodent white adipose tissue. In: Yang K editor. *Methods In molecular biology*. (Vol. 456), Humana Press (2008). doi: 10.1007/978-1-59745-245-8_15

32. Bae J, Ricciardi CJ, Esposito D, Komarnytsky S, Hu P, Curry BJ, et al. Activation of pattern recognition receptors in brown adipocytes induces inflammation and suppresses uncoupling protein 1 expression and mitochondrial respiration. *Am J Physiol Cell Physiol.* (2014) 306:C918–30. doi: 10.1152/ajpcell.00249.2013

33. Overby H, Yang Y, Xu X, Wang S, Zhao L. Indomethacin promotes browning and brown adipogenesis in both murine and human fat cells. *Pharmacol Res Perspect.* (2020) 8:e00592. doi: 10.1002/prp2.592

34. Yang Y, Xu X, Wu H, Yang J, Chen J, Morisseau C, et al. Differential effects of 17,18-EEQ and 19,20-EDP combined with soluble epoxide hydrolase inhibitor t-TUCB on diet-induced obesity in mice. *Int J Mol Sci.* (2021) 22:15. doi: 10.3390/ijms22158267

35. Dawson K, Zhao L, Adkins Y, Vemuri M, Rodriguez RL, Gregg JP, et al. Modulation of blood cell gene expression by DHA supplementation in hypertriglyceridemic men. *J Nutrit Biochem.* (2012) 23:616–21. doi: 10.1016/j.jnutbio.2011.03.004

36. Kim JB, Wright HM, Wright M, Spiegelman BM. ADD1/SREBP1 activates PPARgamma through the production of endogenous ligand. *Proc Natl Acad Sci USA.* (1998) 95:4333–7. doi: 10.1073/pnas.95.8.4333

37. Taxvig C, Dreisig K, Boberg J, Nellemann C, Schelde AB, Pedersen D, et al. Differential effects of environmental chemicals and food contaminants on adipogenesis, biomarker release and PPARγ activation. *Mol Cell Endocrinol.* (2012) 361:106–15. doi: 10.1016/j.mce.2012.03.021

38. Kanaze FI, Bounartzi MI, Georgarakis M, Niopas I. Pharmacokinetics of the citrus flavanone aglycones hesperetin and naringenin after single oral administration in human subjects. *Eur J Clin Nutr.* (2007) 61:472–7. doi: 10.1038/sj.ejcn.1602543

39. Cao W, Daniel KW, Robidoux J, Puigserver P, Medvedev AV, Bai X, et al. p38 mitogen-activated protein kinase is the central regulator of cyclic AMP-dependent transcription of the brown fat uncoupling protein 1 gene. *Mol Cell Biol.* (2004) 24:3057–67. doi: 10.1128/MCB.24.7.3057-3067.2004

40. Cao W, Medvedev AV, Daniel KW, Collins S. β-adrenergic activation of p38 MAP kinase in adipocytes cAMP induction of the uncoupling protein 1 (UCP1) gene requires p38 map kinase. *J Biol Chem.* (2001) 276:27077–82. doi: 10.1074/jbc.M101049200

41. Asano H, Kanamori Y, Higurashi S, Nara T, Kato K, Matsui T, et al. Induction of beige-like adipocytes in 3T3-L1 Cells. *J Vet Med Sci.* (2014) 76:57.

42. Parray HA, Yun JW. Cannabidiol promotes browning in 3T3-L1 adipocytes. *Mol Cell Biochem.* (2016) 416(1–2):131–9. doi: 10.1007/s11010-016-2702-5

43. Choi M, Mukherjee S, Kang NH, Barkat JL, Parray HA, Yun JW. L-rhamnose induces browning in 3T3-L1 white adipocytes and activates HIB1B brown adipocytes. *IUBMB Life.* (2018) 70:563–73. doi: 10.1002/iub.1750

44. Zu Y, Overby H, Ren G, Fan Z, Zhao L, Wang S. Resveratrol liposomes and lipid nanocarriers: comparison of characteristics and inducing browning of white adipocytes. *Colloids Surf B Bio.* (2018) 164:414–23. doi: 10.1016/j.colsurfb.2017.12.044

45. Fan L, Xu H, Yang R, Zang Y, Chen J, Qin H. Combination of capsaicin and capsiate induces browning in 3T3-L1 white adipocytes via activation of the peroxisome proliferator-activated receptor γ/β(3)-adrenergic receptor signaling pathways. *J Agric Food Chem.* (2019) 67:6232–40. doi: 10.1021/acs.jafc.9b02191

46. Kim K, Nam KH, Yi SA, Park JW, Han JW, Lee J. Ginsenoside Rg3 induces browning of 3T3-L1 adipocytes by activating AMPK signaling. *Nutrients.* (2020) 12:427. doi: 10.3390/nu12020427

47. Choi M, Mukherjee S, Yun JW. Trigonelline induces browning in 3T3-L1 white adipocytes. *Phytother Res.* (2021) 35:1113–24. doi: 10.1002/ptr.6892

48. Li Y, Fromme T, Schweizer S, Schottl T, Klingenspor M. Taking control over intracellular fatty acid levels is essential for the analysis of thermogenic function in cultured primary brown and brite/beige adipocytes. *EMBO Rep.* (2014) 15:1069–76. doi: 10.15252/embr.201438775

49. Collins S, Yehuda-Shnaidman E, Wang H. Positive and negative control of Ucp1 gene transcription and the role of beta-adrenergic signaling networks. *Int J Obes.* (2010) 34:S28–33. doi: 10.1038/ijo.2010.180

50. Collins S. β-Adrenoceptor signaling networks in adipocytes for recruiting stored fat and energy expenditure. *Front Endocrinol.* (2011) 2:102. doi: 10.3389/fendo.2011.00102

frontiers | Frontiers in Nutrition

TYPE Review
PUBLISHED 15 November 2022
DOI 10.3389/fnut.2022.1046726

OPEN ACCESS

EDITED BY
Zhiping Yu,
University of North Florida,
United States

REVIEWED BY
Gonzalo Emiliano Aranda-Abreu,
Universidad Veracruzana, Mexico
Min Chen,
Icahn School of Medicine at Mount Sinai, United States
Yuxia Ouyang,
Icahn School of Medicine at Mount Sinai, United States

*CORRESPONDENCE
Ling Wang
lingwang@must.edu.mo

SPECIALTY SECTION
This article was submitted to Nutritional Epidemiology, a section of the journal Frontiers in Nutrition

RECEIVED 17 September 2022
ACCEPTED 31 October 2022
PUBLISHED 15 November 2022

CITATION
Li Z, Li S, Xiao Y, Zhong T, Yu X and Wang L (2022) Nutritional intervention for diabetes mellitus with Alzheimer's disease. *Front. Nutr.* 9:1046726. doi: 10.3389/fnut.2022.1046726

Nutritional intervention for diabetes mellitus with Alzheimer's disease

Zhi Li, Simian Li, Ying Xiao, Tian Zhong, Xi Yu and Ling Wang*

Faculty of Medicine, Macau University of Science and Technology, Macau, China

The combined disease burden of diabetes mellitus (DM) and Alzheimer's disease (AD) is increasing, and the two diseases share some common pathological changes. However, the pharmacotherapeutic approach to this clinical complexity is limited to symptomatic rather than disease-arresting, with the possible exception of metformin. Whether nutritional intervention might extend or synergize with these effects of metformin is of interest. In particular, dietary patterns with an emphasis on dietary diversity shown to affect cognitive function are of growing interest in a range of food cultural settings. This paper presents the association between diabetes and AD. In addition, the cross-cultural nutritional intervention programs with the potential to mitigate both insulin resistance (IR) and hyperglycemia, together with cognitive impairment are also reviewed. Both dietary patterns and nutritional supplementation showed the effects of improving glycemic control and reducing cognitive decline in diabetes associated with AD, but the intervention specificity remained controversial. Multi-nutrient supplements combined with diverse diets may have preventive and therapeutic potential for DM combined with AD, at least as related to the B vitamin group and folate-dependent homocysteine (Hcy). The nutritional intervention has promise in the prevention and management of DM and AD comorbidities, and more clinical studies would be of nutritional scientific merit.

KEYWORDS

nutritional intervention, dietary patterns, diabetes mellitus, Alzheimer's disease, review

Introduction

Diabetes mellitus (DM) is a chronic disease with a metabolic disorder characterized by hyperglycemia, resulting from insufficient insulin secretion in the body or insulin resistance (IR) (1). According to published data, the global prevalence of diabetes was about 9.3% (463 million people) in 2019, and it is estimated that the prevalence will rise to 10.2% (578 million people) by 2030. More than 700 million individuals might be affected by diabetes worldwide by 2045 (2). At present, the treatment methods for DM mainly include five measures: dietary control, exercise, hypoglycemic medicine, health education, and self-monitoring.

Dementia is also a serious public health problem. Alzheimer's disease (AD), the most common type of dementia, is a chronic neurodegenerative disease characterized by impairment of memory and cognition, along with changes in behavior and

personality (3). Pathological features of AD include amyloid plaques composed of fibrillar Aβ and neurofibrillary tangles composed of hyper-phosphorylated tau proteins that could induce oxidative stress, inflammatory damage, cerebrovascular damage, blood-brain barrier dysfunction, and neuronal death (4). The mechanism of AD development is not yet fully discovered and both genetic and environmental factors are involved (5). According to the reports in 2021, AD affected approximately 34 million people worldwide and approximately 5.8 million Americans aged 65 years and older currently have AD. From 2000 to 2019, the number of reported deaths related to AD increased by more than 145% (5, 6). Epidemiological studies have shown that n-3 long-chain polyunsaturated fatty acids (FAs) and docosahexaenoic acid could inhibit Aβ and tau protein production and help the neurons maintain normal function (7). Low intakes of n-3 FAs, B vitamins, and antioxidants have been linked to an increased risk of AD (8, 9). Currently, there is no effective drug that could reverse the symptoms of AD or stop neuronal damage and destruction, and the disease tends to progress gradually.

A substantial body of research indicates that nutrients and phytochemicals including vitamins, folic acid, and polyphenols may have therapeutic effects on DM combined with AD because they could regulate blood glucose concentration, slow the progress of cognitive decline, improve IR, and protect the nervous system from inflammation and/or oxidative damage (10–12). This review discusses and summarizes the effects and potential mechanisms of nutritional intervention of DM and AD, and provides suggestions for nutritional therapy to lower the risk of developing AD in DM individuals.

Methods

CiteSpace visual analysis software and the bibliometric analysis platform were used to analyze the status of the nutritional intervention that improves DM accompanied with AD. PubMed, EMBASE, Cochrane Library, and China National Knowledge Infrastructure (CNKI) databases were searched to identify the relevant and reliable literature up to June 2022. The following search terms were used: Alzheimer's disease, diabetes, dementia, food ingredients, nutrition, and diet. After screening the abstracts and titles, the relevant literature was analyzed and organized, focusing on the last 5 years. In total, 161 potentially relevant articles were included in this review.

Correlation between diabetes and Alzheimer's disease

Type 1 diabetes mellitus (T1DM) is a subtype of diabetes (13). Some links have been found between type 1 diabetes and cognitive impairment (14). A study on cerebral compromise and its underlying mechanisms in type 1 diabetes found altered levels of cerebrospinal fluid (CSF), a biomarker of AD, compared to controls. However, the observed profile does not match the full risk profile seen in pre-AD patients (15). The findings of a large retrospective cohort study of 343,062 hospitalized patients with type 1 diabetes indicate that type 1 diabetes is associated with an elevated risk of any dementia, AD, and vascular dementia, and is particularly pronounced in younger patients with diabetes (16). The mechanisms underlying the association between type 1 diabetes and the development of cognitive impairment are not yet fully understood. Further research is needed in the future.

Numerous epidemiological studies have linked diabetes to dementia caused by AD, especially type 2 diabetes mellitus (T2DM), and it is even considered that AD is likely to represent a brain-specific form of diabetes, namely type 3 diabetes. Some studies indicated that T2DM is a risk factor for AD (17), but there is no validation as to whether AD is a risk factor for T2DM. Type 2 diabetes mellitus accounts for one-tenth of people with dementia worldwide, and T2DM patients have a higher chance (>50%) to develop AD than those non-T2DM individuals (18–20). Alzheimer's disease and T2DM share common risk factors, such as obesity, aging, and IR (21–23). In addition, there are many common pathological mechanisms associated with IR between AD and T2DM, such as oxidative stress, impaired insulin signaling, mitochondrial dysfunction, neuro-inflammation, advanced glycation end products (AGEs), and metabolic syndrome, etc. (3, 24, 25). The insulin signaling pathway is initiated when insulin recognizes and binds to the transmembrane tyrosine kinase receptor (TKR). Activated TKR causes insulin receptor substrates (IRS) to be tyrosine phosphorylated by insulin receptor tyrosine kinase, followed by blocking downstream signaling pathways and impairing insulin signaling pathways, then working together with Aβ deposition and mitochondrial dysfunction to form a vicious circle (26).

Abnormalities of glucose metabolism may contribute to AD development in diabetic patients and the disorder of energy metabolism is directly associated with the pathological development of AD (27). Abnormal metabolism and transportation of glucose in DM could impair the cognitive performance of the patients (28). Therefore, adequate blood glucose control should be the main goal of therapeutic approaches to lower the risk of AD in diabetic individuals. Additionally, oxidative stress and mitochondrial dysfunction are linked to the onset and progression of AD in diabetic patients. It is postulated that the normal function of mitochondria is crucial for delaying aging and avoiding neurodegenerative illnesses (29). Mitochondrial dysfunction is a key factor in the pathogenesis of various diseases, such as diabetes and neurodegenerative diseases (30). The brain is very susceptible to mitochondrial dysfunction due to its high energy requirements (31). Many studies have shown that mitochondrial oxidative stress and the production of reactive oxygen species (ROS) are increased under hyperglycemic conditions, and a

large amount of ROS could lead to a series of common AD pathological changes, such as the oxidative damage of proteins, carbohydrates, and lipids (32). A recent study found for the first time that adipose tissue-derived EVs from high-fat diet (HFD)-fed mice or patients with diabetes induce remarkable synaptic loss and cognitive impairment (33).

Anti-AD drugs, especially piracetam could significantly reduce some diabetic parameters, such as fasting plasma glucose (FPG), HbA1c, and serum insulin concentration in patients with diabetic AD (34). Similarly, epidemiological studies showed that some antidiabetic drugs such as metformin, applied in diabetic patients could reduce the risk of developing AD and all-cause dementia (4, 35). However, the protective effect of metformin on AD is controversial. One study found that metformin had a protective effect in diabetic patients accompanied by cognitive impairment or dementia, while the protective effect was not seen in non-diabetic individuals with cognitive impairment (36). The patients with mild cognitive impairment or mild AD showed little improvement after being treated with metformin in clinical trials (37, 38). In addition, the precise mechanism underlying the therapeutic activity of metformin in AD is unclear. Metformin may act through mechanisms involving glucose homeostasis, decreased amyloid plaque deposition, normalization of tau protein phosphorylation, and increased autophagy (39). More research is needed to confirm the potential role of metformin in DM accompanied by AD.

Nutritional intervention improves DM accompanied with AD

Due to the increasing prevalence, mortality, and complication rates, DM has a great impact on the quality of life in diabetic patients. The effect of pharmacology to cure AD is limited, as whether the nutritional intervention could reduce the risk and progression of AD in diabetic individuals is of significant interest. Changes in dietary intake and lifestyle are more important, and easier and safer to implement than medication. It is particularly important to explore scientific and effective nutritional interventions to improve the disease prognosis of DM patients with AD.

Management of dietary intake

For patients with diabetes and AD, it is common to have both declined cognition and unhealthy dietary intake, overconsumption of some foods makes it difficult to glucose control, while inappropriate strict limitation of food intake might induce hypoglycemia. Management of dietary intake is critical for blood glucose control in diabetic patients. Some studies found that improper dietary control, untimely drug adjustment, and the influence of exercise intensity contributed to poor glucose control in patients with AD accompanied by T2DM (40). Many studies also showed that a reasonable and healthy diet could provide appropriate nutrients and energy required by the patients without inducing significant fluctuation in blood glucose concentration (41–43). Well-planned dietary management could effectively control blood glucose and insulin concentrations and might help to delay further cognitive decline (44) in T2DM patients with AD.

Prevention of hypoglycemia

In cases of DM accompanied by dementia or AD, the patients might have a problem organizing their meals and even be insensitive to hungry, which could induce hypoglycemia (45). The caregiver should try his/her best to persuade him/her to eat, be patient with feeding, and if necessary, give a sugar-free liquid diet through tube feeding or provide intravenous nutrition as prescribed by the doctor to meet the needs of the body's energy (46). To prevent hypoglycemia, it is recommended that these patients should bring some candies and chocolates with them. For the in-patients who are not used to adapt the hospital diet, the dietitian should contact their family members to provide the patient's favorite, but low-sugar, low-fat, and fiber-rich foods (47). For those who have difficulty chewing or swallowing, the food with appropriate nutrients and energy should be ground into a paste and provided to the patients (48).

Reasonable control of the energy intake

According to the patient's physical activity level and eating habits, the dietitian could formulate a diet guide card, and calculate the daily intake of protein, fat, carbohydrate, vegetable, and fruit based on the total amount of food exchange portion. The dietitian could make an individual diet plan based on the daily calorie requirement of the patient. Coarse grains and pasta are the staple food with a low glycemic index (GI), certain types of dark green leafy vegetables are recommended for diabetic patients even at a relatively large amount, while foods rich in simple sugar, e.g., sucrose and honey should be limited. In general, three meals a day are allocated reasonably at the energy distribution of 2/5, 2/5, and 1/5 for breakfast, lunch, and dinner, respectively (49, 50).

Glycemic management

Good glycemic control is crucial for diabetic patients in suppressing disease progress, complications, and even the development of AD. Feeling hungry is a common symptom of DM patients. The quantity and quality of the food consumed should be cautious. Under the condition of enough energy and nutrients, the patients should choose foods that are low GI and rich in dietary fiber, such as coarse grains, potatoes, and miscellaneous beans. Dietary fiber could prevent postprandial

hyperglycemia and be fermented by intestinal flora to produce short-chain FAs in the large bowel. Daily dietary fiber intake could reach up to 40 g for diabetic patients. At the same time, the patient's physical activity level and tolerance capacity should be monitored at the time of exercise to avoid hypoglycemia (49).

Dietary pattern

Improving effects of dietary patterns in DM-only patients

Changes in lifestyle and self-management skills are critical in the treatment of diabetes. A change in eating habits is one of the most important lifestyle changes and challenges for people with diabetes (51). Studies have shown that a low-carbohydrate diet (LCD) can improve glycemic control in people with T2DM, and the effects are even more pronounced with a ketogenic diet (KD) (52). However, there is currently no evidence that LCD or KD can delay or prevent the onset of T1DM (53). In addition, a meta-analysis found that Medi (Mediterranean diet) appears to be the most effective and efficient diet for better glycemic control in patients with T2DM (54). There is also evidence that Medi has beneficial effects on cardiometabolic health and reduces mortality in patients with T2DM (55).

Improving effects of dietary patterns in AD-only patients

For AD patients, observational studies suggested that the MIND (Mediterranean-DASH Diet Intervention for Neurodegenerative Delay) may be more protective against cognitive decline and AD than the Mediterranean and DASH (Dietary Approaches to Stop Hypertension) diets, but more evidence on the MIND diet is required to make a firm judgment (56–58). Ketogenic diet has beneficial effects on enhancing mitochondrial function and cellular metabolism, which are associated with improved cognitive performance in older adults with AD. The level and duration of ketosis affect the improvement of cognitive outcomes (59).

Improving effects of dietary patterns in DM with AD patients

Medi, DASH, and MIND dietary patterns have been found to have a positive influence on DM with AD patients. Both the Medi and DASH dietary patterns emphasize the consumption of plant-based foods and low or limited consumption of red meat. Medi is a traditional diet originating from Mediterranean countries, that focuses on the consumption of abundant fruits, vegetables, legumes, unrefined grains, plenty of fish, and moderate dairy products (such as low-fat cheese and yogurt) and wine, taking olive oil as the cooking oil, while DASH emphasizes consumption of dairy products and low consumption of sodium, industrial sweets, and saturated fat (60). In middle-aged and older adults with T2DM, adherence to the Medi is related to better cognitive function and glycemic control (61, 62). The MIND diet is a combination of the Medi and DASH dietary patterns, emphasizing the consumption of natural plant foods, especially increasing the intake of berries and dark green leafy vegetables, which are rich in folic acid, lutein, lycopene, and alpha and beta carotene, which might play roles in anti-aging for the brain and help to maintain cognitive function (63–65). Adherence to any of the Medi, DASH, and MIND dietary patterns could improve insulin sensitivity, and reduce the likelihood of diabetes and inflammation, in turn reducing the risk of dementia and AD (66–69).

Ketogenic diet has also been found to have a positive influence on DM with AD patients. Ketogenic diets are low-carbohydrate, high-fat, moderate-protein diets that typically provide about 80% of calories from fat, 15% from protein, and 5% from carbohydrates (70). Medium-chain triglyceride (MCT) oil, a major lipid component in KD, may promote ketogenesis and maintain mitochondrial function, in conjunctive therapy for AD patients (71, 72). This dietary pattern could improve glycemic control in T2DM (73) and accompany cognitive impairment in AD (74). Long-term adherence to the KD is difficult with side effects attributable to the compromised dietary quality of micro-nutrient deficiency, along with poor appetite, nausea, constipation, fatigue, dyslipidemia, and unexpected weight loss (53, 75).

Supplements

Some studies have demonstrated that probiotic supplementation could improve T2DM and AD (76–79). For example, the probiotic *Lactobacillus acidophilus* attenuated the inflammatory response in T2DM by modulating hepatic gluconeogenesis, lipid metabolism, and gut microbiota in mice (80). Prebiotic inulin and dietary inulin may suppress inflammation and modulate gut macrobiotics during T2DM progression (81). In AD patients, cognitive function was improved after treatment with probiotics containing Lactobacillus and Bifidobacterium (82, 83).

It remains debatable whether patients with T2DM and AD could benefit from vitamin supplementation. Vitamin A may be involved in nerve regeneration, neurodevelopment, and neurodegeneration, including AD (84, 85). Vitamin C and E have been touted for potentially favorable anti-oxidative effects in T2DM and AD (86, 87). Vitamin D deficiency might increase neurodegenerative risk, in part through ted development of IR and diabetes by reducing insulin signaling (88, 89). Experimental studies indicated that vitamin D had the potential to prevent and treat cognitive decline in dementia (90), and cohort studies suggested that higher concentrations of circulating vitamin D may lower the risk of all-cause dementia and AD in T2DM.

TABLE 1 The effects of nutritional intervention for diabetes mellitus with Alzheimer's disease.

Nutritional intervention	Main findings	Intervention: features of dietary patterns and supplements	Author and Ref. No.
Dietary pattern			
Mediterranean diet (Medi)	Reduce the incidence of diabetes	Carbohydrates, % of energy: 39 ± 6 Protein, % of energy: 14 ± 3 Lipids, % of energy: 47 ± 7	Anastasiou et al. (68)
	Improve insulin sensitivity		
Dietary Approaches to Stop High Blood Pressure (DASH)	Reduce oxidative stress and inflammation	Carbohydrate, % of energy: 55 ± 2 Protein, % of energy: 16 ± 0.9 Total fat, % of energy: 29 ± 1.1 Sodium intake: 2,400 mg/d	Azadbakht et al. (67)
Mediterranean-DASH Delayed Intervention for Neurodegeneration (MIND)	Prevent dementia and reduce the risk of AD	Carbohydrates: 45–55% Protein: 15–20% Total fat: 25–30% Sodium intake: 2,400 mg/d	Asemi et al. (69)
Ketogenic diets (KD)	Control and improve blood glucose in patients with T2DM	14% Carbohydrates (<50 g) 28% Protein 58% Fat (35% MUFA, 13% PUFA, <10% SFA)	Brinkworth et al. (73)
	Improve cognition in AD patients	58% Fat (26% SFA, 32% non-saturated) 29% Protein 7% Fiber 6% Carbohydrates	Abboud et al. (74)
Supplements			
Probiotic *Lactobacillus acidophilus*	Improve the intestinal barrier function	Untreated diabetes mellitus group (DC), diabetic mice treated with *L. acidophilus* KLDS1.1003 (LA1, 1 × 109 CFU/d) and diabetic mice treated with *L. acidophilus* KLDS1.0901 group (LA2, 1 × 109 CFU/d).	Yan et al. (79)
	Suppress inflammatory responses in liver and colon		
	Regulate glucose and lipid metabolism in liver		
Dietary inulin	Reduce the plasma LPS concentration	Six groups (15 mice per group): pre-diabetic group (PDM group); inulin-treated pre-diabetic group (INU/PDM group); early diabetic group (EDM group); inulin-treated early diabetic group (INU/EDM group); diabetic group (DM group); inulin-treated diabetic group (INU/DM group).	Li et al. (81)
	Alter plasma pro-inflammatory and anti-inflammatory cytokines in diverse stages of T2DM		
	Modulate gut dysbiosis in diverse stages of T2DM		
Probiotics containing Lactobacillus and Bifido-bacterium	Decrease the plasma MDA and the serum hs-CRP concentrations	Control group: treat with milk. Probiotic group: take 200 ml/day probiotic milk containing *Lactobacillus acidophilus*, *Lactobacillus casei*, *Bifidobacterium bifidum*, and *Lactobacillus fermentum* (2 × 109 CFU/g for each) for 12 weeks.	Akbari et al. (82)

(Continued)

TABLE 1 (Continued)

Nutritional intervention	Main findings	Intervention: features of dietary patterns and supplements	Author and Ref. No.
	Reduce the HOMA-B index Decrease the serum triglyceride and VLDL concentrations		
Vitamin A	Adequate intake of vitamin A may help protecting against diabetes, especially for men	Vitamin A intakes were assessed by three consecutive 24-h dietary recalls combined with a household food inventory.	Su et al. (84)
	Modulate Aβ formation and aggregation, cholinergic transmission, and inflammatory responses	500 IU (control diet)/100 g of VitA or 2,000 IU (enriched diet)/100 g VitA.	Biyong et al. (85)
Vitamin B	Slow the acceleration of brain atrophy	All patients received treatment with an acetylcholinesterase inhibitor and were randomized to receive add-on mecobalamin (B12) 500 mg + multivitamin supplement, or placebos. (Multivitamin: pyridoxine (B6) 5 mg, folic acid 1 mg, and other vitamins and iron).	Sun et al. (101)
	Reduce plasma homocysteine concentrations in patients with Alzheimer's disease and diabetes Improve cognitive function in AD patients		
Vitamin C	Avoid the pro-oxidative effect Reduce the risk of diabetes mellitus type 2 complications	VC supplementation of 500–1,000 mg/day.	Sun et al. (86)
	A reduced risk of cognitive decline	Exposure to supplements of vitamin E or C was measured at baseline using data collected either from the structured interview at the clinical examination or the selfadministered risk factor questionnaire (RFQ).	Basambombo et al. (87)
Vitamin D	Improve adipocyte metabolic function and protect against obesity	Vitamin D 1,25-dihydroxyvitamin D[1,25(OH)2D] treatment (24 h, 100 nmol/L).	Chang et al. (88)
	Reduce low-grade chronic inflammation caused by IR	2,000 IU of Vitamin D/day.	Wenclewska et al. (89)
	Preserve brain health and lower risk of AD	Plasma 25(OH)D concentrations: ≥50 nmol/L.	Feart et al. (91)
	Slow cognitive decline	Serum 25(OH)D concentrations: ≥50 nmol/L.	Geng et al. (92)
	Delay or prevent the onset of dementia, especially AD		
Polyphenols	Insulin resistance ↓	Resveratrol dose: 500 mg twice a day 45 days.	Movahed et al. (112)
	Blood glucose levels ↓ HOMA-β ↓ Systolic blood pressure ↓		
	Neuroprotection	—	Ben Hmidene et al. (125)
Trace elements (magnesium and zinc)	Lower serum cholesterol and cholesterol/high-density lipoprotein ratio	$ZnSO_4$: 22 mg/day.	Gunasekara et al. (130)
	Maintain normal cell function and normal lipid metabolism Enhance tyrosine kinase activity	Mg supplementation: 4.5 g/day of Mg pidolate (368 mg/day of Mg ion).	Barbagallo et al. (131)

(Continued)

TABLE 1 (Continued)

Nutritional intervention	Main findings	Intervention: features of dietary patterns and supplements	Author and Ref. No.
n-3 Fatty acids (FAs)	Mediate inflammatory and immune responses	Omega-3 fatty acid diet (n-3 diet): add 0.5% of flaxseed oil and 1.2% of docosahexaenoic acid capsule oil.	Agrawal et al. (132)
	Reduce the risk of IR and neurocognitive impairment		
Pentacyclic triterpenoids	Inhibit TNF-α and TGF-β production	0.1% FCS and different concentrations of betulin (1 or 10 μM) or betulinic acid (1 or 5 μM) (Sigma–Aldrich).	Szuster-Ciesielska et al. (133)
	Exert an antifibrotic activity by silencing ethanol-activated HSCs		
Hedera nepalensis crude extract (HNC) and lupin alcohol	HNC and lupeol ameliorate the increase in plasma glucose level and enhance the antioxidant enzymes profile	NC (normal control) group (non-diabetic, non-Alzheimer): given 10% DMSO (10 ml/kg BW/day). STZ + $AlCl_3$ co-treated group: received Rivastigmine (EXCELON®) at 0.8 mg/kg BW/day as positive control (PC). AC group (Alzheimer control): received 10% DMSO (10 ml/kg BW/day) after STZ + $AlCl_3$ co-treatment. HNC group (AC + HNC): received crude extract 400 mg/kg (BW) after STZ + $AlCl_3$ co-treatment. AC + Lupeol group: received lupeol orally at 10 mg/kg (BW) after STZ + AlCl3 co-treatment.	Hashmi et al. (134)
	Decrease DM related complications of AD such as cognitive impairment and anxiety/fear related behavioral indices		
Marine phenolics	Decrease postprandial glucose, insulin, and C-peptide levels	Dieckol-rich extract: 1,500 mg/day.	Lee et al. (135)
Fig leaf extract	The methanol and water extracts of *Ficus carica* leaf extracts have strong antioxidant activity	First 150 μl of the extract was mixed with 50 μl of 1.0×10^{-3} M freshly prepared DPPH• methanol solution in 96-well plates.	Ergül et al. (136)
	Show strong α-glucosidase and α-amylase inhibition activity		
α-lipoic acid (ALA)	Show the improvement in insulin sensitivity and lipid metabolism	ALA: 300 mg/daily for 3 months.	Udupa et al. (137)

Vitamin D supplementation in the elderly might slow cognitive decline and delay the onset of dementia, especially AD (91, 92).

Hyperhomocysteinemia (HHcy) is a risk factor for AD development, and once HHcy is corrected, the development of AD might be postponed (93–95). Homocysteine (Hcy) is a sulfur-containing non-proteinogenic amino acid that enhances excitotoxicity and causes DNA damage and death in neurons, impairing short-term memory and learning (96). Hyperhomocysteinemia is a state in which the body has an excess of Hcy (97). Vitamins B-6, B-12, and folic acid are essential dietary nutrients for maintaining normal physiological concentrations of Hcy (98). Folic acid (also known as the oxidized form of vitamin B-9) supplementation has positive effects on diabetes-related oxidative stress (99) and could improve cognitive function in AD patients (100). Folic acid supplementation alone or the use of multivitamin supplements containing vitamins B-6, and B-12 have been shown to be effective in reducing plasma Hcy concentrations in patients with AD and DM (101–103). Brain atrophy is accelerated in the elderly with cognitive impairment, particularly those who have AD (104). It has been demonstrated that HHcy is linked to brain atrophy. Supplementation with B vitamins to elderly with mild

cognitive impairment may slow the acceleration of brain atrophy by lowering blood Hcy concentrations (105). Additionally, a high baseline of plasma n-3 FA was observed to improve the positive effects of high-dose B vitamin supplementation, which decreased the mean rate of brain shrinkage by 40% in participants with high plasma n-3 FA concentrations compared to those in the placebo group. In contrast, B vitamins had no effect on brain shrinkage in patients with low concentrations of plasma n-3 FA (106). Even though numerous studies explored the association between plasma Hcy and AD, it is not easy to tell the exact effects of Hcy, folate, or vitamin B-12 on cognition and/or AD pathogenesis (107). Understanding the underlying mechanisms of HHcy in AD may help to improve the treatment and bring immediate clinical advantages for the patients.

The antioxidant and anti-inflammatory effects of bioactive compounds, such as polyphenols and carotenoids in vegetables and fruits make them candidates for the prevention and control of DM and AD. Polyphenols such as resveratrol (108–112), gallic acid (11, 113, 114), curcumin (115–118), anthocyanins (119), luteolin (120), hesperetin (121), genistein (122), *Boswellia serrata* gum extract (123), mango leaf extract (124), and flavonoids (125), exist in a variety of plants. They have various functions, such as preventing oxidative stress damage, regulating blood glucose concentration, inhibiting inflammation, improving IR, and neuroprotection, which are all beneficial to DM and AD. A great body of research have confirmed that having foods rich in polyphenols could reduce the risk of DM and AD (12), improve insulin sensitivity in DM patients to inhibit the formation of AGEs, and promote cellular uptake of glucose (126). Polyphenols could also prevent the subsequent development of DM-related complications such as cardiovascular disease, neuropathy, etc., and improve neuronal metabolism and cognitive performance (127), Carotenoids, such as lycopene have been shown having beneficial effects on diabetes and its associated complications in many animal studies, and are potentially effective drug components for the treatment of AD (128, 129).

Supplementation of trace elements, such as magnesium and zinc in diabetic patients could promote glucose transport, maintain normal cell function and lipid metabolism, and enhance tyrosine kinase activity. There was a significant negative association between magnesium intake and all-cause dementia, but the same association was not observed in AD, whereas cognitive improvement was found after zinc therapy in a mouse model of AD, indicating that zinc may play an important role in the pathogenesis of AD (130, 131).

Intake of n-3 FAs (132), pentacyclic triterpenoids (133), Hedera nepalensis crude extract and lupin alcohol (134), marine phenolics (135), fig leaf extract (136), α-lipoic acid (137) has been shown to positively mediate inflammatory and immune responses, reduce the risk of IR and neurocognitive impairment, and ultimately decrease the risk of AD.

The effects of nutritional intervention for DM with AD mentioned above are summarized in Table 1.

Conclusion

The prevalence of DM and AD increases year by year. These two diseases share a common underlying pathological mechanism, and DM patients have a higher risk of developing AD. Therefore, a focus on how to prevent and treat DM accompanied by AD should underscore the potential relevance of nutritional intervention strategies in three respects: food intake management, dietary pattern, and nutrient supplementation. To date, various food factors and dietary components including probiotics, polyphenols, trace elements, and n-3 FAs, have been countenanced as candidates for cognitive maintenance or improvement in diabetic patients who are prone to brain dysfunction. Two dietary patterns, the KD, and the Mediterranean diet have been found to be therapeutically effective in DM and AD. Multi-nutrient supplements together with a healthy dietary pattern may enhance the therapeutic effectiveness. The key to the prevention of DM accompanied by AD is to identify the risk factors such as obesity, lack of exercise, and unhealthy eating habits before the disease is apparent, and to establish effective intervention strategies, especially nutritional measures.

Author contributions

ZL: conducted literature search in different search engines, contributed in preparation of first draft, and final version of the manuscript. SL: conducted literature search in different search engines and contributed in preparation of first draft of the manuscript. YX, TZ, and XY: provided guidance of the manuscript. LW: critically reviewed the manuscript, provided guidance, and approved the final version of the manuscript. All authors contributed to the article and approved the submitted version.

Funding

The work is supported by Macau University of Science and Technology, Faculty Research Grant, FRG-21-036-FMD.

Conflict of interest

The authors declare that the research was conducted in the absence of any commercial or financial relationships that could be construed as a potential conflict of interest.

Publisher's note

References

1. Athanasaki A, Melanis K, Tsantzali I, Stefanou MI, Ntymenou S, Paraskevas SG, et al. Type 2 diabetes mellitus as a risk factor for Alzheimer's disease: review and meta-analysis. *Biomedicines*. (2022) 10:778. doi: 10.3390/biomedicines10040778

2. Saeedi P, Petersohn I, Salpea P, Malanda B, Karuranga S, Unwin N, et al. Global and regional diabetes prevalence estimates for 2019 and projections for 2030 and 2045: results from the international diabetes federation diabetes atlas, 9th edition. *Diabetes Res Clin Pract.* (2019) 157:107843. doi: 10.1016/j.diabres.2019.107843

3. Michailidis M, Moraitou D, Tata DA, Kalinderi K, Papamitsou T, Papaliagkas V. Alzheimer's disease as type 3 diabetes: common pathophysiological mechanisms between Alzheimer's disease and type 2 diabetes. *Int J Mol Sci.* (2022) 23:2687. doi: 10.3390/ijms23052687

4. Cummings J, Ortiz A, Castellino J, Kinney J. Diabetes: risk factor and translational therapeutic implications for Alzheimer's disease. *Eur J Neurosci.* (2022) 2022:10.1111/ejn.1561. doi: 10.1111/ejn.15619

5. Barnes DE, Yaffe K. The projected effect of risk factor reduction on Alzheimer's disease prevalence. *Lancet Neurol.* (2011) 10:819–28. doi: 10.1016/S1474-4422(11)70072-2

6. Alzheimer's disease facts and figures. *Alzheimers Dement.* (2021) 17:327–406. doi: 10.1002/alz.12328

7. Kamphuis PJ, Scheltens P. Can nutrients prevent or delay onset of Alzheimer's disease? *J Alzheimers Dis.* (2010) 20:765–75. doi: 10.3233/jad-2010-091558

8. Farkas M, Keskitalo S, Smith DE, Bain N, Semmler A, Ineichen B, et al. Hyperhomocysteinemia in Alzheimer's disease: the hen and the egg? *J Alzheimers Dis.* (2013) 33:1097–104. doi: 10.3233/jad-2012-121378

9. Faxén-Irving G, Freund-Levi Y, Eriksdotter-Jönhagen M, Basun H, Hjorth E, Palmblad J, et al. Effects on transthyretin in plasma and cerebrospinal fluid by DHA-rich n-3 fatty acid supplemen-tation in patients with Alzheimer's disease: the omegAD study. *J Alzheimers Dis.* (2013) 36:1–6. doi: 10.3233/jad-121828

10. Kaliś K. [Dual action of vitamin C versus degradation and supplementation]. *Postepy Hig Med Dosw (Online).* (2015) 69:1239–44. doi: 10.5604/17322693.1180642

11. Lupaescu AV, Iavorschi M, Covasa M. The use of bioactive compounds in hyperglycemia- and amyloid fibrils-induced toxicity in type 2 diabetes and Alzheimer's disease. *Pharmaceutics.* (2022) 14:235. doi: 10.3390/pharmaceutics14020235

12. Letenneur L, Proust-Lima C, Le Gouge A, Dartigues JF, Barberger-Gateau P. Flavonoid intake and cognitive decline over a 10-year period. *Am J Epidemiol.* (2007) 165:1364–71. doi: 10.1093/aje/kwm036

13. Li W, Huang E, Gao S. Type 1 diabetes mellitus and cognitive impairments: a systematic review. *J Alzheimers Dis.* (2017) 57:29–36. doi: 10.3233/jad-161250

14. Shalimova A, Graff B, Gasecki D, Wolf J, Sabisz A, Szurowska E, et al. Cognitive dysfunction in type 1 diabetes mellitus. *J Clin Endocrinol Metab.* (2019) 104:2239–49. doi: 10.1210/jc.2018-01315

15. Ouwens DM, van Duinkerken E, Schoonenboom SN, Herzfeld de Wiza D, Klein M, van Golen L, et al. Cerebrospinal fluid levels of Alzheimer's disease biomarkers in middle-aged patients with type 1 diabetes. *Diabetologia.* (2014) 57:2208–14. doi: 10.1007/s00125-014-3333-6

16. Smolina K, Wotton CJ, Goldacre MJ. Risk of dementia in patients hospitalised with type 1 and type 2 diabetes in England, 1998–2011: a retrospective national record linkage cohort study. *Diabetologia.* (2015) 58:942–50. doi: 10.1007/s00125-015-3515-x

17. Klimova B, Kuca K, Maresova P. Global view on Alzheimer's disease and diabetes mellitus: threats, risks and treatment Alzheimer's disease and diabetes mellitus. *Curr Alzheimer Res.* (2018) 15:1277–82. doi: 10.2174/1567205015666180925110222

18. Nam GE, Park YG, Han K, Kim MK, Koh ES, Kim ES, et al. BMI, weight change, and dementia risk in patients with new-onset type 2 diabetes: a nationwide cohort study. *Diabetes Care.* (2019) 42:1217–24. doi: 10.2337/dc18-1667

19. Leibson CL, Rocca WA, Hanson VA, Cha R, Kokmen E, O'Brien PC, et al. Risk of dementia among persons with diabetes mellitus: a population-based cohort study. *Am J Epidemiol.* (1997) 145:301–8. doi: 10.1093/oxfordjournals.aje.a009106

20. Li T, Cao HX, Ke D. Type 2 diabetes mellitus easily develops into alzheimer's disease via hyperglycemia and insulin resistance. *Curr Med Sci.* (2021) 41:1165–71. doi: 10.1007/s11596-021-2467-2

21. de la Monte SM. Contributions of brain insulin resistance and deficiency in amyloid-related neurodegeneration in Alzheimer's disease. *Drugs.* (2012) 72:49–66. doi: 10.2165/11597760-000000000-00000

22. Hu Z, Jiao R, Wang P, Zhu Y, Zhao J, De Jager P, et al. Shared causal paths underlying Alzheimer's dementia and type 2 diabetes. *Sci Rep.* (2020) 10:4107. doi: 10.1038/s41598-020-60682-3

23. Nisar O, Pervez H, Mandalia B, Waqas M, Sra HK. Type 3 diabetes mellitus: a link between Alzheimer's disease and type 2 diabetes mellitus. *Cureus.* (2020) 12:e11703. doi: 10.7759/cureus.11703

24. de la Monte SM, Wands JR. Alzheimer's disease is type 3 diabetes-evidence reviewed. *J Diabetes Sci Technol.* (2008) 2:1101–13. doi: 10.1177/193229680800200619

25. Kandimalla R, Thirumala V, Reddy PH. Is Alzheimer's disease a type 3 diabetes? A critical appraisal. *Biochim Biophys Acta Mol Basis Dis.* (2017) 1863:1078–89. doi: 10.1016/j.bbadis.2016.08.018

26. Sun Y, Ma C, Sun H, Wang H, Peng W, Zhou Z, et al. Metabolism: a novel shared link between diabetes mellitus and Alzheimer's disease. *J Diabetes Res.* (2020) 2020:4981814. doi: 10.1155/2020/4981814

27. Banerjee K, Munshi S, Frank DE, Gibson GE. Abnormal glucose metabolism in Alzheimer's disease: relation to autophagy/mitophagy and therapeutic approaches. *Neurochem Res.* (2015) 40:2557–69. doi: 10.1007/s11064-015-1631-0

28. Butterfield DA, Halliwell B. Oxidative stress, dysfunctional glucose metabolism and Alzheimer disease. *Nat Rev Neurosci.* (2019) 20:148–60. doi: 10.1038/s41583-019-0132-6

29. Beal MF. Mitochondria take center stage in aging and neurodegeneration. *Ann Neurol.* (2005) 58:495–505. doi: 10.1002/ana.20624

30. Wijesekara N, Ahrens R, Sabale M, Wu L, Ha K, Verdile G, et al. Amyloid-β and islet amyloid pathologies link Alzheimer's disease and type 2 diabetes in a transgenic model. *FASEB J.* (2017) 31:5409–18. doi: 10.1096/fj.201700431R

31. Islam MT. Oxidative stress and mitochondrial dysfunction-linked neurodegenerative disorders. *Neurol Res.* (2017) 39:73–82. doi: 10.1080/01616412.2016.1251711

32. Kiritoshi S, Nishikawa T, Sonoda K, Kukidome D, Senokuchi T, Matsuo T, et al. Reactive oxygen species from mitochondria induce cyclooxygenase-2 gene expression in human mesangial cells: potential role in diabetic nephropathy. *Diabetes.* (2003) 52:2570–7. doi: 10.2337/diabetes.52.10.2570

33. Wang J, Li L, Zhang Z, Zhang X, Zhu Y, Zhang C, et al. Extracellular vesicles mediate the communication of adipose tissue with brain and promote cognitive impairment associated with insulin resistance. *Cell Metab.* (2022) 34:1264.e8–79.e8. doi: 10.1016/j.cmet.2022.08.004

34. Ahmed AS, Elgharabawy RM, Al-Najjar AH. Ameliorating effect of anti-Alzheimer's drugs on the bidirectional association between type 2 diabetes mellitus and Alzheimer's disease. *Exp Biol Med (Maywood).* (2017) 242:1335–44. doi: 10.1177/1535370217711440

35. Ahn KC, Learman CR, Baker GB, Weaver CL, Chung PS, Kim HG, et al. Regulation of diabetes: a therapeutic strategy for Alzheimer's disease? *J Korean Med Sci.* (2019) 34:e297. doi: 10.3346/jkms.2019.34.e297

36. Campbell JM, Stephenson MD, de Courten B, Chapman I, Bellman SM, Aromataris E. Metformin use associated with reduced risk of dementia in patients with diabetes: a systematic review and meta-analysis. *J Alzheimers Dis.* (2018) 65:1225–36. doi: 10.3233/jad-180263

37. Koenig AM, Mechanic-Hamilton D, Xie SX, Combs MF, Cappola AR, Xie L, et al. Effects of the insulin sensitizer metformin in Alzheimer disease: pilot data from a randomized placebo-controlled crossover study. *Alzheimer Dis Assoc Disord.* (2017) 31:107–13. doi: 10.1097/wad.0000000000000202

38. Luchsinger JA, Perez T, Chang H, Mehta P, Steffener J, Pradabhan G, et al. Metformin in amnestic mild cognitive impairment: results of a pilot randomized placebo controlled clinical trial. *J Alzheimers Dis.* (2016) 51:501–14. doi: 10.3233/jad-150493

39. Ning P, Luo A, Mu X, Xu Y, Li T. Exploring the dual character of metformin in Alzheimer's disease. *Neuropharmacology.* (2022) 207:108966. doi: 10.1016/j.neuropharm.2022.108966

40. Li YW. Analysis and nursing experience of poor blood sugar control in patients with senile dementia complicated by type 2 diabetes mellitus. *Diabetes New World.* (2019) 22:136–8. doi: 10.16658/j.cnki.1672-4062.2019.15.136

41. Wu XY, Lin XR, Zhang SX, Tu WZ. Effects of energy intake management on cognitive function in patients with Alzheimer's disease and diabetes mellitus. *Gen Pract Clin Educ.* (2019) 17:734–6. doi: 10.13558/j.cnki.issn1672-3686.2019.08.020

42. Tang X, Cardoso MA, Yang J, Zhou JB, Simó R. Impact of intensive glucose control on brain health: meta-analysis of cumulative data from 16,584 patients with type 2 diabetes mellitus. *Diabetes Ther.* (2021) 12:765–79. doi: 10.1007/s13300-021-01009-x

43. Xie L, Pu M, Liu Y. The effect of individual nursing on improving the living ability and blood sugar control of alzheimer disease patients with diabetes mellitus. *Am J Translat Res.* (2021) 13:9324–31.

44. Chen Y, Wang J, Wang LJ, Lin H, Huang PJ. Effect of different blood glucose intervention plans on elderly people with type 2 diabetes mellitus combined with dementia. *Eur Rev Med Pharmacol Sci.* (2017) 21:2702–7.

45. Silbert R, Salcido-Montenegro A, Rodriguez-Gutierrez R, Katabi A, McCoy RG. Hypo-glycemia among patients with type 2 diabetes: epidemiology, risk factors, and prevention strategies. *Curr Diab Rep.* (2018) 18:53. doi: 10.1007/s11892-018-1018-0

46. Cruz P. Inpatient hypoglycemia: the challenge remains. *J Diabetes Sci Technol.* (2020) 14:560–6. doi: 10.1177/1932296820918540

47. Bastos M. [Hypoglycemia: prevention and treatment]. *Acta Med Port Suppl.* (1989) 1:27s—8s.

48. Cruz P, Blackburn MC, Tobin GS. A systematic approach for the prevention and reduction of hypoglycemia in hospitalized patients. *Curr Diab Rep.* (2017) 17:117. doi: 10.1007/s11892-017-0934-8

49. Zhong AH. Influence of comprehensive nursing on diabetic patients with Alzheimer's disease. *Chin Health Std Manag.* (2015) 6:256–8. doi: 10.3969/j.issn.1674-9316.2015.28.193

50. Jin JJ, Cui YJ. Observation on dietary care of type 2 diabetes mellitus by dietary guidance card. *Mod Prevent Med.* (2007) 45:94–6. doi: 10.3969/j.issn.1003-8507.2007.23.096

51. Powers MA, Bardsley J, Cypress M, Duker P, Funnell MM, Fischl AH, et al. Diabetes self-management education and support in type 2 diabetes: a joint position statement of the American Diabetes Association, the American Association of Diabetes Educators, and the academy of nutrition and dietetics. *Clin Diabetes.* (2016) 34:70–80. doi: 10.2337/diaclin.34.2.70

52. Chester B, Babu JR, Greene MW, Geetha T. The effects of popular diets on type 2 diabetes management. *Diabetes Metab Res Rev.* (2019) 35:e3188. doi: 10.1002/dmrr.3188

53. Bolla AM, Caretto A, Laurenzi A, Scavini M, Piemonti L. Low-carb and ketogenic diets in type 1 and type 2 diabetes. *Nutrients.* (2019) 11:962. doi: 10.3390/nu11050962

54. Schwingshackl L, Chaimani A, Hoffmann G, Schwedhelm C, Boeing H. A network meta-analysis on the comparative efficacy of different dietary approaches on glycaemic control in patients with type 2 diabetes mellitus. *Eur J Epidemiol.* (2018) 33:157–70. doi: 10.1007/s10654-017-0352-x

55. Becerra-Tomás N, Blanco Mejía S, Viguiliouk E, Khan T, Kendall CWC, Kahleova H, et al. Mediterranean diet, cardiovascular disease and mortality in diabetes: a systematic review and meta-analysis of prospective cohort studies and randomized clinical trials. *Crit Rev Food Sci Nutr.* (2020) 60:1207–27. doi: 10.1080/10408398.2019.1565281

56. Morris MC, Tangney CC, Wang Y, Sacks FM, Bennett DA, Aggarwal NT. MIND diet associated with reduced incidence of Alzheimer's disease. *Alzheimers Dement.* (2015) 11:1007–14. doi: 10.1016/j.jalz.2014.11.009

57. van den Brink AC, Brouwer-Brolsma EM, Berendsen AAM, van de Rest O. The mediterranean, dietary approaches to stop hypertension (DASH), and mediterranean-dash intervention for neurodegenerative delay (MIND) diets are associated with less cognitive decline and a lower risk of Alzheimer's disease-a review. *Adv Nutr.* (2019) 10:1040–65. doi: 10.1093/advances/nmz054

58. Scarmeas N, Anastasiou CA, Yannakoulia M. Nutrition and prevention of cognitive impairment. *Lancet Neurol.* (2018) 17:1006–15. doi: 10.1016/s1474-4422(18)30338-7

59. Rusek M, Pluta R, Ułamek-Kozioł M, Czuczwar SJ. Ketogenic diet in Alzheimer's disease. *Int J Mol Sci.* (2019) 20:3892. doi: 10.3390/ijms20163892

60. Morris MC. Nutrition and risk of dementia: overview and methodological issues. *Ann N Y Acad Sci.* (2016) 1367:31–7. doi: 10.1111/nyas.13047

61. Lotan R, Ravona-Springer R, Shakked J, Lin HM, Ouyang Y, Shahar DR, et al. Greater intake of the medi diet is associated with better cognitive trajectory in older adults with type 2 diabetes. *Diabetes Res Clin Pract.* (2022) 190:109989. doi: 10.1016/j.diabres.2022.109989

62. Mattei J, Bigornia SJ, Sotos-Prieto M, Scott T, Gao X, Tucker KL. The mediterranean diet and 2-year change in cognitive function by status of type 2 diabetes and glycemic control. *Diabetes Care.* (2019) 42:1372–9. doi: 10.2337/dc19-0130

63. Martinis I, Vrca A, Bevanda M, Botić-Štefanec S, Badak J, Kušter D, et al. Nutritional assessment of patients with primary progressive dementia at the time of diagnosis. *Psychiatr Danub.* (2021) 33:226–35.

64. Pistollato F, Iglesias RC, Ruiz R, Aparicio S, Crespo J, Lopez LD, et al. Nutritional patterns associated with the maintenance of neurocognitive functions and the risk of dementia and Alzheimer's disease: a focus on human studies. *Pharmacol Res.* (2018) 131:32–43. doi: 10.1016/j.phrs.2018.03.012

65. Marcason W. What are the components to the MIND diet? *J Acad Nutr Diet.* (2015) 115:1744. doi: 10.1016/j.jand.2015.08.002

66. Jannasch F, Kröger J, Schulze MB. Dietary patterns and type 2 diabetes: a systematic literature review and meta-analysis of prospective studies. *J Nutr.* (2017) 147:1174–82. doi: 10.3945/jn.116.242552

67. Azadbakht L, Surkan PJ, Esmaillzadeh A, Willett WC. The dietary approaches to stop hypertension eating plan affects c-reactive protein, coagulation abnormalities, and hepatic function tests among type 2 diabetic patients. *J Nutr.* (2011) 141:1083–8. doi: 10.3945/jn.110.136739

68. Anastasiou CA, Yannakoulia M, Kosmidis MH, Dardiotis E, Hadjigeorgiou GM, Sakka P, et al. Mediterranean diet and cognitive health: initial results from the hellenic longitudinal investigation of ageing and diet. *PLoS ONE.* (2017) 12:e0182048. doi: 10.1371/journal.pone.0182048

69. Asemi Z, Tabassi Z, Samimi M, Fahiminejad T, Esmaillzadeh A. Favourable effects of the dietary approaches to stop hypertension diet on glucose tolerance and lipid profiles in gestational diabetes: a randomised clinical trial. *Br J Nutr.* (2013) 109:2024–30. doi: 10.1017/s0007114512004242

70. Veech RL. The therapeutic implications of ketone bodies: the effects of ketone bodies in pathological conditions: ketosis, ketogenic diet, redox states, insulin resistance, and mitochondrial metabolism. *Prostaglandins Leukot Essent Fatty Acids.* (2004) 70:309–19. doi: 10.1016/j.plefa.2003.09.007

71. Takeishi J, Tatewaki Y, Nakase T, Takano Y, Tomita N, Yamamoto S, et al. Alzheimer's disease and type 2 diabetes mellitus: the use of mct oil and a ketogenic diet. *Int J Mol Sci.* (2021) 22:12310. doi: 10.3390/ijms222212310

72. Hu Yang I, De la Rubia Ortí JE, Selvi Sabater P, Sancho Castillo S, Rochina MJ, Manresa Ramón N, et al. [Coconut oil: non-alternative drug treatment against Alzheimer's disease]. *Nutr Hosp.* (2015) 32:2822–7. doi: 10.3305/nh.2015.32.6.9707

73. Brinkworth GD, Luscombe-Marsh ND, Thompson CH, Noakes M, Buckley JD, Wittert G, et al. Long-term effects of very low-carbohydrate and high-carbohydrate weight-loss diets on psychological health in obese adults with type 2 diabetes: randomized controlled trial. *J Intern Med.* (2016) 280:388–97. doi: 10.1111/joim.12501

74. Abboud M, AlAnouti F, Georgaki E, Papandreou D. Effect of ketogenic diet on quality of life in adults with chronic disease: a systematic review of randomized controlled trials. *Nutrients.* (2021) 13:4463. doi: 10.3390/nu13124463

75. Lilamand M, Porte B, Cognat E, Hugon J, Mouton-Liger F, Paquet C. Are ketogenic diets promising for Alzheimer's disease? A translational review. *Alzheimers Res Ther.* (2020) 12:42. doi: 10.1186/s13195-020-00615-4

76. Carranza-Naval MJ, Vargas-Soria M, Hierro-Bujalance C, Baena-Nieto G, Garcia-Alloza M, Infante-Garcia C, et al. Alzheimer's disease and diabetes: role of diet, microbiota and inflammation in preclinical models. *Biomolecules.* (2021) 11:262. doi: 10.3390/biom11020262

77. Zhong SR, Kuang Q, Zhang F, Chen B, Zhong ZG. Functional roles of the microbiota-gut-brain axis in Alzheimer's disease: implications of gut microbiota-targeted therapy. *Transl Neurosci.* (2021) 12:581–600. doi: 10.1515/tnsci-2020-0206

78. Sánchez B, Delgado S, Blanco-Míguez A, Lourenço A, Gueimonde M, Margolles A. Probiotics, gut microbiota, and their influence on host health and disease. *Mol Nutr Food Res.* (2017) 61:201600240. doi: 10.1002/mnfr.201600240

79. Luca M, Di Mauro M, Di Mauro M, Luca A. Gut microbiota in Alzheimer's disease, depression, and type 2 diabetes mellitus: the role of oxidative stress. *Oxid Med Cell Longev*. (2019) 2019:4730539. doi: 10.1155/2019/4730539

80. Yan F, Li N, Shi J, Li H, Yue Y, Jiao W, et al. *Lactobacillus acidophilus* alleviates type 2 diabetes by regulating hepatic glucose, lipid metabolism and gut microbiota in mice. *Food Funct*. (2019) 10:5804–15. doi: 10.1039/c9fo01062a

81. Li K, Zhang L, Xue J, Yang X, Dong X, Sha L, et al. Dietary inulin alleviates diverse stages of type 2 diabetes mellitus via anti-inflammation and modulating gut microbiota in db/db mice. *Food Funct*. (2019) 10:1915–27. doi: 10.1039/c8fo02265h

82. Akbari E, Asemi Z, Daneshvar Kakhaki R, Bahmani F, Kouchaki E, Tamtaji OR, et al. Effect of probiotic supplementation on cognitive function and metabolic status in Alzheimer's disease: a randomized, double-blind and controlled trial. *Front Aging Neurosci*. (2016) 8:256. doi: 10.3389/fnagi.2016.00256

83. Téglás T, Ábrahám D, Jókai M, Kondo S, Mohammadi R, Fehér J, et al. Exercise combined with a probiotics treatment alters the microbiome, but moderately affects signalling pathways in the liver of male APP/PS1 transgenic mice. *Biogerontology*. (2020) 21:807–15. doi: 10.1007/s10522-020-09895-7

84. Biyong EF, Tremblay C, Leclerc M, Caron V, Alfos S, Helbling JC, et al. Role of retinoid x receptors (RXRS) and dietary vitamin A in Alzheimer's disease: evidence from clinicopathological and preclinical studies. *Neurobiol Dis*. (2021) 161:105542. doi: 10.1016/j.nbd.2021.105542

85. Su L, He J, Liu Z, Wu S, Chen P, Li K, et al. Dietary total vitamin A, β-carotene, and retinol intake and the risk of diabetes in chinese adults with plant-based diets. *J Clin Endocrinol Metab*. (2022) 107:e4106–14. doi: 10.1210/clinem/dgac439

86. Sun H, Karp J, Sun KM, Weaver CM. Decreasing vitamin C intake, low serum vitamin C level and risk for us adults with diabetes. *Nutrients*. (2022) 14:3902. doi: 10.3390/nu14193902

87. Basambombo LL, Carmichael PH, Côté S, Laurin D. Use of vitamin E and C supplements for the prevention of cognitive decline. *Ann Pharmacother*. (2017) 51:118–24. doi: 10.1177/1060028016673072

88. Chang E, Kim Y. Vitamin D decreases adipocyte lipid storage and increases nad-SIRT1 pathway in 3T3-L1 adipocytes. *Nutrition*. (2016) 32:702–8. doi: 10.1016/j.nut.2015.12.032

89. Wenclewska S, Szymczak-Pajor I, Drzewoski J, Bunk M, Sliwińska A. Vitamin D supplementation reduces both oxidative DNA damage and insulin resistance in the elderly with metabolic disorders. *Int J Mol Sci*. (2019) 20:2891. doi: 10.3390/ijms20122891

90. Dickens AP, Lang IA, Langa KM, Kos K, Llewellyn DJ. Vitamin D, cognitive dysfunction and dementia in older adults. *CNS Drugs*. (2011) 25:629–39. doi: 10.2165/11593080-000000000-00000

91. Feart C, Helmer C, Merle B, Herrmann FR, Annweiler C, Dartigues JF, et al. Associations of lower vitamin d concentrations with cognitive decline and long-term risk of dementia and Alzheimer's disease in older adults. *Alzheimers Dement*. (2017) 13:1207–16. doi: 10.1016/j.jalz.2017.03.003

92. Geng T, Lu Q, Wan Z, Guo J, Liu L, Pan A, et al. Association of serum 25-hydroxyvitamin D concentrations with risk of dementia among individuals with type 2 diabetes: a cohort study in the UK BioBank. *PLoS Med*. (2022) 19:e1003906. doi: 10.1371/journal.pmed.1003906

93. Quadri P, Fragiacomo C, Pezzati R, Zanda E, Forloni G, Tettamanti M, et al. Homocysteine, folate, and vitamin B-12 in mild cognitive impairment, Alzheimer disease, and vascular dementia. *Am J Clin Nutr*. (2004) 80:114–22. doi: 10.1093/ajcn/80.1.114

94. Smith AD. The worldwide challenge of the dementias: a role for B vitamins and homocysteine? *Food Nutr Bull*. (2008) 29:S143–72. doi: 10.1177/15648265080292s119

95. Van Dam F, Van Gool WA. Hyperhomocysteinemia and Alzheimer's disease: a systematic review. *Arch Gerontol Geriatr*. (2009) 48:425–30. doi: 10.1016/j.archger.2008.03.009

96. Škovierová H, Vidomanová E, Mahmood S, Sopková J, Drgová A, Cervenová T, et al. The molecular and cellular effect of homocysteine metabolism imbalance on human health. *Int J Mol Sci*. (2016) 17:1733. doi: 10.3390/ijms17101733

97. Kim J, Kim H, Roh H, Kwon Y. Causes of hyperhomocysteinemia and its pathological significance. *Arch Pharm Res*. (2018) 41:372–83. doi: 10.1007/s12272-018-1016-4

98. Cacciapuoti F. Lowering homocysteine levels with folic acid and B-vitamins do not reduce early atherosclerosis, but could interfere with cognitive decline and Alzheimer's disease. *J Thromb Thrombolysis*. (2013) 36:258–62. doi: 10.1007/s11239-012-0856-x

99. Mutavdzin S, Gopcevic K, Stankovic S, Jakovljevic Uzelac J, Labudovic Borovic M, Djuric D. The effects of folic acid administration on cardiac oxidative stress and cardiovascular biomarkers in diabetic rats. *Oxid Med Cell Longev*. (2019) 2019:1342549. doi: 10.1155/2019/ 1342549

100. Chen H, Liu S, Ji L, Wu T, Ji Y, Zhou Y, et al. Folic acid supplementation mitigates Alzheimer's disease by reducing inflammation: a randomized controlled trial. *Mediators Inflamm*. (2016) 2016:5912146. doi: 10.1155/2016/5912146

101. Malouf M, Grimley EJ, Areosa SA. Folic acid with or without vitamin B12 for cognition and dementia. *Cochrane Database Syst Rev*. (2003) 4:Cd004514. doi: 10.1002/ 14651858.Cd004514

102. Sun Y, Lu CJ, Chien KL, Chen ST, Chen RC. Efficacy of multivitamin supplementation containing vitamins B6 and B12 and folic acid as adjunctive treatment with a cholinesterase inhibitor in Alzheimer's disease: a 26-week, randomized, double-blind, placebo-controlled study in Taiwanese patients. *Clin Ther*. (2007) 29:2204–14. doi: 10.1016/j.clinthera.2007.10.012

103. Gargari BP, Aghamohammadi V, Aliasgharzadeh A. Effect of folic acid supplementation on biochemical indices in overweight and obese men with type 2 diabetes. *Diabetes Res Clin Pract*. (2011) 94:33–8. doi: 10.1016/j.diabres.2011.07.003

104. Jack CR Jr, Shiung MM, Gunter JL, O'Brien PC, Weigand SD, Knopman DS, et al. Comparison of different MRI brain atrophy rate measures with clinical disease progression in AD. *Neurology*. (2004) 62:591–600. doi: 10.1212/01.wnl.0000110315.26026.ef

105. Smith AD, Smith SM, de Jager CA, Whitbread P, Johnston C, Agacinski G, et al. Homocysteine-lowering by B vitamins slows the rate of accelerated brain atrophy in mild cognitive impairment: a randomized controlled trial. *PLoS ONE*. (2010) 5:e12244. doi: 10.1371/journal.pone.0012244

106. Jernerén F, Elshorbagy AK, Oulhaj A, Smith SM, Refsum H, Smith AD. Brain atrophy in cognitively impaired elderly: the importance of long-chain ω-3 fatty acids and B vitamin status in a randomized controlled trial. *Am J Clin Nutr*. (2015) 102:215–21. doi: 10.3945/ajcn.114.103283

107. Farina N, Jernerén F, Turner C, Hart K, Tabet N. Homocysteine concentrations in the cognitive progression of Alzheimer's disease. *Exp Gerontol*. (2017) 99:146–50. doi: 10.1016/j.exger.2017.10.008

108. Szkudelski T, Szkudelska K. Resveratrol and diabetes: from animal to human studies. *Biochim Biophys Acta*. (2015) 1852:1145–54. doi: 10.1016/j.bbadis.2014.10.013

109. Kulashekar M, Stom SM, Peuler JD. Resveratrol's potential in the adjunctive management of cardiovascular disease, obesity, diabetes, Alzheimer disease, and cancer. *J Am Osteopath Assoc*. (2018) 118:596–605. doi: 10.7556/jaoa.2018.133

110. Zhang W, Yu H, Lin Q, Liu X, Cheng Y, Deng B. Anti-inflammatory effect of resveratrol attenuates the severity of diabetic neuropathy by activating the Nrf2 pathway. *Aging (Albany NY)*. (2021) 13:10659–71. doi: 10.18632/aging.202830

111. Ma X, Sun Z, Han X, Li S, Jiang X, Chen S, et al. Neuroprotective effect of resveratrol via activation of SIRT1 signaling in a rat model of combined diabetes and Alzheimer's disease. *Front Neurosci*. (2019) 13:1400. doi: 10.3389/fnins.2019.01400

112. Movahed A, Nabipour I, Lieben Louis X, Thandapilly SJ Yu L, Kalantarhormozi M, et al. Antihyperglycemic effects of short term resveratrol supplementation in type 2 diabetic patients. *Evid Based Complement Alternat Med*. (2013) 2013:851267. doi: 10.1155/2013/851267

113. Jia JJ, Zeng XS, Song XQ, Zhang PP, Chen L. Diabetes mellitus and Alzheimer's disease: the protection of epigallocatechin-3-gallate in streptozotocin injection-induced models. *Front Pharmacol*. (2017) 8:834. doi: 10.3389/fphar.2017.00834

114. Bassiony HS, Zickri MB, Metwally HG, Elsherif HA, Alghandour SM, Sakr W. Comparative histological study on the therapeutic effect of green tea and stem cells in Alzheimer's disease complicating experimentally induced diabetes. *Int J Stem Cells*. (2015) 8:181–90. doi: 10.15283/ijsc.2015.8.2.181

115. Qin B, Panickar KS, Anderson RA. Cinnamon: potential role in the prevention of insulin resistance, metabolic syndrome, and type 2 diabetes. *J Diabetes Sci Technol*. (2010) 4:685–93. doi: 10.1177/193229681000400324

116. Lee MS, Wahlqvist ML, Chou YC, Fang WH, Lee JT, Kuan JC, et al. Turmeric improves post-prandial working memory in pre-diabetes independent of insulin. *Asia Pac J Clin Nutr*. (2014) 23:581–91. doi: 10.6133/apjcn.2014.23.4.24

117. Thota RN, Rosato JI, Dias CB, Burrows TL, Martins RN, Garg ML. Dietary supplementation with curcumin reduce circulating levels of glycogen synthase kinase-3β and islet amyloid polypeptide in adults with high risk of type 2 diabetes and Alzheimer's disease. *Nutrients*. (2020) 12:1032. doi: 10.3390/nu12041032

118. Abdulmalek S, Nasef M, Awad D, Balbaa M. Protective effect of natural antioxidant, curcumin nanoparticles, and zinc oxide nanoparticles against type 2 diabetes-promoted hippocampal neurotoxicity in rats. *Pharmaceutics*. (2021) 13:1937. doi: 10.3390/pharmaceutics13111937

119. Khan MS, Ikram M, Park TJ, Kim MO. Pathology, risk factors, and oxidative damage related to type 2 diabetes-mediated Alzheimer's disease and the rescuing effects of the potent antioxidant anthocyanin. *Oxid Med Cell Longev*. (2021) 2021:4051207. doi: 10.1155/2021/4051207

120. Wagle A, Seong SH, Shrestha S, Jung HA, Choi JS. Korean thistle (*Cirsium japonicum* var. *maackii* (Maxim.) Matsum.): a potential dietary supplement against diabetes and Alzheimer's disease. *Molecules*. (2019) 24:649. doi: 10.3390/molecules24030649

121. Lai MC, Liu WY, Liou SS, Liu IM. The citrus flavonoid hesperetin encounters diabetes-mediated Alzheimer-type neuropathologic changes through relieving advanced glycation end-products inducing endoplasmic reticulum stress. *Nutrients*. (2022) 14:745. doi: 10.3390/nu14040745

122. Li RZ, Ding XW, Geetha T, Al-Nakkash L, Broderick TL, Babu JR. Beneficial effect of genistein on diabetes-induced brain damage in the ob/ob mouse model. *Drug Des Devel Ther*. (2020) 14:3325–36. doi: 10.2147/dddt.S249608

123. Gomaa AA, Makboul RM, Al-Mokhtar MA, Nicola MA. Polyphenol-rich *Boswellia serrata* gum prevents cognitive impairment and insulin resistance of diabetic rats through inhibition of GSK3β activity, oxidative stress and pro-inflammatory cytokines. *Biomed Pharmacother*. (2019) 109:281–92. doi: 10.1016/j.biopha.2018.10.056

124. Infante-Garcia C, Jose Ramos-Rodriguez J, Marin-Zambrana Y, Teresa Fernandez-Ponce M, Casas L, Mantell C, et al. Mango leaf extract improves central pathology and cognitive impairment in a type 2 diabetes mouse model. *Brain Pathol*. (2017) 27:499–507. doi: 10.1111/bpa.12433

125. Ben Hmidene A, Hanaki M, Murakami K, Irie K, Isoda H, Shigemori H. Inhibitory activities of antioxidant flavonoids from tamarix gallica on amyloid aggregation related to Alzheimer's and type 2 diabetes diseases. *Biol Pharm Bull*. (2017) 40:238–41. doi: 10.1248/bpb.b16-00801

126. de Bock M, Derraik JG, Brennan CM, Biggs JB, Morgan PE, Hodgkinson SC, et al. Olive (*Olea europaea* L) leaf polyphenols improve insulin sensitivity in middle-aged overweight men: a randomized, placebo-controlled, crossover trial. *PLoS ONE*. (2013) 8:e57622. doi: 10.1371/journal.pone.0057622

127. Silveira AC, Dias JP, Santos VM, Oliveira PF, Alves MG, Rato L, et al. The action of polyphenols in diabetes mellitus and Alzheimer's disease: a common agent for overlapping pathologies. *Curr Neuropharmacol*. (2019) 17:590–613. doi: 10.2174/1570159x16666180803162059

128. Li W, Wang G, Lu X, Jiang Y, Xu L, Zhao X. Lycopene ameliorates renal function in rats with streptozotocin-induced diabetes. *Int J Clin Exp Pathol*. (2014) 7:5008–15.

129. Yu L, Wang W, Pang W, Xiao Z, Jiang Y, Hong Y. Dietary lycopene supplementation improves cognitive performances in tau transgenic mice expressing P301L mutation via inhibiting oxidative stress and tau hyperphosphorylation. *J Alzheimers Dis*. (2017) 57:475–82. doi: 10.3233/jad-161216

130. Gunasekara P, Hettiarachchi M, Liyanage C, Lekamwasam S. Effects of zinc and multimineral vitamin supplementation on glycemic and lipid control in adult diabetes. *Diabetes Metab Syndr Obes*. (2011) 4:53–60. doi: 10.2147/dmso.S16691

131. Barbagallo M, Dominguez LJ, Galioto A, Pineo A, Belvedere M. Oral magnesium supplementation improves vascular function in elderly diabetic patients. *Magnes Res*. (2010) 23:131–7. doi: 10.1684/mrh.2010.0214

132. Agrawal R, Gomez-Pinilla F. 'Metabolic syndrome' in the brain: deficiency in omega-3 fatty acid exacerbates dysfunctions in insulin receptor signalling and cognition. *J Physiol*. (2012) 590:2485–99. doi: 10.1113/jphysiol.2012.230078

133. Szuster-Ciesielska A, Plewka K, Daniluk J, Kandefer-Szerszeń M. Betulin and betulinic acid attenuate ethanol-induced liver stellate cell activation by inhibiting reactive oxygen species (ROS), cytokine (TNF-α, TGF-β) production and by influencing intracellular signaling. *Toxicology*. (2011) 280:152–63. doi: 10.1016/j.tox.2010.12.006

134. Hashmi WJ, Ismail H, Mehmood F, Mirza B. Neuroprotective, antidiabetic and antioxidant effect of hedera nepalensis and lupeol against STZ + ALCL(3) induced rats model. *Daru*. (2018) 26:179–90. doi: 10.1007/s40199-018-0223-3

135. Lee SH, Jeon YJ. Efficacy and safety of a dieckol-rich extract (ag-dieckol) of brown algae, ecklonia cava, in pre-diabetic individuals: a double-blind, randomized, placebo-controlled clinical trial. *Food Funct*. (2015) 6:853–8. doi: 10.1039/c4fo00940a

136. Ergül M, Ergül M, Eruygur N, Ataş M, Uçar E. *In vitro* evaluation of the chemical composition and various biological activities of *Ficus carica* leaf extracts. *Turk J Pharm Sci*. (2019) 16:401–9. doi: 10.4274/tjps.galenos.2018.70037

137. Udupa AS, Nahar PS, Shah SH, Kshirsagar MJ, Ghongane BB. Study of comparative effects of antioxidants on insulin sensitivity in type 2 diabetes mellitus. *J Clin Diagn Res*. (2012) 6:1469–73. doi: 10.7860/jcdr/2012/4464.2535

frontiers | Frontiers in Nutrition

TYPE Original Research
PUBLISHED 06 December 2022
DOI 10.3389/fnut.2022.1042558

OPEN ACCESS

EDITED BY
Zhi Chai,
Icahn School of Medicine at Mount Sinai, United States

REVIEWED BY
Guoxun Chen,
The University of Tennessee, Knoxville, United States
Han Mei,
Stanford University, United States
Zhaoyue Zhang,
The Rockefeller University, United States
Yuxia Ouyang,
Icahn School of Medicine at Mount Sinai, United States

*CORRESPONDENCE
Gang Liu
cardio2004@163.com
Jun Wang
junwangwh@hotmail.com

†These authors have contributed equally to this work

SPECIALTY SECTION
This article was submitted to Nutrition and Metabolism, a section of the journal Frontiers in Nutrition

RECEIVED 12 September 2022
ACCEPTED 22 November 2022
PUBLISHED 06 December 2022

CITATION
Wang D, Wang N, Zhou J, Luo G, Li Y, Yu W, Tan H, Liu G, Wang J and Hao L (2022) Urine trace element disorder along with renal function injury in vitamin D deficient diabetic rats and intervention effect of 1α,25-dihydroxyvitamin D3. *Front. Nutr.* 9:1042558. doi: 10.3389/fnut.2022.1042558

Urine trace element disorder along with renal function injury in vitamin D deficient diabetic rats and intervention effect of 1α,25-dihydroxyvitamin D3

Dongxia Wang[1,2], Ning Wang[1], Juan Zhou[1], Gang Luo[1], Yanyan Li[3], Wei Yu[3], Hongxing Tan[3], Gang Liu[4*†], Jun Wang[5*†] and Liping Hao[1]

[1]Hubei Key Laboratory of Food Nutrition and Safety, Ministry of Education Key Laboratory of Environment, Department of Nutrition and Food Hygiene, School of Public Health, Tongji Medical College, Huazhong University of Science and Technology, Wuhan, China, [2]Hebei Key Laboratory of Environment and Human Health, Department of Nutrition and Food Hygiene, School of Public Health, Hebei Medical University, Shijiazhuang, China, [3]Shenzhen Center for Chronic Disease Control, Shenzhen, China, [4]Hebei Key Laboratory of Cardiac Injury Repair Mechanism Study, Department of Cardiology, Hebei International Joint Research Center for Structural Heart Disease, The First Hospital of Hebei Medical University, Shijiazhuang, China, [5]School of Food and Drug, Shenzhen Polytechnic, Shenzhen, China

Introduction: Trace element metabolism disorders are often secondary to disorders of glucose metabolism in diabetes. Although 1α,25-dihydroxyvitamin D3 [1,25$(OH)_2D_3$] could ameliorate abnormal glucose metabolism in the development of diabetes, the effect on trace element metabolism is unclear. The objective of this study was to evaluate the influence of 1,25$(OH)_2D_3$ on urinary excretions of trace elements in Zucker diabetic fatty (ZDF) rats.

Methods: At 6 weeks of age, male ZDF (n = 40) rats were subdivided into four groups: diabetic model (ZDF), low-dose (ZDF + VL, 2 μg/kg·bw), middle-dose (ZDF + VM, 8 μg/kg·bw) and high-dose (ZDF + VH, 16 μg/kg·bw) 1,25$(OH)_2D_3$ groups. Another 10 Zucker lean (ZL) rats served as a control group. All rats were given vitamin D deficient Purina #5008 chow and the intervention groups were given the corresponding dose of 1,25$(OH)_2D_3$ by gavage on alternate days for 7 weeks. Microalbuminuria (MALB) and urinary creatinine concentration were detected by a biochemical autoanalyzer. Urine trace element concentrations were measured using inductively coupled plasma mass spectrometry (ICP-MS) and were corrected by urinary creatinine.

Results: Throughout the intervention phase, MALB, UACR and urinary creatinine levels in the ZDF group were significantly higher than those in the ZL group, and showed a gradual increase with the prolongation of the intervention time. These changes were reversed in a dose-dependent manner after 1,25$(OH)_2D_3$ intervention ($P < 0.05$). Correspondingly, most of the urinary trace element excretions in the ZDF rats were significantly increased

compared with the ZL group, and 1,25$(OH)_2D_3$ intervention significantly reduced the urinary copper (Cu), zinc (Zn), selenium (Se) and molybdenum (Mo) levels in the ZDF rats ($P < 0.05$), especially in the medium and high dose groups.

Conclusion: 1,25$(OH)_2D_3$ had improvement effects on urinary Cu, Zn, Se, and Mo excretions in ZDF rats, suggesting that it may be related to the reduction of diabetic renal impairment and renal oxidative damage.

KEYWORDS

1α,25-dihydroxyvitamin D3, diabetes, ZDF rats, renal function, urinary Cu, urinary Zn, urinary Se, urinary Mo

Introduction

Type 2 diabetes mellitus (T2DM) is an endocrine metabolic disease characterized by chronic hyperglycemia and has become a global public health problem that poses a serious threat to human health. According to the latest data published by the International Diabetes Federation, 537 million adults aged 20–79 years have diabetes worldwide in 2021, with a prevalence of 10.5%, of which about 90% are T2DM (1). Among the abovementioned diabetic patients, about 140.9 million are from China, accounting for about a quarter of the global figure. In addition, a nationally representative epidemiological survey showed that the prevalence of diabetes among adults in China was as high as 12.8% in 2017, much higher than 10.9% in 2013 (2). Therefore, the prevention and treatment of T2DM is an important scientific problem that needs to be addressed urgently.

Abnormal glucose metabolism is now recognized as the most fundamental pathophysiological feature in the development of T2DM (3). In addition, the relationship between diabetes and disorders of trace element metabolism has received much attention, largely because most trace elements are involved in glucose metabolism as important components of certain enzymes and hormones (4, 5). It has been shown that trace element metabolism disorders in diabetic patients are often secondary to disorders of glucose metabolism (6). Some studies reported that whole blood levels of zinc, manganese, and chromium were significantly lower while the urinary levels of the same elements were found to be higher in the T2DM patients than in their healthy age-matched counterparts (5). Recent studies found that serum magnesium levels are decreased and serum copper, zinc, and selenium levels are elevated in patients with T2DM (6). In conclusion, we find that the results regarding the association of trace elements and the risk of T2DM are inconsistent.

Vitamin D, an essential fat-soluble vitamin, is mostly converted from 7-dehydrocholesterol in the skin by ultraviolet light exposure. It further undergoes two hydroxylation reactions in the liver and kidney to produce 1α,25-dihydroxyvitamin D3 [1,25$(OH)_2D_3$] before becoming biologically active, and active vitamin D exerts its physiological effects mainly through binding to the Vitamin D Receptor (VDR) (7). Given that VDR is widely distributed in most tissues and cells of the body, vitamin D deficiency is not only associated with disorders of calcium and phosphorus metabolism but also with cancer, autoimmune diseases, metabolic and cardiovascular diseases (diabetes, hypertension, renal diseases, etc.) (8, 9). Evidence from numerous observational studies suggests that vitamin D deficiency is prevalent in patients with T2DM and that the incidence of diabetes is negatively correlated with serum 25(OH)D concentration (10–12). A cross-sectional study based on a Chinese diabetic population showed that 83.5% of patients with T2DM had vitamin D deficiency [serum 25(OH)D concentration < 20 ng/mL], and the prevalence of vitamin D deficiency was more severe in patients with combined diabetic nephropathy than in those without diabetic nephropathy (93.1% vs. 78.9%) (13).

To simulate vitamin D deficiency or insufficiency in T2DM patients, Zucker diabetic fatty (ZDF) rats were fed with vitamin D deficient Purina #5008 chow to establish a vitamin D deficient T2DM animal model. Previous study revealed that vitamin D deficiency accelerated and exacerbated the dysregulation of glucose metabolism in non-obese T2DM rats by increasing insulin resistance and that vitamin D deficiency might be a key factor in the pathogenesis of T2DM (14). The present study further focused on the key role of 1,25$(OH)_2D_3$ supplementation in a vitamin D deficient model of diabetes. No evidence is available regarding the effect of vitamin D supplementation on urinary trace element metabolism in diabetes. The aim of the present study is to clarify whether 1,25$(OH)_2D_3$ supplementation has a protective

Abbreviations: 1,25$(OH)_2D_3$, 1α,25-dihydroxyvitamin D3; MALB, microalbuminuria; T2DM, type 2 diabetes mellitus; UACR, urea microalbuminuria creatinine ratio; ZDF, Zucker diabetic fatty; ZL, Zucker lean.

effect against disorders of trace element excretion in vitamin D-deficient ZDF rats.

Materials and methods

Chemicals

$1,25(OH)_2D_3$ (purity ≥ 97%) was obtained from Cayman Chemical (Item No. 71820, USA). Microalbuminuria (MALB) and creatinine assay kits were supplied by Shenzhen Mindray Biomedical Electronics Co., Ltd. (Shenzhen, China), which were used *via* an automatic biochemical analyzer (BS-200, Mindray, Shenzhen, China). All other reagents were analytical grade.

Animals and diets

Five-week-old male ZDF ($n = 40$) rats and age-matched male Zucker lean (ZL; $n = 10$) rats from Charles River Laboratory (Beijing, China) were maintained on the vitamin D-deficient Purina 5008 chow (500 IU vitamin D3/kg) and tap water *ad libitum*. Animals were kept on a regular 12:12 h light-dark cycle at a controlled temperature (22 ± 2°C) and relative humidity (55 ± 5%). All experimental procedures involving animals complied with the Regulations on the Administration of Laboratory Animals in China and were approved by the Animal Ethical Committee of Tongji Medical College (Approval NO. S432).

Study design

At the age of 6 weeks, male ZDF rats were subdivided into four groups ($n = 10$): diabetic model (ZDF), low-dose (ZDF + VL, 2 μg/kg·bw), middle-dose (ZDF + VM, 8 μg/kg·bw), and high-dose (ZDF + VH, 16 μg/kg·bw) $1,25(OH)_2D_3$ groups. Another 10 ZL rats served as a control group. $1,25(OH)_2D_3$ was dissolved in corn oil and administered by gavage on alternate days for 7 weeks. The vehicle groups (ZL and ZDF) were only gavaged with corn oil.

Sample collection

At the treatment of 1,4,6,7 weeks, the Zucker rats were housed in metabolic cages and their 24 h urine was dynamically collected at least 3 mL per rat to detect indicators of renal function and minerals. Sodium azide was added to all urine samples at a volume ratio of 10 μL/mL before freezing to protect the urine samples from contamination. When fasting blood glucose (FBG) ≥ 16.7 mmol/L, the model of diabetes was established. At the end of the experiment, the rats were weighed after an overnight fast of 8 h. Blood was collected from the eyes, serum was obtained at least 1 mL per rat from blood samples that has been left at room temperature for 2 h and then centrifuged at 4,000 r/min for 15 min, and the kidneys were removed and weighed. All samples were stored at −80°C for subsequent processing.

Determination of serum biochemical parameters

FBG was measured by glucose oxidase method according to the manufacturer's instructions (Biosino Bio-technology and Science Inc., Beijing, China). Serum fasting insulin (FINS) was assayed by double antibody sandwich ELISA using corresponding kit (Millipore Corporation, Billerica, USA). HOMA-IR and HOMA-β were calculated from fasting blood glucose and fasting serum insulin levels with the following formulae:

$$HOMA - IR = (FINS \times FBG)/22.5;$$

$$HOMA - \beta = (20 \times FINS)/(FBG - 3.5)$$ (15, 16).

Serum triglyceride (TG) concentration was detected by phosphoglyceride oxidase-peroxidase method (GPO-PAP). The levels of total cholesterol (TC), low density lipoprotein cholesterol (LDL-C) and high density lipoprotein cholesterol (HDL-C) in serum were measured by the cholesterol oxidase-peroxidase method (CHOD-PAP). The assay kits of lipid indicators mentioned above were supplied by Biosino Bio-technology and Science Inc. Serum adiponectin was detected using ELISA kit (R&D Systems Inc., Minneapolis, USA). All procedures were carried out in strict accordance with the manufacturer's protocol.

Analysis of renal function indicators

24 h urinary collections were taken at 1, 4, 6, and 7 weeks of treatment, respectively. MALB and urinary creatinine concentration were detected by a Mindray BS-200 biochemical autoanalyzer. Subsequently, urea microalbuminuria creatinine ratio (UACR) was calculated *via* the following equation:

$$UACR(\mu g/mg) = MALB/(Urine\ creatinine \times 113).$$

Measurement of trace element concentration in urine

Twenty-four hour urine samples were collected at 1, 4, 6, and 7 weeks of treatment and stored at −80°C for the

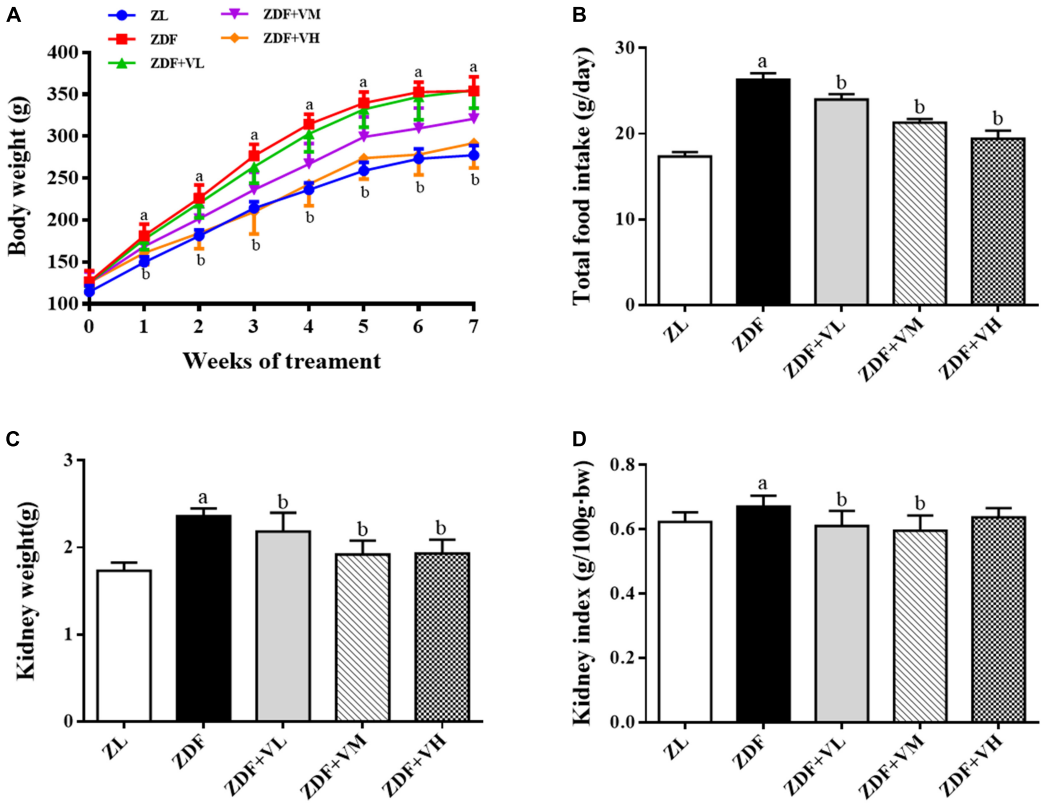

FIGURE 1
Effects of $1,25(OH)_2D_3$ on the body weight, food intake, and kidney index in Zucker rats. **(A)** Variation trends of body weight as weeks of $1,25(OH)_2D_3$ treatment. **(B)** Total food intake. **(C)** Kidney weight. **(D)** Kidney index. ZL, Zucker lean group; ZDF, Zucker diabetic fatty group; ZDF + VL, ZDF + low-dose $1,25(OH)_2D_3$ group (2 μg/kg·bw); ZDF + VM, ZDF + middle-dose $1,25(OH)_2D_3$ group (8 μg/kg·bw); ZDF + VH, ZDF + high-dose $1,25(OH)_2D_3$ group (16 μg/kg·bw). Data are presented as mean ± SD ($n \geq 7$). $^aP < 0.05$ vs. the ZL group, $^bP < 0.05$ vs. the ZDF group.

TABLE 1 Effects of $1,25(OH)_2D_3$ on insulin sensitivity and parameters of lipid metabolism in Zucker rats.

Groups	ZL	ZDF	ZDF + VL	ZDF + VM	ZDF + VH
FBG (mmol/L)	4.39 ± 0.40	17.26 ± 3.17^a	10.05 ± 2.43^b	6.34 ± 0.36^b	6.77 ± 0.43^b
FINS (mIU/L)	14.48 ± 5.80	245.97 ± 69.79^a	439.95 ± 190.94	334.39 ± 99.56	225.89 ± 65.58
HOMA-IR	3.02 ± 1.59	205.08 ± 46.99^a	213.18 ± 55.88	77.05 ± 13.66^b	69.73 ± 19.94^b
HOMA-β	298.48 ± 23.25	364.83 ± 195.55	1121.19 ± 680.80^b	2456.62 ± 706.73^b	1381.12 ± 325.43^b
Serum TG (mmol/L)	2.80 ± 0.83	11.12 ± 4.05^a	12.50 ± 4.21	6.97 ± 1.50^b	5.75 ± 1.28^b
Serum TC (mmol/L)	3.02 ± 0.13	4.47 ± 0.48^a	4.25 ± 0.70	4.13 ± 0.52	3.99 ± 0.44
Serum HDL-C (mmol/L)	0.43 ± 0.13	0.40 ± 0.10	0.44 ± 0.16	0.24 ± 0.05^b	0.26 ± 0.07^b
Serum LDL-C (mmol/L)	1.19 ± 0.12	1.79 ± 0.23^a	1.69 ± 0.51	1.66 ± 0.30	1.59 ± 0.49
Serum adiponectin (ng/mL)	7.46 ± 1.15	5.52 ± 1.12^a	5.61 ± 1.42	8.13 ± 1.62^b	9.29 ± 1.92^b

ZL, Zucker lean group; ZDF, Zucker diabetic fatty group. ZDF + VL, ZDF + low-dose $1,25(OH)_2D_3$ group (2 μg/kg·bw); ZDF + VM, ZDF + middle-dose $1,25(OH)_2D_3$ group (8 μg/kg·bw); ZDF + VH, ZDF + high-dose $1,25(OH)_2D_3$ group (16 μg/kg·bw). Data are presented as the mean ± SD ($n \geq 4$). $^aP < 0.05$ vs. the ZL group, $^bP < 0.05$ vs. the ZDF group using one way ANOVA tests.

dynamic analysis of urinary trace element excretion. Firstly, the urine samples were centrifuged at 4,000 rpm, 4°C for 10 min before being diluted. We mixed 400 μL urine sample and 20 μL of 60% nitric acid solution together and placed them in a refrigerator at 4°C for overnight acidification. Then added 3,580 μL of 1% nitric acid solution to dilute the urine sample 10 times. After centrifuging at 4,000 rpm, 4°C for 10 min, the urine samples were assayed. All samples were measured in triplicate.

Urinary trace element concentrations in the studied samples were detected by inductively coupled plasma mass spectrometer (ICP-MS) at Agilent 7700 (Agilent Technologies, Tokyo, Japan).

The obtained data on urinary trace element contents were corrected with urine creatinine concentration and expressed as μ g/g UCR.

Statistical analysis

Data of urine metal concentration were displayed as mean ± SEM or median (IQR). If the data obeyed normal distribution, the statistical significance of comparisons between multiple groups was analyzed by one-way ANOVA, followed by the Least Significant Difference (LSD) multiple range test if the variances were constant, otherwise the Dunnett's T3 procedure. If the data didn't follow a normal distribution, we performed a non-parametric (Kruskal-Wallis H) test. All statistical analyses were conducted by SPSS 21.0. P-value < 0.05 was considered to show a statistically significant difference.

Results

$1,25(OH)_2D_3$ decreases body weight and kidney index in diabetic rats

ZDF rats were fed with Purina #5008 chow for 7 weeks to establish a spontaneous T2DM rat model, and $1,25(OH)_2D_3$ was administered at the same time. As shown in **Figure 1**, there was no significant difference in the initial body weight (week 0) of the rats in each group. With the prolongation of the intervention time, the body weight of the rats in each group gradually increased. From the first week of intervention to the end of the experiment, the body weight of the rats in the diabetes group (ZDF) was significantly higher than that in the control group (ZL). While the body weight of the rats in the high-dose $1,25(OH)_2D_3$ intervention group (ZDF + VH) was significantly lower than that in the ZDF group ($P < 0.05$). At the 7th week of intervention, the body weight of the rats in the ZDF group increased by 28% compared with the ZL group, while compared with the ZDF group, the figure decreased by 18% in the ZDF + VH group ($P < 0.05$). Meanwhile, the results showed that the weight of kidneys and kidney index in the ZDF group were significantly increased compared with those in the ZL group, and the $1,25(OH)_2D_3$ dose groups effectively reversed the above changes.

$1,25(OH)_2D_3$ improves insulin sensitivity and lipid metabolism in diabetic rats

As shown in **Table 1**, the levels of fasting blood glucose, serum insulin, and HOMA-IR in the ZDF group were significantly higher than those in the ZL group. Although the serum insulin in each $1,25(OH)_2D_3$ intervention group was at a high level, the fasting blood glucose and HOMA-IR in each dose group were significantly lower than those in the ZDF group, and the function of HOMA-β was significantly enhanced ($P < 0.05$). It indicated that $1,25(OH)_2D_3$ played an important role in increasing insulin sensitivity, and the improvement effect was most promising in the middle and high dose groups.

Compared with the ZL group, the serum TG, TC, and LDL-C levels of the ZDF group were increased by 297, 48, and 50%, respectively ($P < 0.05$). On the contrary, the serum TG levels of the ZDF + VM and ZDF + VH groups were decreased by 37 and 48% than the ZDF group ($P < 0.05$), meanwhile the serum TC and LDL-C concentrations showed a dose-dependent decrease. Adiponectin is an adipokine produced by adipose tissue, which is involved in glucose and lipid metabolism and inflammatory response. The serum adiponectin level in the ZDF group was 26% lower than that in the ZL group ($P < 0.05$). However, the serum adiponectin levels in the ZDF + VM and ZDF + VH groups were increased by 47 and 68%, respectively, compared with the ZDF group ($P < 0.05$). The above results indicate that medium and high doses of $1,25(OH)_2D_3$ supplementation can improve the abnormal lipid metabolism in spontaneous diabetic rats, and its lipid-lowering effect is mainly manifested by a significant reduction in TG levels and an increase in adiponectin levels.

$1,25(OH)_2D_3$ alleviates renal function damage in diabetic rats

To investigate whether $1,25(OH)_2D_3$ has a nephroprotective effect on ZDF rats, we used UACR and urinary creatinine levels as indicators to evaluate the progress of DN. As shown in **Figure 2**, the MALB, UACR, and urine creatinine contents in the ZDF group were significantly higher than those in the ZL group during the whole intervention period, and the gap was gradually widened with the extension of the intervention time. These changes were reversed in a dose-dependent manner after $1,25(OH)_2D_3$ intervention ($P < 0.05$).

Effect of $1,25(OH)_2D_3$ on the disturbance of urinary trace element metabolism in diabetic rats

Effect of $1,25(OH)_2D_3$ on urinary trace elements in spontaneously diabetic rats at 1st week of intervention

In this study, 23 trace element concentrations in urine were dynamically determined by ICP-MS and corrected with urinary

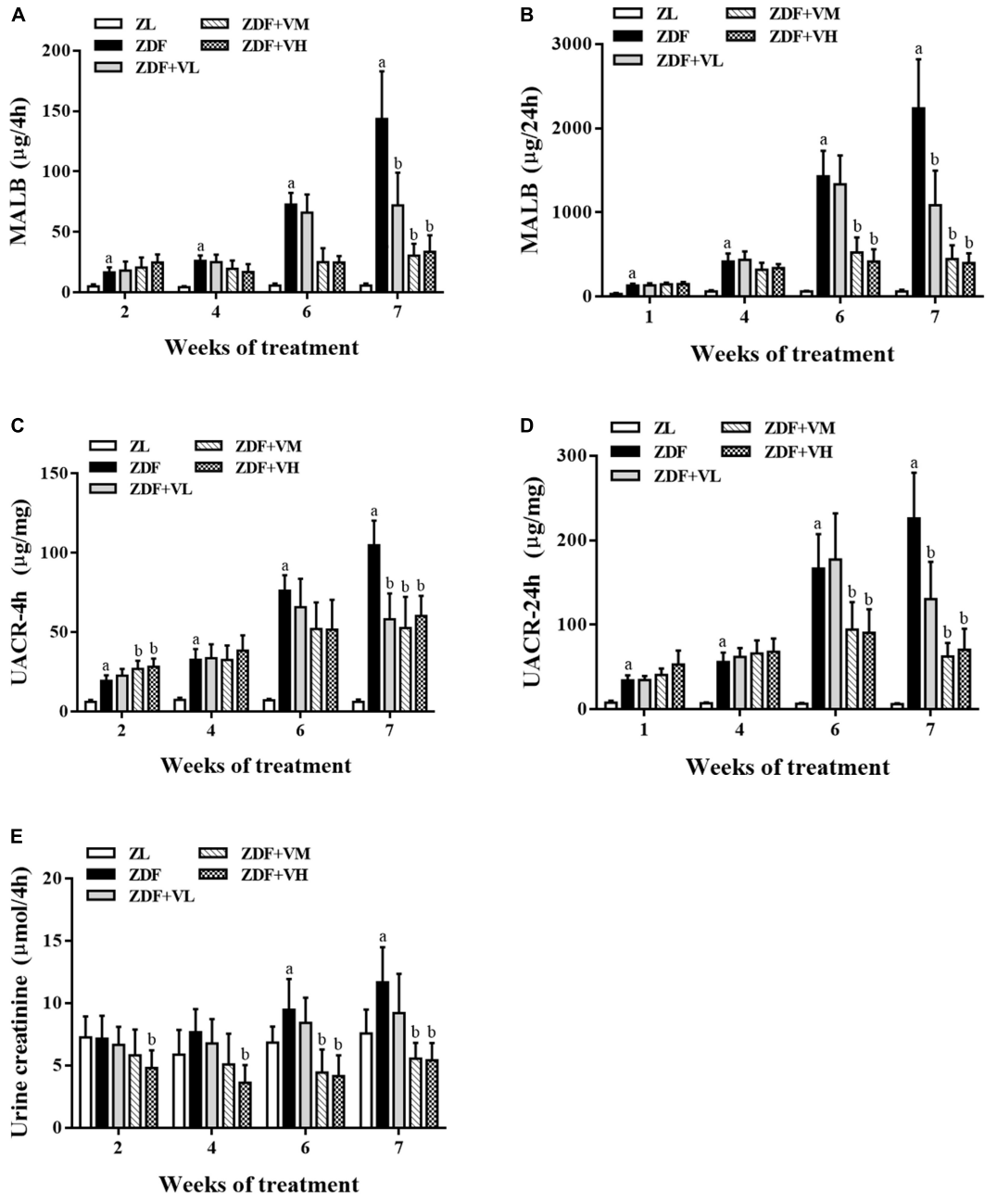

FIGURE 2
Variation trend of renal function indicators as weeks of 1,25$(OH)_2D_3$ treatment. **(A,B)** Four hour-MALB and 24 h-MALB contents. **(C,D)** Four hour-UACR and 24 h-UACR contents. **(E)** Four hour-Urine creatinine content. ZL, Zucker lean group; ZDF, Zucker diabetic fatty group; ZDF + VL, ZDF + low-dose 1,25$(OH)_2D_3$ group (2 μg/kg·bw); ZDF + VM, ZDF + middle-dose 1,25$(OH)_2D_3$ group (8 μg/kg·bw); ZDF + VH, ZDF + high-dose 1,25$(OH)_2D_3$ group (16 μg/kg·bw). Data are presented as mean ± SD ($n \geq 4$). $^{a}P < 0.05$ vs. the ZL group, $^{b}P < 0.05$ vs. the ZDF group.

creatinine concentrations in μg/g UCR, except Tl, Sb, Cd, Sn, and U which were in ng/g UCR. As seen in Table 2, at 1 week of intervention, urinary levels of Cu, Zn, Se, Mo, As, W, Ti, Co, Cr, Ni, Sr, and Cd were significantly increased in the ZDF group of rats compared to the ZL group, and 1,25$(OH)_2D_3$ intervention increased the levels of Se, Tl, Ti, Cr, Al, Mn, Sr, Cd, and Ba in urine compared with the ZDF group ($P < 0.05$).

Effect of 1,25$(OH)_2D_3$ on urinary trace elements in spontaneously diabetic rats at 4th week of intervention

As seen from Table 3, after 4 weeks of intervention, the urinary levels of Zn, Se, Mo, As, Rb, V, W, Tl, Ti, Co, Cr, Ni, Sb, Al, Fe, Mn, Cd, Ba, and U in the ZDF group of rats were significantly increased compared to the ZL group. And

TABLE 2 Effects of $1,25(OH)_2D_3$ on urine metal concentration of Zucker rats in the first week of treatment.

Metals (μg/g UCR)	ZL	ZDF	ZDF + VL	ZDF + VM	ZDF + VH
Cu	184.66 ± 4.98	243.81 ± 7.83[a]	235.21 ± 10.60	223.87 ± 10.49	240.28 ± 13.10
Zn	143.93 ± 23.21	245.87 ± 13.42[a]	262.43 ± 19.72	231.91 ± 7.81	240.25 ± 25.49
Se	7.24 ± 0.18	13.18 ± 0.67[a]	17.03 ± 0.59[b]	16.07 ± 0.88	18.21 ± 1.27[b]
Mo	261.38 ± 5.96	411.78 ± 10.95[a]	406.63 ± 12.99	366.08 ± 27.50	375.01 ± 19.52
As	13.72 ± 0.43	17.43 ± 0.45[a]	17.33 ± 0.68	17.57 ± 0.96	18.51 ± 0.60
Rb	1084.69 ± 48.47	2081.95 ± 57.83	2425.84 ± 56.45	2420.95 ± 85.33	2519.00 ± 93.90
V	1.19 ± 0.10	1.81 ± 0.17	1.98 ± 0.21	1.99 ± 0.24	2.31 ± 0.20
W	0.47 ± 0.02	0.59 ± 0.02[a]	0.58 ± 0.03	0.53 ± 0.03	0.60 ± 0.03
Tl	124.98 ± 11.40	269.56 ± 9.72	350.71 ± 10.55	359.09 ± 18.41	373.69 ± 15.00[b]
Ti	4.07 (2.25,10.63)	38.98 (30.55,44.30)[a]	68.39 (49.09,77.64)[b]	85.09 (66.89,104.78)[b]	100.73 (79.98,122.21)[b]
Co	2.67 (2.16,2.73)	4.54 (3.97, 4.91)[a]	5.44 (4.70, 5.72)	4.34 (4.15, 5.18)	5.03 (4.14, 6.16)
Cr	0.81 (0.56, 0.95)	1.81 (1.37, 2.50)[a]	2.72 (2.05, 3.58)[b]	2.34 (2.04, 2.86)	2.57 (2.01, 3.71)[b]
Ni	8.59 ± 1.62	21.23 ± 2.19[a]	25.62 ± 3.76	23.62 ± 2.02	25.84 ± 2.50
Sb	116.02 ± 9.58	127.94 ± 5.35	112.14 ± 7.09	116.71 ± 12.61	115.42 ± 6.31
Al	13.39 ± 2.30	21.09 ± 1.60	24.39 ± 3.82	24.93 ± 2.69	30.86 ± 3.10[b]
Fe	32.51 ± 8.11	67.53 ± 5.85	86.59 ± 13.06	96.44 ± 9.82	90.59 ± 15.47
Mn	11.36 ± 2.28	32.76 ± 5.64	67.74 ± 17.01	138.94 ± 10.38[b]	116.47 ± 27.24
Sr	91.06 ± 6.55	182.34 ± 13.14[a]	254.26 ± 18.75	329.87 ± 21.10[b]	356.21 ± 24.34[b]
Cd	180.81 ± 7.34	244.99 ± 9.17[a]	277.64 ± 14.74	299.18 ± 22.50[b]	302.94 ± 17.47[b]
Sn	169.89 ± 20.65	123.69 ± 11.00	101.14 ± 10.18	111.74 ± 18.96	95.51 ± 7.48
Ba	6.74 (5.86, 9.34)	8.85 (6.87, 9.29)	11.62 (8.19, 17.08)	18.68 (15.40, 21.96)[b]	18.35 (12.31, 25.70)[b]
Pb	0.40 ± 0.05	0.37 ± 0.07	0.42 ± 0.08	0.32 ± 0.07	0.21 ± 0.03
U	263.85 ± 34.25	134.44 ± 13.09	100.12 ± 8.90	110.48 ± 8.09	108.60 ± 11.88

ZL, Zucker lean group; ZDF, Zucker diabetic fatty group. ZDF + VL, ZDF + low-dose $1,25(OH)_2D_3$ group (2 μg/kg·bw); ZDF + VM, ZDF + middle-dose $1,25(OH)_2D_3$ group (8 μg/kg·bw); ZDF + VH, ZDF + high-dose $1,25(OH)_2D_3$ group (16 μg/kg·bw). The unite of Tl, Sb, Cd, Sn and U was expressed as ng/g UCR. Data are presented as mean ± SEM or median (IQR) ($n \geq 8$). [a]$P < 0.05$ vs. the ZL group, [b]$P < 0.05$ vs. the ZDF group using one way ANOVA tests.

the urinary levels of Se, Mo, As, Rb, W, Ni, Sb, Sn, and U after $1,25(OH)_2D_3$ intervention were significantly decreased compared to the ZDF group, while Sr and Ba levels were increased compared to the ZDF group ($P < 0.05$).

Effect of $1,25(OH)_2D_3$ on urinary trace elements in spontaneously diabetic rats at 6th week of intervention

As seen from Table 4, after 6 weeks of intervention, the urinary levels of Cu, Zn, Se, Mo, As, Rb, V, W, Tl, Ti, Co, Cr, Ni, Sb, Al, Fe, Mn, Cd, Sn, Pb, and U in the ZDF group of rats were significantly increased compared to the ZL group. And the urinary levels of Cu, Zn, Mo, As, Rb, Cr, and U after $1,25(OH)_2D_3$ intervention decreased compared with the ZDF group, while Sr level increased compared with the ZDF group ($P < 0.05$).

Effect of $1,25(OH)_2D_3$ on urinary trace elements in spontaneously diabetic rats at 7th week of intervention

As can be seen from Table 5, after 7 weeks of intervention, the urinary levels of Cu, Zn, Se, Mo, As, Rb, V, W, Tl, Ti, Co, Cr, Ni, Sb, Al, Fe, Mn, Cd, and Sn in the ZDF group of rats were significantly increased compared to the ZL group, and the urinary levels of Cu, Zn, Se, Mo after $1,25(OH)_2D_3$ intervention decreased compared to the ZDF group, while Sr level increased compared to the ZDF group after $1,25(OH)_2D_3$ intervention ($P < 0.05$).

Dynamic analysis of copper, zinc, selenium, and molybdenum levels in the urine of spontaneously diabetic rats and the effect of $1,25(OH)_2D_3$ intervention

From Tables 2–5, it was found that the trend of Cu, Zn, Se, and Mo levels in the urine of spontaneously diabetic rats after $1,25(OH)_2D_3$ intervention was the most obvious. These four trace elements were thus plotted to visualize their dynamic changes with the extension of the intervention time. As shown in Figures 3A–D, the urinary levels of Cu, Zn, Se, and Mo in the ZDF group increased significantly ($P < 0.05$) compared with the ZL group at 1st week of intervention. At 4th week of intervention, the urinary levels of Cu, Zn, Se, and Mo in rats in each dose group of $1,25(OH)_2D_3$ showed a tendency to decrease compared with the ZDF group. And with the extension of the intervention time, the differences of the above four urinary trace elements levels in the rats of ZDF + VM and ZDF + VH groups gradually increased compared with the ZDF group, which to some extent coincided with the trend of urine volume. Additionally, we also measured the urinary levels of calcium (Ca) and magnesium (Mg). As displayed in

TABLE 3 Effects of $1,25(OH)_2D_3$ on urine metal concentration of Zucker rats in the fourth week of treatment.

Metals (μg/g UCR)	ZL	ZDF	ZDF + VL	ZDF + VM	ZDF + VH
Cu	124.73 ± 6.21	175.24 ± 11.69	227.33 ± 15.93	180.33 ± 16.62	155.38 ± 12.27
Zn	78.98 ± 4.09	323.70 ± 13.83[a]	324.78 ± 18.42	251.30 ± 20.77	210.64 ± 25.16
Se	7.23 ± 0.48	17.27 ± 1.10[a]	18.13 ± 1.23	14.58 ± 0.64[b]	13.19 ± 0.44[b]
Mo	179.97 ± 9.65	246.72 ± 12.79[a]	280.37 ± 17.30	214.16 ± 11.76	178.17 ± 7.08[b]
As	10.26 ± 0.42	14.22 ± 0.67[a]	16.14 ± 0.79[b]	14.13 ± 0.72	12.35 ± 0.38[b]
Rb	758.61 ± 39.41	1658.90 ± 65.63[a]	1756.48 ± 89.96	1507.59 ± 76.31	1357.63 ± 62.20[b]
V	0.81 ± 0.07	1.77 ± 0.07[a]	2.15 ± 0.23	1.64 ± 0.12	1.64 ± 0.13
W	0.30 ± 0.01	0.44 ± 0.02[a]	0.48 ± 0.02	0.42 ± 0.02	0.37 ± 0.01[b]
Tl	79.94 ± 7.82	247.06 ± 11.55[a]	278.67 ± 12.78	235.41 ± 10.79	226.95 ± 9.71
Ti	15.86 ± 1.89	68.61 ± 4.20[a]	95.10 ± 6.37	74.15 ± 4.33	63.86 ± 3.42
Co	1.61 ± 0.13	2.71 ± 0.16[a]	3.72 ± 0.27	2.95 ± 0.24	2.43 ± 0.14
Cr	1.01 (0.81,1.45)	3.64 (2.85, 4.77)[a]	2.99 (2.04, 4.19)	1.78 (1.54, 3.07)	2.39 (1.63, 2.96)
Ni	7.05 (5.76, 7.79)	22.86 (22.13, 25.07)[a]	23.92 (17.44, 32.54)	17.17 (13.62, 20.68)	15.78 (13.17, 19.29)[b]
Sb	64.24 ± 4.06	122.21 ± 5.96[a]	129.47 ± 10.90	88.16 ± 6.85[b]	83.05 ± 6.71[b]
Al	16.28 ± 1.15	47.98 ± 3.08[a]	45.80 ± 6.62	40.69 ± 3.66	41.22 ± 4.70
Fe	37.00 (30.06, 42.73)	160.15 (130.83, 187.32)[a]	157.40 (118.70, 234.62)	143.06 (103.51, 232.23)	130.34 (104.25, 301.02)
Mn	7.82 ± 0.80	136.11 ± 14.05[a]	176.39 ± 20.69	191.75 ± 25.01	178.98 ± 28.79
Sr	35.38 ± 2.08	82.67 ± 3.98	240.48 ± 23.86[b]	223.33 ± 19.04[b]	171.14 ± 15.84
Cd	107.04 ± 5.34	200.58 ± 12.13[a]	262.67 ± 20.53	225.79 ± 20.18	213.79 ± 20.61
Sn	203.23 ± 16.88	193.63 ± 19.15	141.30 ± 13.97	97.07 ± 3.83[b]	85.28 ± 6.63[b]
Ba	3.93 ± 0.43	11.13 ± 0.40[a]	19.86 ± 2.24[b]	20.48 ± 1.56[b]	19.81 ± 2.05[b]
Pb	0.20 (0.16, 0.30)	0.46 (0.24, 0.65)	0.26 (0.16, 0.90)	0.19 (0.14, 0.49)	0.33 (0.11, 0.63)
U	201.42 ± 13.23	270.76 ± 19.36[a]	160.84 ± 18.68[b]	173.86 ± 17.90[b]	186.53 ± 24.42[b]

ZL, Zucker lean group; ZDF, Zucker diabetic fatty group. ZDF + VL, ZDF + low-dose $1,25(OH)_2D_3$ group (2 μg/kg·bw); ZDF + VM, ZDF + middle-dose $1,25(OH)_2D_3$ group (8 μg/kg·bw); ZDF + VH, ZDF + high-dose $1,25(OH)_2D_3$ group (16 μg/kg·bw). The unite of Tl, Sb, Cd, Sn, and U was expressed as ng/g UCR. Data are presented as mean ± SEM or median (IQR) ($n \geq 9$). [a] $P < 0.05$ vs. the ZL group, [b] $P < 0.05$ vs. the ZDF group using one way ANOVA tests.

Figures 3E,F, the urinary levels of Ca and Mg in the ZDF group increased compared with the ZL group during the whole intervention, but the differences were not significant for urinary Ca. Relatively, the urinary levels of Ca and Mg in rats in each dose group of $1,25(OH)_2D_3$ maintained high levels even upper than the ZDF group.

Discussion

The present study provides evidence that $1,25(OH)_2D_3$ improves kidney index, insulin sensitivity, abnormal glucose and lipid metabolism, renal function injury and urine trace element metabolism disorder in spontaneous diabetic rats. We found that spontaneous diabetes could lead to renal function damage by increasing MALB, UACR, urine creatinine contents, and exacerbate the disorder of most trace elements in urine. As predicted, we showed that $1,25(OH)_2D_3$ treatment significantly attenuated renal damage and decreased urine Cu, Zn, Se, and Mo contents. However, given that there are few studies on vitamin D reducing urinary trace elements in diabetic patients or models, more studies are needed to confirm this conclusion in the future.

Evidence has reported that MALB is a marker of early kidney damage in DN. In our study, the continuous increase of MALB content confirmed the occurrence and development of renal dysfunction in spontaneous diabetic rats, accompanied by the continuous increase of UACR and urinary creatinine content. Importantly, treatment with $1,25(OH)_2D_3$ decreased the impairment of renal function. Similarly, $1,25(OH)_2D_3$ has been reported to ameliorate renal dysfunction in rats with chronic renal failure (17) or may contribute to delay the deterioration in glomerular function and reduce the occurrence of ESRD in patients with diabetes (18). Besides, our previous research has revealed the positive effect of $1,25(OH)_2D_3$ on renal morphological, pathological changes and oxidative stress damage (19). Considering that trace elements are closely related to diabetes, the levels of trace elements in urine were further detected. It was found that the metabolism of trace elements in the urine of spontaneous diabetic rats was disordered, and the intervention of $1,25(OH)_2D_3$ could significantly reverse the urinary Cu, Zn, Se, and Mo contents of ZDF rats. The results also suggested that the disturbance of trace element metabolism in ZDF rats might be related to kidney damage.

Both a cross-sectional study and a multisite, multiethnic cohort study indicated that increased urinary excretion of zinc was associated with elevated risk of diabetes (20, 21). Some scholars have studied the effect of STZ-induced insulin-dependent diabetes on urinary excretion of zinc, copper and iron, and found that the onset of diabetes symptoms was

TABLE 4 Effects of $1,25(OH)_2D_3$ on urine metal concentration of Zucker rats in the sixth week of treatment.

Metals (μg/g UCR)	ZL	ZDF	ZDF + VL	ZDF + VM	ZDF + VH
Cu	109.08 ± 5.42	199.31 ± 14.34[a]	164.56 ± 11.00[b]	142.63 ± 8.53[b]	166.97 ± 6.29[b]
Zn	62.54 ± 2.22	393.50 ± 27.54[a]	313.71 ± 29.80	250.58 ± 23.82[b]	257.75 ± 26.79[b]
Se	6.26 ± 0.31	22.07 ± 2.02[a]	18.83 ± 1.75	14.79 ± 0.69	16.03 ± 0.80
Mo	148.06 ± 8.49	233.96 ± 10.46[a]	207.62 ± 10.57	178.25 ± 6.12[b]	166.84 ± 12.83[b]
As	9.26 ± 0.39	15.88 ± 0.92[a]	15.58 ± 0.81	12.88 ± 0.54[b]	12.11 ± 0.85[b]
Rb	668.60 ± 25.85	1773.86 ± 84.74[a]	1646.44 ± 78.37	1359.78 ± 51.40	1161.21 ± 104.14[b]
V	0.85 (0.79, 1.04)	2.25 (1.61, 3.25)[a]	2.01 (1.49, 2.56)	1.63 (1.51, 2.08)	2.10 (1.48, 2.76)
W	0.23 ± 0.01	0.47 ± 0.04[a]	0.45 ± 0.03	0.37 ± 0.01	0.35 ± 0.04
Tl	56.24 ± 4.08	261.25 ± 15.29[a]	245.89 ± 12.34	225.46 ± 12.09	203.13 ± 15.32
Ti	12.42 ± 1.15	73.87 ± 5.19[a]	90.49 ± 8.03	74.94 ± 3.53	72.49 ± 7.36
Co	1.62 ± 0.05	3.12 ± 0.25[a]	3.16 ± 0.29	2.69 ± 0.09	2.64 ± 0.30
Cr	0.71 ± 0.04	4.84 ± 0.76[a]	3.22 ± 0.48	1.83 ± 0.25[b]	2.04 ± 0.22
Ni	7.87 ± 0.65	33.84 ± 3.91[a]	29.32 ± 4.40	19.95 ± 1.83	21.00 ± 3.89
Sb	33.89 ± 1.85	118.03 ± 11.32[a]	90.52 ± 3.30	80.52 ± 5.90	84.91 ± 8.67
Al	13.09 ± 0.99	67.87 ± 9.30[a]	53.41 ± 9.35	38.68 ± 4.85	43.17 ± 7.43
Fe	37.26 (32.80, 49.50)	194.24 (142.57, 285.08)[a]	180.67 (125.17, 217.62)	153.23 (106.00, 355.21)	263.92 (111.32, 390.51)
Mn	4.62 ± 0.48	238.38 ± 29.77[a]	258.95 ± 45.63	279.53 ± 42.50	320.14 ± 68.20
Sr	29.53 ± 1.63	95.48 ± 4.76	197.15 ± 16.00	218.55 ± 16.94[b]	247.38 ± 24.49[b]
Cd	76.57 ± 4.04	201.91 ± 16.74[a]	235.17 ± 25.16	238.33 ± 19.34	258.73 ± 38.69
Sn	32.72 ± 1.40	165.66 ± 26.52[a]	94.59 ± 12.36	76.02 ± 6.63	92.63 ± 16.55
Ba	2.51 ± 0.23	12.89 ± 1.31	18.37 ± 1.45	20.30 ± 1.34	20.12 ± 2.18
Pb	0.13 ± 0.01	0.84 ± 0.22[a]	0.41 ± 0.11	0.33 ± 0.09	0.38 ± 0.07
U	156.91 ± 10.00	261.99 ± 22.49[a]	148.10 ± 18.01[b]	201.41 ± 35.95	226.30 ± 32.70

ZL, Zucker lean group; ZDF, Zucker diabetic fatty group. ZDF + VL, ZDF + low-dose $1,25(OH)_2D_3$ group (2 μg/kg·bw); ZDF + VM, ZDF + middle-dose $1,25(OH)_2D_3$ group (8 μg/kg·bw); ZDF + VH, ZDF + high-dose $1,25(OH)_2D_3$ group (16 μg/kg·bw). The unite of Tl, Sb, Cd, Sn, and U was expressed as ng/g UCR. Data are presented as mean ± SEM or median (IQR) ($n \geq 9$). [a]$P < 0.05$ vs. the ZL group, [b]$P < 0.05$ vs. the ZDF group using one way ANOVA tests.

associated with a rapid and sustained increase in the daily excretion of these three trace elements in urine, which was significantly reduced by insulin treatment (22). Combined with our study, it can be indicated that $1,25(OH)_2D_3$ intervention can achieve the efficacy of insulin therapy to a certain extent. Another study indicated that diabetes can alter levels of copper, zinc, magnesium, and lipid peroxidation, and it also highlighted that disturbance in mineral metabolism was more pronounced in diabetic patients with specific complications (23). Gong later suggested that an imbalance in copper homeostasis may be a key event in triggering the development of diabetic nephropathy (24). Our present study further found that $1,25(OH)_2D_3$ may reduce diabetic kidney injury by restoring urinary copper levels.

Currently, urinary trace element levels are expressed in different ways. Data from a study in Northeast China showed an increase in urinary Zn levels, a decrease in the Zn/Cu ratio, and a decrease in urinary Se levels in patients with T2DM (25). A cross-sectional study has indicated significantly higher urinary Zn levels and no significant changes in urinary Cu, Mo, and Se levels in diabetic patients as compared to healthy subjects (26). However, it is worth noting that these studies present trace element concentrations rather than contents. In a STZ-induced mild diabetic rat model, 24-h urinary excretion of zinc, copper, iron, calcium, and magnesium was found to be positively correlated with urine volume (27), whose daily mineral excretion was determined by multiplying the daily urine volume by the concentration of each mineral in the urine. In most studies, however, such results are calculated by the ratio of the concentration of minerals in urine to the concentration of urinary creatinine. Our research used the latter method, while suggesting that the excretions of minerals in urine were proportional to the amount of urine. The reason could be that hyperglycemia may cause hyperosmolar urine or impair tubular reabsorption of trace elements which may further hamper tubular function and lead to hyperfiltration.

In a STZ-induced diabetic rat model, it showed increased levels of Fe and Cu and decreased levels of Zn and Mg in liver and kidney tissues, decreased contents of 24 h urinary Cu and increased contents of 24 h urinary Zn and Mg (28). This study suggests that impaired trace element metabolism may be associated with disturbances in oxidative homeostasis in liver and kidney tissues. More importantly, vitamin D supplementation modulated blood and tissue zinc concentrations, hepatic glutathione, and blood biochemical parameters in diabetic rats (29). However, studies on whether vitamin D supplementation modulates urinary trace elements in diabetic rats are relatively rare. Compared with previous studies, this study used ICP-MS to dynamically detect the concentrations of more than 20 trace elements in urine, and at the same time

TABLE 5 Effects of $1,25(OH)_2D_3$ on urine metal concentration of Zucker rats in the seventh week of treatment.

Metals (μg/g UCR)	ZL	ZDF	ZDF + VL	ZDF + VM	ZDF + VH
Cu	83.46 ± 4.68	165.69 ± 6.73[a]	129.57 ± 12.55[b]	115.86 ± 8.45[b]	138.64 ± 6.27[b]
Zn	58.34 ± 5.06	364.47 ± 26.67[a]	289.48 ± 34.78	182.51 ± 17.71[b]	176.57 ± 9.78[b]
Se	6.24 ± 0.31	23.44 ± 2.34[a]	18.68 ± 1.98	12.46 ± 0.63[b]	12.97 ± 0.58[b]
Mo	134.93 ± 6.24	211.04 ± 6.79[a]	204.13 ± 12.74	179.93 ± 5.14[b]	176.77 ± 10.52[b]
As	8.03 ± 0.30	14.30 ± 0.94[a]	13.40 ± 0.80	11.49 ± 0.39	12.15 ± 0.34
Rb	593.46 ± 20.74	1689.40 ± 58.11[a]	1551.81 ± 106.79	1503.00 ± 50.90	1520.98 ± 76.37
V	0.83 ± 0.07	1.89 ± 0.18[a]	1.58 ± 0.12	1.71 ± 0.19	2.29 ± 0.21
W	0.21 ± 0.01	0.41 ± 0.03[a]	0.36 ± 0.03	0.35 ± 0.01	0.36 ± 0.02
Tl	42.80 ± 2.83	244.11 ± 8.85[a]	247.83 ± 12.76	219.54 ± 3.50	223.77 ± 12.35
Ti	6.50 ± 1.27	63.26 ± 4.70[a]	65.23 ± 5.03	50.09 ± 2.19	50.38 ± 2.63
Co	1.12 ± 0.07	2.63 ± 0.20[a]	2.72 ± 0.28	2.17 ± 0.12	2.31 ± 0.04
Cr	0.65 ± 0.06	3.67 ± 0.74[a]	1.83 ± 0.37	1.25 ± 0.14	2.42 ± 0.52
Ni	5.60 (4.71, 7.29)	24.44 (18.16, 31.77)[a]	16.58 (13.18, 21.17)	12.87 (11.31, 18.29)	17.94 (15.56, 21.99)
Sb	28.43 ± 1.66	75.25 ± 9.27[a]	74.19 ± 7.07	69.79 ± 5.04	83.22 ± 6.63
Al	8.79 ± 0.94	48.90 ± 5.65[a]	35.03 ± 7.34	31.14 ± 5.84	39.99 ± 5.72
Fe	26.08 ± 3.76	151.82 ± 13.84[a]	140.00 ± 11.97	143.16 ± 15.32	223.45 ± 23.37
Mn	4.47 ± 0.79	189.60 ± 17.49[a]	200.76 ± 23.82	169.96 ± 14.34	227.92 ± 22.15
Sr	25.64 ± 1.95	93.12 ± 5.09	163.37 ± 6.59[b]	139.96 ± 13.47	143.47 ± 10.97
Cd	68.60 ± 2.47	169.88 ± 9.64[a]	190.23 ± 12.46	176.55 ± 13.37	187.58 ± 9.15
Sn	23.10 (20.84, 24.77)	55.44 (37.00, 80.77)[a]	63.84 (45.82, 104.49)	48.76 (43.89, 55.70)	52.79 (46.52, 66.67)
Ba	1.75 ± 0.18	10.46 ± 0.73	15.26 ± 0.93	14.22 ± 1.21	15.05 ± 1.58
Pb	0.11 (0.08, 0.17)	0.25 (0.16, 0.49)	0.12 (0.10, 0.30)	0.11 (0.09, 0.17)	0.29 (0.16, 0.78)
U	124.09 ± 13.98	172.70 ± 20.56	111.73 ± 8.90	157.34 ± 15.67	191.45 ± 24.99

ZL, Zucker lean group; ZDF, Zucker diabetic fatty group. ZDF + VL, ZDF + low-dose $1,25(OH)_2D_3$ group (2 μg/kg·bw); ZDF + VM, ZDF + middle-dose $1,25(OH)_2D_3$ group (8 μg/kg·bw); ZDF + VH, ZDF + high-dose $1,25(OH)_2D_3$ group (16 μg/kg·bw). The unite of Tl, Sb, Cd, Sn and U was expressed as ng/g UCR. Data are presented as mean ± SEM or median (IQR) ($n \geq 9$). [a]$P < 0.05$ vs. the ZL group, [b]$P < 0.05$ vs. the ZDF group using one way ANOVA tests.

normalized and corrected the concentration of urine creatinine. It has made a comprehensive and systematic evaluation of the preventive effect of $1,25(OH)_2D_3$ on urinary trace elements disorders in diabetic rats. Zinc (Zn) is an essential trace element in many enzymes and is involved in antioxidant defense. Numerous studies have shown that zinc supplementation has a protective effect against diabetic renal damage by promoting metallothionein synthesis (30, 31) and regulating oxidative stress (32–34). Meanwhile, triethylenetetramine (TETA) is a Copper (II)-selective chelation that inhibits copper-mediated oxidative stress and restores antioxidant defenses. A growing body of research suggests that TETA may reduce the chronic complications of diabetes by enhancing antioxidant defense mechanisms (35, 36).

Since copper and zinc are important components of superoxide dismutase (SOD), selenium is a component of the antioxidant enzyme GSH-Px, both of which are major natural antioxidants capable of scavenging excess free radicals from the body. Therefore, we speculate that renal function damage in spontaneous diabetic rats induces an increase in the excretion of urinary trace elements, which in turn causes trace element metabolism disorders. However, $1,25(OH)_2D_3$ intervention may improve the metabolic disorder of trace elements by reducing the renal function damage in ZDF rats, among which copper, zinc, and selenium are most closely related to oxidative stress. Ito further pointed out that increased urinary copper excretion in patients with advanced diabetic nephropathy may be due to the copper-albumin and ceruloplasmin-copper complexes through the impaired glomeruli (37). Considering that the related mechanism of $1,25(OH)_2D_3$ improving specific trace elements in urine is unknown, future research is warranted to explore the underlying mechanisms. Except for urine trace elements, we also focused the urinary levels of Ca and Mg. In brief, $1,25(OH)_2D_3$ may accelerate urinary Ca and urinary Mg excretion in the early period, which is less pronounced with the extension of the intervention. This phenomenon needs to be further confirmed by other relevant studies.

Eventually, from our study, we speculate that $1,25(OH)_2D_3$ supplementation may have a positive effect in diabetic rats that are deficient or inadequate in vitamin D status. Conversely, if vitamin D levels are adequate in diabetic rats, $1,25(OH)_2D_3$ intervention may have no significant improvement. This is an important hypothesis that we need to validate in our next study.

10.3389/fnut.2022.1042558

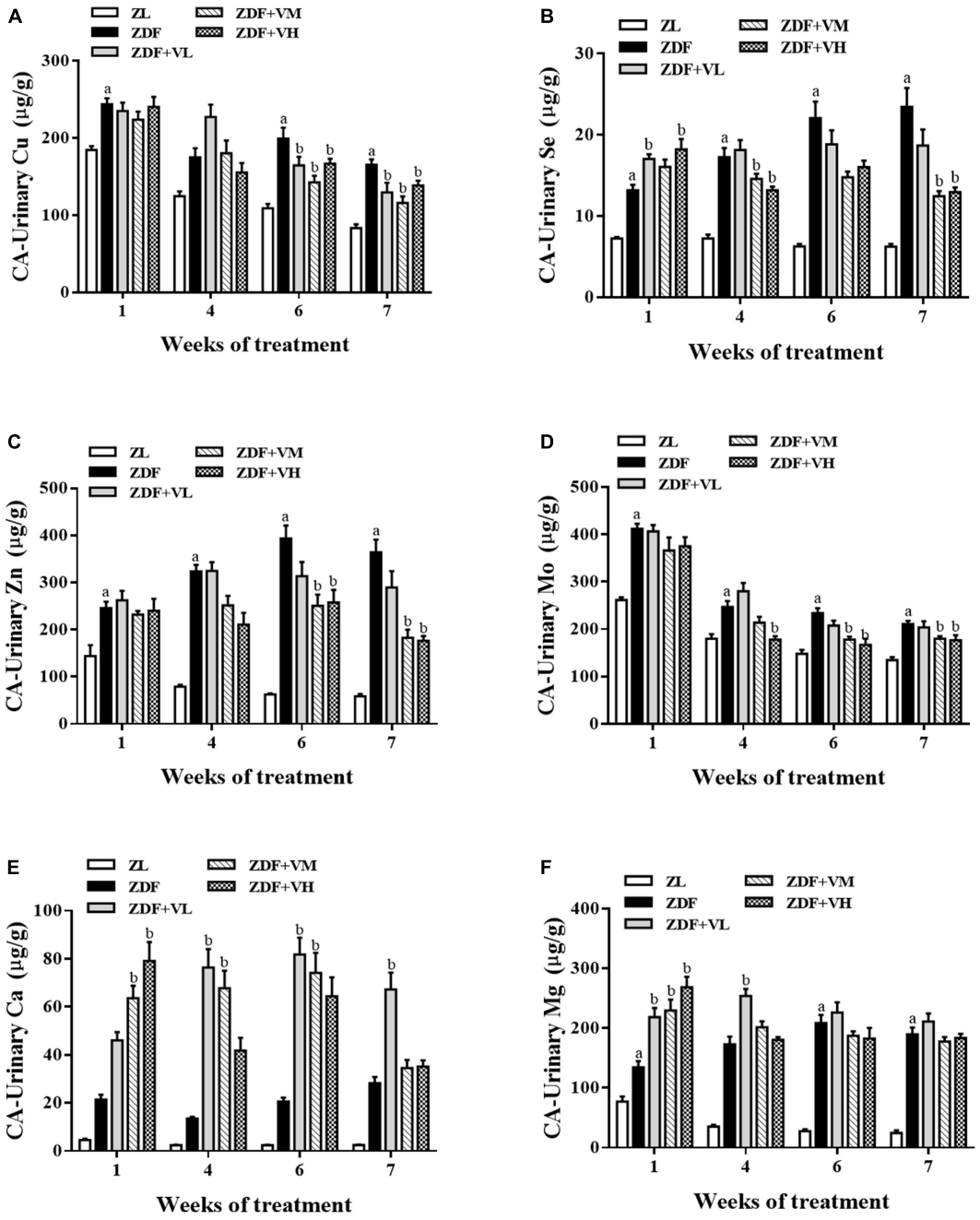

FIGURE 3
Effect of 1,25$(OH)_2D_3$ on urinary mineral levels in Zucker rats. **(A)** Urinary Cu/UCR. **(B)** Urinary Se/UCR. **(C)** Urinary Zn/UCR. **(D)** Urinary Mo/UCR. **(E)** Urinary Ca/UCR. **(F)** Urinary Mg/UCR. ZL, Zucker lean group; ZDF, Zucker diabetic fatty group; ZDF + VL, ZDF + low-dose 1,25$(OH)_2D_3$ group (2 μg/kg·bw); ZDF + VM, ZDF + middle-dose 1,25$(OH)_2D_3$ group (8 μg/kg·bw); ZDF + VH, ZDF + high-dose 1,25$(OH)_2D_3$ group (16 μg/kg·bw). Data are presented as mean ± SEM ($n \geq 9$). $^{a}P < 0.05$ vs. the ZL group, $^{b}P < 0.05$ vs. the ZDF group.

Conclusion

In summary, our research confirmed that vitamin D-deficient diabetic rats suffered from renal injury and disturbance of trace element metabolism, manifested by increased production of MALB, UACR, urine creatinine content, and urinary excretion of trace elements. Interestingly, we found that 1,25$(OH)_2D_3$ reversed renal impairment and improved urinary excretions of Cu, Zn, Se, and Mo in ZDF rats. Our study indicated that 1,25$(OH)_2D_3$ may be a potential therapeutic strategy for correcting trace element disorders in DN patients in the near future.

Data availability statement

The original contributions presented in this study are included in the article/supplementary material, further inquiries can be directed to the corresponding authors.

Ethics statement

This animal study was reviewed and approved by the Animal Ethical Committee of Tongji Medical College.

Author contributions

DW: conceptualization, performing the experiment, and writing—original draft preparation. NW and JZ: performing the experiment. GLu: interpreting the results. YL: conceptualization. WY and HT: data analysis. GLi and JW: funding acquisition. LH: revising the manuscript. All authors contributed to the article and approved the submitted version.

Funding

This study was financially supported by the Science and Technology Project of Hebei Education Department (grant no. QN2022016), the National Natural Science Foundation of China (grant no. 81703226), and the Hubei Key Laboratory of Kidney Disease Pathogenesis and Intervention (grant no. SB202107).

Acknowledgments

We thank Xiaohao Liu from Beijing Normal University for helping to polish English language.

Conflict of interest

The authors declare that the research was conducted in the absence of any commercial or financial relationships that could be construed as a potential conflict of interest.

Publisher's note

References

1. International Diabetes Federation. *IDF Diabetes Atlas*. 9th ed. Brussels: International Diabetes Federation (2019).

2. Li Y, Teng D, Shi X, Qin G, Qin Y, Quan H, et al. Prevalence of diabetes recorded in mainland china using 2018 diagnostic criteria from the American diabetes association: national cross sectional study. *BMJ.* (2020) 369:m997. doi: 10.1136/bmj.m997

3. DeFronzo R, Ferrannini E, Groop L, Henry R, Herman W, Holst J, et al. Type 2 diabetes mellitus. *Nat Rev Dis Primers.* (2015) 1:15019. doi: 10.1038/nrdp.2015.19

4. Chen M, Lin P, Tsou C, Wang J, Lin W. Selected metals status in patients with noninsulin-dependent diabetes mellitus. *Biol Trace Elem Res.* (1995) 50:119–24. doi: 10.1007/bf02789414

5. Kazi T, Afridi H, Kazi N, Jamali M, Arain M, Jalbani N, et al. Copper, chromium, manganese, iron, nickel, and zinc levels in biological samples of diabetes mellitus patients. *Biol Trace Elem Res.* (2008) 122:1–18. doi: 10.1007/s12011-007-8062-y

6. Zhang H, Yan C, Yang Z, Zhang W, Niu Y, Li X, et al. Alterations of serum trace elements in patients with type 2 diabetes. *J Trace Elem Med Biol.* (2017) 40:91–6. doi: 10.1016/j.jtemb.2016.12.017

7. Holick M. The vitamin d deficiency pandemic: approaches for diagnosis, treatment and prevention. *Rev Endocr Metab Disord.* (2017) 18:153–65. doi: 10.1007/s11154-017-9424-1

8. Thacher T, Clarke B. Vitamin D insufficiency. *Mayo Clin Proc.* (2011) 86:50–60. doi: 10.4065/mcp.2010.0567

9. Verstuyf A, Carmeliet G, Bouillon R, Mathieu C. Vitamin D: a pleiotropic hormone. *Kidney Int.* (2010) 78:140–5. doi: 10.1038/ki.2010.17

10. Shen L, Zhuang Q, Ji H. Assessment of vitamin D levels in type 1 and type 2 diabetes patients: results from metaanalysis. *Mol Nutr Food Res.* (2016) 60:1059–67. doi: 10.1002/mnfr.201500937

11. Gagnon C, Lu Z, Magliano D, Dunstan D, Shaw J, Zimmet P, et al. Serum 25-hydroxyvitamin d, calcium intake, and risk of Type 2 diabetes after 5 years: results from a national, population-based prospective study (the Australian diabetes, obesity and lifestyle study). *Diabetes Care.* (2011) 34:1133–8. doi: 10.2337/dc10-2167

12. Lucato P, Solmi M, Maggi S, Bertocco A, Bano G, Trevisan C, et al. Low Vitamin d levels increase the risk of type 2 diabetes in older adults: a systematic review and meta-analysis. *Maturitas.* (2017) 100:8–15. doi: 10.1016/j.maturitas.2017.02.016

13. Peng Y, Li L. Serum 25-hydroxyvitamin d level and diabetic nephropathy in patients with type 2 diabetes mellitus. *Int Urol Nephrol.* (2015) 47:983–9. doi: 10.1007/s11255-015-0983-3

14. Park S, Kim D, Kang S. Vitamin D deficiency impairs glucose-stimulated insulin secretion and increases insulin resistance by reducing Ppar-gamma expression in nonobese type 2 diabetic rats. *J Nutr Biochem.* (2016) 27:257–65. doi: 10.1016/j.jnutbio.2015.09.013

15. Matthews D, Hosker J, Rudenski A, Naylor B, Treacher D, Turner R. Homeostasis model assessment: insulin resistance and beta-cell function from fasting plasma glucose and insulin concentrations in man. *Diabetologia.* (1985) 28:412–9. doi: 10.1007/bf00280883

16. Reaven G. Homa-beta in the Ukpds and adopt. Is the natural history of type 2 diabetes characterised by a Progressive and inexorable loss of insulin secretory function? Maybe? Maybe not? *Diab Vasc Dis Res.* (2009) 6:133–8. doi: 10.1177/1479164109336038

17. Yang X, Wan J, Yuan J, Dong R, Da J, Sun Z, et al. Effects of calcitriol on peripheral endothelial progenitor cells and renal renovation in rats with chronic renal failure. *J Steroid Biochem Mol Biol.* (2021) 214:105956. doi: 10.1016/j.jsbmb.2021.105956

18. Nakhoul N, Thawko T, Farber E, Dahan I, Tadmor H, Nakhoul R, et al. The therapeutic effect of active vitamin D supplementation in preventing the progression of diabetic nephropathy in a diabetic mouse model. *J Diabetes Res.* (2020) 2020:7907605. doi: 10.1155/2020/7907605

19. Wang D, Li Y, Wang N, Luo G, Wang J, Luo C, et al. 1α,25-dihydroxyvitamin D_3 prevents renal oxidative damage via the Parp1/Sirt1/Nox4 pathway in zucker diabetic fatty rats. *Am J Physiol Endocrinol Metab.* (2020) 318:E343–56. doi: 10.1152/ajpendo.00270.2019

20. Wang X, Karvonen-Gutierrez C, Herman W, Mukherjee B, Harlow S, Park S. Urinary metals and incident diabetes in midlife women: study of women's health across the nation (Swan). *BMJ Open Diabetes Res Care.* (2020) 8:e001233. doi: 10.1136/bmjdrc-2020-001233

21. Velmurugan G, Swaminathan K, Veerasekar G, Purnell J, Mohanraj S, Dhivakar M, et al. Metals in urine in relation to the prevalence of pre-diabetes, diabetes and atherosclerosis in rural India. *Occup Environ Med.* (2018) 75:661–7. doi: 10.1136/oemed-2018-104996

22. Lau A, Failla M. Urinary excretion of zinc, copper and iron in the streptozotocin-diabetic rat. *J Nutr.* (1984) 114:224–33. doi: 10.1093/jn/114.1.224

23. Walter R Jr, Uriu-Hare J, Olin K, Oster M, Anawalt B, Critchfield J, et al. Copper, zinc, manganese, and magnesium status and complications of diabetes mellitus. *Diabetes Care.* (1991) 14:1050–6. doi: 10.2337/diacare.14.11.1050

24. Gong D, Lu J, Chen X, Reddy S, Crossman D, Glyn-Jones S, et al. A copper(Ii)-selective chelator ameliorates diabetes-evoked renal fibrosis and albuminuria, and suppresses pathogenic Tgf-beta activation in the kidneys of rats used as a model of diabetes. *Diabetologia.* (2008) 51:1741–51. doi: 10.1007/s00125-008-1088-7

25. Zhou Q, Guo W, Jia Y, Xu J. Serum and urinary selenium status in patients with the pre-diabetes and diabetes in northeast China. *Biol Trace Elem Res.* (2019) 191:61–9. doi: 10.1007/s12011-018-1604-7

26. Flores C, Puga M, Wrobel K, Garay Sevilla M, Wrobel K. Trace elements status in diabetes mellitus type 2: possible role of the interaction between molybdenum and copper in the progress of typical complications. *Diabetes Res Clin Pract.* (2011) 91:333–41. doi: 10.1016/j.diabres.2010.12.014

27. Gomez T, Bequer L, Mollineda A, Molina J, Alvarez A, Lavastida M, et al. Concentration of zinc, Copper, iron, calcium, and magnesium in the serum, tissues, and urine of streptozotocin-induced mild diabetic rat model. *Biol Trace Elem Res.* (2017) 179:237–46. doi: 10.1007/s12011-017-0962-x

28. Ozcelik D, Tuncdemir M, Ozturk M, Uzun H. Evaluation of trace elements and oxidative stress levels in the liver and kidney of streptozotocin-induced experimental diabetic rat model. *Gen Physiol Biophys.* (2011) 30:356–63. doi: 10.4149/gpb_2011_04_356

29. Kechrid Z, Hamdi M, Nazıroğlu M, Flores-Arce M. Vitamin D supplementation modulates blood and tissue zinc, liver glutathione and blood biochemical parameters in diabetic rats on a zinc-deficient diet. *Biol Trace Elem Res.* (2012) 148:371–7. doi: 10.1007/s12011-012-9383-z

30. Tang Y, Yang Q, Lu J, Zhang X, Suen D, Tan Y, et al. Zinc Supplementation partially prevents renal pathological changes in diabetic rats. *J Nutr Biochem.* (2010) 21:237–46. doi: 10.1016/j.jnutbio.2008.12.010

31. Ozcelik D, Naziroglu M, Tuncdemir M, Celik O, Ozturk M, Flores-Arce M. Zinc supplementation attenuates metallothionein and oxidative stress changes in kidney of streptozotocin-induced diabetic rats. *Biol Trace Elem Res.* (2012) 150:342–9. doi: 10.1007/s12011-012-9508-4

32. Zhang X, Zhao Y, Chu Q, Wang Z, Li H, Chi Z. Zinc modulates high glucose-induced apoptosis by suppressing oxidative stress in renal tubular epithelial cells. *Biol Trace Elem Res.* (2014) 158:259–67. doi: 10.1007/s12011-014-9922-x

33. Yang F, Li B, Dong X, Cui W, Luo P. The beneficial effects of zinc on diabetes-induced kidney damage in murine rodent model of type 1 diabetes mellitus. *J Trace Elem Med Biol.* (2017) 42:1–10. doi: 10.1016/j.jtemb.2017.03.006

34. Barman S, Pradeep S, Srinivasan K. Zinc supplementation alleviates the progression of diabetic nephropathy by inhibiting the overexpression of oxidative-stress-mediated molecular markers in streptozotocin-induced experimental rats. *J Nutr Biochem.* (2018) 54:113–29. doi: 10.1016/j.jnutbio.2017.11.008

35. Lu J, Gong D, Choong S, Xu H, Chan Y, Chen X, et al. Copper(Ii)-selective chelation improves function and antioxidant defences in cardiovascular tissues of rats as a model of diabetes: comparisons between triethylenetetramine and three less copper-selective transition-metal-targeted treatments. *Diabetologia.* (2010) 53:1217–26. doi: 10.1007/s00125-010-1698-8

36. Cooper G. Selective divalent copper chelation for the treatment of diabetes mellitus. *Curr Med Chem.* (2012) 19:2828–60. doi: 10.2174/092986712800609715

37. Ito S, Fujita H, Narita T, Yaginuma T, Kawarada Y, Kawagoe M, et al. Urinary copper excretion in type 2 diabetic patients with nephropathy. *Nephron.* (2001) 88:307–12. doi: 10.1159/000046013

frontiers | Frontiers in Nutrition

TYPE Mini Review
PUBLISHED 13 February 2023
DOI 10.3389/fnut.2023.1091067

OPEN ACCESS

EDITED BY
Ling Zhao,
The University of Tennessee, Knoxville,
United States

REVIEWED BY
Guoxun Chen,
The University of Tennessee, Knoxville,
United States
Jin-Rong Zhou,
Harvard Medical School,
United States

*CORRESPONDENCE
Ling Tao
✉ ling_tao@fudan.edu.cn

SPECIALTY SECTION
This article was submitted to Nutrition and Metabolism, a section of the journal Frontiers in Nutrition

RECEIVED 06 November 2022
ACCEPTED 25 January 2023
PUBLISHED 13 February 2023

CITATION
Wang K, Yang T, Zhang Y, Gao X and Tao L (2023) The opportunities and challenges for nutritional intervention in childhood cancers.
Front. Nutr. 10:1091067.
doi: 10.3389/fnut.2023.1091067

The opportunities and challenges for nutritional intervention in childhood cancers

Kaiyue Wang[1], Tianyou Yang[2], Yubin Zhang[1], Xiang Gao[1] and Ling Tao[1]*

[1]Department of Nutrition and Food Hygiene, School of Public Health, Institute of Nutrition, Fudan University, Shanghai, China, [2]Department of Pediatric Surgery, Guangzhou Women and Children's Medical Center, Guangzhou Medical University, Guangzhou, China

Diet dictates nutrient availability in the tumor microenvironment, thus affecting tumor metabolic activity and growth. Intrinsically, tumors develop unique metabolic features and are sensitive to environmental nutrient concentrations. Tumor-driven nutrient dependencies provide opportunities to control tumor growth by nutritional restriction or supplementation. This review summarized the existing data on nutrition and pediatric cancers after systematically searching articles up to 2023 from four databases (PubMed, Web of Science, Scopus, and Ovid MEDLINE). Epidemiological studies linked malnutrition with advanced disease stages and poor clinical outcomes in pediatric cancer patients. Experimental studies identified several nutrient dependencies (i.e., amino acids, lipids, vitamins, etc.) in major pediatric cancer types. Dietary modifications such as calorie restriction, ketogenic diet, and nutrient restriction/supplementation supported pediatric cancer treatment, but studies remain limited. Future research should expand epidemiological studies through data sharing and multi-institutional collaborations and continue to discover critical and novel nutrient dependencies to find optimal nutritional approaches for pediatric cancer patients.

KEYWORDS

malnutrition, pediatric cancer, nutrient dependency, dietary modifications, precision nutrition

Introduction

Childhood cancers represent the leading cause of disease-related mortality in childhood (1). Major childhood cancer types include leukemias (i.e., acute lymphoblastic leukemia ALL, acute myeloid leukemia AML), lymphomas (i.e., Hodgkin lymphoma HL, non-Hodgkin lymphoma NHL), brain and spinal cord tumors (i.e., glioblastoma GBM, medulloblastoma MB), peripheral nervous system tumors (i.e., neuroblastoma NB), renal cancers (i.e., Wilms tumor WT), liver cancers (i.e., hepatoblastoma HB), eye cancers (i.e., retinoblastoma RB), bone cancers (i.e., osteosarcoma OS and Ewing sarcoma ES), and soft tissue sarcomas (i.e., rhabdomyosarcoma RMS). The mutational burden in most childhood cancers is substantially lower than that in adult cancers (2, 3). Instead, fusion oncoproteins and epigenetic dysregulations frequently occur in childhood cancers (1, 4). For example, the EWS-FLI1 fusion protein plays a central role in the pathogenesis of ES (4). Oncohistones and aberrant DNA methylations have been identified in pediatric brain tumors (5–7). In addition, copy number alterations such as *MYCN* amplification occurs in many pediatric cancer types, such as NB (8), MB (9), WT (10), RB (11), and RMS (12).

Malnutrition (undernutrition and overnutrition) problems are increasing worldwide (13), raising concerns about the relationship between nutrition and childhood cancers (Table 1).

TABLE 1 Dietary associations and tumor-driven nutrient dependencies in pediatric cancers.

Pediatric cancer type	Pediatric cancer name	Associations between nutrient/diets and pediatric cancers	Tumor-driven nutrient dependencies
Leukemias	Acute lymphoblastic leukemia (ALL)	Protein-energy malnutrition (+) (14, 15) Magnesium and zinc deficiency (+) (16) Maternal obesity and diabetes (+) (17, 18) Maternal diet during pregnancy (vegetables, fruits, protein sources, and folate supplementation) (19–21)	Amino acids: glutamine (22), arginine (23), asparagine (24) Glycolysis and oxidative phosphorylation: glucose uptake (25) Lipids: mevalonate pathway (26) Vitamins: vitamin D (27)
	Acute myeloid leukemia (AML)	Maternal intake of dietary DNA topoisomerase II inhibitors (+) (28)	Amino acids: glutamine (29), arginine (23, 30) Glycolysis and oxidative phosphorylation: PDK1 pathway (31) Lipids: phosphatidylinositol, sphingolipids, free cholesterol, monounsaturated fatty acids (32, 33)
Lymphomas	Hodgkin lymphoma (HL)	Undernutrition (+) (34) Zinc deficiency (+) (16)	Not available
	Non-Hodgkin lymphoma (NHL)	Undernutrition (+) (34) Zinc deficiency (+) (16)	Glycolysis and oxidative phosphorylation: *HK* (35) Vitamins: vitamin D (36)
Brain and spinal cord cancers	Glioblastoma (GBM)	Not available	Amino acids: glutamine (37) Glycolysis and oxidative phosphorylation: *PDK1* (38) Lipids: ketone bodies (39)
	Medulloblastoma (MB)	Maternal diets during pregnancy (candy, chili peppers, and oil products +; fruits, −; yellow-orange vegetables, −) (40, 41)	Amino acids: glutamine (42) Glycolysis and oxidative phosphorylation: *HK* (43) Lipids: Smoothened-activating sterol lipids (i.e., cholesterol and 7-keto-cholesterol) (44)
Peripheral nervous system cancers	Neuroblastoma (NB)	Undernutrition (+) (45) Maternal folate fortification (−) (46)	Amino acids: glutamine (47, 48), SGOC metabolism (49, 50), polyamines (51–53) Glycolysis and oxidative phosphorylation: *HK* (54), *LDHA* (55), *GLUT1* (56), mitochondrial activity (57, 58) Lipids: fatty acid metabolism [*SLC27A2* (59), *FASN* and *SCD* (60, 61), *CPT1* (58)] Vitamins and Minerals: vitamin B12 (62), iron (63, 64)
Eye cancers	Retinoblastoma (RB)	Vitamin D (−) (36)	Glycolysis and oxidative phosphorylation: PDK1 pathway (65) Vitamins: vitamin D (36)
Renal cancers	Wilms tumor (WT)	Folate fortification (−) (66)	Glycolysis and oxidative phosphorylation: *GLUT1* (67), mitochondrial activity (68)
Liver cancers	Hepatoblastoma (HB)	Vitamin D deficiency (+) (36)	Glycolysis and oxidative phosphorylation: *LDHB* (69), *GLUT3* (69) Lipids: fatty acid metabolism (*SREBP-1c* (70)) Vitamins: vitamin D (36)
Bone cancers	Osteosarcoma (OS)	Vitamin D deficiency (+) (36)	Amino acids: SGOC metabolism Glycolysis and oxidative phosphorylation: *HK* (71) Lipids: lipid catabolism and hydroxylation (72) Vitamins: vitamin D (36)
	Ewing sarcoma (ES)	Zinc deficiency (+) (73)	Amino acids: SGOC metabolism (74) Glycolysis and oxidative phosphorylation: *LDHA* (75)
Soft tissue sarcomas	Rhabdomyosarcoma (RMS)	Not available	Lipids: fatty acid oxidation (76)

(+) positive association; (−) negative association.

Abbreviations: ALL, acute lymphoblastic leukemia; AML, acute myeloid leukemia; CPT1, carnitine palmitoyltransferase 1; DHA, docosahexaenoic acid; EPA, eicosapentaenoic acid; ES, Ewing sarcoma; FASN, fatty acid synthase; GBM, glioblastoma; GLUT, glucose transporter; HB, hepatoblastoma; HK, hexokinase; HL, Hodgkin lymphoma; LDHA, lactate dehydrogenase; MB, medulloblastoma; MTHFD, methylenetetrahydrofolate dehydrogenase; NB, neuroblastoma; NHL, non-Hodgkin lymphoma; ODC1, ornithine decarboxylase; OS, osteosarcoma; PDK, pyruvate dehydrogenase kinase; RB, retinoblastoma; RMS, rhabdomyosarcoma; SCD, stearoyl-CoA desaturase; SGOC, serine-glycine-one-carbon; SLC27A2, fatty acid transporter; SLC3A2, Polyamine transporter; SREBP-1c, sterol regulatory element-binding protein-1c; WT, Wilms tumor.

Nutrient deficiency and obesity at diagnosis are associated with poor clinical outcomes in childhood cancers (34, 45, 77–79). Maternal nutritional status also links to the risk of developing hematopoietic and solid childhood tumors (17–21). Overall, the current epidemiological studies are limited. This is partly due to a lower incidence of childhood cancers and little nutritional evaluation at diagnosis (80). On the other side of the coin, multi-omics technology corroborating with basic and translational cancer research sheds light on discovering new metabolic dependencies of pediatric cancers. Like adult cancers, aggressive pediatric tumors require specific lipids, amino acids, carbohydrates, vitamins, and minerals for survival (63, 81, 82). The most vulnerable metabolite is determined under a particular context of cancer and is associated with the tumor microenvironment (83). Finding critical nutrient dependencies for each cancer type will aid in developing optimal treatment regimens.

Here, we summarize recent findings on the associations between nutrition and pediatric cancers, nutritional dependencies under different tumor contexts, and dietary approaches during pediatric cancer treatment. Much remains to be uncovered in pediatric cancers compared to adult cancers. Thus, we also discuss the current challenges and research gaps in the field and point to interesting future directions. The ultimate goal is finding optimal and precise nutritional strategies to improve patient survival and quality of life.

The link between nutrition and childhood cancers

The State of Food Security and Nutrition in the World reported that 9.8 percent of the global population (768 million) were undernourished in 2021 (13). Infants and children are more susceptible populations due to the high demand for energy and essential nutrients, especially for cancer patients. In a prospective study of 1,787 newly diagnosed pediatric patients, 18% had moderate nutritional depletion, and 45–59% were severely depleted (34). Another study showed that 50% of children with stage IV NB (high-risk patients) were undernourished at diagnosis (45). Undernourished children abandoned therapy more frequently, resulting in inferior event-free survival (34). Protein-energy malnutrition, a specific undernutrition defined as an energy deficit due to a lack of macronutrients, is commonly seen in leukemias and solid tumors (14, 15). Apart from the macronutrients, deficiencies of micronutrients such as magnesium, zinc, selenium, vitamin D, and vitamin B12 were reported in pediatric cancer patients (Table 1) (16, 36, 73, 84). There is a lack of standard clinical practice guidelines for monitoring the nutritional status of children with cancer. Therefore, a systematic comparison of different evaluation methods and longitudinal nutritional assessment throughout diagnosis and treatment is urgently needed.

The number of overweight and obese individuals (85) and the cancer risk (16–18) have increased over the years. A recent study of 640 pediatric ALL patients found that 27% were overweight/obese, and 79% exceeded the dietary reference amount (79). Obese pediatric acute leukemia patients had a higher mortality risk than non-obese patients (77, 78). In recent years, the consumption of food-added sugars has also increased dramatically. High sugar consumption was associated with increased incidences of multiple adult malignancies, such as pancreatic and endometrial cancers (86, 87). However, whether sugar contributes to pediatric cancers is poorly understood.

Maternal obesity and diabetes also increase the risk of childhood cancers. Children born to mothers with a body mass index of ≥40 had a 57% higher leukemia risk (18). Maternal diabetes was associated with an increased risk of childhood cancers, particularly ALL, and medications reduced the risk of offspring childhood cancers (17). Additionally, maternal diets correlate with the risk of childhood cancers. Maternal consumption of vegetables and fruits before or during pregnancy was inversely associated with offspring ALL and AML incidence (19, 20, 28). In contrast, consuming flavonoid-rich foods may interfere with DNA topoisomerase II and increase the risk of AML (28). Maternal folate fortification correlated with a reduced risk of ALL, NB, and WT (21, 46, 66). Additionally, a maternal diet rich in yellow-orange vegetables, fresh fish, and grains decreased the risk of childhood brain tumors, whereas a maternal diet rich in cured meats, eggs/dairy, oil products, non-chocolate candy, and chili increased the risk (41).

The current epidemiological studies remain limited, particularly for rare diseases. Future efforts should increase subjects through data sharing and multi-institutional collaborations.

Nutrient dependencies in childhood cancers

Metabolic reprogramming has emerged as an essential cancer hallmark (88). Mutation of tumor suppressors and activation of oncogenic signaling make tumor cells promote the synthesis and uptake of nutrients for survival (89), thus enhancing tumor dependency on certain nutrients (81) (Table 1).

Amino acids

Amino acids are the building blocks of proteins. They also regulate the redox state and contribute to epigenetic and immune responses linked to tumorigenesis and metastasis (90). Therefore, tumors present a heightened amino acid dependence.

Glutamine, the most abundant amino acid in serum, is surprisingly depleted in developing cancers (91). Glutamine supported childhood AML and ALL survival and contributed to adipocyte-induced cell resistance to asparaginase (22, 29). Inhibition of glucose metabolism or Akt signaling also activated glutamine metabolism in GBM (37). In NB, the oncogenic driver MYCN promoted glutamine uptake and catabolism (47, 48). Similarly, high *MYC*-expressing atypical teratoid/rhabdoid tumors demonstrated higher glutamine metabolism activity compared to low *MYC*-expressing tumors (92). TAp73, which is frequently overexpressed in human tumors, sustained a subset of MB growth and proliferation by upregulating glutamine metabolism (42).

Another critical amino acid pathway is the serine-glycine-one-carbon (SGOC) metabolism. SGOC incorporates serine–glycine biosynthesis, one-carbon metabolism, and purine nucleotide biosynthesis in a positive feedback loop, generating diverse metabolites (93). In NB, high expression of an SGOC gene signature (49) or glycine decarboxylase (50), the enzyme which catalyzes glycine breakdown to produce one-carbon metabolism intermediate 5,10-methylene-tetrahydrofolate, was identified in *MYCN*-amplified patients and was associated with advanced disease stage and poor prognosis. In OS, the rate-limiting enzyme in serine biosynthesis 3-phosphoglycerate dehydrogenase is inversely correlated with patient survival (94). In ES, two methylenetetrahydrofolate dehydrogenase genes (*MTHFD2* and

MTHFD1L) were upregulated by EWS-FLI1, and high expressions were linked with high-risk disease and poor survival (74).

Arginine is a semi-essential amino acid and an intermediate in many biological pathways, such as the urea cycle and tricarboxylic acid cycle (95). AML depends on arginine, as depletion of intracellular arginine (*via* a pegylated arginine deiminase ADI-PEG20) and extracellular arginine (*via* a pegylated human recombinant arginase BCT-100) decreased proliferation of AML (23, 30). Depletion of arginine in combination with chemotherapy cytarabine exerted greater efficacy compared to single therapy in AML and ALL. Still, resistance eventually occurred (30, 96), likely due to compensatory activation of endogenous production of arginine (23, 97). Therefore, additional metabolic dependencies in AML must be targeted.

Asparagine is a nonessential amino acid that facilitates glycoprotein synthesis and the uptake of extracellular amino acids such as arginine, histidine, and serine (98). Asparagine presents a potential nutrient dependency in leukemias as these tumors lack asparagine synthetase (24, 99). Deprivation of exogenous asparagine by asparaginase resulted in a remission rate of >90% in children with ALL (24).

Polyamines are active organic compounds with at least two amino groups (100). They can be synthesized by ornithine decarboxylase (*ODC1*), the rate-limiting enzyme in polyamine synthesis (100), and imported by transporters such as *SLC3A2* (53). Polyamines are frequently deregulated in cancer because they involve fundamental processes related to cell growth and survival (100). For example, putrescine, spermidine, and spermine levels were elevated in children with leukemias (101). MYCN directly increased polyamine synthesis in NB and promoted NB tumor growth by upregulating *ODC1* and *SLC3A2* (51–53).

Glycolysis and oxidative phosphorylation

As discovered by Otto Warburg in the 1920s, cancer cells exhibit an increased dependence on glycolysis, preferentially catalyzing the conversion of glucose to lactate in the presence of oxygen (102). Despite a relatively low mutational burden, pediatric cancers exhibit aberrant expressions of key glycolytic enzymes, suggesting an increased dependence on glycolysis. Expression of hexokinase (*HK1/2*), which converts glucose to glucose-6-phosphate, was raised in several pediatric cancers and high *HK* expression predicted poor prognosis [i.e., metastatic NB (54), the SHH subtype of MB (43), diffuse large B-cell lymphoma (35) and OS (71)]. High expression of lactate dehydrogenase (*LDHA/B*) that converts pyruvate to lactate is linked to poor prognosis in NB, ES, and HB (55, 69, 75). Additionally, glucose transporter *GLUT1* was highly expressed in ALL (25), NB (56), and WT (67), and *GLUT3* upregulated in HB (69).

More recent work has demonstrated that mitochondrial respiration also plays a significant role in tumor growth and survival (103). WT and NB exhibited heterogeneity in mitochondrial phenotypes and energy metabolism (57, 58, 68). Stromal regions of WT showed reduced mtDNA copy number, whereas the epithelial and blastemal regions were normal (68). *MYCN*-amplified NB demonstrated higher mitochondrial activity than non-*MYCN*-amplified NB (57, 58). The pyruvate dehydrogenase kinase 1 (PDK1) phosphorylates pyruvate dehydrogenase and in turn, lowers its activity, which reduces the conversion of pyruvate to acetyl-CoA. PDK1 was activated in AML, GBM, and RB, and its inhibition blocked cell proliferation and restored sensitivity to chemotherapy (31, 38, 65).

Lipids

Lipids are also critical for cancer cell proliferation by serving as membrane components, providing energy sources, maintaining redox homeostasis, and acting as signaling molecules (104). Several pediatric cancers heavily rely on lipids for survival. For example, fatty acid transport (*via* fatty acid transporter *SLC27A2*), biosynthesis (*via* fatty acid synthase *FASN* and stearoyl-CoA desaturase *SCD*), and oxidation (*via* carnitine palmitoyltransferase 1 *CPT1*) were activated in *MYCN*-amplified NB (58–61). Inhibition of fatty acid oxidation by malonyl-CoA decarboxylase inhibitor prohibited RMS growth, and knockdown of fatty acid metabolism regulator sterol regulatory element-binding protein-1c (*SREBP-1c*) suppressed HB, suggesting a dependency on lipid metabolism (70, 76). Lipids such as phosphatidylinositol, sphingolipids, free cholesterol, and monounsaturated fatty acids were increased in isocitrate dehydrogenases mutant AML cells (32). Moreover, AML blasts activated adipocyte lipolysis, thus allowing fatty acids to be transferred from adipocytes to blasts (33). A recent study identified the mevalonate pathway as a novel vulnerability in early T-cell ALL (26). Inhibition of 3-hydroxy-3-methylglutaryl-CoA reductase, the rate-limiting enzyme in the mevalonate pathway, significantly blocked T-cell ALL growth (26). Besides, smoothened-activating sterol lipids such as cholesterol and 7-keto-cholesterol sustained oncogenic Hedgehog signaling in MB (44).

Vitamins and minerals

Besides the macronutrients, vitamins and minerals are essential as substrates and cofactors for critical metabolic processes (105). Pediatric cancer patients were disproportionately vitamin D deficient (27, 36, 82), suggesting sequestration of this vitamin by tumor cells. Vitamin B12 has also been identified as a pediatric cancer dependency, specifically in NB cells, such that B12 depletion induced cell-cycle arrest and neuronal differentiation (62).

Among minerals, iron serves as a significant dependency across pediatric cancers. Iron depletion by iron chelator deferoxamine or sodium ascorbate has demonstrated anti-proliferative activity in NB (63, 64). However, exogenous iron exposure induced ferroptosis in malignant brain tumors and NB (106–108), indicating that tight control of iron levels is required for cancer cell survival.

Dietary modifications in pediatric cancers

Inhibitors used to disrupt active cancer metabolism have been extensively summarized in many reviews (81, 109–111). Nevertheless, a majority of drugs fail to enter clinical trials. Compensatory activation of other metabolic routes or uptake of the source metabolite reduces the anti-tumor effects (59, 112). Moreover, the specificity of the metabolic inhibitors to tumor cells and their potential toxicities remain a question. Therefore, supportive approaches such as dietary modifications should be considered during cancer treatment. Dietary composition determines nutrient availability in the microenvironment of cells in the body (113). Accumulating evidence suggests that dietary modifications, including calorie and nutrient restriction/supplementation,

reprogram tumor metabolic activity and produce shifts in proliferation rate and drug sensitivity (114, 115). Herein, this review will focus on dietary modifications applied to pediatric cancers.

Calorie restriction and ketogenic diet

Calorie restriction emphasizes a chronic 20–30% reduction of the standard calorie intake (116). This approach reduces tumor growth in several adult tumor models, including breast cancer, pancreatic cancer, and lymphoma (117–119). Interestingly, calorie restriction also inhibited tumor growth in neuroblast mouse xenograft models, although its molecular mechanism remains unknown (120). However, it remains a concern to use calorie restriction during childhood, given the risk of malnutrition and disrupted endocrine function (121).

Consequently, researchers have sought a safer approach that sustains overall calorie intake but modifies the diet composition. The ketogenic diet was introduced to meet such demand. Ketogenic diets have normal calorie, low-carbohydrate but high-fat content, leading to increased ketone bodies in plasma (122). The ketogenic diet showed anticancer effects in preclinical models of NB and GBM (39, 120, 123). Researchers further identified that a medium-chain fatty acid-containing ketogenic diet was more effective than a long-chain fatty acid-containing diet (120, 123). It remains uncertain whether ketogenic diet can be applied to all cancer types.

Nutrient restriction

Germline mutations in the methionine synthase gene have been associated with childhood leukemia risk (124), and methionine depletion augmented the anticancer activities of chemotherapeutics against pediatric sarcoma cells *in vitro* (125). However, it remains unknown whether methionine dependence is a broader feature across pediatric cancers and whether this dependency can be effectively exploited against tumors in children. Besides methionine, serine deprivation has also been shown to induce oxidative stress and prohibit tumor growth in adult cancer models (126, 127). Given that NB and ES showed active serine metabolism (50, 74), it will be interesting to determine whether serine restriction is effective in treating those cancers.

Besides amino acids, restriction of vitamins can be used in tumors that rely on those vitamins for survival. Restriction of vitamin B9 (folate) and B12 (cobalamin) together with other methyl donors (methionine and choline) inhibited one-carbon metabolism and protected against adenoma development (128). Restriction of minerals like iron may selectively target cancer cells (63, 64). However, care must be taken to avoid restriction toxicity since pediatric cancer patients are frequently vitamin deficient already (82, 129).

Nutrient supplementation

Omega-3 fatty acids exert anti-inflammatory and anti-tumor effects (130). Docosahexaenoic acid (DHA) and eicosapentaenoic acid (EPA) slowed MB tumor growth by alleviating the inflammatory tumor microenvironment (131). *MYCN*-amplified NB contained lower DHA levels than non-*MYCN*-amplified NB. DHA supplementation delayed the progression of NB in cell line-derived mouse xenograft models (132). However, another study using TH-*MYCN* transgenic NB model did not observe significant DHA effects (133). More studies and standard treatment strategies are needed to evaluate the efficacy of DHA supplementation in NB.

Folate and vitamin B12 deficiency was found in ALL patients who showed anemia on maintenance therapy (134). Supplementation of these deficient micronutrients significantly alleviated anemia. Supplementation of vitamin K2 and D3 improved bone mineral density in ALL patients during intensive steroid therapy (135). Further research is needed to comprehensively characterize micronutrient status before and after treatment and to precisely monitor the effects of micronutrient supplementation on patients' health conditions.

Cachexia is a complex syndrome presenting with decreased food intake, weight loss, muscle and adipose tissue wasting, and hormonal/metabolic abnormalities (136). Muscle wasting is associated with reduced protein synthesis and increased protein degradation (137). Oral supplementation of a mixture of amino acids partially reversed cachexia in patients with advanced solid tumors (138). Similarly, a diet enriched in leucine or branch-chain amino acids stimulated muscle protein synthesis and alleviated cachexia (139, 140). However, most studies were conducted on adult cancer patients. Further investigations into the effects of cachexia on pediatric tumor development and strategies for its reversal through dietary modifications are urgently needed.

Challenges for nutritional interventions and future directions

Studies on dietary modifications for adult cancer treatment have provided insights into pediatric cancer interventions. Nevertheless, there is still a long way to go. First, additional studies are needed to understand specific nutrient dependencies in different pediatric cancers and to evaluate the efficacies of various dietary interventions. Second, because dietary modifications induce systemic responses that impact both tumor and tumor microenvironment, a holistic understanding of how the nutrient restriction or supplementation affects tumor and tumor microenvironment such as anti-/pro-tumor immune response, stromal cell activity, angiogenesis, and whole-body homeostasis is highly demanded. Third, the duration and start time for nutritional therapy as well as the long-term toxicity from nutrient deprivation or supplementation should be evaluated. Fourth, it should be emphasized that no treatment works for all types of cancers. For example, histidine supplementation made leukemia xenografted tumors more sensitive to methotrexate (141), whereas histidine depletion in a Drosophila model selectively limited the growth of *MYC*-dependent neural tumors (142). Thus, specific tumor context needs to be mentioned when advertising nutritional therapies.

Conclusion

Compared to adult cancers, the understanding of crosstalks between nutrition and pediatric cancers remains poor, thus providing tremendous opportunities for studying how nutrition can help prevent and treat childhood cancers (Figure 1). Large-scale epidemiological studies of pediatric cancers could uncover additional relationships between nutrients and pediatric cancers. Moreover, omics technology combined with mechanistic studies can reveal novel nutrient dependencies. This will further guide preclinical and clinical nutritional interventions to optimize therapeutic strategies. This process can be applied to populations, subgroups, and individuals. Each patient's

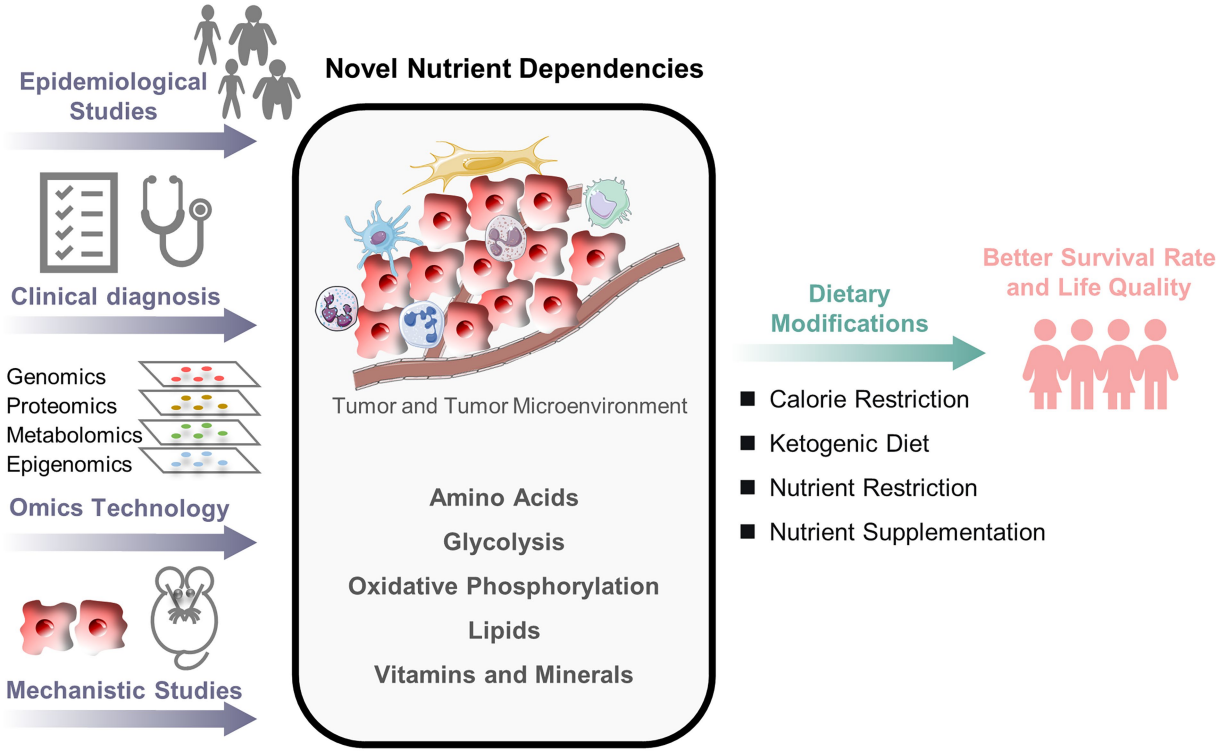

FIGURE 1
An outlook of nutritional research in pediatric cancers. The crosstalks between nutrition and pediatric cancers remain poorly understood. A combined approach of epidemiological investigation, clinical diagnosis, omics technology, and mechanistic study is necessary to understand better how nutrients alter cancer fate and to develop the optimal nutritional strategy for pediatric cancer patients.

genetic information may guide the discovery of personalized nutrient dependencies and nutritional interventions. There is still much to learn, but additional studies will enlighten the future by overlapping nutrition and pediatric cancer fields.

Author contributions

LT and KW wrote the manuscript and prepared the figure. LT and TY conceived and organized the structure of the review. KW, TY, YZ, XG, and LT reviewed the manuscript. LT revised the manuscript and supervised the entire writing process. All authors approved the final manuscript before submission and publication.

Funding

This work was supported by Start-up Funding from Fudan University (to LT) and Sub-project of the Shanghai Local High-Level University Construction Program from Shanghai Municipal Education Commission (to LT).

Acknowledgments

We thank Nathan Drolet for assisting with the language editing of this manuscript.

Conflict of interest

The authors declare that the research was conducted in the absence of any commercial or financial relationships that could be construed as a potential conflict of interest.

Publisher's note

References

1. Filbin, M, and Monje, M. Developmental origins and emerging therapeutic opportunities for childhood cancer. *Nat Med*. (2019) 25:367–76. doi: 10.1038/s41591-019-0383-9

2. Grobner, SN, Worst, BC, Weischenfeldt, J, Buchhalter, I, Kleinheinz, K, Rudneva, VA, et al. The landscape of genomic alterations across childhood cancers. *Nature*. (2018) 555:321–7. doi: 10.1038/s41586-018-0167-2

3. Ma, X, Liu, Y, Liu, Y, Alexandrov, LB, Edmonson, MN, Gawad, C, et al. Pan-cancer genome and transcriptome analyses of 1,699 paediatric leukaemias and solid tumours. *Nature*. (2018) 555:371–6. doi: 10.1038/nature25795

4. Tanaka, K, Iwakuma, T, Harimaya, K, Sato, H, and Iwamoto, Y. EWS-Fli1 antisense oligodeoxynucleotide inhibits proliferation of human Ewing's sarcoma and primitive neuroectodermal tumor cells. *J Clin Invest*. (1997) 99:239–47. doi: 10.1172/JCI119152

5. Schwartzentruber, J, Korshunov, A, Liu, XY, Jones, DT, Pfaff, E, Jacob, K, et al. Driver mutations in histone H3.3 and chromatin remodelling genes in paediatric glioblastoma. *Nature*. (2012) 482:226–31. doi: 10.1038/nature10833

6. Bender, S, Tang, Y, Lindroth, AM, Hovestadt, V, Jones, DT, Kool, M, et al. Reduced H3K27me3 and DNA hypomethylation are major drivers of gene expression in K27M mutant pediatric high-grade gliomas. *Cancer Cell*. (2013) 24:660–72. doi: 10.1016/j.ccr.2013.10.006

7. Bayliss, J, Mukherjee, P, Lu, C, Jain, SU, Chung, C, Martinez, D, et al. Lowered H3K27me3 and DNA hypomethylation define poorly prognostic pediatric posterior fossa ependymomas. *Sci Transl Med*. (2016) 8:366ra161. doi: 10.1126/scitranslmed.aah6904

8. Weiss, WA, Aldape, K, Mohapatra, G, Feuerstein, BG, and Bishop, JM. Targeted expression of MYCN causes neuroblastoma in transgenic mice. *EMBO J*. (1997) 16:2985–95. doi: 10.1093/emboj/16.11.2985

9. Aldosari, N, Bigner, SH, Burger, PC, Becker, L, Kepner, JL, Friedman, HS, et al. MYCC and MYCN oncogene amplification in medulloblastoma. A fluorescence in situ hybridization study on paraffin sections from the Children's oncology group. *Arch Pathol Lab Med*. (2002) 126:540–4. doi: 10.5858/2002-126-0540-MAMOAI

10. Williams, RD, Al-Saadi, R, Natrajan, R, Mackay, A, Chagtai, T, Little, S, et al. Molecular profiling reveals frequent gain of MYCN and anaplasia-specific loss of 4q and 14q in Wilms tumor. *Genes Chromosomes Cancer*. (2011) 50:982–95. doi: 10.1002/gcc.20907

11. Lee, WH, Murphree, AL, and Benedict, WF. Expression and amplification of the N-myc gene in primary retinoblastoma. *Nature*. (1984) 309:458–60. doi: 10.1038/309458a0

12. Driman, D, Thorner, PS, Greenberg, ML, Chilton-MacNeill, S, and Squire, J. MYCN gene amplification in rhabdomyosarcoma. *Cancer*. (1994) 73:2231–7. doi: 10.1002/1097-0142(19940415)73:8<2231::AID-CNCR2820730832>3.0.CO;2-E

13. FAO I, UNICEF, WFP and WHO. *The State of Food Security and Nutrition in the World 2022. Repurposing Food and Agricultural Policies to Make Healthy Diets More Affordable*. Rome: FAO (2022).

14. Yu, LC, Kuvibidila, S, Ducos, R, and Warrier, RP. Nutritional status of children with leukemia. *Med Pediatr Oncol*. (1994) 22:73–7. doi: 10.1002/mpo.2950220202

15. Revuelta Iniesta, R, Paciarotti, I, Davidson, I, McKenzie, JM, Brougham, MFH, and Wilson, DC. Nutritional status of children and adolescents with cancer in Scotland: a prospective cohort study. *Clin Nutr ESPEN*. (2019) 32:96–106. doi: 10.1016/j.clnesp.2019.04.006

16. Sahin, G, Ertem, U, Duru, F, Birgen, D, and Yuksek, N. High prevelance of chronic magnesium deficiency in T cell lymphoblastic leukemia and chronic zinc deficiency in children with acute lymphoblastic leukemia and malignant lymphoma. *Leuk Lymphoma*. (2000) 39:555–62. doi: 10.3109/10428190009113385

17. Seppala, LK, Vettenranta, K, Pitkaniemi, J, Hirvonen, E, Leinonen, MK, and Madanat-Harjuoja, LM. Maternal diabetes and risk of childhood cancer in the offspring. *Int J Cancer*. (2020) 147:662–8. doi: 10.1002/ijc.32757

18. Stacy, SL, Buchanich, JM, Ma, ZQ, Mair, C, Robertson, L, Sharma, RK, et al. Maternal obesity, birth size, and risk of childhood cancer development. *Am J Epidemiol*. (2019) 188:1503–11. doi: 10.1093/aje/kwz118

19. Abiri, B, Kelishadi, R, Sadeghi, H, and Azizi-Soleiman, F. Effects of maternal diet during pregnancy on the risk of childhood acute lymphoblastic leukemia: a systematic review. *Nutr Cancer*. (2016) 68:1065–72. doi: 10.1080/01635581.2016.1206581

20. Kwan, ML, Jensen, CD, Block, G, Hudes, ML, Chu, LW, and Buffler, PA. Maternal diet and risk of childhood acute lymphoblastic leukemia. *Public Health Rep*. (2009) 124:503–14. doi: 10.1177/003335490912400407

21. Metayer, C, Milne, E, Dockerty, JD, Clavel, J, Pombo-de-Oliveira, MS, Wesseling, C, et al. Maternal supplementation with folic acid and other vitamins and risk of leukemia in offspring: a Childhood Leukemia International Consortium study. *Epidemiology*. (2014) 25:811–22.

22. Ehsanipour, EA, Sheng, X, Behan, JW, Wang, X, Butturini, A, Avramis, VI, et al. Adipocytes cause leukemia cell resistance to L-asparaginase via release of glutamine. *Cancer Res*. (2013) 73:2998–3006.

23. Miraki-Moud, F, Ghazaly, E, Ariza-McNaughton, L, Hodby, KA, Clear, A, Anjos-Afonso, F, et al. Arginine deprivation using pegylated arginine deiminase has activity against primary acute myeloid leukemia cells in vivo. *Blood*. (2015) 125:4060–8. doi: 10.1182/blood-2014-10-608133

24. Story, MD, Voehringer, DW, Stephens, LC, and Meyn, RE. L-asparaginase kills lymphoma cells by apoptosis. *Cancer Chemother Pharmacol*. (1993) 32:129–33. doi: 10.1007/BF00685615

25. Liu, T, Kishton, RJ, Macintyre, AN, Gerriets, VA, Xiang, H, Liu, X, et al. Glucose transporter 1-mediated glucose uptake is limiting for B-cell acute lymphoblastic leukemia anabolic metabolism and resistance to apoptosis. *Cell Death Dis*. (2014) 5:e1470. doi: 10.1038/cddis.2014.431

26. Rashkovan, M, Albero, R, Gianni, F, Perez-Duran, P, Miller, HI, Mackey, AL, et al. Intracellular cholesterol pools regulate oncogenic signaling and epigenetic circuitries in early T-cell precursor acute lymphoblastic leukemia. *Cancer Discov*. (2022) 12:856–71. doi: 10.1158/2159-8290.CD-21-0551

27. Oosterom, N, Dirks, NF, Heil, SG, de Jonge, R, Tissing, WJE, Pieters, R, et al. A decrease in vitamin D levels is associated with methotrexate-induced oral mucositis in children with acute lymphoblastic leukemia. *Support Care Cancer*. (2019) 27:183–90. doi: 10.1007/s00520-018-4312-0

28. Spector, LG, Xie, Y, Robison, LL, Heerema, NA, Hilden, JM, Lange, B, et al. Maternal diet and infant leukemia: the DNA topoisomerase II inhibitor hypothesis: a report from the children's oncology group. *Cancer Epidemiol Biomarkers Prev*. (2005) 14:651–5. doi: 10.1158/1055-9965.EPI-04-0602

29. Matre, P, Velez, J, Jacamo, R, Qi, Y, Su, X, Cai, T, et al. Inhibiting glutaminase in acute myeloid leukemia: metabolic dependency of selected AML subtypes. *Oncotarget*. (2016) 7:79722–35.

30. Mussai, F, Egan, S, Higginbotham-Jones, J, Perry, T, Beggs, A, Odintsova, E, et al. Arginine dependence of acute myeloid leukemia blast proliferation: a novel therapeutic target. *Blood*. (2015) 125:2386–96. doi: 10.1182/blood-2014-09-600643

31. Qin, L, Tian, Y, Yu, Z, Shi, D, Wang, J, Zhang, C, et al. Targeting PDK1 with dichloroacetophenone to inhibit acute myeloid leukemia (AML) cell growth. *Oncotarget*. (2016) 7:1395–407. doi: 10.18632/oncotarget.6366

32. Stuani, L, Riols, F, Millard, P, Sabatier, M, Batut, A, Saland, E, et al. Stable isotope labeling highlights enhanced fatty acid and lipid metabolism in human acute myeloid leukemia. *Int J Mol Sci*. (2018) 19:3325. doi: 10.3390/ijms19113325

33. Shafat, MS, Oellerich, T, Mohr, S, Robinson, SD, Edwards, DR, Marlein, CR, et al. Leukemic blasts program bone marrow adipocytes to generate a protumoral microenvironment. *Blood*. (2017) 129:1320–32. doi: 10.1182/blood-2016-08-734798

34. Sala, A, Rossi, E, Antillon, F, Molina, AL, de Maselli, T, Bonilla, M, et al. Nutritional status at diagnosis is related to clinical outcomes in children and adolescents with cancer: a perspective from Central America. *Eur J Cancer*. (2012) 48:243–52. doi: 10.1016/j.ejca.2011.06.006

35. Gu, JJ, Singh, A, Xue, K, Mavis, C, Barth, M, Yanamadala, V, et al. Up-regulation of hexokinase II contributes to rituximab-chemotherapy resistance and is a clinically relevant target for therapeutic development. *Oncotarget*. (2018) 9:4020–33. doi: 10.18632/oncotarget.23425

36. Rosen, GP, Beebe, KL, and Shaibi, GQ. Vitamin D levels differ by cancer diagnosis and decline over time in survivors of childhood cancer. *Pediatr Blood Cancer*. (2013) 60:949–52. doi: 10.1002/pbc.24349

37. Yang, C, Sudderth, J, Dang, T, Bachoo, RM, McDonald, JG, and DeBerardinis, RJ. Glioblastoma cells require glutamate dehydrogenase to survive impairments of glucose metabolism or Akt signaling. *Cancer Res*. (2009) 69:7986–93. doi: 10.1158/0008-5472.CAN-09-2266

38. Damanskiene, E, Balnyte, I, Valanciute, A, Lesauskaite, V, Alonso, MM, and Stakisaitis, D. The comparative experimental study of sodium and magnesium dichloroacetate effects on pediatric PBT24 and SF8628 cell glioblastoma tumors using a chicken embryo chorioallantoic membrane model and on cells in vitro. *Int J Mol Sci*. (2022) 23:10455. doi: 10.3390/ijms231810455

39. Vallejo, FA, Shah, SS, de Cordoba, N, Walters, WM, Prince, J, Khatib, Z, et al. The contribution of ketone bodies to glycolytic inhibition for the treatment of adult and pediatric glioblastoma. *J Neuro Oncol*. (2020) 147:317–26. doi: 10.1007/s11060-020-03431-w

40. Bunin, GR, Kushi, LH, Gallagher, PR, Rorke-Adams, LB, McBride, ML, and Cnaan, A. Maternal diet during pregnancy and its association with medulloblastoma in children: a children's oncology group study (United States). *Cancer Causes Control*. (2005) 16:877–91. doi: 10.1007/s10552-005-3144-7

41. Pogoda, JM, Preston-Martin, S, Howe, G, Lubin, F, Mueller, BA, Holly, EA, et al. An international case-control study of maternal diet during pregnancy and childhood brain tumor risk: a histology-specific analysis by food group. *Ann Epidemiol*. (2009) 19:148–60. doi: 10.1016/j.annepidem.2008.12.011

42. Niklison-Chirou, MV, Erngren, I, Engskog, M, Haglof, J, Picard, D, Remke, M, et al. TAp73 is a marker of glutamine addiction in medulloblastoma. *Genes Dev*. (2017) 31:1738–53. doi: 10.1101/gad.302349.117

43. Bhatia, B, Potts, CR, Guldal, C, Choi, S, Korshunov, A, Pfister, S, et al. Hedgehog-mediated regulation of PPARgamma controls metabolic patterns in neural precursors and shh-driven medulloblastoma. *Acta Neuropathol*. (2012) 123:587–600. doi: 10.1007/s00401-012-0968-6

44. Daggubati, V, Hochstelter, J, Bommireddy, A, Choudhury, A, Krup, AL, Kaur, P, et al. Smoothened-activating lipids drive resistance to CDK4/6 inhibition in hedgehog-associated medulloblastoma cells and preclinical models. *J Clin Invest*. (2021) 131:e141171. doi: 10.1172/JCI141171

45. Green, GJ, Weitzman, SS, and Pencharz, PB. Resting energy expenditure in children newly diagnosed with stage IV neuroblastoma. *Pediatr Res*. (2008) 63:332–6. doi: 10.1203/PDR.0b013e318163a2d4

46. French, AE, Grant, R, Weitzman, S, Ray, JG, Vermeulen, MJ, Sung, L, et al. Folic acid food fortification is associated with a decline in neuroblastoma. *Clin Pharmacol Ther*. (2003) 74:288–94. doi: 10.1016/S0009-9236(03)00200-5

47. Wang, T, Liu, L, Chen, X, Shen, Y, Lian, G, Shah, N, et al. MYCN drives glutaminolysis in neuroblastoma and confers sensitivity to an ROS augmenting agent. *Cell Death Dis*. (2018) 9:220. doi: 10.1038/s41419-018-0295-5

48. Ren, P, Yue, M, Xiao, D, Xiu, R, Gan, L, Liu, H, et al. ATF4 and N-Myc coordinate glutamine metabolism in MYCN-amplified neuroblastoma cells through ASCT2 activation. *J Pathol*. (2015) 235:90–100. doi: 10.1002/path.4429

49. Xia, Y, Ye, B, Ding, J, Yu, Y, Alptekin, A, Thangaraju, M, et al. Metabolic reprogramming by MYCN confers dependence on the serine-glycine-one-carbon biosynthetic pathway. *Cancer Res*. (2019) 79:3837–50. doi: 10.1158/0008-5472.CAN-18-3541

50. Alptekin, A, Ye, B, Yu, Y, Poole, CJ, van Riggelen, J, Zha, Y, et al. Glycine decarboxylase is a transcriptional target of MYCN required for neuroblastoma cell proliferation and tumorigenicity. *Oncogene*. (2019) 38:7504–20. doi: 10.1038/s41388-019-0967-3

51. Hogarty, MD, Norris, MD, Davis, K, Liu, X, Evageliou, NF, Hayes, CS, et al. ODC1 is a critical determinant of MYCN oncogenesis and a therapeutic target in neuroblastoma. *Cancer Res*. (2008) 68:9735–45. doi: 10.1158/0008-5472.CAN-07-6866

52. Evageliou, NF, Haber, M, Vu, A, Laetsch, TW, Murray, J, Gamble, LD, et al. Polyamine antagonist therapies inhibit neuroblastoma initiation and progression. *Clin Cancer Res*. (2016) 22:4391–404. doi: 10.1158/1078-0432.CCR-15-2539

53. Gamble, LD, Purgato, S, Murray, J, Xiao, L, Yu, DMT, Hanssen, KM, et al. Inhibition of polyamine synthesis and uptake reduces tumor progression and prolongs survival in mouse models of neuroblastoma. *Sci Transl Med*. (2019) 11:eaau1099. doi: 10.1126/scitranslmed.aau1099

54. Botzer, LE, Maman, S, Sagi-Assif, O, Meshel, T, Nevo, I, Yron, I, et al. Hexokinase 2 is a determinant of neuroblastoma metastasis. *Br J Cancer*. (2016) 114:759–66. doi: 10.1038/bjc.2016.26

55. Dorneburg, C, Fischer, M, Barth, TFE, Mueller-Klieser, W, Hero, B, Gecht, J, et al. LDHA in neuroblastoma is associated with poor outcome and its depletion decreases neuroblastoma growth independent of aerobic glycolysis. *Clinical Cancer Res*. (2018) 24:5772–83. doi: 10.1158/1078-0432.CCR-17-2578

56. Matsushita, K, Uchida, K, Saigusa, S, Ide, S, Hashimoto, K, Koike, Y, et al. Glycolysis inhibitors as a potential therapeutic option to treat aggressive neuroblastoma expressing GLUT1. *J Pediatr Surg*. (2012) 47:1323–30. doi: 10.1016/j.jpedsurg.2011.12.007

57. Feichtinger, RG, Zimmermann, F, Mayr, JA, Neureiter, D, Hauser-Kronberger, C, Schilling, FH, et al. Low aerobic mitochondrial energy metabolism in poorly-or undifferentiated neuroblastoma. *BMC Cancer*. (2010) 10:149. doi: 10.1186/1471-2407-10-149

58. Oliynyk, G, Ruiz-Perez, MV, Sainero-Alcolado, L, Dzieran, J, Zirath, H, Gallart-Ayala, H, et al. MYCN-enhanced oxidative and glycolytic metabolism reveals vulnerabilities for targeting neuroblastoma. *iScience*. (2019) 21:188–204. doi: 10.1016/j.isci.2019.10.020

59. Tao, L, Mohammad, MA, Milazzo, G, Moreno-Smith, M, Patel, TD, Zorman, B, et al. MYCN-driven fatty acid uptake is a metabolic vulnerability in neuroblastoma. *Nat Commun*. (2022) 13:3728. doi: 10.1038/s41467-022-31331-2

60. Moreno-Smith, M, Milazzo, G, Tao, L, Fekry, B, Zhu, B, Mohammad, MA, et al. Restoration of the molecular clock is tumor suppressive in neuroblastoma. *Nat Commun*. (2021) 12:4006. doi: 10.1038/s41467-021-24196-4

61. Ruiz-Perez, MV, Sainero-Alcolado, L, Oliynyk, G, Matuschek, I, Balboni, N, Ubhayasekera, S, et al. Inhibition of fatty acid synthesis induces differentiation and reduces tumor burden in childhood neuroblastoma. *iScience*. (2021) 24:102128. doi: 10.1016/j.isci.2021.102128

62. Battaglia-Hsu, SF, Akchiche, N, Noel, N, Alberto, JM, Jeannesson, E, Orozco-Barrios, CE, et al. Vitamin B12 deficiency reduces proliferation and promotes differentiation of neuroblastoma cells and up-regulates PP2A, proNGF, and TACE. *Proc Natl Acad Sci U S A*. (2009) 106:21930–5. doi: 10.1073/pnas.0811794106

63. Wijesinghe, TP, Dharmasivam, M, Dai, CC, and Richardson, DR. Innovative therapies for neuroblastoma: the surprisingly potent role of iron chelation in up-regulating metastasis and tumor suppressors and down-regulating the key oncogene. *N-myc Pharmacol. Res*. (2021) 173:105889. doi: 10.1016/j.phrs.2021.105889

64. Carosio, R, Zuccari, G, Orienti, I, Mangraviti, S, and Montaldo, PG. Sodium ascorbate induces apoptosis in neuroblastoma cell lines by interfering with iron uptake. *Mol Cancer*. (2007) 6:55. doi: 10.1186/1476-4598-6-55

65. Sradhanjali, S, Tripathy, D, Rath, S, Mittal, R, and Reddy, MM. Overexpression of pyruvate dehydrogenase kinase 1 in retinoblastoma: a potential therapeutic opportunity for targeting vitreous seeds and hypoxic regions. *PLoS One*. (2017) 12:e0177744. doi: 10.1371/journal.pone.0177744

66. Linabery, AM, Johnson, KJ, and Ross, JA. Childhood cancer incidence trends in association with US folic acid fortification (1986-2008). *Pediatrics*. (2012) 129:1125–33. doi: 10.1542/peds.2011-3418

67. Rakheja, D, Khokhar, S, Mitui, M, and Cost, NG. Immunohistochemical expression of GLUT1 and its correlation with unfavorable histology and TP53 codon 72 polymorphism in Wilms tumors. *Pediatric Dev Pathol*. (2012) 15:286–92. doi: 10.2350/12-01-1151-OA.1

68. Feichtinger, RG, Neureiter, D, Royer-Pokora, B, Mayr, JA, Zimmermann, FA, Jones, N, et al. Heterogeneity of mitochondrial energy metabolism in classical triphasic Wilms' tumor. *Front Biosci*. (2011) 3:187–93. doi: 10.2741/e232

69. Crippa, S, Ancey, PB, Vazquez, J, Angelino, P, Rougemont, AL, Guettier, C, et al. Mutant CTNNB1 and histological heterogeneity define metabolic subtypes of hepatoblastoma. *EMBO Mol Med*. (2017) 9:1589–604. doi: 10.15252/emmm.201707814

70. Hu, Y, Zai, H, Jiang, W, Ou, Z, Yao, Y, and Zhu, Q. The mutual inhibition of FoxO1 and SREBP-1c regulated the progression of hepatoblastoma by regulating fatty acid metabolism. *Mediat Inflamm*. (2021) 2021:5754592. doi: 10.1155/2021/5754592

71. Zhuo, B, Li, Y, Li, Z, Qin, H, Sun, Q, Zhang, F, et al. PI3K/Akt signaling mediated Hexokinase-2 expression inhibits cell apoptosis and promotes tumor growth in pediatric osteosarcoma. *Biochem Biophys Res Commun*. (2015) 464:401–6. doi: 10.1016/j.bbrc.2015.06.092

72. Qian, H, Lei, T, Hu, Y, and Lei, P. Expression of lipid-metabolism genes is correlated with immune microenvironment and predicts prognosis in osteosarcoma. *Front Cell Dev Biol*. (2021) 9:673827. doi: 10.3389/fcell.2021.673827

73. Chanihoon, GQ, Afridi, HI, Kazi, TG, Talpur, FN, and Baig, JA. Evaluation of zinc and cadmium levels in the biological samples of Ewing sarcomas patients and healthy subjects, clin chim acta 522 (2021)1-7. *Clin. Chim. Acta*. (2021) 522:1–7. doi: 10.1016/j.cca.2022.01.011

74. Sen, N, Cross, AM, Lorenzi, PL, Khan, J, Gryder, BE, Kim, S, et al. EWS-FLI1 reprograms the metabolism of Ewing sarcoma cells via positive regulation of glutamine import and serine-glycine biosynthesis. *Mol Carcinog*. (2018) 57:1342–57. doi: 10.1002/mc.22849

75. Yeung, C, Gibson, AE, Issaq, SH, Oshima, N, Baumgart, JT, Edessa, LD, et al. Targeting glycolysis through inhibition of lactate dehydrogenase impairs tumor growth in preclinical models of Ewing sarcoma. *Cancer Res*. (2019) 79:5060–73. doi: 10.1158/0008-5472.CAN-19-0217

76. Miyagaki, S, Kikuchi, K, Mori, J, Lopaschuk, GD, Iehara, T, and Hosoi, H. Inhibition of lipid metabolism exerts antitumor effects on rhabdomyosarcoma. *Cancer Med*. (2021) 10:6442–55. doi: 10.1002/cam4.4185

77. Amankwah, EK, Saenz, AM, Hale, GA, and Brown, PA. Association between body mass index at diagnosis and pediatric leukemia mortality and relapse: a systematic review and meta-analysis. *Leuk Lymphoma*. (2016) 57:1140–8. doi: 10.3109/10428194.2015.1076815

78. Orgel, E, Genkinger, JM, Aggarwal, D, Sung, L, Nieder, M, and Ladas, EJ. Association of body mass index and survival in pediatric leukemia: a meta-analysis. *Am J Clin Nutr*. (2016) 103:808–17. doi: 10.3945/ajcn.115.124586

79. Ladas, EJ, Orjuela, M, Stevenson, K, Cole, PD, Lin, M, Athale, UH, et al. Dietary intake and childhood leukemia: the diet and acute lymphoblastic leukemia treatment (DALLT) cohort study. *Nutrition*. (2016) 32:1103–1109.e1. doi: 10.1016/j.nut.2016.03.014

80. Johnston, WT, Erdmann, F, Newton, R, Steliarova-Foucher, E, Schuz, J, and Roman, E. Childhood cancer: estimating regional and global incidence. *Cancer Epidemiol*. (2021) 71:101662. doi: 10.1016/j.canep.2019.101662

81. Issaq, SH, and Heske, CM. Targeting metabolic dependencies in pediatric cancer. *Curr Opin Pediatr*. (2020) 32:26–34. doi: 10.1097/MOP.0000000000000853

82. Revuelta Iniesta, R, Rush, R, Paciarotti, I, Rhatigan, EB, Brougham, FHM, McKenzie, JM, et al. Systematic review and meta-analysis: prevalence and possible causes of vitamin D deficiency and insufficiency in pediatric cancer patients. *Clin Nutr*. (2016) 35:95–108. doi: 10.1016/j.clnu.2014.12.023

83. Balkwill, FR, Capasso, M, and Hagemann, T. The tumor microenvironment at a glance. *J Cell Sci*. (2012) 125:5591–6. doi: 10.1242/jcs.116392

84. Ganguly, S, Srivastava, R, Agarwala, S, Dwivedi, S, Bansal, PG, Gonmei, Z, et al. Prevalence of micronutrient deficiency and its impact on the outcome of childhood cancer: a prospective cohort study. *Clin Nutr*. (2022) 41:1501–11. doi: 10.1016/j.clnu.2022.05.010

85. Sahoo, K, Sahoo, B, Choudhury, AK, Sofi, NY, Kumar, R, and Bhadoria, AS. Childhood obesity: causes and consequences. *J Family Med Prim Care*. (2015) 4:187–92. doi: 10.4103/2249-4863.154628

86. Larsson, SC, Bergkvist, L, and Wolk, A. Consumption of sugar and sugar-sweetened foods and the risk of pancreatic cancer in a prospective study. *Am J Clin Nutr*. (2006) 84:1171–6. doi: 10.1093/ajcn/84.5.1171

87. Friberg, E, Wallin, A, and Wolk, A. Sucrose, high-sugar foods, and risk of endometrial cancer--a population-based cohort study. *Cancer Epidemiol Biomarkers Pre.* (2011) 20:1831–7. doi: 10.1158/1055-9965.EPI-11-0402

88. Hanahan, D, and Weinberg, RA. Hallmarks of cancer: the next generation. *Cells*. (2011) 144:646–74. doi: 10.1016/j.cell.2011.02.013

89. DeBerardinis, RJ, and Chandel, NS. Fundamentals of cancer metabolism. *Sci Adv*. (2016) 2:e1600200. doi: 10.1126/sciadv.1600200

90. Lieu, EL, Nguyen, T, Rhyne, S, and Kim, J. Amino acids in cancer. *Exp Mol Med*. (2020) 52:15–30. doi: 10.1038/s12276-020-0375-3

91. Souba, WW. Glutamine and cancer. *Ann Surg*. (1993) 218:715–28. doi: 10.1097/00000658-199312000-00004

92. Wang, SZ, Poore, B, Alt, J, Price, A, Allen, SJ, Hanaford, AR, et al. Unbiased metabolic profiling predicts sensitivity of high MYC-expressing atypical teratoid/rhabdoid tumors to glutamine inhibition with 6-Diazo-5-Oxo-L-Norleucine. *Clin Cancer Res*. (2019) 25:5925–36. doi: 10.1158/1078-0432.CCR-19-0189

93. Zhao, E, Hou, J, and Cui, H. Serine-glycine-one-carbon metabolism: vulnerabilities in MYCN-amplified neuroblastoma. *Oncogenesis*. (2020) 9:14. doi: 10.1038/s41389-020-0200-9

94. Rathore, R, Caldwell, KE, Schutt, C, Brashears, CB, Prudner, BC, Ehrhardt, WR, et al. Metabolic compensation activates pro-survival mTORC1 signaling upon 3-phosphoglycerate dehydrogenase inhibition in osteosarcoma. *Cell Rep*. (2021) 34:108678. doi: 10.1016/j.celrep.2020.108678

95. Patil, MD, Bhaumik, J, Babykutty, S, Banerjee, UC, and Fukumura, D. Arginine dependence of tumor cells: targeting a chink in cancer's armor. *Oncogene*. (2016) 35:4957–72. doi: 10.1038/onc.2016.37

96. Hernandez, CP, Morrow, K, Lopez-Barcons, LA, Zabaleta, J, Sierra, R, Velasco, C, et al. Pegylated arginase I: a potential therapeutic approach in T-ALL. *Blood*. (2010) 115:5214–21. doi: 10.1182/blood-2009-12-258822

97. Tsai, HJ, Jiang, SS, Hung, WC, Borthakur, G, Lin, SF, Pemmaraju, N, et al. A phase II study of arginine deiminase (ADI-PEG20) in relapsed/refractory or poor-risk acute myeloid leukemia patients. *Sci Rep*. (2017) 7:11253. doi: 10.1038/s41598-017-10542-4

98. Krall, AS, Xu, S, Graeber, TG, Braas, D, and Christofk, HR. Asparagine promotes cancer cell proliferation through use as an amino acid exchange factor. *Nat Commun*. (2016) 7:11457. doi: 10.1038/ncomms11457

99. Chiu, M, Taurino, G, Bianchi, MG, Kilberg, MS, and Bussolati, O. Asparagine synthetase in cancer: beyond acute lymphoblastic leukemia. *Front Oncol*. (2019) 9:1480. doi: 10.3389/fonc.2019.01480

100. Casero, RA Jr, Murray Stewart, T, and Pegg, AE. Polyamine metabolism and cancer: treatments, challenges and opportunities. *Nat Rev Cancer*. (2018) 18:681–95. doi: 10.1038/s41568-018-0050-3

101. Rennert, O, Miale, T, Shukla, J, Lawson, D, and Frias, J. Polyamine concentrations in bone marrow aspirates of children with leukemia and other malignancies. *Blood*. (1976) 47:695–701.

102. Warburg, O, Wind, F, and Negelein, E. The metabolism of tumors in the body. *J Gen Physiol*. (1927) 8:519–30. doi: 10.1085/jgp.8.6.519

103. Martinez-Reyes, I, Diebold, LP, Kong, H, Schieber, M, Huang, H, Hensley, CT, et al. TCA cycle and mitochondrial membrane potential are necessary for diverse biological functions. *Mol Cell*. (2016) 61:199–209. doi: 10.1016/j.molcel.2015.12.002

104. Snaebjornsson, MT, Janaki-Raman, S, and Schulze, A. Greasing the wheels of the cancer machine: the role of lipid metabolism in cancer. *Cell Metab*. (2020) 31:62–76. doi: 10.1016/j.cmet.2019.11.010

105. Hathcock, JN. Vitamins and minerals: efficacy and safety. *Am J Clin Nutr*. (1997) 66:427–37. doi: 10.1093/ajcn/66.2.427

106. Zhao, J, Wang, Y, Tao, L, and Chen, L. Iron transporters and ferroptosis in malignant brain tumors. *Front Oncol*. (2022) 12:861834. doi: 10.3389/fonc.2022.861834

107. Floros, KV, Cai, J, Jacob, S, Kurupi, R, Fairchild, CK, Shende, M, et al. MYCN-amplified neuroblastoma is addicted to iron and vulnerable to inhibition of the system xc−/glutathione axis. *Cancer Res*. (2021) 81:1896–908. doi: 10.1158/0008-5472.CAN-20-1641

108. Lu, Y, Yang, Q, Su, Y, Ji, Y, Li, G, Yang, X, et al. MYCN mediates TFRC-dependent ferroptosis and reveals vulnerabilities in neuroblastoma. *Cell Death Dis*. (2021) 12:511. doi: 10.1038/s41419-021-03790-w

109. Martinez-Outschoorn, UE, Peiris-Pages, M, Pestell, RG, Sotgia, F, and Lisanti, MP. Cancer metabolism: a therapeutic perspective. *Nat Rev Clin Oncol*. (2017) 14:11–31. doi: 10.1038/nrclinonc.2016.60

110. Farhadi, P, Yarani, R, Dokaneheifard, S, and Mansouri, K. The emerging role of targeting cancer metabolism for cancer therapy. *Tumour Biol*. (2020) 42:1010428320965284. doi: 10.1177/1010428320965284

111. Stine, ZE, Schug, ZT, Salvino, JM, and Dang, CV. Targeting cancer metabolism in the era of precision oncology. *Nat Rev Drug Discov*. (2022) 21:141–62. doi: 10.1038/s41573-021-00339-6

112. Sabnis, HS, Bradley, HL, Tripathi, S, Yu, WM, Tse, W, Qu, CK, et al. Synergistic cell death in FLT3-ITD positive acute myeloid leukemia by combined treatment with metformin and 6-benzylthioinosine. *Leuk Res*. (2016) 50:132–40. doi: 10.1016/j.leukres.2016.10.004

113. Sullivan, MR, Danai, LV, Lewis, CA, Chan, SH, Gui, DY, Kunchok, T, et al. Quantification of microenvironmental metabolites in murine cancers reveals determinants of tumor nutrient availability. *Elife*. (2019) 8:e44235. doi: 10.7554/eLife.44235

114. Kanarek, N, Petrova, B, and Sabatini, DM. Dietary modifications for enhanced cancer therapy. *Nature*. (2020) 579:507–17. doi: 10.1038/s41586-020-2124-0

115. Tajan, M, and Vousden, KH. Dietary approaches to cancer therapy. *Cancer Cell*. (2020) 37:767–85. doi: 10.1016/j.ccell.2020.04.005

116. Holloszy, JO, and Fontana, L. Caloric restriction in humans. *Exp Gerontol*. (2007) 42:709–12. doi: 10.1016/j.exger.2007.03.009

117. Berrigan, D, Perkins, SN, Haines, DC, and Hursting, SD. Adult-onset calorie restriction and fasting delay spontaneous tumorigenesis in p53-deficient mice. *Carcinogenesis*. (2002) 23:817–22. doi: 10.1093/carcin/23.5.817

118. Fernandes, G, Chandrasekar, B, Troyer, DA, Venkatraman, JT, and Good, RA. Dietary lipids and calorie restriction affect mammary tumor incidence and gene expression in mouse mammary tumor virus/v-Ha-ras transgenic mice. *Proc Natl Acad Sci U S A*. (1995) 92:6494–8. doi: 10.1073/pnas.92.14.6494

119. Harvey, AE, Lashinger, LM, Hays, D, Harrison, LM, Lewis, K, Fischer, SM, et al. Calorie restriction decreases murine and human pancreatic tumor cell growth, nuclear factor-kappaB activation, and inflammation-related gene expression in an insulin-like growth factor-1-dependent manner. *PLoS One*. (2014) 9:e94151. doi: 10.1371/journal.pone.0094151

120. Morscher, RJ, Aminzadeh-Gohari, S, Feichtinger, RG, Mayr, JA, Lang, R, Neureiter, D, et al. Inhibition of neuroblastoma tumor growth by ketogenic diet and/or calorie restriction in a CD1-Nu mouse model. *PLoS One*. (2015) 10:e0129802. doi: 10.1371/journal.pone.0129802

121. Chen, JH, Cottrell, EC, and Ozanne, SE. Early growth and ageing. *Nestle Nutr Workshop Ser Pediatr Program*. (2010) 65:41–50; discussion-4. doi: 10.1159/000281144

122. De Feyter, HM, Behar, KL, Rao, JU, Madden-Hennessey, K, Ip, KL, Hyder, F, et al. A ketogenic diet increases transport and oxidation of ketone bodies in RG2 and 9L gliomas without affecting tumor growth. *Neuro Oncology*. (2016) 18:1079–87. doi: 10.1093/neuonc/now088

123. Aminzadeh-Gohari, S, Feichtinger, RG, Vidali, S, Locker, F, Rutherford, T, O'Donnel, M, et al. A ketogenic diet supplemented with medium-chain triglycerides enhances the anti-tumor and anti-angiogenic efficacy of chemotherapy on neuroblastoma xenografts in a CD1-nu mouse model. *Oncotarget*. (2017) 8:64728–44. doi: 10.18632/oncotarget.20041

124. Ma, LM, Yang, HP, Yang, XW, and Ruan, LH. Methionine synthase A2756G polymorphism influences pediatric acute lymphoblastic leukemia risk: a meta-analysis. *Biosci Rep*. (2019) 39:BSR20181770. doi: 10.1042/BSR20181770

125. Stern, PH, and Hoffman, RM. Enhanced in vitro selective toxicity of chemotherapeutic agents for human cancer cells based on a metabolic defect. *J Natl Cancer Inst*. (1986) 76:629–39. doi: 10.1093/jnci/76.4.629

126. Maddocks, OD, Berkers, CR, Mason, SM, Zheng, L, Blyth, K, Gottlieb, E, et al. Serine starvation induces stress and p53-dependent metabolic remodelling in cancer cells. *Nature*. (2013) 493:542–6. doi: 10.1038/nature11743

127. Maddocks, ODK, Athineos, D, Cheung, EC, Lee, P, Zhang, T, van den Broek, NJF, et al. Modulating the therapeutic response of tumours to dietary serine and glycine starvation. *Nature*. (2017) 544:372–6. doi: 10.1038/nature23471

128. Hanley, MP, Kadaveru, K, Perret, C, Giardina, C, and Rosenberg, DW. Dietary methyl donor depletion suppresses intestinal adenoma development. *Cancer Prev Res*. (2016) 9:812–20. doi: 10.1158/1940-6207.CAPR-16-0042

129. Muggeo, P, Muggeo, VMR, Giordano, P, Delvecchio, M, Altomare, M, Novielli, C, et al. Cardiovascular dysfunction and vitamin D status in childhood acute lymphoblastic leukemia survivors. *World J Pediatr*. (2019) 15:465–70. doi: 10.1007/s12519-019-00258-y

130. Wei, L, Wu, Z, and Chen, YQ. Multi-targeted therapy of cancer by omega-3 fatty acids-an update. *Cancer Lett*. (2022) 526:193–204. doi: 10.1016/j.canlet.2021.11.023

131. Ljungblad, L, Bergqvist, F, Tummler, C, Madawala, S, Olsen, TK, Andonova, T, et al. Omega-3 fatty acids decrease CRYAB, production of oncogenic prostaglandin E2 and suppress tumor growth in medulloblastoma. *Life Sci*. (2022) 295:120394. doi: 10.1016/j.lfs.2022.120394

132. Gleissman, H, Segerstrom, L, Hamberg, M, Ponthan, F, Lindskog, M, Johnsen, JI, et al. Omega-3 fatty acid supplementation delays the progression of neuroblastoma in vivo. *Int J Cancer*. (2011) 128:1703–11. doi: 10.1002/ijc.25473

133. Ljungblad, L. *Omega-3 Fatty Acids in the Treatment of Childhood Cancer*. Stockholm: Karolinska Institute (2022).

134. Pattnaik, J, Kayal, S, Dubashi, B, Basu, D, Vinod, KV, Nandeesha, H, et al. Profile of anemia in acute lymphoblastic leukemia patients on maintenance therapy and the effect of micronutrient supplementation. *Support Care Cancer*. (2020) 28:731–8. doi: 10.1007/s00520-019-04862-6

135. Solmaz, I, Ozdemir, MA, Unal, E, Abdurrezzak, U, Muhtaroglu, S, and Karakukcu, M. Effect of vitamin K2 and vitamin D3 on bone mineral density in children with acute lymphoblastic leukemia: a prospective cohort study. *J Pediatr Endocrinol Metab*. (2021) 34:441–7. doi: 10.1515/jpem-2020-0637

136. Baracos, VE, Martin, L, Korc, M, Guttridge, DC, and Fearon, KCH. Cancer-associated cachexia. *Nat Rev Dis Primers*. (2018) 4:17105. doi: 10.1038/nrdp.2017.105

137. Argiles, JM. Cancer-associated malnutrition. *Eur J Oncol Nurs*. (2005) 9:S39–50. doi: 10.1016/j.ejon.2005.09.006

138. May, PE, Barber, A, D'Olimpio, JT, Hourihane, A, and Abumrad, NN. Reversal of cancer-related wasting using oral supplementation with a combination of beta-hydroxy-beta-methylbutyrate, arginine, and glutamine. *Am J Surg*. (2002) 183:471–9. doi: 10.1016/S0002-9610(02)00823-1

139. Deutz, NE, Safar, A, Schutzler, S, Memelink, R, Ferrando, A, Spencer, H, et al. Muscle protein synthesis in cancer patients can be stimulated with a specially formulated medical food. *Clin Nutr*. (2011) 30:759–68. doi: 10.1016/j.clnu.2011.05.008

140. Hunter, DC, Weintraub, M, Blackburn, GL, and Bistrian, BR. Branched chain amino acids as the protein component of parenteral nutrition in cancer cachexia. *Br J Surg*. (1989) 76:149–53. doi: 10.1002/bjs.1800760215

141. Kanarek, N, Keys, HR, Cantor, JR, Lewis, CA, Chan, SH, Kunchok, T, et al. Histidine catabolism is a major determinant of methotrexate sensitivity. *Nature*. (2018) 559:632–6. doi: 10.1038/s41586-018-0316-7

142. Froldi, F, Pachnis, P, Szuperak, M, Costas, O, Fernando, T, Gould, AP, et al. Histidine is selectively required for the growth of Myc-dependent dedifferentiation tumours in the drosophila CNS. *EMBO J*. (2019) 38:e99895. doi: 10.15252/embj.201899895

frontiers | Frontiers in Nutrition

TYPE Mini Review
PUBLISHED 01 March 2023
DOI 10.3389/fnut.2023.1139339

OPEN ACCESS

EDITED BY
Ling Zhao,
The University of Tennessee, Knoxville,
United States

REVIEWED BY
Guoxun Chen,
The University of Tennessee, Knoxville,
United States

*CORRESPONDENCE
Chaodong Wu
✉ chaodong.wu@ag.tamu.edu

SPECIALTY SECTION
This article was submitted to
Nutrition and Metabolism,
a section of the journal
Frontiers in Nutrition

RECEIVED 06 January 2023
ACCEPTED 14 February 2023
PUBLISHED 01 March 2023

CITATION
Li H, Guo X, Aquino E and Wu C (2023) Mini review: STING activation during non-alcoholic fatty liver disease.
Front. Nutr. 10:1139339.
doi: 10.3389/fnut.2023.1139339

Mini review: STING activation during non-alcoholic fatty liver disease

Honggui Li, Xinlei Guo, Eduardo Aquino and Chaodong Wu*

Department of Nutrition, Texas A&M University, College Station, TX, United States

Non-alcoholic fatty liver disease (NAFLD) is one of the most common chronic diseases serving as a major threat to human health. While the pathogenesis of NAFLD is multi-factorial, inflammation is considered a critical factor driving the development and progression of NAFLD phenotype, including liver fibrosis. As an essential mediator of innate immunity, stimulator of interferon genes (STING) functions to promote anti-viral immunity. Accumulating evidence also indicates that STING functions to promote the proinflammatory activation of several types of liver cells, especially macrophages/Kupffer cells, in a manner independent of interferon production. Over the past several years, a significant body of literature has validated a detrimental role for STING in regulating the pathogenesis of hepatic steatosis and inflammation. In particular, the STING in macrophages/Kupffer cells has attracted much attention due to its importance in not only enhancing macrophage proinflammatory activation, but also generating macrophage-derived mediators to increase hepatocyte fat deposition and proinflammatory responses, and to activate hepatic stellate cell fibrogenic activation. Both intracellular and extracellular signals are participating in STING activation in macrophages, thereby critically contributing to NAFLD phenotype. This mini review summarizes recent advances on how STING is activated in macrophages in the context of NAFLD pathophysiology.

KEYWORDS

non-alcoholic fatty liver disease, liver fibrosis, inflammation, stimulator of interferon genes, macrophage

1. Introduction

Non-alcoholic fatty liver disease (NAFLD), comprised of a spectrum of chronic liver diseases whose pathogenesis is not associated with alcohol consumption, is characterized by excessive fat deposition in hepatocytes (steatosis). Subjects with certain health conditions such as obesity, metabolic disease, and insulin resistance, are more prone to develop NAFLD. Indeed, epidemiological data indicate that the incidence of NAFLD in populations with obesity is increased by about sevenfold relative to that of general populations. While simple steatosis may be benign and have few or no symptoms, NAFLD progresses to non-alcoholic steatohepatitis (NASH), the advanced form of NAFLD, when the liver displays overt inflammatory damage. The diagnosis of NAFLD relies on medical history, a physical exam, and laboratory tests. However, liver histology is required to diagnose NASH. Healthy eating and lifestyle changes are recommended to manage NALFD, particularly hepatic steatosis. However, currently there is no effective treatment for NASH.

The outcomes of numerous basic research and translational studies have demonstrated that NASH is one of the most common causes of terminal liver diseases including hepatocellular carcinoma. Because of this, a significant number of investigations have focused on how inflammation arises and then triggers or exacerbates the development and progression of NAFLD under obese conditions. As a critical mediator in innate immunity, stimulator of interferon genes (STING) has been implicated to promote inflammation. This property enables STING to be involved in the pathogenesis of NAFLD. This mini review focuses on the recent advances in understanding STING activation in macrophages during the pathogenesis of NAFLD.

2. Role of STING in the pathogenesis of NAFLD

While studying DNA-binding agents for their anti-tumor properties, researchers synthesized and functionally characterized the effect of 5,6-dimethylxanthenone-4-acetic acid (DMXAA) in 1990 (1). Since then, the investigations concerning DMXAA actions have been extended to studying the regulation of macrophage activation as it related to anti-tumor immunology. In 1994, Perera et al. showed that DMXAA was able to induce a subset of lipopolysaccharide (LPS)-inducible genes within primary murine macrophages (2). Several years later, the lab where DMXAA was initially synthesized showed that DMXAA was capable of inducing interferon (IFN) expression (3), suggesting an effect of DMXAA on stimulating antiviral defensive responses in addition to its role in promoting the proinflammatory responses. Following these findings, numerous studies had focused on the mechanisms by which DMXAA induces IFN expression. In 2007, Roberts et al. demonstrated DMXAA as a novel and specific activator of the TANK-binding kinase 1 (TBK1)-IFN regulatory factor 3 (IRF-3) signaling pathway (4). A year later, the adaptor protein mediator of IRF3 activation (MITA), known as STING, was functionally validated to serve as a critical mediator of virus-induced IFN beta (IFNβ) expression (5). Since then, STING has been studied for its role in regulating innate immunity and the proinflammatory responses (6, 7).

The discovery of cyclic 2′,5′-GMP-AMP (cGAMP), generated by cGAMP synthase (cGAS) in response to cytosolic aberrant presence of double-stranded DNA (dsDNA), has drawn much attention to STING for its role in anti-viral immunity. While examining the effects of cGAMP, the studies by Guo et al. and Luo et al. showed interesting findings concerning macrophage activation. Specifically, treatment of bone marrow cell-derived macrophages (BMDMs) that were prepared from wild-type (WT) mice with exogenous cGAMP potentiated the effect of LPS on stimulating macrophage proinflammatory activation (8). However, in the absence of functional STING, treatment of mouse BMDMs with exogenous cGAMP significantly decreased the effect of LPS on stimulating macrophage proinflammatory activation (9). These findings led Luo et al. to postulate a role for STING in regulating inflammation as a key driving factor to promote the pathogenesis of NAFLD. Accordingly, Luo et al. performed the first study to examine STING expression in livers from patients with NAFLD and demonstrated a significant increase in STING expression in liver non-parenchymal cells (NPCs) relative to that in livers from subjects without NAFLD (9). Notably, using various mouse models involving adoptive transfer of STING-disrupted bone marrow cells to lethally irradiated WT mice or adoptive transfer of WT bone marrow cells to lethally irradiated STING-disrupted mice, the study by Luo et al. validated a deleterious role for STING-driven macrophage activation in promoting hepatic steatosis and inflammation, as well as liver fibrosis. The concept that STING-driven macrophage activation critically contributes to the development and progression of NAFLD or NASH with liver fibrosis is substantiated by the findings from the study by Wang et al. upon analyzing STING expression in liver monocyte-derived macrophages and Kupffer cells (10). Notably, using liver sections from human subjects with or without NAFLD, Wang et al. demonstrated that STING expression is significantly increased in liver sections from patients with NAFLD (10). More importantly, the intensities of STING expression in macrophages, particular monocyte-derived macrophages, were positively correlated with the severities of NASH and/or grades of liver fibrosis. To be noted, since the first study addressing STING promotion of NAFLD by Luo et al., a significant number of new studies have confirmed the importance of STING in NAFLD or NASH pathogenesis, as well as liver inflammation and related injuries (11–15), and provided novel insights into STING activation in macrophages, which are highlighted below.

3. Hepatocyte-driven STING activation

The earliest evidence concerning the role for STING in regulating liver inflammation and fibrosis may come from the results of the study by Petrasek et al. (16). Notably, global deficiency of IRF3, a transcription factor whose activation is induced in response to STING activation, protected mice from ethanol-induced liver inflammatory damage. Due to its role in activating IRF3 and related downstream events, STING was also studied for its role in ethanol-induced liver inflammation. Specifically, STING was detectable at high abundance in whole liver extracts and associated with phosphorylated IRF3. Moreover, STING disruption blunted the effect of thapsigargin, a non-competitive inhibitor of the sarcoendoplasmic reticulum Ca^{2+} ATPase, on activating (phosphorylating) IRF3 in mouse primary hepatocytes and alleviated the severity of ethanol-induced liver inflammation. Based on this, the authors speculated a role for STING in hepatocytes in promoting liver inflammation (16). A similar study by Iracheta-Vellve et al. also indicated a role for STING in hepatocytes in its association with IRF3 in the context of promoting carbon tetrachloride (CCl4)-induced hepatocyte apoptosis and

Abbreviations: ADK, adenosine kinase; BMDM, bone marrow-derived macrophages; cGAMP, cyclic 2′,5′-GMP-AMP; cGAS, cyclic GMP-AMP synthase; DMXAA, 5,6-dimethylxanthenone-4-acetic acid; dsDNA, double-stranded DNA; ER, endoplasmic reticulum; HFD, high-fat diet; IFNβ, interferon beta; IL-1β, interleukin 1β; LPS, lipopolysaccharide; IRF3, interferon regulatory factor 3; JNK, c-Jun N-terminal kinases; MCD, methionine- and choline-deficient diet; mEVs, microbial DNA-containing extracellular vesicles; mtDNA, mitochondrial DNA; NAFLD, non-alcoholic fatty liver disease; NFκB, nuclear factor kappa B; NASH, non-alcoholic steatohepatitis; Pp65, phosphorylated p65 subunit of NFκB; Pp46, phosphorylated JNK1 (p46); STING, stimulator of interferon genes; TBK1, TANK-binding kinase 1; TNFα, tumor necrosis factor α; TGFβ1, transforming growth factor β1.

liver fibrosis (17). Interestingly, in either of the two studies the researchers only provided the data concerning STING expression in whole liver extracts, but not hepatocytes, while a role for the STING in hepatocytes has been speculated. In contrast, increasing evidence from the studies involving both human subjects and rodent models indicates that STING expression in hepatocytes is likely at an undetectable level as this is supported by the data from immunoblots for STING expression in the isolated primary hepatocytes or liver immunohistochemistry staining for STING (9, 11, 14, 18). Because of this, the STING in macrophages, but not hepatocytes, appears to be primarily responsible for the regulation of liver inflammation. In addition, macrophage STING activation is attributable to, in large part, hepatocyte-derived mediators. This is particularly true under conditions with hepatic steatosis; given that hepatocyte fat deposition is an event that commonly precedes inflammation.

In terms of how hepatocyte fat deposition causes or exacerbates liver inflammation, multiple studies have demonstrated the importance of palmitate as a key component of fats in triggering or enhancing hepatocyte proinflammatory responses. For instance, the study by Nakamura et al. showed that palmitate induced hepatocyte JNK activation, at least through promoting the production of mitochondrial dysfunction-associated reactive oxygen species (ROS) (19). Since palmitate-treated hepatocytes revealed increased production of proinflammatory mediators that are capable of enhancing macrophage proinflammatory activation (20, 21), it is conceivable that excessive fat deposition-associated hepatocyte mediators function to stimulate macrophage proinflammatory activation and this process involves STING. This, indeed, was validated by the findings from the study by Yu et al. Initially, Yu et al. verified that STING was highly expressed in liver Kupffer cells and was nearly undetectable in hepatocytes of WT mice while showing that global STING disruption protected mice from either high-fat die (HFD)-induced NAFLD or methionine- and choline-deficient diet (MCD)-induced NASH. This led the researchers to validate hepatocyte-derived mitochondrial DNA (mtDNA) as a key mediator that functions to stimulate the STING in Kupffer cells, as a result of cGAS activation and cGAMP production, and increase the expression of proinflammatory cytokines in Kupffer cells. This in turn accounts for liver inflammation. In addition, STING promotion of the expression of proinflammatory cytokines in Kupffer cells was largely independent of IRF3. However, it remains an important question whether hepatocyte-derived mtDNA is sufficient to trigger or exacerbate NAFLD or NASH phenotype while stimulating STING in liver Kupffer cells and promoting proinflammatory cytokine expression.

While increased mtDNA production is a hallmark of hepatocyte mitochondrial dysfunction/stress, excessive fat deposition is considered to trigger or exacerbate hepatocyte mitochondrial dysfunction. Indeed, the study by Yu et al. hinted at a link between excessive fat deposition and hepatocyte mitochondrial dysfunction as this was evidenced by the finding that hepatocyte mtDNA production is increased in mice fed an HFD. However, palmitate, proposed as a primary fatty acid that functions to induce hepatocyte mitochondrial dysfunction, is a hydrolytic product of VLDL, whose secretion by hepatocytes is not necessarily elevated during hepatic steatosis. Considering this, aberrant subcellular deposition of fatty acids must exist

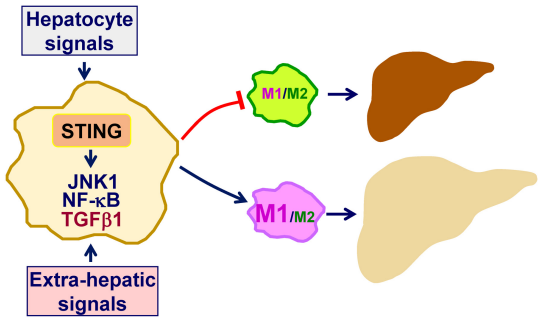

FIGURE 1
Macrophage STING promotes the pathogenesis of NAFLD. As a mediator of innate immunity, stimulator of interferon genes (STING) also exerts a crucial role in regulating inflammation. Within macrophages, double-stranded DNA (dsDNA) generated in response to mitochondrial dysfunction or endoplasmic reticulum stress activates cyclic GMP-AMP (cGAMP) synthase (cGAS) to increase cGAMP production. The latter, in turn, activates STING to promote macrophage proinflammatory activation. Inside the liver, hepatocytes are a key source that releases dsDNA including mitochondrial DNA and fragment DNA when under stress conditions. This, in turn, acts through cGAS-cGAMP signaling to activate the STING in macrophages. In addition, extra-hepatic mediators, i.e., gut-derived microbial DNA, exert a similar function in terms of activating macrophage STING in the liver. When activated, STING-stimulated macrophage activation promotes the development and progression of hepatic steatosis and inflammation. See text for details.

in hepatocytes and account for, to a certain extent, hepatocyte mitochondrial dysfunction and mtDNA production during hepatic steatosis. This notion is supported by the findings of a recent study investigating the role for hepatocyte adenosine kinase (ADK) in regulating fat deposition and liver inflammation. In that study, Li et al. showed that hepatocyte-specific ADK overexpression caused excessive fat deposition in hepatocytes, which was characterized by increased mitochondrial membrane accumulation of multiple bis-monoacylglycerol phosphate and lysophosphatidylcholine species and significantly decreased membrane levels of tetralinoleoyl cardiolipin (18:2-18:2-18:2-18:2), indicating increased oxidative stress and mitochondrial dysfunction (22). The latter was accompanied with increased hepatic mtDNA production and increased STING activation in liver macrophages (22). As such, intracellular accumulation of fats in excessive amount is one of the primary causes of increased production of hepatocyte mtDNA, which in turn functions to stimulate macrophage cGAS-cGAMP signaling and STING activation.

During liver injury in the absence of excessive fat deposition, hepatocyte production/release of mtDNA is increased and causes STING activation, in response to increased cGAS-cGAMP signaling, in liver macrophages/Kupffer cells (13). Specifically, the study by Chen et al. showed that hepatocyte-specific deletion of Sam50, a key component of the sorting and assembly machinery (SAM) necessary for the assembly of β-barrel proteins in the mitochondrial outer membrane, induced cardiolipin-dependent mitochondrial membrane remodeling to trigger mtDNA release. The latter was accompanied by increased STING amount and signaling in liver cells including macrophages, which in turn accounted for increased liver inflammatory injury. Similarly, the study by Liu et al. showed that the X-box binding protein 1

(XBP1) in hepatocytes was linked to macrophage STING activation through hepatocyte-derived mtDNA (23).

4. Extrahepatic mediator-stimulated STING activation

While the interplays among liver cells are key to the pathogenesis of NAFLD, extra-hepatic tissues have been shown to also regulate the development and progression of hepatic steatosis and inflammation as this is highlighted by the multiple-hit theory for NAFLD. For instance, under obese conditions, various mediators associated with adipose tissue dysfunction participate in the initiation and progression of NAFLD phenotype. These mediators include fatty acids, adipokines, and cytokines (24), many of which have been implicated to trigger or enhance liver inflammation through their actions on both hepatocytes and liver NPCs (24). It is worth noting that intestinal inflammation is increased not only under obese conditions, but also under conditions of lipoatrophy or absence of abdominal fat as this is supported by outcomes from mice fed an obesogenic/pro-NAFLD HFD or MCD diet (25–28). In particular, MCD-fed mice displayed increased intestinal inflammation that was correlated with corresponding degrees of liver inflammation while showing almost no abdominal fat. This suggests that intestinal inflammation could be more important than white adipose tissue inflammation in terms of triggering or exacerbating liver inflammation under certain conditions, e.g., lipoatrophy.

As it is extensively reviewed elsewhere, gut dysbiosis is a key factor contributing to NAFLD pathogenesis (29–32). Of note, "leaky gut" is shown to increase the delivery of nutrients and proinflammatory mediators to the liver to promote NAFLD phenotype. This role of gut-derived mediator(s) is well exemplified by the effect of bacterial DNA on promoting liver inflammation in the context of STING involvement in the development of liver inflammation (12). Initially, Luo et al. validated that gut microbial DNA-containing extracellular vesicles (mEVs) were translocated in the circulation and metabolic tissues including the liver in both HFD-fed WT mice and obese humans relative to their respective control. This type of mEVs is shown to enhance liver inflammation in mice primarily through stimulating STING activation in liver cells including hepatocytes. The same outcome could be expected for liver macrophages, whose response to mEVs in terms of STING activation, however, was not examined. It is worth noting that liver CRIg+ macrophages were shown to exert a unique function of clearing intestinal mEVs from circulation, thereby protecting against liver inflammation. As substantial evidence, treatment of chow diet-fed CRIg-deficient mice with obese mEVs significantly increased the abundance of liver cytokines including interleukin 1 beta and tumor necrosis factor alpha relative to control-treated CRIg-deficient mice. This effect of mEVs was significantly lighter in WT mice, and was due to, in large part, the less activation of STING pathway in the liver. Based on these findings, it is conceivable that microbial DNA, when translocated to the liver, is capable of stimulating liver inflammation in a manner involving STING. While it remains debatable if normal hepatocytes express STING, it is very likely that the STING in liver macrophages can be activated by microbial DNA and account for liver inflammation.

5. Conclusion

Inflammation not only underlies the pathogenesis of NAFLD, but also drives the progression of simple hepatic steatosis to NASH (9, 10, 21, 33–36). In terms of regulating inflammation, STING, an essential mediator of innate immunity, has also been implicated to exert a crucial role in promoting macrophage proinflammatory activation in a manner independent of IFNβ production (11, 17). Within the liver, macrophage STING can be activated by increased cGAS-cGAMP signaling in response to intracellular dsDNA due to mitochondrial stress or endoplasmic reticulum (ER) stress (14, 23). Moreover, under stress conditions, e.g., excessive fat deposition in hepatocytes, macrophage STING can be activated by increased cGAS-cGAMP signaling in response to exogeneous dsDNA, e.g., mtDNA, derived from hepatocytes (11, 16, 17, 22). This paracrine effect of hepatocyte-driven mediators on macrophage STING activation exemplifies dysregulation of crosstalk between macrophages and hepatocytes in the context of promoting the pathogenesis of NAFLD/NASH. In addition, during obesity, gut-derived microbial DNA can also be translocated to the liver and is expected to activate macrophage STING through cGAS-cGAMP signaling (12). The combined effects of hepatic and extrahepatic mediators on activating STING lead to enhanced macrophage proinflammatory activation, which in turn promotes liver inflammation and causes dysregulation of hepatocyte fat metabolism to trigger or exacerbate hepatic steatosis. The latter is attributable to, in large part, the paracrine effects of macrophage-driven mediators including proinflammatory cytokines on hepatocytes as reviewed elsewhere. As summarized in **Figure 1**, the STING in macrophages plays a central role in the pathogenesis of NAFLD. Accordingly, inhibiting STING in liver macrophages/Kupffer cells may be a viable approach for the management of NAFLD/NASH.

Author contributions

HL, XG, and EA wrote in part of the manuscript. CW came up the concept and finalized the manuscript. All authors contributed to the article and approved the submitted version.

Funding

This work was supported in whole or in part by grants from the National Institutes of Health (DK095862 and DK124854 to CW). Also, CW was supported by the Hatch Program of the National Institute of Food and Agriculture (NIFA).

Conflict of interest

The authors declare that the research was conducted in the absence of any commercial or financial relationships that could be construed as a potential conflict of interest.

Publisher's note

References

1. Thomsen LL, Ching LM, Baguley BC. Evidence for the production of nitric oxide by activated macrophages treated with the antitumor agents flavone-8-acetic acid and xanthenone-4-acetic acid. *Cancer Res.* (1990) 50:6966–70.

2. Perera PY, Barber SA, Ching LM, Vogel SN. Activation of LPS-inducible genes by the antitumor agent 5,6-dimethylxanthenone-4-acetic acid in primary murine macrophages. Dissection of signaling pathways leading to gene induction and tyrosine phosphorylation. *J Immunol.* (1994) 153:4684.

3. Cao Z, Baguley BC, Ching LM. Interferon-inducible protein 10 induction and inhibition of angiogenesis in vivo by the antitumor agent 5,6-dimethylxanthenone-4-acetic acid (DMXAA). *Cancer Res.* (2001) 61:1517–21.

4. Roberts ZJ, Goutagny N, Perera P-Y, Kato H, Kumar H, Kawai T, et al. The chemotherapeutic agent DMXAA potently and specifically activates the TBK1–IRF-3 signaling axis. *J Exp Med.* (2007) 204:1559–69. doi: 10.1084/jem.20061845

5. Zhong B, Yang Y, Li S, Wang Y-Y, Li Y, Diao F, et al. The adaptor protein MITA links virus-sensing receptors to IRF3 transcription factor activation. *Immunity.* (2008) 29:538–50.

6. Ahn J, Gutman D, Saijo S, Barber GN. STING manifests self DNA-dependent inflammatory disease. *Proc Natl Acad Sci U.S.A.* (2012) 109:19386–91. doi: 10.1073/pnas.1215006109

7. Conlon J, Burdette DL, Sharma S, Bhat N, Thompson M, Jiang Z, et al. Mouse, but not human STING, binds and signals in response to the vascular disrupting agent 5,6-dimethylxanthenone-4-acetic acid. *J Immunol.* (2013) 190:5216–25.

8. Guo X, Shu C, Li H, Pei Y, Woo S-L, Zheng J, et al. Cyclic GMP-AMP ameliorates diet-induced metabolic dysregulation and regulates proinflammatory responses distinctly from STING activation. *Sci Rep.* (2017) 7:6355. doi: 10.1038/s41598-017-05884-y

9. Luo X, Li H, Ma L, Zhou J, Guo X, Woo S-L, et al. Expression of STING is increased in liver tissues from patients with NAFLD and promotes macrophage-mediated hepatic inflammation and fibrosis in mice. *Gastroenterology.* (2018) 155:1971–84. doi: 10.1053/j.gastro.2018.09.010

10. Wang X, Rao H, Zhao J, Wee A, Li X, Fei R, et al. STING expression in monocyte-derived macrophages is associated with the progression of liver inflammation and fibrosis in patients with nonalcoholic fatty liver disease. *Lab Invest.* (2020) 100:542–52. doi: 10.1038/s41374-41019-40342-41376

11. Yu Y, Liu Y, An W, Song J, Zhang Y, Zhao X. STING-mediated inflammation in Kupffer cells contributes to progression of nonalcoholic steatohepatitis. *J Clin Invest.* (2019) 129:546–55. doi: 10.1172/JCI121842

12. Luo Z, Ji Y, Gao H, Gomes Dos Reis FC, Bandyopadhyay G, Jin Z, et al. CRIg+ macrophages prevent gut microbial DNA–containing extracellular vesicle–induced tissue inflammation and insulin resistance. *Gastroenterology.* (2021) 160:863–74. doi: 10.1053/j.gastro.2020.10.042

13. Chen L, Dong J, Liao S, Wang S, Wu Z, Zuo M, et al. Loss of Sam50 in hepatocytes induces cardiolipin-dependent mitochondrial membrane remodeling to trigger mtDNA release and liver injury. *Hepatology.* (2022) 76:1389–408.

14. Zhang Q, Wei J, Liu Z, Huang X, Sun M, Lai W, et al. STING signaling sensing of DRP1-dependent mtDNA release in kupffer cells contributes to lipopolysaccharide-induced liver injury in mice. *Redox Biol.* (2022) 54:102367. doi: 10.1016/j.redox.2022.102367

15. Zhong W, Rao Z, Xu J, Sun Y, Hu H, Wang P, et al. Defective mitophagy in aged macrophages promotes mitochondrial DNA cytosolic leakage to activate STING signaling during liver sterile inflammation. *Aging Cell.* (2022) 21:e13622. doi: 10.1111/acel.13622

16. Petrasek J, Iracheta-Vellve A, Csak T, Satishchandran A, Kodys K, Kurt-Jones EA, et al. STING-IRF3 pathway links endoplasmic reticulum stress with hepatocyte apoptosis in early alcoholic liver disease. *Proc Natl Acad Sci U.S.A.* (2013) 110:16544–9. doi: 10.1073/pnas.1308331110

17. Iracheta-Vellve A, Petrasek J, Gyongyosi B, Satishchandran A, Lowe P, Kodys K, et al. Endoplasmic reticulum stress-induced hepatocellular death pathways mediate liver injury and fibrosis via stimulator of interferon genes. *J Biol Chem.* (2016) 291:26794–805. doi: 10.1074/jbc.M116.736991

18. Thomsen MK, Nandakumar R, Stadler D, Malo A, Valls RM, Wang F, et al. Lack of immunological DNA sensing in hepatocytes facilitates hepatitis B virus infection. *Hepatology.* (2016) 64:746–59. doi: 10.1002/hep.28685

19. Nakamura S, Takamura T, Matsuzawa-Nagata N, Takayama H, Misu H, Noda H, et al. Palmitate induces insulin resistance in H4IIEC3 hepatocytes through reactive oxygen species produced by mitochondria. *J Biol Chem.* (2009) 284:14809–18. doi: 10.1074/jbc.M901488200

20. Woo S-L, Xu H, Li H, Zhao Y, Hu X, Zhao J, et al. Metformin ameliorates hepatic steatosis and inflammation without altering adipose phenotype in diet-induced obesity. *PLoS One.* (2014) 9:e91111. doi: 10.1371/journal.pone.0091111

21. Ma L, Li H, Hu J, Zheng J, Zhou J, Botchlett R, et al. Indole alleviates diet-induced hepatic steatosis and inflammation in a manner involving myeloid cell PFKFB3. *Hepatology.* (2020) 72:1191–203. doi: 10.1002/hep.31115

22. Li H, Zheng J, Xu Q, Yang Y, Zhou J, Guo X, et al. Hepatocyte adenosine kinase promotes excessive fat deposition and liver inflammation. *Gastroenterology.* (2023) 164:134–46. doi: 10.1053/j.gastro.2022.09.027

23. Liu Z, Wang M, Wang X, Bu Q, Wang Q, Su W, et al. XBP1 deficiency promotes hepatocyte pyroptosis by impairing mitophagy to activate mtDNA-cGAS-STING signaling in macrophages during acute liver injury. *Redox Biol.* (2022) 52:102305. doi: 10.1016/j.redox.2022.102305

24. Wang X, Rao H, Liu F, Wei L, Li H, Wu C. Recent advances in adipose tissue dysfunction and its role in the pathogenesis of non-alcoholic fatty liver disease. *Cells.* (2021) 10:3300.

25. Ding S, Chi MM, Scull BP, Rigby R, Schwerbrock NMJ, Magness S, et al. High-fat diet: bacteria interactions promote intestinal inflammation which precedes and correlates with obesity and insulin resistance in mouse. *PLoS One.* (2010) 5:e12191. doi: 10.1371/journal.pone.0012191

26. Guo X, Li H, Xu H, Halim V, Thomas LN, Woo S-L, et al. Disruption of inducible 6-phosphofructo-2-kinase impairs the suppressive effect of PPARg activation on diet-induced intestine inflammatory response. *J Nutr Biochem.* (2013) 24:770–5. doi: 10.1016/j.jnutbio.2012.04.007

27. Matthews DR, Li H, Zhou J, Li Q, Glaser S, Francis H, et al. Methionine- and choline-deficient diet–induced nonalcoholic steatohepatitis is associated with increased intestinal inflammation. *Am J Pathol.* (2021) 191:1743–53.

28. Zhu B, Li H, Lu B, Guo X, Wu C, Wang F, et al. Indole supplementation ameliorates MCD-induced NASH in mice. *J Nutr Biochem.* (2022) 107:109041. doi: 10.1016/j.jnutbio.2022.109041

29. Leung C, Rivera L, Furness JB, Angus PW. The role of the gut microbiota in NAFLD. *Nat Rev Gastroenterol Hepatol.* (2016) 13:412.

30. Yu J, Marsh S, Hu J, Feng W, Wu C. The pathogenesis of nonalcoholic fatty liver disease: interplay between diet, gut microbiota, and genetic background. *Gastroenterol Res Pract.* (2016) 2016:2862173.

31. Kolodziejczyk AA, Zheng D, Shibolet O, Elinav E. The role of the microbiome in NAFLD and NASH. *EMBO Mol Med.* (2019) 11:e9302.

32. Jiang X, Zheng J, Zhang S, Wang B, Wu C, Guo X. Advances in the involvement of gut microbiota in pathophysiology of NAFLD. *Front Med.* (2020) 7:361. doi: 10.3389/fmed.2020.00361

33. Deng Z, Liu Y, Cunren Liu C, Xiang X, Wang J, Cheng Z, et al. Immature myeloid cells induced by a high-fat diet contribute to liver inflammation. *Hepatology.* (2009) 50:1412–20. doi: 10.1002/hep.23148

34. Huang W, Metlakunta A, Dedousis N, Zhang P, Sipula I, Dube JJ, et al. Depletion of liver Kupffer cells prevents the development of diet-induced hepatic steatosis and insulin resistance. *Diabetes.* (2010) 59:347–57. doi: 10.2337/db09-0016

35. Xu H, Li H, Woo S-L, Kim S-M, Shende VR, Neuendorff N, et al. Myeloid cell-specific disruption of Period1 and Period2 exacerbates diet-induced inflammation and insulin resistance. *J Biol Chem.* (2014) 289:16374–88. doi: 10.1074/jbc.M113.539601

36. Cai Y, Li H, Liu M, Pei Y, Zheng J, Zhou J, et al. Disruption of adenosine 2A receptor exacerbates NAFLD through increasing inflammatory responses and SREBP1c activity. *Hepatology.* (2018) 68:48–61. doi: 10.1002/hep.29777

frontiers | Frontiers in Nutrition

TYPE Original Research
PUBLISHED 09 March 2023
DOI 10.3389/fnut.2023.1116278

OPEN ACCESS

EDITED BY
Ding-Tao Wu,
Chengdu University,
China

REVIEWED BY
Kiran Veer Sandhu,
University College Cork,
Ireland
Wen Zhou,
Nanjing University of Chinese Medicine,
China
Ming Cai,
Shanghai University of Medicine and Health Sciences,
China

*CORRESPONDENCE
Jin-Rong Zhou
✉ jrzhou@bidmc.harvard.edu

SPECIALTY SECTION
This article was submitted to Nutrition and Microbes, a section of the journal Frontiers in Nutrition

RECEIVED 06 December 2022
ACCEPTED 10 February 2023
PUBLISHED 09 March 2023

CITATION
Abdolmaleky HM, Sheng Y and Zhou J-R (2023) Bioactive nutraceuticals oligo-lactic acid and fermented soy extract alleviate cognitive decline in mice in part *via* anti-neuroinflammation and modulation of gut microbiota.
Front. Nutr. 10:1116278.
doi: 10.3389/fnut.2023.1116278

Bioactive nutraceuticals oligo-lactic acid and fermented soy extract alleviate cognitive decline in mice in part *via* anti-neuroinflammation and modulation of gut microbiota

Hamid M. Abdolmaleky, Yin Sheng and Jin-Rong Zhou*

Nutrition/Metabolism Laboratory, Department of Surgery, Beth Israel Deaconess Medical Center, Harvard Medical School, Boston, MA, United States

Introduction: Cognition decline is associated with aging and certain diseases, such as neurodegenerative or neuropsychiatric disorders, diabetes and chronic kidney disease. Inflammation/neuroinflammation is considered an important causal factor, and experimental evidence suggests that anti-inflammatory natural compounds may effectively prevent cognitive decline. The goal of this study was to evaluate the effects of two natural bioactive agents, oligo-lactic acid (LAP) and fermented soy extract (ImmunBalance, IMB), on cognition in an adenine-induced cognitive impairment mouse model and to investigate the modulation of related biomarkers.

Methods: Male C57 black mice were randomly assigned into the following experimental groups and received the corresponding treatments for 2 weeks before the use of adenine for model development: (1) negative control; (2) model control: injection of adenine at 50mg/kg daily for 4 weeks; (3, 4) IMB groups: adenine injection and IMB oral gavage at 250 and 1,000mg/kg BW, respectively; and (5) LAP group: adenine injection and LAP oral gavage at 1,000mg/kg BW. One week after the model was developed, mice were evaluated for cognitive performances by using Y maze test, novel object recognition test, open field test, and Barnes maze tests. At the end of the experiment, brain tissues and cecum fecal samples were collected for analysis of gene expression and gut microbiota.

Results: Mice treated with LAP or IMB had significantly improved spatial working memory, spatial recognition memory (LAP only), novel object recognition, and spatial learning and memory, compared with those in the model group. Gene expression analysis showed that, among a panel of cognition related genes, six of them (ELOVL2, GLUT4, Nestein, SNCA, TGFB1, and TGFB2) were significantly altered in the model group. LAP treatment significantly reversed expression levels of inflammatory/neuroinflammatory genes (SNCA, TGFB1), and IMB significantly reversed expression levels of genes related to inflammation/neuroinflammation, neurogenesis, and energy metabolism (ELOVL2, GLUT4, Nestin, TGFB1, and TGFB2). The altered microbiome was attenuated only by IMB.

Discussion: In conclusion, our data showed that LAP improved cognition associated with regulating biomarkers related to neuroinflammation and energy metabolism, whereas IMB improved cognition associated with regulating biomarkers related to neuroinflammation, energy metabolism, and neurogenesis, and modulating gut microbiota. Our results suggest that LAP and IMB may improve cognitive performance in mice *via* distinct mechanisms of action.

KEYWORDS

cognition, nutraceuticals, oligo-lactic acid, fermented soy extract, neuroinflammation, microbiota, gene expression

Introduction

Cognition is regarded as a higher function of the central nervous system (CNS) and includes attention, learning, memory, and executive processes (1). Cognition decline is associated with aging and certain diseases, such as neurodegenerative or neuropsychiatric disorders, diabetes, and chronic kidney disorder (CKD) (2). Despite efforts to develop novel therapeutic agents to improve cognitive function, few viable treatment options exist. However, several lines of evidence indicate that natural bioactive agents may provide effective preventive and/or therapeutic strategies to delay cognitive decline (3). More recent research data also provided strong evidence that nutritional compounds not only mediate their effects though their natural bioactive agents, their influence on gut microbiome alterations may also have significant beneficial or harmful consequences (4).

The science of microbial colonization of gut was limited before the development of microbial 16S rRNAs sequencing technology. Now, it has been shown that the mammals gut contains diverse bacterial elements which their total number is 10 times more than their body cells. Surprisingly, the gut microbial population collectively contain 100 times more genes than human which are involved in the digestion of many nutritional compounds or production of nutrients and vitamins (Reviewed in Alam et al. (4)). There is also evidence that nutritional elements and food compounds affect the gut microbiome composition and thus their function as well. For example, it has been shown that in mice fed with high-fat diet, silybin decreases *Firmicutes*, *Lactobacillus*, *Lachnoclostridium*, and *Lachnospiraceae_UCG-006*, and increases the gut level of *Bacteroidetes*, *Bacteroides*, *Blautia*, and *Akkermansia* (5), while epigallocatechin-3-gallate (EGCG) increases *Verrucomicrobia*, *Enterococcaceae*, and *Verrucomicrobiaceae*, but decreases *Deferribacteres*, *Lachnospiraceae*, *Desulfovibrionaceae*, *Bacteroidaceae*, *Proteobacteria*, *Prevotellaceae*, *Deferribacteraceae*, and *Rikenellaceae* (6).

Furthermore, it has been shown that gut microbiota not only plays an important role in normal brain development, but also has significant impacts on animal behavior and cognitive status. For example, metabolomic analysis showed that four metabolites linked to neuropsychiatric disorders were down-regulated in germ-free mice (7). Additionally, gut microbiota manipulation in germ-free mice impacts fear extinction learning that is associated with gene expression alterations in single-nucleus RNA sequencing analysis of glia, excitatory neurons, and other brain cells in the medial prefrontal cortex (7). These mice also exhibit postsynaptic dendritic spines remodeling and hypoactivity of cue-encoding neurons in transcranial two-photon imaging analysis. However, selective microbiota re-establishment could restore normal extinction learning (7). Notably, increases in plasma tryptophan and hippocampal concentration of serotonin and its metabolite (5-hydroxyindoleacetic acid) was also shown in germ-free mice compared to the control mice. While the brain neurochemical changes remained stable until adulthood, restoring microbial colonization post weaning could reverse behavioral alterations in affected mice (8).

It has been reported that mice treated with adenine showed depressed locomotor activity associated with cognitive impairment, depleted brain norepinephrine, dopamine and serotonin, disrupted blood–brain barrier, and increased brain inflammation (9–12). In our previous study applying this mouse model to investigate the effect of bioactive components on CKD (13), we found that the adenine-treated mice had increased inflammation in circulation and in kidney tissues. Bioactive components, an oligo-lactic acid product (LAP) and/or a fermented soy extract (ImmunBalance, IMB), alleviated adenine-induced CKD associated with decreased circulating inflammatory cytokines and tissue inflammation. Our preliminary observation also indicated that mice in the model group had cognitive problems. Interestingly, LAP- and IMB-treated groups showed improved cognition and were more energetic and healthier than positive control mice (adenine treated). These results and observations suggest that LAP and/or IMB may have beneficial effects on improving cognition/alleviating inflammation-associated cognitive impairment.

In this study, we propose to investigate the effects of LAP and/or IMB on improving cognition in adenine-induced mouse model of cognitive impairment, and to determine if improved cognition is associated with modulation of gut microbiota using and expression of inflammation related genes in brain tissue.

Materials and methods

Materials

A soy extract, IMB was prepared by a koji fermentation of defatted soybeans with *Aspergillus oryzae* and lactic acid bacteria (*Pediococcus parvulus* and *Enterococcus faecium*) according to a proprietary fermentation technology, followed by water extraction and purification of Koji polysaccharides®. IMB was provided by Nichimo Biotics Co., Ltd., Japan. Oligo-lactic acid product (LAP) was a condensate of about nine ester-linked molecules of L-lactic acid that was purified from fermentation products of sugar beet and corn with *Lactobacilli* according to a proprietary process. LAP was provided by LifeTrade Co., Ltd., Japan.

Animal study

Male C57BL/6 mice (8–9 weeks of age) were purchased from Taconic (Germantown, NY, United States), housed in a room at a temperature of 22 ± 2°C, relative humidity of about 60%, with a 12 h light–dark cycle, and free access to an AIN-93 M diet. After an acclimatization period of 1 week, mice were randomly assigned into the following five groups ($n = 8$/group) and receive the corresponding treatment for 2 weeks before the use of adenine for model

development: (1) negative control (NC): PBS injection and PBS oral gavage daily; (2) model control (MC): adenine injection intraperitoneally (i.p.) at a dose of 50 mg/kg daily for 28 days and PBS oral gavage daily; (3) IMB-low treatment (IMB-L): adenine injection, oral gavage of IMB at 250 mg/kg BW; (4) IMB-high treatment (IMB-H): adenine injection, oral gavage of IMB at the 1,000 mg/kg BW; and (5) LAP treatment: adenine injection, oral gavage of LAP at 1,000 mg/kg BW. Our previous animal study indicated that IMB had a dose-dependent effect, whereas LAP did not show clear dose-dependent effect (13). Therefore, we used two doses of IMB (250 and 1,000 mg/kg BW) and one dose of LAP (1,000 mg/kg BW) in this study to evaluate the effect of treatments on cognition improvement and biomarkers alterations. Body weight and food intake were measured weekly. The cognition/memory evaluations were started 1 week after adenine injection was finished. A diagram of experimental protocol is included as Figure 1.

Methods for memory/cognition tests

Y maze test

The Y maze was used to measure spatial working and recognition memory by making use of a rodent's natural exploratory instincts (14). The Y-maze consists of three arms of equal length interconnected at 120°. The Y Maze test includes two sessions. The first session measures spatial working memory, and the second session measures spatial recognition memory. The experimental procedures are described as follows:

Spatial working memory test: During the first session of the experiment to measure spatial working memory, all three arms of the maze were open. Specifically, mice were placed onto the end of one arm and allowed to explore freely for 5 min. The sequences of the arms entries were recorded. The spontaneous alternation behavior was calculated as the number of triads (three different arms, ABC not ABB) that contain entries into all three arms divided by the total visits. The first session represents a classic spontaneous alternation test of spatial working memory.

Spatial recognition memory test: The second session measures spatial recognition memory. During the testing phase, one of the arms of the maze was blocked while the mouse was allowed for a 5-min exploration of only two arms of the maze. After a 30 min break, the partition was removed and the mouse was allowed for another 5-min exploration. Since the first 2 min of activities were the most sensitive to measure spatial preference for a new arm, the time and number of visits to the new arm were calculated for the first 2 min of testing. The first 5 min of activities were also recorded and the motor activity was calculated as the number of arms visited for the whole period of the test. This experiment takes advantage of the innate tendency of mice to explore novel unexplored areas (e.g., the previously blocked arm). Mice with intact recognition memory prefer to explore a novel arm over the familiar arms, whereas mice with impaired spatial recognition memory enter all arms randomly. Thus, this experiment represents a classic test for spatial recognition memory.

Data were recorded and analyzed by using the Smartsuper software (Harvard Apparatus, Holliston, MA, United States) for the time spent in each arm overall, and the time spent in each arm for the first 2 and 5 min.

Novel object recognition test

This test was used to examine memory in animals. The mouse was presented with an object during acclimation and then in testing presented with a novel (new) object, and the amount of time the animal spends exploring the novel object was recorded. The mouse was then challenged further with a subsequent test where the novel object was moved. Here instead of a three-chamber apparatus, which was used in previous experiments (thus mice were familiar with), a rectangle chamber was used. The experimental protocols are described as follows:

Acclimation: Each animal was placed in a rectangle chamber without objects and was allowed to explore for 10 min. The procedures were repeated 24 and 48 h later, thus the total acclimation was 3 days.

Experiment setup-day 4: In the rectangle chamber apparatus, two identical objects were placed in the test chamber. The animal activity was recorded to track how much time was spent to interact with each of the objects, the "right object" and "left object," for a fixed session length of 10 min. The animal's nose must be within 1 cm of the object and directed at the object, or actually touch the object in order to be considered time spent exploring the object. After 10 min, we removed the animal was putted back in its home cage and the chamber and objects were cleaned with 70% ethanol to remove any smell.

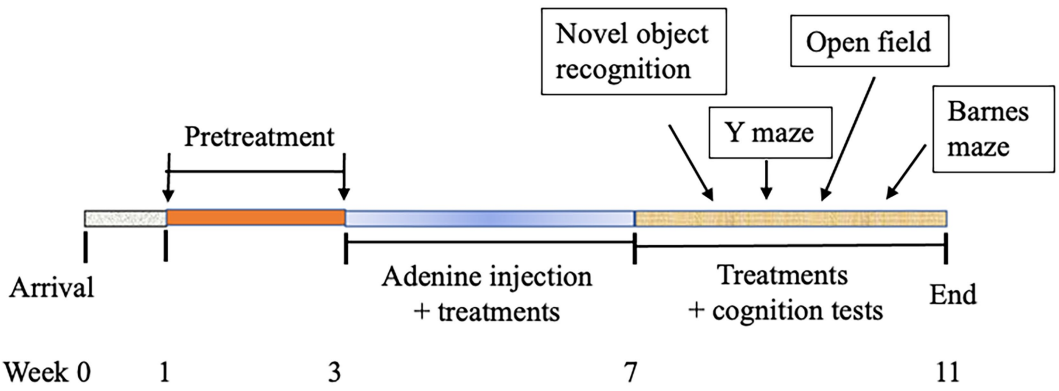

FIGURE 1
Diagram of experimental schedule.

Experiment setup-day 5: One old object and one novel (new) object were putted in the chamber, and the animal activity was recorded for 5 min instead of 10 min. After an intertrial interval (ITI) of approximately 2 h, the location of the old object was moved so that it was located on a different wall and the steps were repeated, again using a 5 min trial length.

Open field test

Open field test was used to evaluate mouse fear and anxiety levels. In this test, a mouse was placed in rectangle apparatus and its activity was recorded for 10 min. Mouse instinct drives it to search in the corners and angles of the chamber instead of the middle part (open field) of the chamber. In this test, we also placed two identical objects in the chamber, one in a corner and another one in the middle of the chamber to assess the frequency and time the mouse spent with each object. The mouse was expected to spend more time with the object placed in the corner than that in the middle.

Barnes maze for spatial learning and memory test

Mice spatial learning and memory were assessed using Barnes maze test (Harvard Apparatus). Barnes maze is one of the best and ideal apparatus for testing spatial learning and memory in mice (14, 15). The Barnes maze motivates animals to hide from the bright, open platform by finding the small, dark "escape box." Animals learn the escape box's location without the stress of swimming or food deprivation, and false escape boxes remove the possibility of inadvertent cues. With a variety of color options, Barnes maze adjusts to fit a wide range of experiments. In Barnes test, mice are trained in 3–5 sessions to find the escape box and after 5–7 days mice are tested for the time spent to find the escape box. We tested the mice for two successive days after 6 days interval. The data were collected and analyzed using the Smartsuper software (Harvard Apparatus).

At the end of Barnes maze test, mice were sacrificed, and biological samples (blood, brain, and cecum) were collected for analyses. A piece of mouse brain sample from the left frontal lobe (~30 mg) was used for RNA and DNA extraction. The fecal sample of mouse cecum was used for DNA extraction and microbiome profiling.

Gene expression analysis by quantitative real-time PCR (qRT-PCR)

An aliquot of hippocampus-containing brain tissues was used for gene expression analysis. In brief, following RNA extraction using Direct-Zol DNA/RNA MiniPrep kit (Zymo Research, Irvine, CA, United States) and cDNA synthesis using Bio-Rad iScript cDNA synthesis kit (Hercules, CA, United States), expression levels of genes related to neurotransmission, inflammation, metabolism, and neuronal protection/regeneration were determined using CFX384 Touch real-time PCR detection system and *Power* SYBR™ Green PCR Master Mix (Applied Biosystems, Bedford, MA, United States) by following the established procedures (13). These genes included brain-derived neurotrophic factor (BDNF), dopamine beta-hydroxylase (DBH), dopamine receptor D2 (DRD2), ELOVL fatty acid elongase 2 (ELOVL2), glucose transporter 4 (GLUT4), Huntington-associated protein 1 (HAP1), 5-hydroxytryptamine receptor 2A (HTR2A), interleukin 1β (IL1B), IL4, IL6, NESTIN, phosphoinositide 3-kinase (PI3K), solute carrier family 6 member 4 (SLC6A4), synuclein alpha (SNCA), transforming growth factor beta 1 (TGFB1), TGFB2, and TSC complex subunit 1 (TSC1). All mRNA quantification data were calculated using the $2^{\Delta\Delta Ct}$ method and normalized to GAPDH, presented as folds to the negative control (NC). The primer sequences of genes were taken from Harvard Primer Bank (listed in Table 1) designed for real-time PCR analysis and tested to assure that they generated a single PCR product.

Microbiome analysis of cecum fecal samples

DNA was extracted using Quick-DNA Fecal/Soil Microbiome Miniprep kit (Zymo research, cat # D6010) from 30 mg of fecal sample from the mouse cecum for microbiota analysis. After quantitation and quality control using NanoDrop One (Thermo Scientific), the extracted DNA (each ~100 ng/μl, in total volume of 100 μl) was diluted (10 ng/μl) and subjected to examination with one set of universal and one set of Lactobacillus specific primers (Table 2) (16) to reconfirm DNA quality. Then, DNA samples were sent to CoreBiome, Inc.[1] for microbiome profiling using amplicon sequencing targeting variable region 4 of the bacterial 16S ribosomal RNA gene (16S rRNA). All quality control measures by CoreBiome experts confirmed the reliability of data presented in the result section.

The details of the methods are presented in www.corebiome.com and elsewhere by the developers (17).

Statistical analysis

Data were expressed as the group mean ± standard error and analyzed by one-way analysis of variance (ANOVA) test, followed by multiple comparison of least-significant difference (equal variances assumed) or Dunnett's T3-test (equal variances not assumed) to evaluate the difference of parametric samples among groups. A p-value of <0.05 was considered statistically significant.

Results

Effects of treatments on body weight and food intake

There was no significant difference in the baseline body weight among experimental groups (Figure 2A). As expected, model induction *via* daily adenine injection reduced body weight (Figure 2B) in all modeled groups, compared with the negative control group, whereas there were no significant differences of body weight among the modeled groups. Similarly, mice in the modeled groups reduced food intake, compared with the NC group, but there were no significant differences of food intake among the modeled groups (data not shown).

1 www.corebiome.com

TABLE 1 The primer sequences for qRT-PCR.

Genes	Forward	Reverse
BDNF	TCATACTTCGGTTGCATGAAGG	AGACCTCTCGAACCTGCCC
DBH	GAGGCGGCTTCCATGTACG	TCCAGGGGGATGTGGTAGG
DRD2	ACCTGTCCTGGTACGATGATG	GCATGGCATAGTAGTTGTAGTGG
ELOVL2	CCTGCTCTCGATATGGCTGG	AAGAAGTGTGATTGCGAGGTTAT
GAPDH	AGGTCGGTGTGAACGGATTTG	GGGGTCGTTGATGGCAACA
GLUT-4	ATCATCCGGAACCTGGAGG	CGGTCAGGCGCTTTAGACTC
HAP1	AGGTGAACCTGCGAGATGAC	TGCTGGTCTTGATCCCTCTGT
HTR2A	TAATGCAATTAGGTGACGACTCG	GCAGGAGAGGTTGGTTCTGTTT
IL1B	GCAACTGTTCCTGAACTCAACT	TGGATGCTCTCATCAGGACAG
IL4	GGTCTCAACCCCCAGCTAGT	GCCGATGATCTCTCTCAAGTGAT
IL6	CCAAGAGGTGAGTGCTTCCC	CTGTTGTTCAGACTCTCTCCCT
Nestin	CCCTGAAGTCGAGGAGCTG	CTGCTGCACCTCTAAGCGA
PI3K	TTATTGAACCAGTAGGCAACCG	GCTATGAGGCGAGTTGAGATCC
SLC6A4	GTCATTGGCTATGCCGTGGA	CACCCATTTCGGTGGTACTG
SNCA	GACAAAAGAGGGTGTTCTCTATGTAG	GCTCCTCCAACATTTGTCACTT
TGFB1	CTCCCGTGGCTTCTAGTGC	GCCTTAGTTTGGACAGGATCTG
TGFB2	CTTCGACGTGACAGACGCT	TTCGCTTTTATTCGGGATGATGT
TSC1	ATGGCCCAGTTAGCCAACATT	CAGAATTGAGGGACTCCTTGAAG

TABLE 2 Primer sequences of microbiota analysis.

Lac-F	AGCAGTAGGGAATCTTCCA	*Lactobacillus* genus
Lac-R	CACCGCTACACATGGAG	*Lactobacillus* genus
Uni331F	TCCTACGGGAGGCAGCAGT	All bacteria
Uni797R	GGACTACCAGGGTATCTATCCTGTT	All bacteria

Effects of LAP and IMB treatments on spatial working memory and recognition memory

Spatial working memory and recognition memory tests were performed using Y maze as described in methods. There were no significant changes in the total activity (numbers of arm entry) among different groups (Figure 3A). The model development significantly impaired spatial working memory (Figure 3B, $p < 0.05$) but did not significantly affect recognition memory (Figure 3C). Compared with the MC, mice treated with LAP had significantly better spatial working memory (Figure 3B, $p < 0.05$) and recognition memory (Figure 3C, $p < 0.05$). IMB treatment improved spatial working memory in a dose-dependent manner and mice treated with the high dose IMB had significantly increased spatial working memory (Figure 3B, $p < 0.05$).

Effects of LAP and IMB treatments on novel object recognition and spatial learning and memory

As shown in Figure 4A, the MC mice had non-significant impairment of novel object recognition memory; mice treated with LAP significantly improved novel object recognition by over 30% ($p < 0.05$). IMB showed a dose-dependent effect on novel object recognition memory, and the high dose IMB treatment showed a significant effect ($p < 0.05$).

Barnes maze test was applied to determine spatial learning and memory. Compared with the NC, mice in the MC showed significantly impaired spatial learning and memory (Figure 4B, $p < 0.05$). This impaired memory was significantly improved by the treatment of LAP ($p < 0.05$) or IMB ($p < 0.05$ for IMB-L; $p < 0.001$ for IMB-H). Overall, IMB treatment showed a suggestive dose-dependent effect.

The results of open field test did not show significant alterations among any experimental groups (data not shown).

Effects of LAP and IMB treatments on gene expression levels of related biomarkers in brain tissues

We explored the expression levels of a panel of genes related to neurotransmission, inflammation, metabolism, and neuronal regeneration at RNA levels (including, BDNF, DBH, DRD2, ELOVL2, GLUT4, HAP1, HTR2A, IL1B, IL4, IL6, NESTIN, PI3K, SLC6A4, SNCA, TGFB1, TGFB2, and TSC1) aiming to identify candidate genes whose expressions were significantly altered in the model group and were significantly reversed by LAP and/or IMB treatments. Six candidate genes (ELOVL2, GLUT4, SNCA, Nestein, TGFB1, and TGFB2) were identified. As shown in Figure 5, compared with the NC, the model development (MC) significantly decreased the expression levels of GLUT4, NESTIN, TGFB1, and TGFB2 genes by 75, 80, 60, and 50%, respectively (p at least <0.05), and significantly increased the expression levels of ELOVL2 and SNCA genes by 60 and 55%, respectively ($p < 0.05$). Expression of TGFB1 was significantly increased by LAP (>100%, $p < 0.05$) and

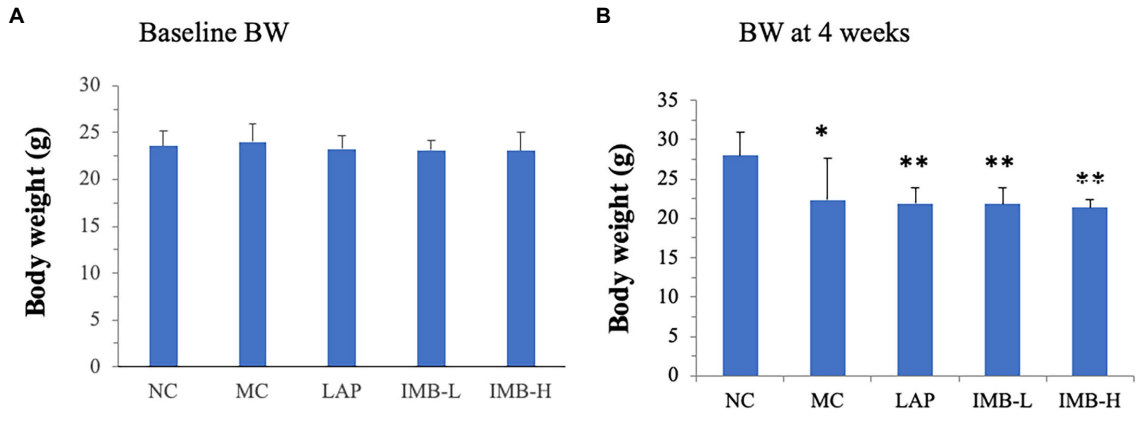

FIGURE 2
Effects of treatments on body weights (BW). **(A)** Baseline BW; **(B)** BW after 4weeks of model induction. Values are expressed as mean±standard error. Within each panel, values with a superscript symbol are significantly different from the NC. *p<0.05; **p<0.01.

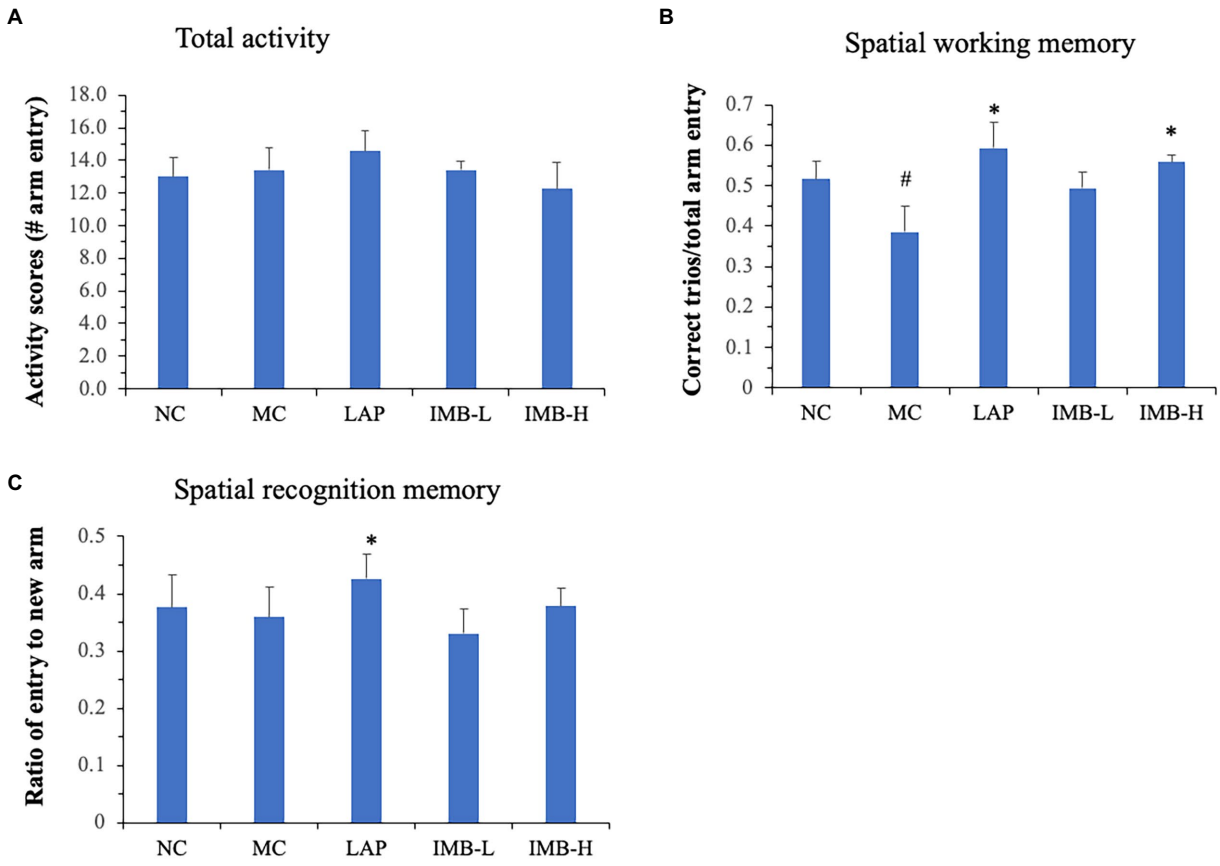

FIGURE 3
Effects of treatments on spatial working memory and spatial recognition memory, as measured by Y maze test. **(A)** Total activity measured as the total numbers of arm entries in 5min; **(B)** Spatial working memory measured as the correct trios (ABC or ACB) vs. total arm entry in 5min; **(C)** Spatial recognition memory measured as the average number of entries to new arm in 5min. Values are expressed as mean±SE (n=8). Within each panel, values with a superscript symbol "*" are significantly different from that of the MC. *p<0.05.

IMB-H (>150%, $p < 0.05$; Figure 5E); the decreased expression of TGFB2 in model mice trended to be normalized by IMB treatment (Figure 5F). The reduced expression levels of GLUT4 (Figure 5B) and NESTIN (Figure 5C) in the MC mice were increased significantly by IMB-H treatment (>100 and 150%, respectively, $p < 0.05$). The increased expression of ELOVL2 in the MC mice was reversed only by IMB-L or IMB-H treatment (Figure 5A, ~40%, $p < 0.05$), whereas the increased expression of SNCA in the MC

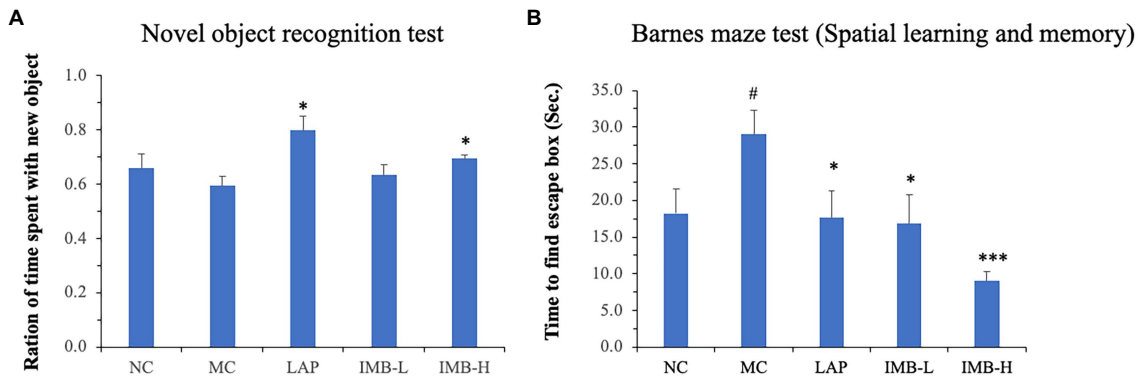

FIGURE 4
Effects of treatments on novel object recognition memory and spatial learning and memory. Mouse novel object recognition memory was tested 24h after training **(A)**; mouse spatial learning and memory was evaluated in Barnes maze test **(B)**. Values are expressed as mean±SE (n=7–8). Within each panel, values with a superscript symbol "*" is significantly different from that of the MC (*p<0.05; ***p<0.001); and the value in the MC with a superscript symbol "#" is significantly different from that of the NC ($^{\#}p$<0.05).

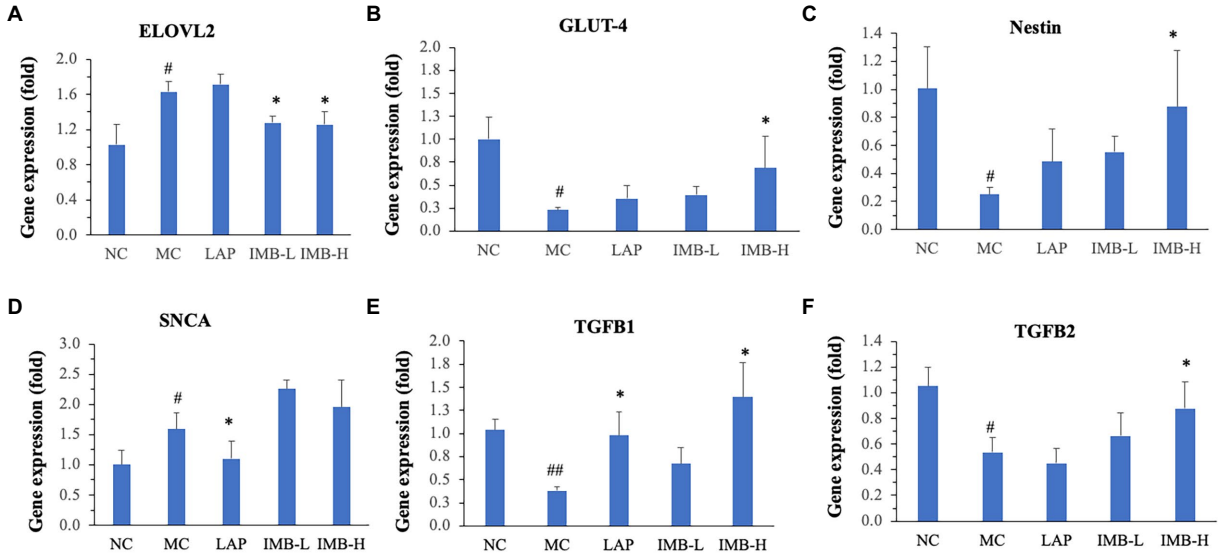

FIGURE 5
Effects of treatments on expression levels of genes that were significantly altered by model development and recovered by LAP and/or IMB treatment. ELOVL2 **(A)**, GLUT-4 **(B)**, Nestin **(C)**, SNCA **(D)**, TGFB1 **(E)**, and TGFB2 **(F)**. Values are expressed as mean±SE (n=7–8). Within each panel, values with a superscript symbol "*" are significantly different from that of the MC (*p<0.05; **p<0.01); and the value of the MC with a superscript symbol "#" is significantly different from that of the NC ($^{\#}p$<0.05; $^{\#\#}p$<0.01).

mice was significantly altered by the LAP treatments (Figure 5D, $p < 0.05$).

Effects of LAP and IMB treatments on gut microbiota

In general, the abundance of almost 60% (30 out of 51) of bacterial species exhibited significant changes in the MC, compared with that in the NC. As shown in Figure 6A the diversity of bacterial species decreased in the MC group which was recovered in part by IMB-H. Figure 6B shows the abundances of three common bacteria that were significantly altered in the MC group and were also reversed/normalized in the IMB-H group. Compared with the NC, model development (MC) significantly decreased the abundance of *Lachnospiraceae bacterium* 28-4 ($p < 0.05$), but significantly increased abundances of *Bifidobacterium pseudolongum* and *Faecalibaculum rodentium* ($p < 0.001$). In general, IMB treatments recovered aberrant alterations in a dose-dependent manner and the high dose IMB (IMB-H) treatment had significant effects. On the other hand, LAP treatment did not show significant effects on reversing the abundance of these common bacteria altered in the MC group (Figure 6B).

The abundances of two phyla (out of seven phyla) were also altered significantly in the MC group (Figure 6C). Compared with the NC, the MC significantly increased the abundance of *Actinobacteria* ($p < 0.01$) and significantly decreased the abundance of *Bacteroidetes* ($p < 0.001$) (Figure 6C). Those alterations were significantly reversed by the treatment of high dose IMB (IMB-H), but not LAP or IMB-L.

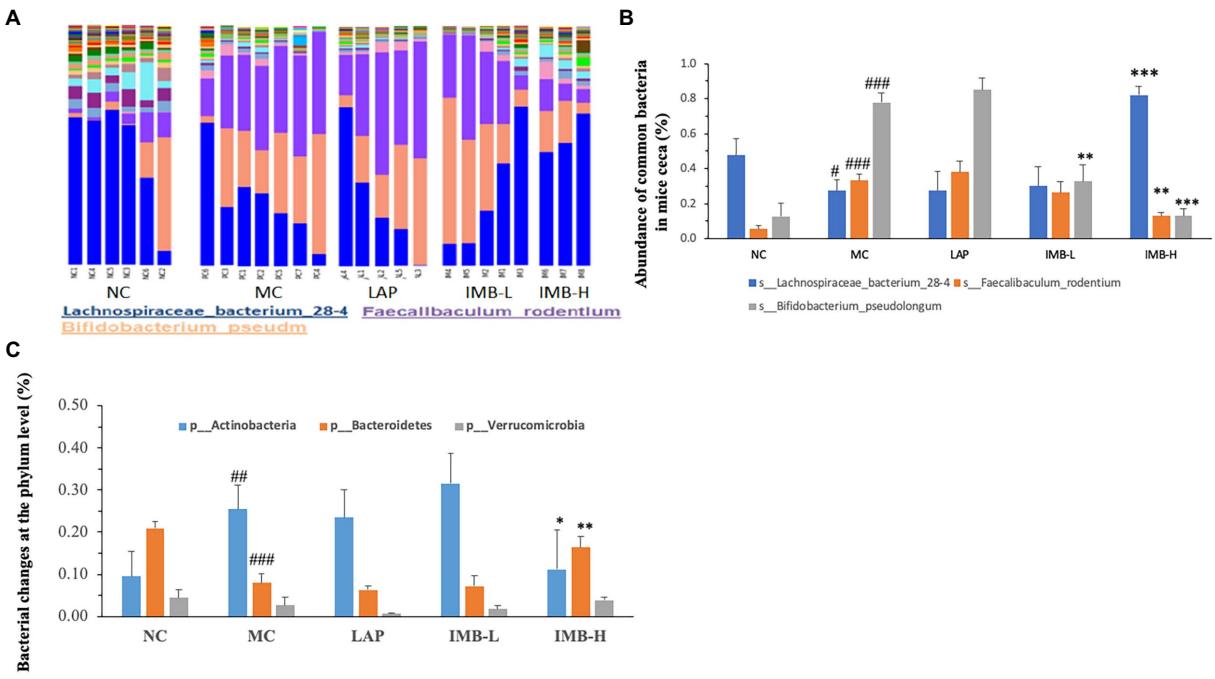

FIGURE 6
Effects of treatments on gut microbiota. **(A)**. A portray of cecum bacterial changes; **(B)**. Effects of treatments on the abundance of three common bacteria; **(C)**. Effects of treatments on the abundance of three phyla. Values are expressed as mean±SE (n=3–7). Within each panel **(B or C)**, values with a superscript symbol "*" are significantly different from that of the corresponding MC (*p<0.05; **p<0.01; ***p<0.001); and the value of the MC with a superscript symbol "#" is significantly different from that of the corresponding NC ($^{\#}p$<0.05; $^{\#\#}p$<0.01; $^{\#\#\#}p$<0.001).

We also found that the model development significantly altered the abundances of several rare (Figure 7A) and very rare (Figure 7B) bacteria, and some treatments significantly reversed these alterations. In general, IMB treatment showed a dose-dependent effect on reversing model-induced alterations and the high dose IMB treatment effects were statistically significant. On the other hand, LAP treatment did not show significant effect on the abundances of those bacteria.

Discussion

In this study, we evaluated the effects of two nutraceutical components, LAP and IMB, on cognitive status of adenine-induced cognitive impairment mouse model. Mice treated with LAP had significantly improved spatial working memory (Figure 3B), spatial recognition memory (Figure 3C), novel object recognition (Figure 4A), and spatial learning and memory (Figure 4B), compared with those in the MC group. Similarly, IMB treatment significantly improved spatial working memory (Figure 3B), novel object recognition (Figure 4A), and spatial learning and memory (Figure 4B) in a dose-dependent manner. Gene expression analysis showed that, among a panel of genes, six of them (ELOVL2, GLUT4, Nestein, SNCA, TGFB1, and TGFB2) were significantly altered in the model group, and their expression levels were significantly reversed by LAP (SNCA and TGFB1) and/or IMB (ELOVL2, GLUT4, Nestin, TGFB1, and TGFB2). On the other hand, the altered microbiome was attenuated only by IMB-H.

Our study showed that LAP could significantly alleviate adenine-induced cognitive impairment. While the mechanisms of LAP actions may remain elusive, it is possible that reduction of inflammation/neuroinflammation may be one of the important mechanisms. The causal role of inflammation/neuroinflammation in cognitive impairment is well recognized. Our previous study showed that LAP reduced inflammatory lesions in kidney tissues, circulating levels of proinflammatory cytokines (IL-6 and IL-12p70), and mRNA levels of proinflammatory cytokines (IL-6, TLR-4, F4/F80, and IL-1ß) in kidney tissues (13). While histopathological evaluation of inflammation in brain tissues was not performed (in part due to insufficient tissue availability), we found that adenine significantly increased SNCA mRNA level and decreased TGFB1 mRNA level, and these alterations could be significantly reversed by LAP treatment. SNCA has recently been shown to be associated with decline of cognitive functions in older adults including Alzheimer's disease patients possibly *via* mediation/induction of neuroinflammation (18, 19), supporting that SNCA may serve as an additional biomarker for determining poor cognitive functions (19). TGFB1 is an important anti-inflammatory cytokine. It has been shown that its lower production may predict a longitudinal functional and cognitive decline in oldest-old individuals (20). Cumulatively, these results strongly suggest that one of the mechanisms by which LAP alleviates adenine-induced cognitive impairment may *via* modulating SNCA- and/or TGFB1- mediated neuroinflammation. Further research on studying how LAP may alter SNCA and/or TGFB1 expression and function is warranted.

LAP is a chain of nine lactate molecules, it is likely that LAP is broken to lactate and then lactate affect gene expression pattern and cognitive functions. Lactate has long been considered a byproduct

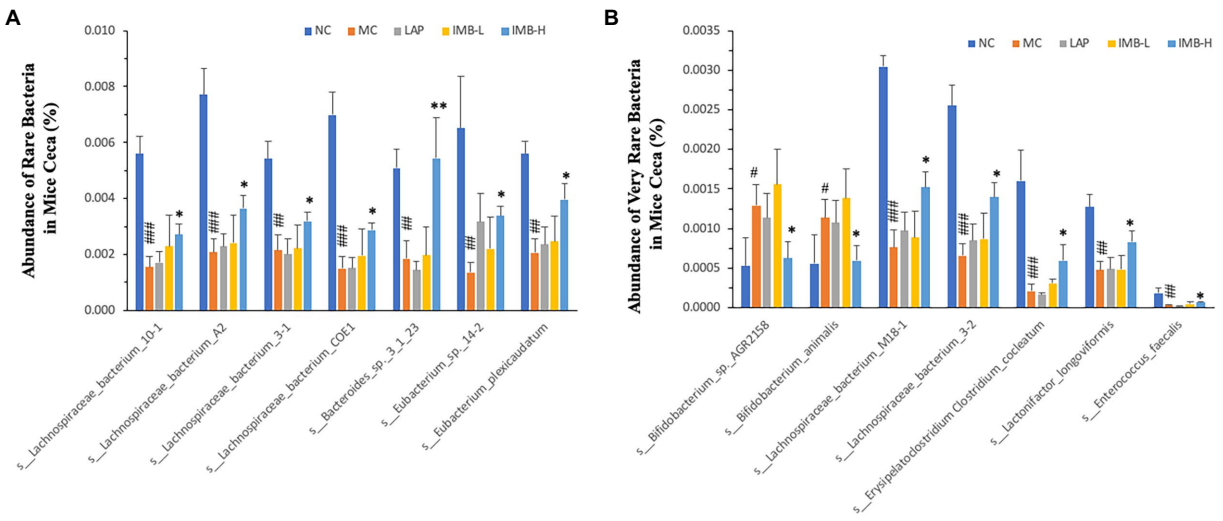

FIGURE 7
Effects of treatments on abundance of rare **(A)** and very rare **(B)** bacteria in mice ceca. Within each panel, values with a superscript symbol "*" are significantly different from that of the corresponding MC (*p<0.05; **p<0.01; ***p<0.001); and the value of the MC with a superscript symbol "#" is significantly different from that of the corresponding NC ($^{\#}p$<0.05; $^{\#\#}p$<0.01; $^{\#\#\#}p$<0.001).

of glycolysis (glucose breakdown) in anaerobic metabolism and a product of oxygen-limited metabolism. However, subsequent studies revealed that lactate is formed under both aerobic and anaerobic conditions (21). It was shown that lactate is taken up by liver and is converted to pyruvate by LDH to be used in Krebs cycle. Nevertheless, other studies proposed the lactate shuttle hypothesis and demonstrated that lactate generated in peripheral tissue is transferred to other tissues to be used as fuel. For instance, lactate produced in muscles (during physical exercise) could be taken by heart and other tissues (e.g., brain) and used as fuel (22, 23). Therefore, it is also likely that LAP exerts its effects though these mechanisms.

Our study showed that IMB significantly alleviated adenine-induced cognitive impairment. It is also possible that reduction of inflammation/neuroinflammation may be one of the important mechanisms. IMB, to the less extend than LAP, reduced inflammatory lesions in kidney tissues, circulating levels of proinflammatory cytokines, and mRNA levels of proinflammatory cytokines in kidney tissues (13). In this study, we found that IMB significantly reversed adenine-induced alterations of mRNA levels of ELOVL2, GLUT4, Nestin, TGFB1, and TGFB2 genes. ELOVL2 improves synaptic functionality and regulates/mitigates brain inflammatory activity (24). It also inhibits apoptosis in pancreatic beta cells supporting its involvement in metabolic processes (25). GLUT4 is an insulin-regulated glucose transporter. Animal models of insulin resistance showed memory deficit and a decrease in GLUT4 and hippocampal insulin signaling (26). The reduced GLUT4 expression in brain tissues of adenine-treated mice indicated that cognitive impairment is associated with impaired glucose utilization/energy metabolism in brain. The reduced GLUT4 expression in brain tissues of adenine-treated mice indicated impaired neural stem cell production and reduced neurogenesis in brain. While the primary function of Nestin is related to neurogenesis from neural stem cells, neuroinflammation is also involved in Nestin-mediated neurogenesis (27). The significantly reduced Nestin expression in adenine-treated mice indicated impaired neurogenesis, which could be reversed by IMB treatment. In addition to TGFB1, TGFB2 also has anti-inflammatory functions (28). Similar to TGFB1, the reduced expression level of TGFB2 in adenine-treated mice was significantly increased by IMB. These cumulative experimental results strongly suggest that IMB may improve cognition in part *via* inhibiting neuroinflammation, increasing energy metabolism, and increasing neurogenesis processes.

IMB was prepared by a koji fermentation of defatted soybeans with *Aspergillus oryzae* and lactic acid bacteria (*Pediococcus parvulus* and *Enterococcus faecium*), followed by water extraction and purification of koji polysaccharides. Hydrolysis analysis showed that this polysaccharide was mainly consisted with arabinose (41.4%), galactose (23.7%), and xylose (10.4%) (13). The functional roles of polysaccharides in modulating gut microbiota have been well-established. In this study, our microbiome analysis revealed that adenine treatment drastically altered the microbiome profile of the fecal samples of mice cecum. In fact, the abundance of almost 2/3 of bacterial species was changed at a significant level. Interestingly, IMB (especially IMB-H), but not LAP, could normalize the abundance of 30% of the altered bacteria.

We found that mice in the MC had significantly increased abundance of *Actinobacteria* phylum and significantly decreased abundance of *Bacteroidetes* phylum. Previous research has suggested that *Actinobacteria* (mainly Bifidobacterium) may play a functional role in cognition. Patients with cognitive impairment had a higher abundance of *Actinobacteria* than that of the controls (29). Mice with depression also had increased abundance of *Actinobacteria* (30). Ovariectomized (OVX) mice fed a high-fat diet experienced impaired object recognition and spatial memory associated with increased *Bifidobacteriales*; administration of epigallocatechin gallate (EGCG) significantly improved cognition and memory and inhibited the increase of *Bifidobacteriales* (31). The results in our current study showed that IMB supplementation significantly improved cognition associated with significant reduction of *Actinobacteria* abundance. Further analysis also

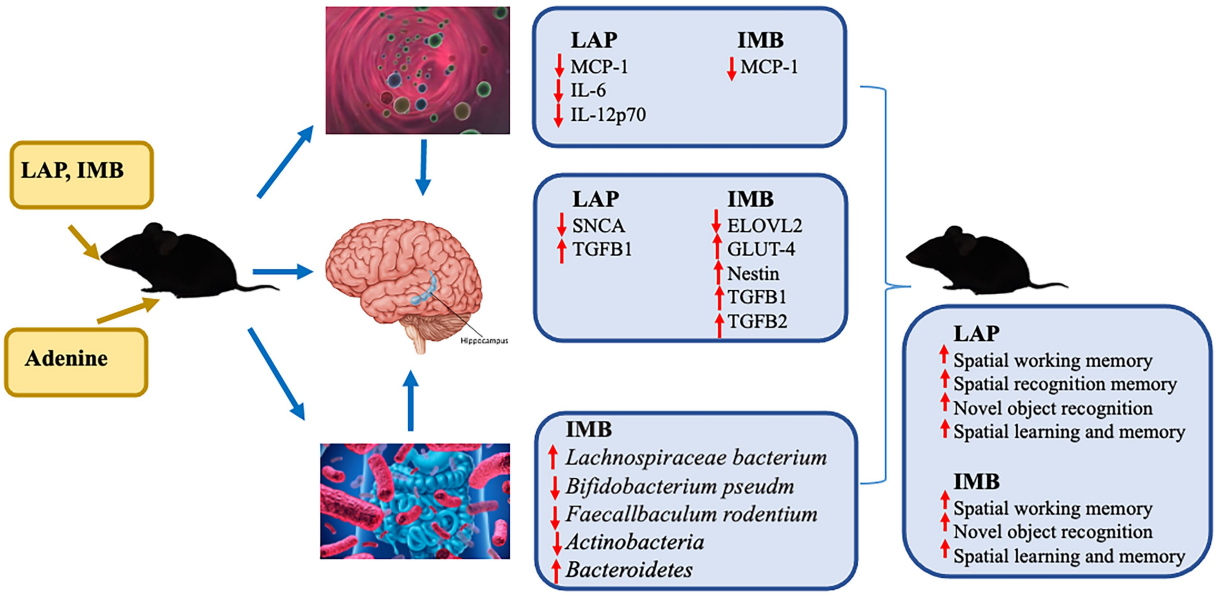

FIGURE 8
A diagram of suggested mechanisms of IMB and LAP actions. The results of circulating inflammatory cytokines are from our previous study (13).

showed that some *Bifidobacterium* species in the *Actinobacteria* phylum, such as the common bacteria *s_Bifidobacterium_pseudolongum* (Figure 6B), and the very rare bacteria s_*Bifidobacterium*_sp._*AGR2158* and *s_Bifidobacterium_animalis* (Figure 7B), had significantly increased abundances in MC mice, which were reversed/normalized by IMB supplementation. These results suggest that IMB may improve cognition in part *via* inhibition of the abundance/function of bacteria species in *Actinobacteria* phylum.

Our results showed that the abundance of *Bacteroidetes* phylum (which includes notably *Bacteroides* and *Prevotella* genera) was significantly decreased in mice of adenine-induced cognitive impairment, and IMB treatment improved cognition associated with increased abundance of *Bacteroidetes*. It is well recognized that cognitive impairment is correlated to decreased abundance of *Bacteroidetes* and the increased *Firmicutes*/*Bacteroidetes* ratio. Alzheimer's disease patients had significantly increased fecal abundance of *Firmicutes* but decreased abundance of *Bacteroidetes* compared to normal controls (32). Fecal microbiota transplantation improved cognition in patients with cognitive decline associated with enrichment of *Bacteroidetes* (33). Administration of young blood plasma significantly diminished the gut *Firmicutes*/*Bacteroidetes* ratio in middle-aged rats (34). Again, these results suggest that IMB may improve cognition in part *via* inhibition of the function of bacteria species in *Bacteroidetes* phylum.

In conclusion, our data demonstrated that LAP and IMB could improve cognitive performance in mice *via* distinct mechanisms of action. LAP may improve cognition in part *via* inhibiting inflammation/neuroinflammation and modulating metabolic process, whereas IMB may improve cognition in part *via* inhibiting inflammation/neuroinflammation, enhancing energy metabolism, increasing neurogenesis, and modulating gut microbiota (Figure 8).

Data availability statement

The data presented in the study are deposited in the Harvard Dataverse, accession number (https://doi.org/10.7910/DVN/XUJYVB).

Ethics statement

The animal study was reviewed and approved by Beth Israel Deaconess Medical Center.

Author contributions

HA and YS contributed to the animal study, sample analysis, and manuscript preparation. HA and J-RZ contributed to experimental design and data analyses. J-RZ contributed to supervision and project administration. All authors contributed to the article and approved the submitted version.

Funding

This research was funded by Nichimo Biotics Co., Ltd., Japan and LifeTrade Co., Ltd., Japan. The funders were not involved in the study design, collection, analysis, interpretation of data, the writing of this article or the decision to submit it for publication.

Conflict of interest

The authors declare that this study received funding from Nichimo Biotics Co., Ltd and LifeTrade Co., Ltd. The funders were not involved in the study design, collection, analysis, interpretation of data, the writing of this article or the decision to submit it for publication.

Publisher's note

References

1. Harvey, PD. Domains of cognition and their assessment. *Dialogues Clin Neurosci*. (2019) 21:227–37. doi: 10.31887/DCNS.2019.21.3/pharvey

2. Zammit, AR, Katz, MJ, Bitzer, M, and Lipton, RB. Cognitive impairment and dementia in older adults with chronic kidney disease: a review. *Alzheimer Dis Assoc Disord*. (2016) 30:357–66. doi: 10.1097/WAD.0000000000000178

3. Dominguez, LJ, and Barbagallo, M. Nutritional prevention of cognitive decline and dementia. *Acta Biomed*. (2018) 89:276–90. doi: 10.23750/abm.v89i2.7401

4. Alam, R, Abdolmaleky, HM, and Zhou, JR. Microbiome, inflammation, epigenetic alterations, and mental diseases. *Am J Med Genet B Neuropsychiatr Genet*. (2017) 174:651–60. doi: 10.1002/ajmg.b.32567

5. Li, X, Wang, Y, Xing, Y, Xing, R, Liu, Y, and Xu, Y. Changes of gut microbiota during silybin-mediated treatment of high-fat diet-induced non-alcoholic fatty liver disease in mice. *Hepatol Res*. (2020) 50:5–14. doi: 10.1111/hepr.13444

6. Ushiroda, C, Naito, Y, Takagi, T, Uchiyama, K, Mizushima, K, Higashimura, Y, et al. Green tea polyphenol (epigallocatechin-3-gallate) improves gut dysbiosis and serum bile acids dysregulation in high-fat diet-fed mice. *J Clin Biochem Nutr*. (2019) 65:34–46. doi: 10.3164/jcbn.18-116

7. Chu, C, Murdock, MH, Jing, D, Won, TH, Chung, H, Kressel, AM, et al. The microbiota regulate neuronal function and fear extinction learning. *Nature*. (2019) 574:543–8. doi: 10.1038/s41586-019-1644-y

8. Clarke, G, Grenham, S, Scully, P, Fitzgerald, P, Moloney, RD, Shanahan, F, et al. The microbiome-gut-brain axis during early life regulates the hippocampal serotonergic system in a sex-dependent manner. *Mol Psychiatry*. (2013) 18:666–73. doi: 10.1038/mp.2012.77

9. Akintonwa, A, and Auditore, JV. Reversal of adenine-induced depression of mouse locomotor activity by amphetamine. *Arch Int Pharm Ther*. (1978) 235:248–53.

10. Mazumder, MK, Giri, A, Kumar, S, and Borah, A. A highly reproducible mice model of chronic kidney disease: evidences of behavioural abnormalities and blood-brain barrier disruption. *Life Sci*. (2016) 161:27–36. doi: 10.1016/j.lfs.2016.07.020

11. Mazumder, MK, Paul, R, Bhattacharya, P, and Borah, A. Neurological sequel of chronic kidney disease: from diminished acetylcholinesterase activity to mitochondrial dysfunctions, oxidative stress and inflammation in mice brain. *Sci Rep*. (2019) 9:3097. doi: 10.1038/s41598-018-37935-3

12. Nakagawa, T, Hasegawa, Y, Uekawa, K, and Kim-Mitsuyama, S. Chronic kidney disease accelerates cognitive impairment in a mouse model of Alzheimer's disease, through angiotensin II. *Exp Gerontol*. (2017) 87:108–12. doi: 10.1016/j.exger.2016.11.012

13. He, LX, Abdolmaleky, HM, Yin, S, Wang, Y, and Zhou, JR. Dietary fermented soy extract and oligo-lactic acid alleviate chronic kidney disease in mice via inhibition of inflammation and modulation of gut microbiota. *Nutrients*. (2020) 12:2376. doi: 10.3390/nu12082376

14. Patil, SS, Sunyer, B, Hoger, H, and Lubec, G. Evaluation of spatial memory of C57BL/6J and CD1 mice in the Barnes maze, the multiple T-maze and in the Morris water maze. *Behav Brain Res*. (2009) 198:58–68. doi: 10.1016/j.bbr.2008.10.029

15. Rosenfeld, CS, and Ferguson, SA. Barnes maze testing strategies with small and large rodent models. *J Vis Exp*. (2014) 84:e51194. doi: 10.3791/51194

16. Kwok, LY, Zhang, J, Guo, Z, Gesudu, Q, Zheng, Y, Qiao, J, et al. Characterization of fecal microbiota across seven Chinese ethnic groups by quantitative polymerase chain reaction. *PLoS One*. (2014) 9:e93631. doi: 10.1371/journal.pone.0093631

17. Gohl, DM, Vangay, P, Garbe, J, MacLean, A, Hauge, A, Becker, A, et al. Systematic improvement of amplicon marker gene methods for increased accuracy in microbiome studies. *Nat Biotechnol*. (2016) 34:942–9. doi: 10.1038/nbt.3601

18. Gallardo-Fernandez, M, Hornedo-Ortega, R, Alonso-Bellido, IM, Rodriguez-Gomez, JA, Troncoso, AM, Garcia-Parrilla, MC, et al. Hydroxytyrosol decreases LPS- and alpha-Synuclein-induced microglial activation in vitro. *Antioxidants*. (2019) 9:36. doi: 10.3390/antiox9010036

19. Dabiri, S, Ramirez Ruiz, MI, Jean-Louis, G, Ntekim, OE, Obisesan, TO, Campbell, AL, et al. The mediating role of inflammation in the relationship between alpha-synuclein and cognitive functioning. *J Gerontol A Biol Sci Med Sci*. (2022). doi: 10.1093/gerona/glac217

20. Fraga, VG, Guimaraes, HC, Lara, VP, Teixeira, AL, Barbosa, MT, Carvalho, MG, et al. TGF-beta1 codon 10 T>C polymorphism influences short-term functional and cognitive decline in healthy oldest-old individuals: the pieta study. *J Alzheimers Dis*. (2015) 48:1077–81. doi: 10.3233/JAD-150397

21. Brooks, GA. Mammalian fuel utilization during sustained exercise. *Comp Biochem Physiol B Biochem Mol Biol*. (1998) 120:89–107. doi: 10.1016/S0305-0491(98)00025-X

22. Gertz, EW, Wisneski, JA, Stanley, WC, and Neese, RA. Myocardial substrate utilization during exercise in humans. Dual carbon-labeled carbohydrate isotope experiments. *J Clin Invest*. (1988) 82:2017–25. doi: 10.1172/JCI113822

23. Bergersen, LH. Is lactate food for neurons? Comparison of monocarboxylate transporter subtypes in brain and muscle. *Neuroscience*. (2007) 145:11–9. doi: 10.1016/j.neuroscience.2006.11.062

24. Talamonti, E, Sasso, V, To, H, Haslam, RP, Napier, JA, Ulfhake, B, et al. Impairment of DHA synthesis alters the expression of neuronal plasticity markers and the brain inflammatory status in mice. *FASEB J*. (2020) 34:2024–40. doi: 10.1096/fj.201901890RR

25. Bellini, L, Campana, M, Rouch, C, Chacinska, M, Bugliani, M, Meneyrol, K, et al. Protective role of the ELOVL2/docosahexaenoic acid axis in glucolipotoxicity-induced apoptosis in rodent beta cells and human islets. *Diabetologia*. (2018) 61:1780–93. doi: 10.1007/s00125-018-4629-8

26. de Nazareth, AM. Type 2 diabetes mellitus in the pathophysiology of Alzheimer's disease. *Dement Neuropsychol*. (2017) 11:105–13. doi: 10.1590/1980-57642016dn11-020002

27. Wilhelmsson, U, Lebkuechner, I, Leke, R, Marasek, P, Yang, X, Antfolk, D, et al. Nestin regulates neurogenesis in mice through notch signaling from astrocytes to neural stem cells. *Cereb Cortex*. (2019) 29:4050–66. doi: 10.1093/cercor/bhy284

28. Maheshwari, A, Kelly, DR, Nicola, T, Ambalavanan, N, Jain, SK, Murphy-Ullrich, J, et al. TGF-beta2 suppresses macrophage cytokine production and mucosal inflammatory responses in the developing intestine. *Gastroenterology*. (2011) 140:242–53. doi: 10.1053/j.gastro.2010.09.043

29. Lu, S, Yang, Y, Xu, Q, Wang, S, Yu, J, Zhang, B, et al. Gut microbiota and targeted biomarkers analysis in patients with cognitive impairment. *Front Neurol*. (2022) 13:834403. doi: 10.3389/fneur.2022.834403

30. Sun, Y, Pei, J, Chen, X, Lin, M, Pan, Y, Zhang, Y, et al. The role of the gut microbiota in depressive-like behavior induced by chlorpyrifos in mice. *Ecotoxicol Environ Saf*. (2023) 250:114470. doi: 10.1016/j.ecoenv.2022.114470

31. Qu, Y, Wu, Y, Cheng, W, Wang, D, Zeng, L, Wang, Y, et al. Amelioration of cognitive impairment using epigallocatechin-3-gallate in ovariectomized mice fed a high-fat diet involves remodeling with Prevotella and Bifidobacteriales. *Front Pharmacol*. (2022) 13:1079313. doi: 10.3389/fphar.2022.1079313

32. Jeong, S, Huang, LK, Tsai, MJ, Liao, YT, Lin, YS, Hu, CJ, et al. Cognitive function associated with gut microbial abundance in sucrose and S-Adenosyl-L-methionine (SAMe) metabolic pathways. *J Alzheimers Dis*. (2022) 87:1115–30. doi: 10.3233/JAD-215090

33. Park, SH, Lee, JH, Kim, JS, Kim, TJ, Shin, J, Im, JH, et al. Fecal microbiota transplantation can improve cognition in patients with cognitive decline and Clostridioides difficile infection. *Aging*. (2022) 14:6449–66. doi: 10.18632/aging.204230

34. Ceylani, T, and Teker, HT. The effect of young blood plasma administration on gut microbiota in middle-aged rats. *Arch Microbiol*. (2022) 204:541. doi: 10.1007/s00203-022-03154-8

Frontiers in Nutrition

Explores what and how we eat in the context of health, sustainability and 21st century food science

A multidisciplinary journal that integrates research on dietary behavior, agronomy and 21st century food science with a focus on human health.

Discover the latest Research Topics

See more →

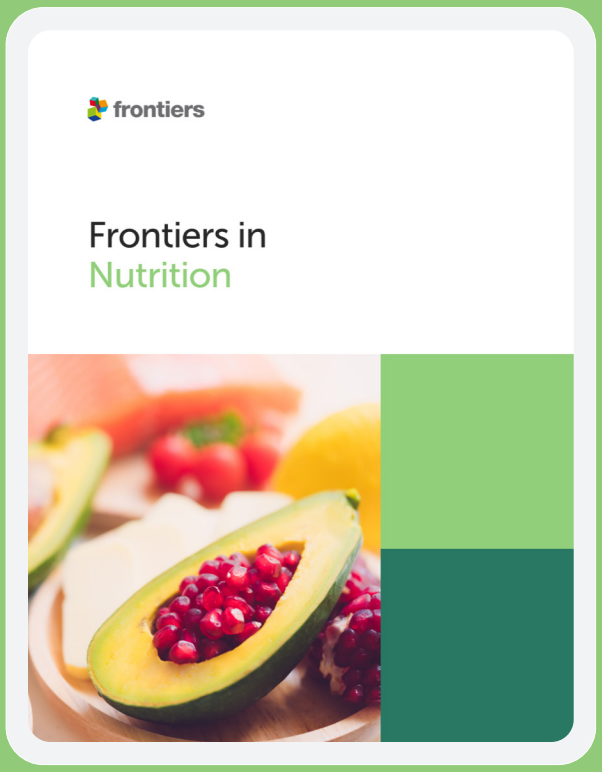

Frontiers

Avenue du Tribunal-Fédéral 34
1005 Lausanne, Switzerland
frontiersin.org

Contact us

+41 (0)21 510 17 00
frontiersin.org/about/contact